RADIOSENSITIZATION STRATEGIES FOR ENHANCED E-BEAM IRRADIATION TREATMENT OF FRESH PRODUCE

A Dissertation

by

CARMEN LUIZA FEITOSA DE LIMA GOMES

Submitted to the Office of Graduate Studies of
Texas A&M University
in partial fulfillment of the requirements for the degree of

DOCTOR OF PHILOSOPHY

May 2010

Major Subject: Biological and Agricultural Engineering

Radiosensitization Strategies for Enhanced E-beam Irradiation Treatment of Fresh Produce

RADIOSENSITIZATION STRATEGIES FOR ENHANCED E-BEAM IRRADIATION TREATMENT OF FRESH PRODUCE

A Dissertation

by

CARMEN LUIZA FEITOSA DE LIMA GOMES

Submitted to the Office of Graduate Studies of
Texas A&M University
in partial fulfillment of the requirements for the degree of

DOCTOR OF PHILOSOPHY

Approved by:

Chair of Committee,	Rosana G. Moreira
Committee Members,	Elena Castell-Perez
	Zivko Nikolov
	Luis Cisneros-Zevallos
	Marcos X. Sanches-Plata
Head of Department,	Gary Riskowski

May 2010

Major Subject: Biological and Agricultural Engineering

ABSTRACT

Radiosensitization Strategies for Enhanced E-beam Irradiation Treatment of Fresh Produce. (May 2010)

Carmen Luiza Feitosa de Lima Gomes, B.S., Federal University of Vicosa

Chair of Advisory Committee: Dr. Rosana G. Moreira

Fresh produce is increasingly implicated in outbreaks of foodborne illness. Internalization of bacterial pathogens into produce is of particular concern as internalized pathogens are unlikely to be removed by surface sanitizers. It is therefore necessary to develop treatments that will reduce their prevalence and numbers on fresh produce.

Irradiation is a penetrating nonthermal treatment that effectively eliminates bacteria. Irradiated baby spinach leaves up to 1.0 kGy showed negligible ($P>0.05$) changes in color, texture, vitamin C, total carotenoids, and chlorophyll content compared to non-irradiated controls throughout storage (15 days at $4^{o}C$).

This research also shows that irradiation effectively reduces viable *Escherichia coli* cells internalized in lettuce, and that decontamination is not influenced ($P>0.05$) by lettuce variety. Irradiation effectively reduced the population of internalized pathogens in a dose-dependent manner (3-4 log reduction at 1.0 kGy). Microscopy images suggest that the contamination sites of pathogens in leafy vegetables are mainly localized on

crevices and in the stomata. A careful design of the treatment (understanding dose distribution) will effectively eliminate pathogens while maintaining produce quality.

The use of modified atmosphere packaging increased ($P<0.05$) the sensitivity of pathogens (*Salmonella* spp. and *Listeria* spp.) to irradiation in baby spinach leaves (up to 25%). Increasing concentration of oxygen increased ($P<0.05$) sensitivity of both microorganisms. Radiosensitization could be affected ($P<0.05$) by production of ozone, which increases with increasing dose-rate and oxygen concentration, and reducing temperatures.

Antimicrobial effectiveness of various active compounds was determined against *Salmonella* spp. and *Listeria* spp. Inclusion complexes were prepared with antimicrobial compounds and β-cyclodextrin. The effectiveness of the microencapsulated compounds was tested by spraying them on the surface of baby spinach leaves inoculated with *Salmonella* spp. The increase in radiosensitivity (up to 40%) varied with the antimicrobial compound.

Spherical poly (DL-lactide-*co*-glycolide) (PLGA) nanoparticles with entrapped eugenol and *trans*-cinnamaldehyde were synthesized for future antimicrobial delivery applications. All loaded nanoparticles proved to be efficient in inhibiting growth of *Salmonella* spp. and *Listeria* spp. The entrapment efficiency for eugenol and *trans*-cinnamaldehyde was 98% and 92%, respectively. Controlled release experiments (*in vitro* at 37^{o}C for 72 hrs) showed an initial burst followed by a slower release rate of the antimicrobial entrapped inside the PLGA matrix.

DEDICATION

To my parents, Luiz Clairmont and Heloisa Helena de Lima Gomes

To my siblings, Clarissa and Paulo Feitosa de Lima Gomes

To my boyfriend, Paulo Cesar Fortes Da Silva

For their unconditional love. Thank you.

ACKNOWLEDGEMENTS

I would like to express my deepest appreciation to my major professor, Dr. Rosana G. Moreira for the guidance, patience and knowledge she shared while serving as Chair of the Advisory Committee, as well as for her generosity and encouragement throughout my entire graduate program. She has been very supportive in helping me to finish this dissertation and to have a vision for my future research and career. Thanks to Dr. Elena Castell-Perez, member of my committee, for all the support, encouragement and help.

I would like to thank Dr. Zivko Nikolov, Dr. Marcos X. Sanchez-Plata, and Dr. Cisneros-Zevallos for giving their time and advice and also kindly allowing me to use their laboratory space and instruments. Thanks to them for serving as my Advisory Committee members.

Profound thanks to Jong-Soon Kim and Paulo Da Silva in the Food Engineering Lab for sacrificing their time and generously providing help and resources vital to the completion of this study. I will always be grateful to their assistance and good friendship during my entire stay in graduate school. My special thanks to all my friends in the Food Engineering Lab for always having a smile and a nice word to say. I also want to extend my gratitude to my friends and colleagues and the department faculty and staff for making my time at Texas A&M University a great experience.

Finally, I would like to thank my parents and boyfriend, Paulo Da Silva, for all their love and patience, for believing in me, and for making hard times much easier. They have provided me with unconditional love.

TABLE OF CONTENTS

Page

ABSTRACT iii

DEDICATION v

ACKNOWLEDGEMENTS vi

TABLE OF CONTENTS viii

LIST OF FIGURES xii

LIST OF TABLES xvii

CHAPTER

I INTRODUCTION 1

II LITERATURE REVIEW 6

2.1 Fresh Fruits and Vegetables as Vehicles of Foodborne Illness 6
2.2 Irradiation Treatment and Radiosensitization Approaches 8
2.3 Modified Atmosphere Packaging 10
2.4 Natural Antimicrobial Agents and Novel Delivery Systems ... 12

III E-BEAM IRRADIATION OF BAGGED, READY-TO-EAT SPINACH LEAVES (*SPINACEA OLERACEA*): AN ENGINEERING APPROACH 17

3.1 Overview 17
3.2 Introduction 18
3.3 Materials and Methods 20
3.3.1 Produce Quality Study 20
3.3.2 Produce Quality Attributes 21
3.3.3 Statistical Analysis 23
3.3.4 Experimental Determination of Radiation D_{10} value of *E. coli* O157:H7 in Irradiated Bagged Spinach Leaves..... 24
3.3.5 Simulation Studies of Pathogen Survival within a Bag of Baby Spinach Leaves 26
3.4 Results and Discussion 29

CHAPTER Page

3.4.1 Effect of Electron Beam Irradiation on Quality of Baby Spinach Leaves 29
3.4.2 Dose Distribution and Microbial Survival within a Bag of Baby Spinach Leaves 36
3.5 Conclusions 42

IV UNDERSTANDING *E. COLI* INTERNALIZATION IN LETTUCE LEAVES FOR OPTIMIZATION OF IRRADIATION TREATMENT 44

4.1 Overview 44
4.2 Introduction 45
4.3 Materials and Methods 48
4.3.1 Determination of Radiation D_{10}-values 48
4.3.2 Scanning Electron Microscopy 52
4.4 Results and Discussion 53
4.4.1 Radiation Sensitivity of Internalized Microorganisms 53
4.4.2 Does Variety Affect Radiation Sensitivity? 59
4.4.3 Mechanisms of Internalization 61
4.5 Conclusions 68

V RADIOSENSITIZATION OF *SALMONELLA* SPP. AND *LISTERIA* SPP. IN READY-TO-EAT BABY SPINACH LEAVES 70

5.1 Overview 70
5.2 Introduction 71
5.3 Materials and Methods 74
5.3.1 Bacterial Cultures 74
5.3.2 Inoculation and Preparation of Baby Spinach 75
5.3.3 Irradiation 76
5.3.4 Microbiological Analysis 77
5.3.5 Radiosynthesis Study of Ozone by Electron Beam Irradiation 78
5.3.6 Ozone Radiosynthesis under Different Atmospheres 79
5.3.7 Effect of Dose Rate on Ozone Radiosynthesis 79
5.3.8 Ozone Decomposition with Time 79
5.3.9 Statistical Analysis 80
5.4 Results and Discussion 81
5.4.1 Bacterial Radiosensitization under Different Atmospheres 81
5.4.2 Radiosynthesis Study of Ozone by Electron Beam Irradiation 87
5.5 Conclusions 93

CHAPTER Page

VI MICROENCAPSULATED ANTIMICROBIAL COMPOUNDS AS A MEANS TO ENHANCE ELECTRON BEAM IRRADIATION TREATMENT OF FRESH PRODUCE 95

6.1 Overview 95
6.2 Introduction 96
6.3 Materials and Methods 101
6.3.1 Materials 101
6.3.2 β-cyclodextrins in Inclusion Complexes with Antimicrobial Compounds 103
6.3.3 Minimum Inhibitory Concentration (MIC) 105
6.3.4 Radiosensitization Analysis 107
6.3.5 Irradiation 108
6.3.6 Microbiological Analysis 109
6.3.7 Statistical Analysis 110
6.4 Results and Discussion 110
6.4.1 Garlic Extract and Characterization 110
6.4.2 Bee Resin Extract and Characterization 110
6.4.3 β-cyclodextrins Inclusion Complexes with Antimicrobial Compounds 111
6.4.4 Minimum Inhibitory Concentration (MIC) 116
6.4.5 Radiosensitization Analysis 122
6.5 Conclusions 125

VII POLY (DL-LACTIDE-CO-GLYCOLIDE) (PLGA) NANOPARTICLES WITH ENTRAPPED *TRANS*-CINNAMALDEHYDE AND EUGENOL FOR ANTIMICROBIAL DELIVERY APPLICATIONS 127

7.1 Overview 127
7.2 Introduction 128
7.3 Materials and Methods 132
7.3.1 Materials 132
7.3.2 Synthesis of Nanoparticles with Entrapped *trans*-Cinnamaldehyde and Eugenol 132
7.3.3 Size and Size Distribution 134
7.3.4 Nanoparticle Morphology Characterization 135
7.3.5 Determination of *trans*-Cinnamaldehyde and Eugenol Entrapment Efficiency 135
7.3.6 Controlled Release Study 136
7.3.7 Minimum Inhibitory Concentration (MIC) 139
7.3.8 Statistical Analysis 140

CHAPTER Page

7.4 Results and Discussion 141
7.4.1 Size and Polydispersity of Nanoparticles 141
7.4.2 Nanoparticle Morphology Characterization 144
7.4.3 Determination of *trans*-Cinnamaldehyde and Eugenol Entrapment Efficiency 147
7.4.4 Controlled Release Study 147
7.4.5 Minimum Inhibitory Concentration (MIC) 151
7.5 Conclusions 155

VIII CONCLUSIONS 157

IX RECOMMENDATIONS FOR FURTHER STUDY 161

REFERENCES 163

APPENDIX 189

VITA 213

LIST OF FIGURES

FIGURE Page

3.1 Survival curve of a cocktail of *E. coli* O157:H7 in irradiated bagged spinach (10-MeV LINAC at room temperature). Log [CFU/g]=7.07156-5.37615*dose, D_{10} value = 0.186 kGy, R^2 = 0.993.. 27

3.2 Effect of dose and storage (days) on overall appearance of baby spinach leaves stored for 15d at 4^{o}C and 90% RH. 31

3.3 Effect of dose and storage (days) on total chlorophyll (g/100 g d.b.) of baby spinach leaves stored for 15d at 4^{o}C and 90% R.H. 35

3.4 Effect of dose and storage (days) on total carotenoids (g/100 g d.b.) of baby spinach leaves stored for 15d at 4^{o}C and 90% R.H. 35

3.5 Effect of dose and storage (days) on total vitamin C content (mg ascorbic acid/g d.b.) of baby spinach leaves stored for 15d at 4^{o}C and 90% RH..... 36

3.6 (a) A leaf of baby spinach; (b) Density distribution within a bag of spinach leaves using CT data 37

3.7 Simulated dose distribution within a bag of baby spinach leaves (a) single-top-beam configuration, 10-MeV, entrance dose 0.5 kGy; (b) double-beam configuration, 10-MeV, entrance dose 0.5 kGy/beam.... 38

3.8 Spinach dose data (a) along the vertical direction at the horizontal points with single (top) beam direction; entrance dose = 0.5 kGy; (b) along the horizontal direction in the vertical point of 5.63 cm with double (top and bottom) beam direction , entrance dose for each beam = 0.5 kGy ; (c) along the vertical direction at the horizontal points (6.56 and 14.1 cm) with double beam direction, entrance dose for each beam = 0.5 kGy; (d) along the vertical direction at the horizontal points (6.56 and 14.1 cm) with double beam direction, the entrance dose for each beam = 1 kGy..... 40

3.9 (a) Simulated dose distribution within a bag of spinach leaves: double-beam, 10-MeV, entrance dose 1.0 kGy/beam; (b) Simulated microbial (*E. coli* O157:H7) survival distribution within a bag of spinach leaves: double beam, 10-MeV, entrance dose 1.0 kGy/beam..... 42

FIGURE Page

4.1 (a) Experimental setup showing gas ion-chamber dosimeters locations at the front and back of the box holding the samples; (b) location of RCF (radio-chromic films) dosimeters between the sample bags. Dimensions for the lanthanum plate and the box were 1m x 1m and 30.48cm x 30.48cm, respectively 51

4.2 (a) Dose distribution within the lettuce bag samples; (b) buildup region for gamma rays in water 56

4.3 Log reduction (log No/N) of internalized *E. coli* in lettuce leaf pieces of four lettuce varieties (iceberg, green leaf, red leaf, and Boston) (dots = experimental data; line = linear regression) 58

4.4 Microflora density of the surface of lettuce leaf of (a) iceberg, (b) Boston, (c) green leaf, and (d) red leaf inoculated with *E. coli*. Inoculated (top) and irradiated at 1.0 kGy (bottom) 61

4.5 Images of (a) iceberg, (b) Boston (b), (c) green leaf, and (d) red leaf (d) surface of non-inoculated control 61

4.6 Deep internalization of inoculated *E. coli* cells in lettuce leaf stomata (clockwise from top-left - iceberg, Boston, red leaf, green leaf) 63

4.7 Localization of *E. coli* cells on crevices in lettuce leaf. (clockwise from top-left - iceberg, Boston, red leaf, green leaf)..... 63

4.8 Absence of *E. coli* cells on cut edges of lettuce leaf (showing iceberg lettuce) 64

4.9 Biofilm formation by *E. coli* on lettuce surface and stomata after 24 hours. (Clockwise from top-left – Boston, iceberg, red leaf, green leaf)..... 65

4.10 Lettuce surface field-of-view (a) iceberg, (b) Boston, (c) green leaf, and (d) red leaf for the determination of stomata density and size. Bottom image shows a zoom of image (c) showing location of stomata..... 67

4.11 Structural characteristics: (a) stomatal density; and (b) length of the stomatal aperture; (error bars indicate standard deviation)..... 68

FIGURE Page

5.1 Radiosensitization of *Salmonella* spp. in baby spinach under different atmospheres (air, N_2:O_2 (1:1) and 100% O_2) irradiated at room temperature (21^oC) 83

5.2 Radiosensitization of *Listeria* spp. in baby spinach under different atmospheres (air, N_2:O_2 (1:1) and 100% O_2) irradiated at room temperature (21^oC) 83

5.3 Radiosensitization of *Salmonella* spp. in baby spinach under different atmospheres (air, N_2:O_2 (1:1) and 100% O_2) irradiated at -5^oC 84

5.4 Radiosensitization of *Listeria* spp. in baby spinach under different atmospheres (air, N_2:O_2 (1:1) and 100% O_2) irradiated at -5^oC 84

5.5 Ozone production as a function of dose at room temperature (21^oC) under different package atmospheres 89

5.6 Ozone formation as a function of dose at -5^oC under different package atmospheres 90

5.7 Ozone concentration at 1 kGy as a function of dose rate (100% O_2 atmosphere) 91

5.8 Ozone decomposition within time after electron beam irradiation at 1 kGy at room temperature, and with a dose rate of 0.002512 kGy/s ± 0.0001909 94

6.1 HPLC chromatogram of ethanolic extract of propolis 111

6.2 DSC thermograms of a) propolis extract , b) β-cyclodextrin, c) physical mixture of propolis and β-cyclodextrin, d) inclusion complex of propolis and β-cyclodextrin..... 113

6.3 DSC thermograms of a) garlic extract, b) β-cyclodextrin, c) garlic extract β-cyclodextrin inclusion complex 114

6.4 DSC thermograms of pure *trans*-cinnamaldehyde and inclusion complex of *trans*-cinnamaldehyde and β-cyclodextrin under oxidative conditions 115

FIGURE Page

6.5 DSC thermograms of eugenol and inclusion complex of eugenol and β-cyclodextrin under oxidative conditions 116

6.6 Growth of *Salmonella* spp. in tryptic soy broth as a function of active compound 117

6.7 Growth of *Listeria* spp. in tryptic soy broth as a function of active compound 118

6.8 Growth of *Salmonella* spp. and *Listeria* spp. in tryptic soy broth as a function of active compound 118

6.9 Growth of *Salmonella* spp. in tryptic soy broth as a function of active compounds and their respective inclusion complexes with β-cyclodextrin 120

6.10 Growth of *Salmonella* spp. and *Listeria* spp.in tryptic soy broth as a function of active compounds and their respective inclusion complexes with β-cyclodextrin 121

6.11 Effect of microencapsulated antimicrobial compounds (0.5% w/v) sprayed on baby spinach on radiation inactivation of *Salmonella* spp. at room temperature 124

7.1 Schematic diagram of nanoparticle synthesis with entrapped *trans*-cinnamaldehyde and eugenol using PVA as surfactant 134

7.2 TEM images of unloaded PLGA nanoparticles (x 50,000 magnification) 145

7.3 TEM images of PLGA-*trans*-cinnamaldehyde loaded nanoparticles (x 50,000 magnification) 146

7.4 TEM images of PLGA-eugenol loaded nanoparticles (x 50,000 magnification**)** 146

7.5 *trans*-cinnamaldehyde release kinetic by PLGA nanospheres as a function of time (hours). See text for equations used in the fitting procedure 147

FIGURE Page

7.6 Eugenol release kinetic by PLGA nanospheres as a function of time (hours). See text for equations used in the fitting procedure 148

7.7 Eugenol (left) and *trans*-cinnamaldehyde (right) chemical structures..... 149

7.8 Growth of *Salmonella* spp. in tryptic soy broth as a function of active compound concentration (Top: PLGA-*trans*-cinnamaldehyde; Bottom: PLGA-eugenol). Concentration units are μg/ml 153

7.9 Growth of *Listeria* spp. in tryptic soy broth as a function of active compound concentration (Top: PLGA-*trans*-cinnamaldehyde; Bottom: PLGA-eugenol). Concentration units are μg/ml 154

1A Absorbance growth curves for *Salmonella enteriditis* 190

2A Log CFU growth curves for *Salmonella enteriditis* 190

3A Absorbance growth curves for *Salmonella typhimurium* 191

4A Log CFU growth curves for *Salmonella typhimurium* 191

5A Absorbance growth curves for *Listeria monocytogenes Strain A* 193

6A Log CFU growth curves for *Listeria monocytogenes Strain A* 193

7A Absorbance growth curves for *Listeria monocytogenes Scott A* 194

8A Log CFU growth curves for *Listeria monocytogenes Scott A* 194

LIST OF TABLES

TABLE		Page
3.1	Color values of control and irradiated baby spinach leaves stored for 15 days at 4°C and 90% R.H.	30
3.2	Sensory scores for control and irradiated baby spinach leaves stored for 15 days at 4°C and 90% R.H.	33
3.3	Texture characteristics (force and work to shear) of control and irradiated baby spinach leaves stored for 15 days at 4°C and 90% R.H.	34
4.1	Target and measured doses and calculated D_{10}-values for different locations in different bags of lettuces (see Figure 4.1 for location of the dosimeters)	55
4.2	Composition of selected lettuces and calculated effective atomic number (Z_{eff}).	60
5.1	Radiation sensitivity of *Salmonella* spp. or *Listeria* spp. inoculated in baby spinach leaves irradiated at room temperature (21°C) and at -5°C under MAP	82
6.1	Minimal Inhibitory Concentration (MIC) of natural compounds and their respective inclusion complexes with β-cyclodextrin against Gram-positive and negative bacteria	119
6.2	Radiation sensitivity of *Salmonella* spp. in baby spinach leaves when sprayed with antimicrobial compounds and irradiated at room temperature (20°C)	122
6.3	Log reduction of *Salmonella* spp. in baby spinach leaves when sprayed with antimicrobial compounds during storage at 4°C for 15 days	125
7.1	Effect of treatment (unloaded PLGA, PLGA loaded with *trans*-cinnamaldehyde (PLGA-C), PLGA loaded with eugenol (PLGA-E), and processing parameter (evaporation, ultrafiltration, and freeze-drying) during synthesis on size of nanoparticles	142

TABLE Page

7.2 Polydispersity of nanoparticles as a function of treatments (unloaded PLGA, PLGA loaded with *trans*-cinnamaldehyde (PLGA-C), PLGA loaded with eugenol (PLGA-E)), and processing parameter during synthesis 143

7.3 Release constant values for *trans*-cinnamaldehyde and eugenol antimicrobial agents determined by fitting Eqn. (7.3) to the experimental data 149

A1 Growth data for *Salmonella enteriditis (SE)* and *Salmonella typhimurium(ST)*..... 189

A2 Growth data for *Listeria strain A (LA)* and *Listeria Scott A (LS)* 192

A3 Growth of *Salmonella* spp. in tryptic soy broth as a function of active compound 195

A4 Growth of *Listeria* spp. in tryptic soy broth as a function of active compounds 198

A5 Growth of *Salmonella* spp. in tryptic soy broth as a function of active compounds and their respective inclusion complexes with β-cyclodextrin 203

A6 Growth of *Listeria* spp. in tryptic soy broth as a function of active compounds and their respective inclusion complexes with β-cyclodextrin 206

A7 Growth of *Salmonella* spp. in tryptic soy broth as a function of active compounds loaded nanoparticles 209

A8 Growth of *Listeria* spp. in tryptic soy broth as a function of active compounds loaded nanoparticles 210

A9 Controlled release data for the nanoparticles loaded with active compounds 211

CHAPTER I

INTRODUCTION

The emergence of outbreaks of foodborne illness associated with fresh fruits and vegetables has revived interest among public health agencies and sparked a new wave of research on food safety issues related to microbial contamination of fresh produce. Therefore, actions are required to identify an effective antimicrobial intervention that can be incorporated into the infrastructure of the food supply chain.

Furthermore, one needs to take into account the produce quality. To preserve the typical fresh character, only mild stabilizing treatments are used on such products, combining chemical and physical barriers (i.e. surface sanitizers, low temperatures). However, the potential for internalization of pathogens into produce tissues is existent and surface treatments, such as use of antimicrobial rinses, are ineffective in eliminating pathogens that have been internalized.

Ionizing radiation is a non-thermal technology known to penetrate food tissues and effectively eliminate food pathogens from fresh produce. Since radiation degradation of sensory quality of a product is dose dependent, it follows that reduction of the treatment dose would result directly in improved sensory quality of the treated product. By increasing sensitivity of the pathogens (radiosensitization) to a certain irradiation dose, one would successfully reduce detrimental effects in produce quality.

This dissertation follows the style of the Journal of Food Engineering.

∗ Reprinted with permission from Gomes, C. Moreira, R. Castell-Perez, E. Kim, J.; Da Silva, P. and Castillo, A. E-beam irradiation of bagged, ready-to-eat spinach leaves (Spinacea oleracea): An engineering approach. Journal of Food Science 73 (2):E95-E102. Copyright 2008 by John Wiley and Sons.

Currently, there is an interest in developing treatments to reduce the radiation dose necessary to achieve these objectives.

One approach is to use modified atmosphere packaging (MAP) with ionizing irradiation. The use of MAP can help to control bacterial populations in food products. Bacteria will be more sensitive to irradiation in the presence of oxygen. The presence of oxygen in the modified atmosphere increases the radiosensitivity of bacteria because of the formation of oxygen radical and ozone (O_3). Ozone is produced when ionizing radiation passes through oxygen. High reactivity, penetrability, and spontaneous decomposition to a nontoxic product (i.e., O_2) make ozone a viable disinfectant for ensuring the microbiological safety of food products.

Therefore, the understanding of the composition and concentration of gases in a MAP system subjected to ionizing irradiation could make the process more effective in terms of quality and safety assurance, and consequently increasing the potential of the process.

Another approach is to investigate the synergistic effect of antimicrobial agents from natural sources combined with ionizing radiation treatments. Naturally derived antimicrobial agents have a positive public perception, broad regulatory approvals, and environmentally friendly appeal to the consumers. Phenolic compounds and their subclasses, such as coumarins, flavonoids, and essential oils, have antimicrobial function. Usually, the active compound that confers the antimicrobial action is also responsible for flavor/odor characteristic of its source. Therefore, their use in foods as

preservatives is often limited due to flavor/odor considerations, since effective antimicrobial doses may exceed organoleptically acceptable levels.

An alternative is to use encapsulation (micro- or nano-) to carry, protect, and deliver antimicrobial compounds. The characteristic of the delivery system are one of the most important factors influencing the efficacy of functional ingredients in many industrial products. Each type of delivery system (i.e. biopolymer matrices, inclusion complexes, association colloids, etc) has its own specific advantages and disadvantages for encapsulation, protection, and delivery of functional ingredients, as well as cost, regulatory status, ease of use, biodegradability, and biocompatibility. These novel encapsulated materials may have great potential as a microbial hurdle against pathogenic bacteria in food systems in combination with irradiation, as controlled release system. And they could also be applied to medical and pharmaceutical supplies, and packaging for active packaging applications.

Therefore, when irradiation is used in combination with other preservation methods such as MAP and antimicrobial agents (encapsulated for controlled release and protection), the global efficiency is reinforced through synergistic action, and the irradiation doses can be reduced without affecting the product quality.

The main goal of this research was to develop a reliable technology that ensures the safety and quality of fresh and fresh-cut produce using ionizing radiation. The main hypothesis was that the use of a combination of technologies (i.e. MAP and antimicrobial agents) with ionizing radiation for treatment of fresh produce provides a

synergistic preservative effect that will reduce the risk of outbreaks with negligible effect on quality of fresh produce.

The specific objectives are:

1. To assess the efficacy of electron beam irradiation to ensure the safety (inactivation of *Escherichia coli* O157:H7) and quality (objective and sensory) of baby spinach leaves (*Spinacia oleracea* L.).
2. To verify the radiation sensitivity of internalized *E. coli* spp. cells in lettuce leaves (*Lactuca sativa*), determine the effect of lettuce variety on the efficacy of the irradiation treatment, and to understand the mechanisms of pathogen colonization of plants relative to lettuce leafy structures using microscopy.
3. To determine the effectiveness of using different modified atmosphere packaging with electron beam irradiation at different temperatures on sensitivity of Gram-positive (*Listeria* spp.) and negative (*Salmonella* spp.) bacteria, and to understand the radiochemistry of ozone by electron beam irradiation.
4. To establish the antimicrobial effectiveness of natural antimicrobial compounds and extracts against of Gram-positive (*Listeria* spp.) and negative (*Salmonella* spp.) bacteria, and to develop inclusion complexes (microencapsulation) among these natural antimicrobial compounds with β-cyclodextrin to mask their flavor/odor and protection. Furthermore, to assess the degree of radiosensitization of *Salmonella* spp. in baby spinach leaves sprayed with different microencapsulated antimicrobial compounds.

5. To synthesize poly (D,L-lactide-co-glycolide) (PLGA) nanoparticles with entrapped *trans*-cinnamaldehyde and eugenol, and to characterize (i.e. size, size distribution, morphology, entrapment efficiency and controlled release profile) of the synthesized nanoparticles; to determine the minimum inhibitory concentration (MIC) in order to establish their antimicrobial efficiency; and to determine the diffusion kinetics of *trans*-cinnamaldehyde and eugenol from the nanoparticles.

CHAPTER II

LITERATURE REVIEW

2.1 Fresh Fruits and Vegetables as Vehicles of Foodborne Illness

In recent years, the increased consumption of fresh and minimally processed fruits and vegetables has lead to an increase in the number of foodborne illnesses linked to these products (Beuchat, 1996; Tauxe et al., 1997).

Pathogens can readily contaminate fresh produce via contact with the decaying vegetation, soil, polluted water, manure or sewage sludge (Beuchat, 1998). In addition, contamination with pathogens such as *Salmonella typhimurium, Escherichia coli,* and *Listeria monocytogenes* may also occur during post-harvest handling, processing, distribution and marketing, as demonstrated by several studies (Beuchat and Brackett, 1990; Brandl, 2006). Since these products are often consumed raw or following minimal processing, the potential for ingestion of viable pathogens is a concern.

Epidemics of foodborne illness linked to fresh produce increased in the United States from 1973 through 1997, both in absolute number and in the proportion of total food-linked outbreaks with a known etiologic agent (Sivapalasingam et al., 2004). Several bacterial pathogens have caused fresh produce-associated epidemics of enteric illness, including *Salmonella enterica*, pathogenic *E. coli, Shigella* spp., *Campylobacter* spp., *Listeria monocytogenes, Staphylococcus aureus, Yersinia* spp., and *Bacillus cereus*. *S. enterica*, the most frequent etiologic agent of outbreaks from fresh produce, caused 48% of such outbreaks with a known etiology between 1973 and 1997 in the United

States. Pathogenic *E. coli* is the second most important causal agent of outbreaks from fresh produce (Brandl, 2006; Sivapalasingam et al., 2004). The unexpected increase in produce-associated bacterial infections is indicative of a much more important role of plants as a secondary habitat for enteric pathogens than previously thought. Furthermore, the low infective dose of just a few cells as low as 10 cell ingested can for *Salmonella* spp. and pathogenic *E. coli* and high risk, of complications are cause of concern, since it can cause enteric fever, enterocolitis, systemic infections (*Salmonella* spp.) hemolytic uremic syndrome (*E. coli* O157:H7) and lead to death, particularly in children, the elderly, and the immune-compromised ((D'Aoust, 1997; Doyle et al., 1997).

Internalization of bacterial pathogens into the edible portions of plants is of particular concern as internalized pathogens are unlikely to be removed by washing or surface sanitization methods (Jablasone et al., 2005). The uncertainties that persist with respect to the mechanism of contamination, and potential for continuing problems, have reduced consumer confidence in bagged spinach, lettuce, and other leafy vegetables ((USFDA), 2005). Researchers are continuing to study ways to reduce the food safety risks associated with fresh produce. Despite the use of proper hygiene and good agricultural practices, under specific conditions, contamination of fresh produce may occur at any point along the farm to table continuum ((USFDA), 2008a).

The potential for human pathogens and other bacteria to infiltrate into fresh fruits and vegetables was reviewed by (USFDA) (1999). The effectiveness of conventional surface decontamination measures to reduce internalized bacteria was also evaluated. It was concluded that a variety of opportunities exist for internalization events to occur,

and that surface treatments are generally ineffective in eliminating pathogens that have been internalized.

There is an urgency to develop effective interventions technologies that will inactivate microorganisms (including those internalized) and provide consumers with safe fresh produce with minimal quality deterioration. Non-thermal interventions capable of maintaining the intrinsic organoleptic profiles of produce are the only alternatives currently available to include as a lethality step in fresh produce processing.

2.2 Irradiation Treatment and Radiosensitization Approaches

Irradiation is a process with excellent potential to control or eliminate foodborne pathogens in food. Ionizing radiation is a non-thermal technology known to penetrate food tissues and effectively eliminate food pathogens from fresh produce. Ionizing radiation from Cobalt-60, Cesium-137, or machine generated electron beams, either alone or in combination with other preservative treatments, is used to extend shelf-life or enhance safety of produce (Diehl, 1995b; Thayer et al., 1996).

The biological effects of ionizing radiation on cells can be due both to direct interactions with critical cell components and to indirect actions on these critical targets caused by radiolytic products of other molecules in the cell, particularly free radicals formed from water. The DNA in the chromosomes is the most critical target of ionizing radiation. Effects on cytoplasmic membrane appear to play an additional important role in radiation-induced damage of cells (Grecz et al., 1983). Ionizing radiation can affect DNA directly by ionizing ray or indirectly by the primary water radicals $^{\cdot}H$, $^{\cdot}OH$, and e_{aq}^{-}. The most important of these three radicals in DNA damage is the $^{\cdot}OH$ radical. The $^{\cdot}OH$

radicals formed in the hydration layer around the DNA molecule are responsible for 90% of DNA damage. Thus, in living cells, the indirect radiation damage is predominant, resulting in a break in the phosphodiester backbone in one strand of the molecule (single-strand break) or in both strands at the same place (double-strand break) (Farkas, 1997; Moseley, 1989).

Although the changes by radiation are at the cellular level, the consequences of these changes vary with the organism. The correlation of radiation sensitivity is roughly inversely proportional to the size a complexity of an organism. This correlation is related to genome size: the DNA in the nuclei of the insect cells represents a target much larger than the genomes of bacteria. Differences in radiation sensitivities within groups of similar organisms are related to differences in their chemical and physical structure and the ability to recover from radiation injury. In general, gram-negative bacteria, including common spoilage organisms, and enteric species including pathogens, are more sensitive to irradiation than gram-positive bacteria. Irradiation resistance generally can be represented by the following sequence (Adams and Moss, 2000; Farkas, 1997):

gram-negative < gram-positive ≈ molds < spores ≈ yeast < virus

Radiations sensitivity itself is not a constant for a given organism; instead, an organism's response will depend on its repair capabilities as well as its environment and its physiological status at the time of irradiation. Many chemical agents have been found that alter radiation sensitivity. This generalization has virtually no exceptions: oxidizing agents are radiation sensitizers, whereas reducing agents are usually radiation protectors. The gas during irradiation affects the sensitivity of a particular microorganism. Survival

curves in oxygen re steeper (i.e. they show a more sensitive response) than those in 100% nitrogen (Ewing, 1987).

On August 22, 2008, the U. S. Food and Drug Administration ((USFDA), 1999) published a final rule that allows the use of ionizing radiation to make fresh iceberg lettuce and fresh spinach safer and last longer without spoiling. Therefore, proper treatment protocols are needed for effective inactivation of foodborne pathogens in fresh produce. Whenever irradiation is used to treat a fresh produce, a balance must be achieved between the quality of the treatment (i.e.., decontamination, surface pasteurization, disinfestation) and the organoleptic quality of the produce. The challenge is how to reduce the damage to produce quality while applying sufficient doses of radiation to inactivate pathogens. There is an interest in developing treatments to reduce the radiation dose necessary to achieve these objectives. The use of treatments involving antimicrobial agents and modified atmosphere packaging, combined with irradiation, could be effective in reducing the dose necessary to inactivate pathogenic bacteria. The radiosensitization phenomenon may be of practical utility for enhancement of irradiation effectiveness and feasibility for a variety of food products.

2.3 Modified Atmosphere Packaging

The use of modified atmosphere packaging (MAP) is also well documented to control the bacterial population of several food products (Farber, 1991; Hintlian and Hotchkiss, 1986).

MAP for respiring (“live”) product, i.e., fresh fruits and vegetables, is rather complicated since proper gas permeability of the packaging film is required to achieve

an equilibrium atmosphere in the package while both respiration rate and the gas permeability change with temperature (Keteleer and Tobback, 1994). Being living materials, fresh-cut produce can modify the atmosphere in their packages as a result of respiratory O_2 consumption and CO_2 evolution (Pirovani et al., 1998).

It has been reported that treatment of super atmospheric oxygen is an effective means for both inhibiting microbial growth and enzymatic discoloration and preventing anaerobic fermentation reactions (Day, 1996, 2000; Jacxsens et al., 2001). The improved effect of super atmospheric oxygen, when combined with increased CO_2 concentrations on fresh-cut vegetables, was previously demonstrated (Allende et al., 2002; Amanatidou et al., 1999). For instances, Allende et al. (2004) evaluated the effect of super atmospheric O_2 (80 and 100kPa) on quality of baby spinach. They reported that adding super atmospheric O_2 to the packages alleviated tissue injury in addition to reducing microbial growth and was beneficial in maintaining quality of baby spinach.

Furthermore, gas ozone (O_3) is produced when ionizing radiation (e.g., electrons and x-rays) passes through oxygen. The highest local concentrations will be in the region where the highest radiation doses are imparted. In air an efficient charge transfer mechanism (N_2^+ ions to O_2) enhances the O_3 yield, with the number of O_3 molecules produced per 100 eV of energy deposited varying between 7.4 and 10.3 depending on the rate of energy deposition (Swanson, 1979; Miller, 2005; Spears and Sutherland, 1968).

Ozone is one of the most potent sanitizers known and is effective against a wide spectrum of microorganisms at relatively low concentration (Khadre et al., 2001).

Sensitivity of microorganisms to ozone depends largely on the medium, the method of application, and the species. Because of its very high oxidation reduction potential, ozone acts as an oxidant of the constituent elements of cell walls before penetrating inside microorganisms and oxidizing certain essential components, e.g., unsaturated lipids, enzymes, proteins, nucleic acids, etc (Mahapatra et al., 2005). Ozone can react up to 3,000 times faster than chlorine with organic materials. In 2001, the Food and Drug Administration (FDA) allowed for the use of ozone as a direct contact food sanitizing agent ((CFR), 2009c). The gas does not leave any residual toxic by-products and does not alter a food's chemistry (Mahapatra et al., 2005). By generating ozone inside a packaging the risk related to human exposure to ozone is inexistent. Therefore, the combination of irradiation with ozone production using adequate gas composition inside a packaging could work synergistically to reduce microbial contamination.

2.4 Natural Antimicrobial Agents and Novel Delivery Systems

The recent years have also witnessed a revival of traditional natural products in medicine and in food and cosmetics preservation. There has been a growing interest in natural products due to their availability, fewer side effects or toxicity as well as better biodegradability as compared to the available antibiotics and preservatives. In this regard, plant essential oils and extracts and enzymes offer great potential and hope.

Eugenol and *trans*-cinnamaldehyde are phenolic compounds present in the essential oil fraction of clove (*Eugenia caryophyllata*) and cinnamon (*Cinnamomum verum*) plants. Cloves, cinnamon, oregano, and thyme and to a lesser extent sage and rosemary have the strongest antimicrobial activity among spices (Davidson, 1997).

Among the plants widely consumed in the human diet, the *Allium* spp. (*A. sativum* (garlic)) probably have been recognized longest and studied most extensively for their antimicrobial properties. Most of the foodborne bacterial pathogens examined are sensitive to extracts from garlic and onion. The principal component of garlic exhibiting bactericidal activity is allicin, a dially thisoufinate (2-propenyl-2propenethiol sulfinate) (Beuchat and Golden, 1989).

In the antimicrobial action of essential oil components, the lipophilic character of their hydrocarbon skeleton and the hydrophilic character of their functional groups are of main importance. The activity rank of essential oil components is as follows:

phenols> aldehydes> ketones> alcohols> ether> hydrocarbons

Essential oils with phenols as main compounds express the highest activity against microorganisms, and their activity spectrum is the broadest. (Kalemba and Kunicka, 2003).

Bee resin or propolis is a resinous mixture of substances collected by honey bees (*Apis mellifera*) from various plant sources. It is used by the bees e.g., to seal holes in their honeycombs and protect the hive entrance (Ghisalberti, 1979; Greenaway et al., 1990). The variety and high concentration of phenolic compounds present in propolis extracts is responsible for its antimicrobial properties (Scazzocchio et al., 2006).

Several enzymes, as well as other proteins present in milk and eggs, are known to exhibit antimicrobial activity. Lysozyme is present in both milk and eggs. Lysozyme is active against most Gram-positive bacteria. Gram-negative are usually resistant to lysozyme activity, although susceptibility can be induced following certain

environmental stresses such as treatment with lysozyme in the presence of EDTA (ethylenediaminetetraacetate). Lysozyme offers potential as food preservative, since it is specific for bacterial cell walls and harmless to humans (Beuchat and Golden, 1989). Since these natural compounds occurring in edible and medicinal plants and animal, herbs and spices are of GRAS (Generally Recognized As Safe) status, the safety concern of using them to control foodborne pathogens is minimal.

Nevertheless, the use of these compounds at a commercial level is still limited due to several factors such as impact on sensory attributes, water solubility and volatility. Consequently, there is a need to develop/design delivery systems to overcome these issues. An edible delivery system must perform a number of different roles. First, it serves as a vehicle for carrying the functional ingredient to the desired site of action. Second, it may have to protect the functional ingredient from chemical or biological degradation (e.g., oxidation) during processing, storage, and utilization. Third, it may have to be capable of controlling the release of the functional ingredient, such as the release rate or the specific environmental conditions that trigger release (for example, pH, ionic strength, temperature, or humidity). Fourth, the delivery system has to be compatible with the outer components in the system, as well as being compatible with the physicochemical and qualitative attributes (appearance, texture, taste, and shelf-life) of the final product (Weiss et al., 2006).

Delivery systems may take many forms: liposomes, niosomes, nanoparticles, and microemulsions. Colloidal particles (i.e. nanoparticles) are currently prepared from various materials with different shapes and morphologies. Nowadays the interest in these

systems has been dramatically increased due to fast developing fields like novel materials and drug delivery. Colloidal particles can be made of the material of interest or from a mixture with a suitable matrix in which the material of interest is encapsulated or embedded. Colloidal particles can have different internal structures ranging from crystalline (e.g. nanocrystals, cubosomos) to amorphous (e.g. solid-lipid nanoparticles or polymeric nanoparticles). Colloidal particles can be made with different morphologies, including homogenous spheres, core-shell type particles, and hollow particles (Velikov and Pelan, 2008).

One example of hollow particles would be cyclodextrins (six, seven, or eight-membered cyclic glucose molecules) which are produced from starch by enzymatic process using cyclodextrin glycosyltransferase. Cyclodextrin are hollow truncated cone-shaped molecules having an inner diameter of approximately 5-8 Å, sufficient to hold typically 6-17 molecules of water. Small organic molecules can displace the water from the inner cavity and form thermodynamically stable complexes (binding constant up to 100). The main advantage of the cyclodextrin encapsulation is the unique release characteristics and the thermal and chemical stability imparted to the compounds while entrapped within the cyclodextrin. In aqueous solution there is a dynamic equilibrium between the free and complexed states of the guest compound and cyclodextrin. The payload typically achieved with cyclodextrins is generally 10% w/w, depending on the size and steric conformation of the guest molecule. Usually 1:1 (cyclodextrin : guest) complex is formed although other molar compositions have also been observed in some cases (Gouin, 2004; Hedges et al., 1998).

Synthetic-preformed biodegradable polymers and natural macromolecules have been extensively researched as colloidal materials for nanoparticle production designed for delivery systems. The later have the advantage of high purity and reproducibility over natural polymers. Among them, the polyester family, such as poly(lactic acid) (PLA), poly(β-hydroxybutyrate) (PHB), poly(lactide-*co*-glycolide) (PLGA), and poly(ε-caprolactone) (PCL), which have shown good biocompatibility, biodegradability, and biodegradability properties. Furthermore, the safety of these polymers for human use has been extensively documented during the last three decades, and several drug-delivery systems designed with polyesters have been approved and commercialized (Quintanar-Guerrero et al., 1998).

CHAPTER III

E-BEAM IRRADIATION OF BAGGED, READY-TO-EAT SPINACH LEAVES (*SPINACEA OLERACEA*): AN ENGINEERING APPROACH*

3.1 Overview

We experimentally assessed the efficacy of electron beam irradiation to ensure the safety and quality of ready-to-eat spinach leaves using a 2-MeV Van de Graff accelerator. Spinach leaves (approximately 8 g) inside petri dishes were irradiated up to 1 kGy and stored at 4^{o}C for 15 d. Nonirradiated samples served as controls. Color, texture, vitamin C, total carotenoids, and chlorophyll content were measured using standard methods. Sensory analysis was performed by 15 untrained panelists using a 9-point hedonic scale. Color of control and irradiated samples showed slight variation throughout storage. Firmness of all samples changed significantly ($P < 0.05$) by half the storage time; however, exposure to radiation did not cause significant differences by the end of shelf-life. Irradiation did not affect the chlorophyll and total carotenoid content, though it produced samples with significantly lower ($P< 0.05$) vitamin C content. For all treatments, chlorophyll content decreased by day 15 while total carotenoids remained constant. Although, by the end of refrigerated storage, all the irradiated samples received slightly lower odor scores, sensory analysis revealed that irradiation had little or no effect on the overall quality of spinach leaves. We also simulated the dose distribution

---

* Reprinted with permission from Gomes, C. Moreira, R. Castell-Perez, E. Kim, J.; Da Silva, P. and Castillo, A. E-beam irradiation of bagged, ready-to-eat spinach leaves (Spinacea oleracea): An engineering approach. Journal of Food Science 73 (2):E95-E102. Copyright 2008 by John Wiley and Sons.

within a bag of spinach leaves irradiated using a 10-MeV linear accelerator (0.3 to 1 kGy) to quantify the problem of nonuniform dose absorbed at different parts of the bag and predict death of a pathogen such as *Escherichia coli* O157:H7. The simulation results confirmed that it is feasible to irradiate baby spinach leaves (up to 1 kGy) to eliminate *E. coli* 0157:H7 while maintaining the overall quality of the produce.

3.2 Introduction

The prevention of cross contamination during handling and processing of leafy vegetables has been implemented in the United States with relative success using a set of standardized Good Agricultural Practices (GAPs); however, these efforts have not been sufficient to eliminate the problem once the product is contaminated and while the contamination is undetected by our current monitoring capabilities. In addition, recent studies indicate the potential internalization of pathogenic organisms into the core of fruits and vegetables rather than contamination in the exposed surface only (Hora et al., 2005; Ibarra-Sanchez et al., 2004). This bacterial mobility makes surface treatments to reduce pathogenic presence very ineffective. Most of these commercially used interventions employ chemical agents. In addition to potential detrimental effects on the organoleptic properties of these products, pathogen reduction studies associated with these agents at the laboratory level do not always correlate with the results observed in field applications. Thermal processing of fruits and vegetables is not an option due to significant detrimental effects in quality and organoleptic integrity. Therefore, nonthermal interventions with minimal effects in quality deterioration of produce are the

only alternatives currently available to include as a lethality step in leafy vegetable processing.

Electron beam irradiation has the potential to ensure the safety and quality of whole and fresh-cut fruits and vegetables (Han et al., 2004; Moreno et al., 2006; Moreno et al., 2007a; Moreno et al., 2007b). The main assets of this technology include its high lethality, low quality detrimental effects, unmatched penetration into the product core, cold application, capabilities to be applied in a conveyor belt, and tested safety of the intervention technology (Miller, 2005). A preliminary study on the reduction of *Escherichia coli* O157:H7 on baby spinach by electron beam irradiation using a 10-MeV linear accelerator (LINAC) showed that doses as low as 0.9 kGy reduced the population of different strains of *E. coli* O157:H7 by 5-6 log cycles. At doses of 1.2 kGy or higher, no pathogens were detected in any of the samples. The respiration rate of irradiated spinaches was not different from non-irradiated controls except at 3 kGy. Sensory characteristics such as crispiness or color were not affected by irradiation up to 2 kGy (Castillo, 2006); however, whenever e-beams are used to irradiate a food product, a compromise must be achieved between the quality of the treatment (i.e., decontamination, surface pasteurization) and the radiation dose received by the food. When individual electrons or photons, which are particles mainly used in food irradiation, strike a target, their reactions depend on the geometry and physical properties (e.g., density) of the target (the food). In the case of bagged spinach leaves, although uniform energy from the radiation source is shot to the food, some areas may receive excessive dose while others are underexposed to ionizing radiation. This is due

to the uncertainty encountered in density variations of the surrounding product (the spinach leaf) due to the presence of air pockets and the heterogeneous arrangement of the leaves inside the package. Thus, dose distribution within the bag must be determined to assure proper treatment of the produce.

The objectives of this research were to (1) verify that e-beam irradiation of the produce (up to 1 kGy) does not affect the physicochemical and sensory quality of the food, and (2) obtain dose distribution data within a bag of baby spinach leaves using Monte Carlo simulation techniques to establish the survival distribution of *E. coli* O157:H7 within the bag.

3.3 Materials and Methods

3.3.1 *Produce Quality Study*

Sample preparation: Twenty (20) bags with approximately 170 g of baby spinach (*Spinacia oleracea* L.) were purchased from a local grocery market. The packages were obtained from the same supplier (Fresh Express Inc, Salinas, CA, USA) and day of purchasing. The bags were kept refrigerated (4^{o}C) overnight and irradiated the next day.

Irradiation test: Irradiation of samples was carried out with a Van De Graaff accelerator (2.0 MeV) located at Texas A&M University. Eight (8) gram portions (about 3 leaves) of baby spinach leaves were removed from the original packaging and placed in the center of petri dishes at a thickness of 0.5 cm, which is the penetration depth of the accelerator. A total of 60 petri dishes were irradiated at each dose level (0.3, 0.6, and 1.0 kGy). Leaves that appeared defective (with bruises or stained) were discarded. Irradiation dosage was measured by placing radiochromic film dosimeters (GEX

Corporation, Centennial, CO, USA) at the center of the front and back of the petri dish containing the spinach leaves. After irradiation, the baby spinach leaves were placed in polyethylene bags (Ziploc®) and stored in a cold chamber at 4^{o}C and 90% RH for the entire shelf-life study. Non-irradiated samples served as controls. Quality and sensory attributes of the produce were determined at 1, 7, and 15-day intervals.

3.3.2 ***Produce Quality Attributes***

Color: A Labscan XE (16437) colorimeter (HunterLab, Inc., Reston, VA, USA) with the CIELAB system with measuring aperture diameter of 36 mm, and illuminant/viewing geometry of D65/10^{o} was used. The colorimeter was calibrated using the standard white and black plates. Fifteen baby spinach leaves were used for each treatment (dose) and four readings made on each set of leaves. The mean values were used to determine the color coordinates L* (lightness - darkness), a* (redness - greenness), and b* (yellowness - blueness) (Han et al., 2004).

Texture: Firmness of the spinach leaves at room temperature (21°C) was measured using a Texture Analyzer (TA.XT2i, Texture Technologies Corporation, Scardale, NY, USA) equipped with a Kramer Shear Press with 5 blades (TA-91). Fifteen grams of baby spinach leaves were weighed and placed into the sample holder (internal dimensions 82x 63x 89 mm^{3}) with the stems positioned perpendicular to the path of the blade. A 5 flat-plate plunger (1.5 mm thickness) was forced through the leaves. The probe was set at an initial height of 65 mm from the bottom of the plunger to move at 1.0 mm/s (Han et al., 2004). The Texture Expert software program recorded the maximum force (N) and work

(J) required to shear (cut) the samples. Five measurements were performed for each treatment (irradiated and control).

Moisture content: Measurement of moisture was performed to report results of vitamin C, chlorophylls and carotenoids content on a dry weight basis. Approximately 2 g of samples were dried at 60-65^{o}C ($\leq$ 13.3 kPa) to a constant weight (for about 10-12 h) in a vacuum oven (Squared Lab Line Instruments, Melrose Park, IL, USA) following the AOAC method 930.04 (AOAC, 1990).

Vitamin C analysis: The effect of dose on vitamin C content was evaluated according to AOAC Official Method 985.33 (2,6-Dichloroindophenol titrimetric method (1998)). Seven grams of baby spinach leaves were ground with 25 mL of extracting solution (metaphosphoric acid-acetic acid solution). The homogenate was vacuum-filtered (vacuum pump - KNF Neuberger, USA) with qualitative paper (Whatman No. 4) and 10 mL of the filtered solution was titrated with 2,6-dichloroindophenol standard solution. The volume of titration was recorded and used to quantify vitamin C content of the sample. The indophenol solution was standardized by titrating an ascorbic acid standard solution (1mg/mL) and sample blanks. Vitamin C content was expressed in milligrams of ascorbic acid per g of sample on wet basis. Three repetitions for each treatment and two duplicates for each repetition were performed throughout the shelf-life study.

Total chlorophyll and carotenoids extraction and analysis: The procedure described by Lichtenthaler (1987) was followed. Baby spinach leaves (about 100 grams) were frozen at -80^{o}C, the frozen leaves crushed into small pieces and freeze-dried (Labconco Freeze Dry-5 - Labconco, Kansas City, MO, USA) for 48 hours. Next, the samples were

collected and stored in glass vials, flushed with nitrogen and protected from light. One-hundred mg of the freeze-dried baby spinach leaves were mixed with 10 mL of 80% acetone (v/v) solution and stored in the dark at room temperature. After filtration (paper Whatman No. 4), the filtrate volume was brought up to 25 mL with 80% acetone (v/v). Absorbance was measured at 663.2, 646.8, and 470 nm using a UV-visible spectrophotometer (UV 1601, Shimadzu Scientific Instruments, Inc., USA) and the chlorophyll and carotenoids content determined using the equation given by Lichtenthaler (1987). The analyses were made in triplicate. Results were expressed as percentage (w/w) of total chlorophyll and carotenoids on dry weight basis.

Sensory test: Approximately fifteen students, staff, and faculty at Texas A&M University formed the consumer test panel. Panelists were asked to evaluate the samples by visual inspection of color, odor, texture, and overall quality for days 0, 7, and 15 of storage. Panelists scored the samples using a nine-hedonic scale (Meilgaard et al., 1999), where a score of 1 represented attributes most disliked and a score of 9 represented attributes most liked. Scores higher or equal to 5 were considered acceptable. About 30-g samples from each treatment (three dose levels and the non-irradiated control) were placed in covered glass containers labeled with a random 3-digit number and presented to each panelist at once for a total of 4 samples.

3.3.3 *Statistical Analysis*

Data analysis was performed using SPSS software for Windows, v. 11.5.1 (SPSS, 2002). The effect of radiation dose, length of refrigerated storage (shelf-life) and their interaction were evaluated. Differences between variables were tested for

significance by one-way ANOVA. Significant different means ($p \leq 0.05$) were separated by the Tukey test.

3.3.4 *Experimental Determination of Radiation D_{10} value of* E. coli *O157:H7 in Irradiated Bagged Spinach Leaves*

This parallel study was conducted to experimentally obtain the radiation D_{10} value of a cocktail of 5 strains of *E. coli* O157:H7 inoculated in baby spinach leaves (Castillo, 2006).

Microorganisms and inoculum preparation: The organisms used in this study were obtained from the Texas A&M Food Microbiology laboratory culture collection. For differential purposes, rifampicin-resistant (Rif+) mutants were selected from the parent strains following the procedure described by Kaspar and Tamplin (1993). Their identity was verified prior to use by biochemical and serological tests. Preliminary trials were conducted to ensure that the modified organisms had the same resistance to heat, acid and irradiation, as well as the same growth characteristics, as the parent strains.

The microorganisms were kept frozen in beads with cryoprotective agent (Cryocare, Key Scientific Products, Round Rock, Texas). Before use, the organisms were resuscitated by two consecutive transfers to tryptic soy broth (TSB, Difco, Sparks, MD), incubating at 35°C for 18 hours. To prepare the inoculum, the organisms were grown separately at 35°C in 9 ml of TSB and then the cells were harvested by centrifuging (Centrifuge B4i, Jouan, Winchester, VA) at 1,620 x g in sterile tubes and washing 3 times with equal volume of sterile 0.1% peptone water.

Inoculation and preparation of spinach: Fresh baby spinach leaves were obtained from a major supplier (Fresh Express Inc, Salinas, CA, USA). All leaves showing decay, cuts or bruises were removed and then 10-g portions were dispensed into sterile stomacher bags and inoculated with 1 ml of the cocktail containing *E. coli* O157:H7. The bags then were vigorously shaken manually for 1 min to spread the inoculum over the sample. The stomacher bags then were sealed (Food Saver Vac 800, Tilia Inc., San Francisco, CA) and placed into a second stomacher bag to prevent leaks as per standard procedures of the irradiation facility and transported to the Food Technology Facility for Electron Beam and Space Food Research at Texas A&M University, College Station, Texas. Triplicate bags with inoculated spinach were exposed to no treatment (control) or 0.7, 1.2, or 2.5 kGy electron beam irradiation using a 10-MeV linear accelerator (LINAC) at room temperature in the double beam fixture (top and bottom). Dosimetry was performed using alanine dosimeters (Harwell Dosimeters, UK).

Microbiological analysis: Ninety ml of sterile 0.1% peptone water was added to each treatment bag and subsequent decimal dilutions were made in sterile peptone water and plated onto plates of lactose sulfite phenol red rifampicin (LSPR) agar, which was designed in the laboratory for simultaneous, differential count of Rif+ *E. coli* O157:H7 and *Salmonella* (Castillo et al., 1998).

The radiation D_{10} value was calculated as 0.186 kGy from the slope of the survivors vs. dose plot (Figure 3.1). The next section provides the definition of the radiation D_{10} value and its application in the simulation of survival distribution in a bag of spinach leaves.

3.3.5 *Simulation Studies of Pathogen Survival within a Bag of Baby Spinach Leaves*

The dose distribution within a bag of baby spinach leaves was calculated using the procedure described by Kim et al. (2007). First, a 3-D geometric model of the bagged product was developed using multi-sliced Computer Tomography (CT) data. Then, the product geometry and densities were extracted using image-processing methods. The source energy input spectrum and source size were entered into the Monte Carlo N-Particle radiation transport code (MCNP5) to obtain dose distributions in the bag of spinach leaves irradiated with a 10-MeV (19 kW) LINAC accelerator. The e-beam source was assumed as a parallel plane large enough to cover the target, and the electrons were emitted in a plane and distributed evenly within the scan (Kim et al., 2007).

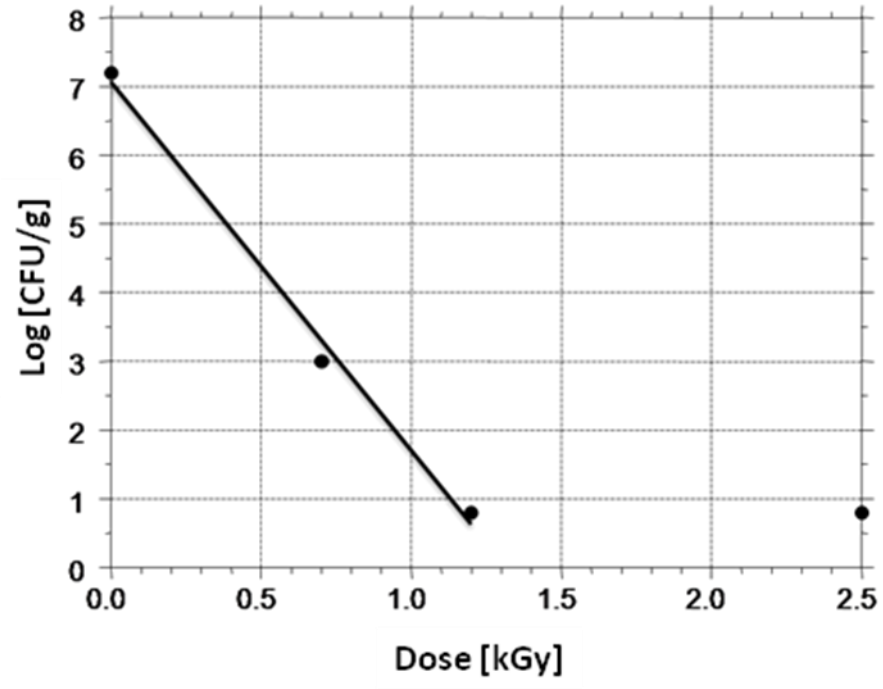

Figure 3.1. Survival curve of a cocktail of *E. coli* O157:H7 in irradiated bagged spinach (10-MeV LINAC at room temperature). Log [CFU/g]=7.07156-5.37615*dose, D_{10} value = 0.186 kGy, R^2 = 0.993.

Using the experimental D_{10} value for *E. coli* O157:H7 of 0.186 kGy, the microbial survival distribution within the bag of spinach was simulated using both the "target theory" approach initially described by Lea (1955) and the single-hit inactivation model to solve the general survival equation (Alpen, 1998), a classical first-order relationship of logarithmic survival on dose. The assumptions for the development of the single-hit inactivation model are: (1) the deposition of energy as ionizing or excitation in the critical volume leads to the production of molecular lesions in the cell and thus inactivation of the microorganisms and, (2) a cell will survive only if it has received no hits at all and that it will always die if it has received one or more hits. Thus, the survival equation for this model was written as:

$$S = \frac{N}{N_o} = e^{-D/D_o} \rightarrow \ln S = -\frac{D}{D_o} \quad [3.1]$$

where D is the dose in [kGy] and D_o the mean lethal dose, defined as the dose required to reduce the survival fraction S to 1/e (i.e., 37%) of the initial value, or 1/k from:

$$N = N_o e^{-kD} \quad [3.2]$$

where N_o is the initial number of undamaged cells (e.g., microorganisms), N is the number of remaining cells after dose D (in kGy), and k is the inactivation constant (1/kGy). At dose D_o the average number of target hits per cell is 1 (Alpen, 1998).

The relationship between D_o and D_{10} was found by comparing Eq. (3.1) to:

$$S = 10^{-D/D_{10}} \rightarrow \log S = -\frac{D}{D_{10}} \quad [3.3]$$

where D_{10} is the decimal reduction time, i.e., the dose required for 90% reduction in the microbial population. By changing the logarithmic base from natural log (Eq. (3.1)) to log10:

$$2.303 \log S = -\frac{D}{D_o} \quad [3.4]$$

$$\log S = -\frac{D}{2.303 D_o} \quad [3.5]$$

By comparison of equations 3.3 and 3.5:

$$D_o = \frac{D_{10}}{2.303} \quad [3.6]$$

with D_{10} = 0.186 kGy, microorganism survival was calculated as:

$$S = e^{-D/D_0} = e_{-D/0.186} = e^{-12.382D} \quad [3.7]$$

3.4 Results and Discussion

3.4.1 *Effect of Electron Beam Irradiation on Quality of Baby Spinach Leaves*

Overall, exposure to ionizing radiation up to 1 kGy did not ($p < 0.05$) affect the color attributes of the spinach leaves (Table 3.1); however, after seven days of storage, the samples radiated at 1 kGy showed significantly higher b* values (more yellowish) than the rest of the samples (Figure 3.2). All irradiated samples had lower a* values by day 1 and the trend continued throughout storage, indicating a decrease in greenness during storage; however, the final a* values were not significantly different from the irradiated controls by day 15 (Table 3.1). This finding may be associated with the decrease in the content of chlorophylls. These color differences were not found significant by the sensory panelists (Table 3.2).

Table 3.1. Color values of control and irradiated baby spinach leaves stored for 15 days at 4°C and 90% R.H.

	L*			
Day/Dose [kGy]	**0.0 ***	**0.3**	**0.6**	**1.0**
1	$_{w}$ 34.47 ^{a} (0.63)	$_{w}$ 34.44 ^{a} (0.83)	$_{x}$ 35.88 ^{a} (0.50)	$_{w, x}$ 35.45 ^{a} (0.89)
7	$_{w}$ 34.66 ^{a} (0.37)	$_{w}$ 34.83 ^{a} (1.78)	$_{w, x}$ 36.33 ^{a} (1.74)	$_{x}$ 37.77 ^{a} (1.13)
15	$_{w}$ 36.24 ^{b} (1.11)	$_{w}$ 36.95 ^{a} (2.64)	$_{w}$ 37.35 ^{a} (0.79)	$_{w}$ 37.54 ^{a} (3.84)
	a*			
Day/Dose [kGy]	**0.0***	**0.3**	**0.6**	**1.0**
1	$_{w}$ -8.65 ^{a} (0.33)	$_{w}$ -8.38 ^{b} (0.26)	$_{w}$ -8.60 ^{a} (0.44)	$_{w}$ -8.39 ^{b} (0.42)
7	$_{w}$ -8.72 ^{a} (0.09)	$_{w}$ -8.77 ^{b} (0.25)	$_{w}$ -9.01 ^{a} (0.47)	$_{w}$ -9.21 ^{a} (0.25)
15	$_{w}$ -8.99 ^{a} (0.20)	$_{w}$ -9.22 ^{a} (0.27)	$_{w}$ -9.18 ^{a} (0.30)	$_{w}$ -9.18 ^{a} (0.24)
	b*			
Day/Dose [kGy]	**0.0***	**0.3**	**0.6**	**1.0**
1	$_{w}$ 19.69 ^{a} (0.99)	$_{w}$ 18.98 ^{a} (0.73)	$_{w}$ 20.11 ^{a} (0.98)	$_{w}$ 19.05 ^{a} (1.49)
7	$_{w}$ 20.14 ^{a} (0.68)	$_{w}$ 20.44 ^{a} (1.77)	$_{w, x}$ 22.32 $^{a, b}$ (1.44)	$_{x}$ 23.69 ^{b} (1.33)
15	$_{w}$ 22.41 ^{b} (0.89)	$_{w}$ 23.95 ^{b} (2.49)	$_{w}$ 24.29 ^{b} (1.86)	$_{w}$ 23.69 ^{b} (1.65)

*Non-irradiated samples.

^{a,b}Means within a column, which are not followed by a common superscript letter are significantly different ($p < 0.05$). $_{w,x}$Means within a row, which are not preceded by a common superscript letter, are significantly different ($p < 0.05$).

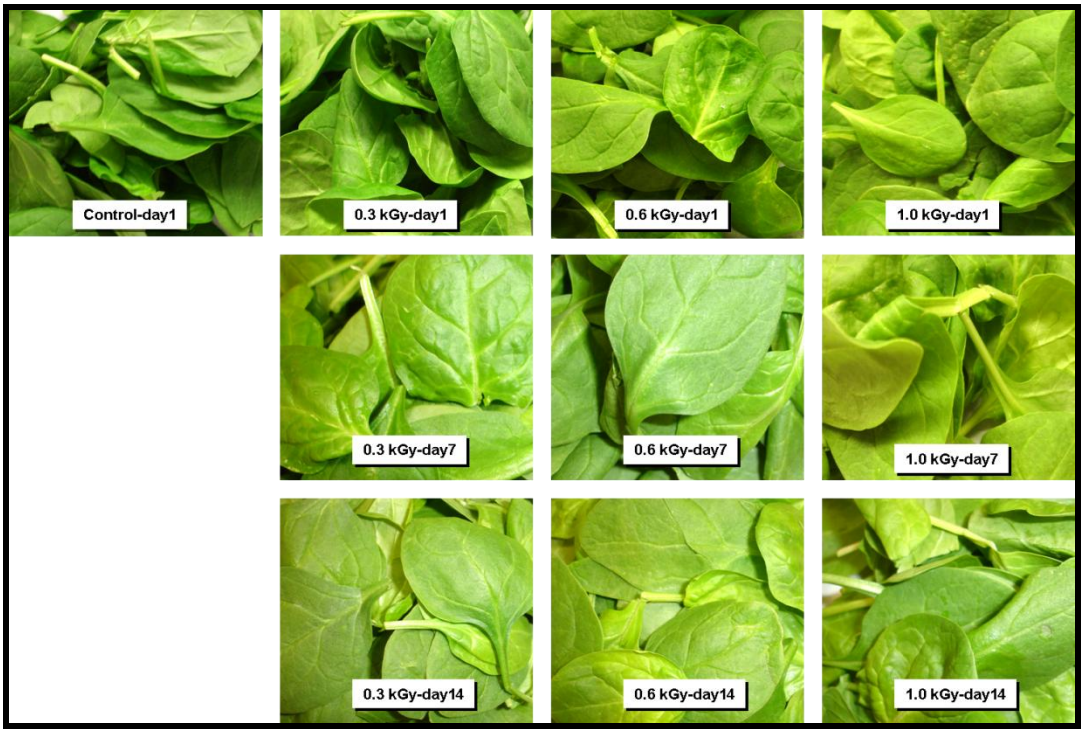

Figure 3.2. Effect of dose and storage (days) on overall appearance of baby spinach leaves stored for 15 days at 4^{o}C and 90% R.H.

Irradiation had some effect on the force required to cut the spinach leaves (Table 3.3). For all samples, the leaves were significantly ($p > 0.05$) harder (higher value of force needed for shearing the leaf) by day 7 of storage and softer by day 15. This effect was dose-independent since the control samples showed the same trend. Exactly the same was found for the work to shear the leaves. The production of lignin and suberin in cells adjacent to damaged tissues prevents water loss (Jacobsson et al., 2004; Rittinger et al., 1987). This might contribute to the hardening of the spinach tissue during wound healing, in accordance with observations made on asparagus, potatoes and other fresh produce (Jacobsson et al., 2004; Lipton, 1990; Thomson et al., 1995); however, by the end of the shelf-life study, all samples had similar values of force and work. These

results are similar to the findings of Jacobsson et al. (2004) who observed an increase in the cutting energy for broccoli stored at 4^{o}C in four different packaging materials after different storage times. These texture differences were not found significant by the sensory panelists (Table 3.2).

The consumer panel found all the irradiated samples acceptable with scores higher than 5 for color, texture, and overall quality (Table 3.2). By the end of storage, slightly lower odor ratings were given to all the irradiated spinach samples, with several panelists noticing a "different" odor compared to the non-irradiated controls.

Irradiation did not affect the chlorophyll and total carotenoids content significantly ($p > 0.05$) (Fig. 3.3 and Fig. 3.4), but it yielded samples with lower ($p < 0.05$) vitamin C content (Fig. 3.5). This decrease in vitamin C concentration during storage is in agreement with previous studies of spinach under different storage conditions (Bergquist et al., 2006; Favell, 1998; Hodges and Forney, 2003; Izumi and Muraoka, 1997; Watada et al., 1987); however, by the end of the shelf-life study, all samples had similar values of vitamin C content.

For all treatments, total chlorophyll content decreased by the end of storage. Loss of green color is the most important problem during the postharvest life of spinach, since yellowing reduces the quality of the product (Burton, 1982).

Table 3.2. Sensory scores for control and irradiated baby spinach leaves stored for 15 days at 4°C and 90% R.H.

	Color			
Day/Dose (kGy)	**0.0***	**0.3**	**0.6**	**1.0**
1	$_{w}$ 7.69 ^{a}	$_{w}$ 7.75 ^{a}	$_{w}$ 7.92 ^{a}	$_{w}$ 7.00 ^{a}
	(0.95)	(0.97)	(0.86)	(1.68)
7	$_{w}$ 8.00 ^{a}	$_{w}$ 7.64 ^{a}	$_{w}$ 8.00 ^{a}	$_{w}$ 7.00 ^{a}
	(1.05)	(1.75)	(1.26)	(0.67)
15	$_{w}$ 7.82 ^{a}	$_{w}$ 6.55 ^{a}	$_{w}$ 6.91 ^{a}	$_{w}$ 7.27 ^{a}
	(0.87)	(2.07)	(1.38)	(1.27)
	Odor			
Day/Dose [kGy]	**0.0***	**0.3**	**0.6**	**1.0**
1	$_{w}$ 7.23 ^{a} (1.24)	$_{w}$ 7.50 ^{b} (1.17)	$_{w}$ 7.67 ^{b} (1.23)	$_{w}$ 7.23 ^{b} (1.54)
7	$_{w}$ 7.09 ^{a} (1.58)	$_{w}$ 6.82 $^{a, b}$ (1.99)	$_{w}$ 6.82 $^{a, b}$ (1.54)	$_{w}$ 5.55 $^{a, b}$ (1.81)
15	$_{w}$ 5.73 ^{a} (1.90)	$_{w}$ 5.00 ^{a} (2.79)	$_{w}$ 4.91 ^{a} (2.74)	$_{w}$ 5.00 ^{a} (2.45)
	Texture			
Day/Dose [kGy]	**0.0***	**0.3**	**0.6**	**1.0**
1	$_{w}$ 7.12 ^{a} (1.58)	$_{w}$ 7.33 ^{a} (0.78)	$_{w}$ 7.77 ^{a} (1.01)	$_{w}$ 7.08 ^{a} (1.55)
7	$_{w, x}$ 7.64 ^{a} (1.03)	$_{w, x}$ 7.27 ^{a} (0.90)	$_{x}$ 7.80 ^{a} (0.79)	$_{w}$ 6.36 ^{a} (1.63)
15	$_{w}$ 7.73 ^{a} (1.01)	$_{w}$ 7.00 ^{a} (1.61)	$_{w}$ 7.80 ^{a} (0.92)	$_{w}$ 6.82 ^{a} (1.66)
	Overall Quality			
Day/Dose [kGy]	**0.0***	**0.3**	**0.6**	**1.0**
1	$_{w}$ 7.33 ^{a} (1.07)	$_{w}$ 7.67 ^{a} (0.89)	$_{w}$ 7.77 ^{a} (0.93)	$_{w}$ 7.50 ^{a} (1.09)
7	$_{x}$ 7.64 ^{a} (1.21)	$_{w, x}$ 7.36 ^{a} (1.36)	$_{x}$ 7.64 ^{a} (1.36)	$_{w}$ 6.00 ^{a} (1.55)
15	$_{w}$ 7.50 ^{a} (1.08)	$_{w}$ 6.09 ^{a} (2.30)	$_{w}$ 6.27 ^{a} (2.57)	$_{w}$ 6.55 ^{a} (1.92)

*Non-irradiated samples. All analyses were made in SPSS, SNK procedure 95% confidence. Means are values of at least 3 replications for each treatment. $^{a\text{-}c}$Means within a column (storage day) which are not followed by a common superscript letter are significantly different ($p \leq 0.05$). $^{w\text{-}z}$Means within a row (dose treatment) which are not preceded by a common superscript letter are significantly different ($p \leq 0.05$). A score of 1 = dislike extremely, 5 = neither like nor dislike and 9 = like extremely.

Table 3.3. Texture characteristics (force and work to shear) of control and irradiated baby spinach leaves stored for 15 days at 4°C and 90% R.H.

	Force [N]			
Day/Dose [kGy]	**0.0 ***	**0.3**	**0.6**	**1.0**
1	$_{w}$ 3524.61 ^{a} (412.18)	$_{w}$ 2927.72 ^{a} (58.25)	$_{w}$ 3194.50 ^{a} (325.63)	$_{w}$ 2962.34 ^{a} (376.44)
7	$_{w}$ 4817.93 ^{b} (431.65)	$_{w}$ 5033.02 ^{b} (146.65)	$_{w}$ 4752.83 ^{b} (640.10)	$_{w}$ 4128.08 ^{b} (840.87)
15	$_{w}$ 3059.01 ^{a} (173.53)	$_{w}$ 3182.86 ^{a} (235.50)	$_{w}$ 3239.61 ^{a} (658.44)	$_{w}$ 3112.91 ^{a} (200.14)
	Work [N.m]			
Day/Dose [kGy]	**0.0***	**0.3**	**0.6**	**1.0**
1	$_{x}$ 43.31 ^{b} (1.30)	$_{w}$ 36.39 ^{a} (1.84)	$_{w, x}$ 41.17 ^{a} (2.55)	$_{w}$ 35.95 ^{a} (4.85)
7	$_{w}$ 66.25 ^{c} (6.19)	$_{w}$ 71.93 ^{b} (3.63)	$_{w}$ 68.58 ^{b} (11.18)	$_{w}$ 58.06 ^{b} (11.97)
15	$_{w}$ 35.77 ^{a} (1.98)	$_{w}$ 39.23 ^{a} (4.38)	$_{w}$ 38.55 ^{a} (5.58)	$_{w}$ 35.58 ^{a} (2.37)

*Non-irradiated samples. ^{a,b}Means within a row, which are not followed by a common superscript letter are significantly different ($p < 0.05$). $_{w,x}$Means within a column, which are not preceded by a common superscript letter, are significantly different ($p < 0.05$).

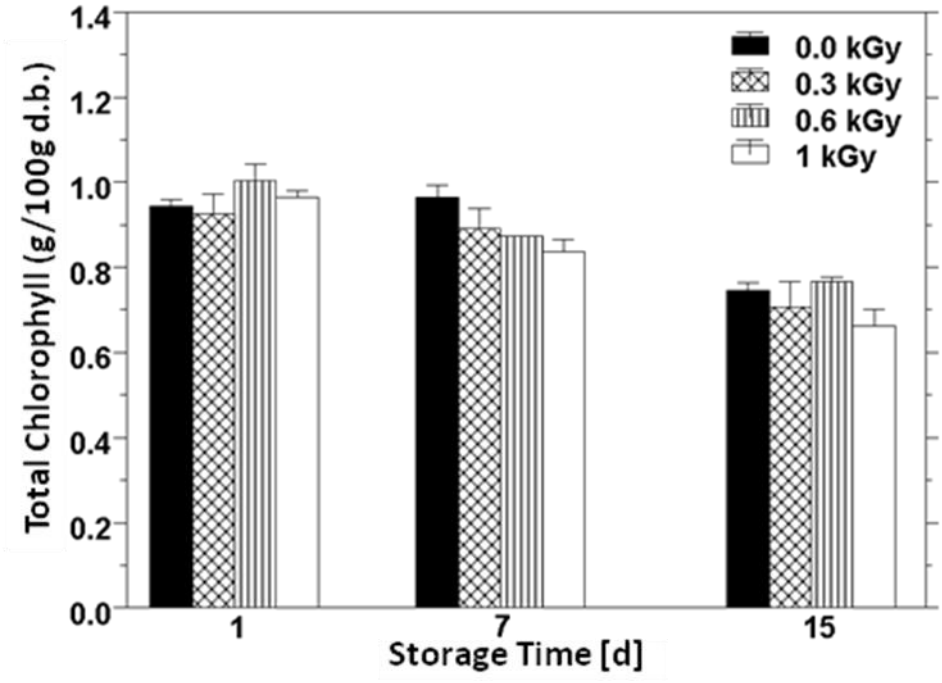

Figure 3.3. Effect of dose and storage (days) on total chlorophyll (g/100 g d.b.) of baby spinach leaves stored for 15 days at 4^{o}C and 90% R.H.

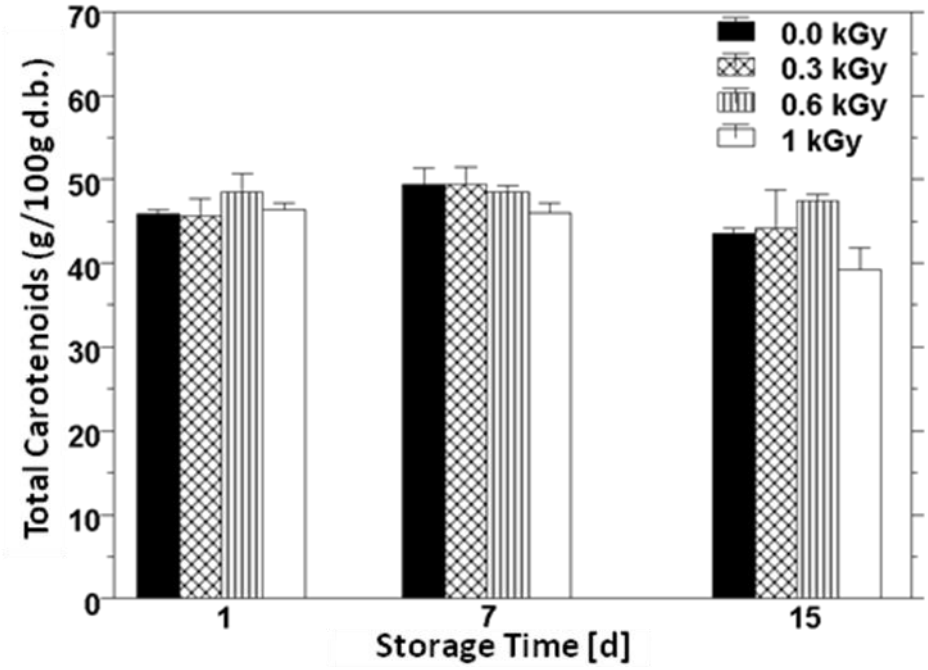

Figure 3.4. Effect of dose and storage (days) on total carotenoids (g/100 g d.b.) of baby spinach leaves stored for 15 days at 4^{o}C and 90% R.H.

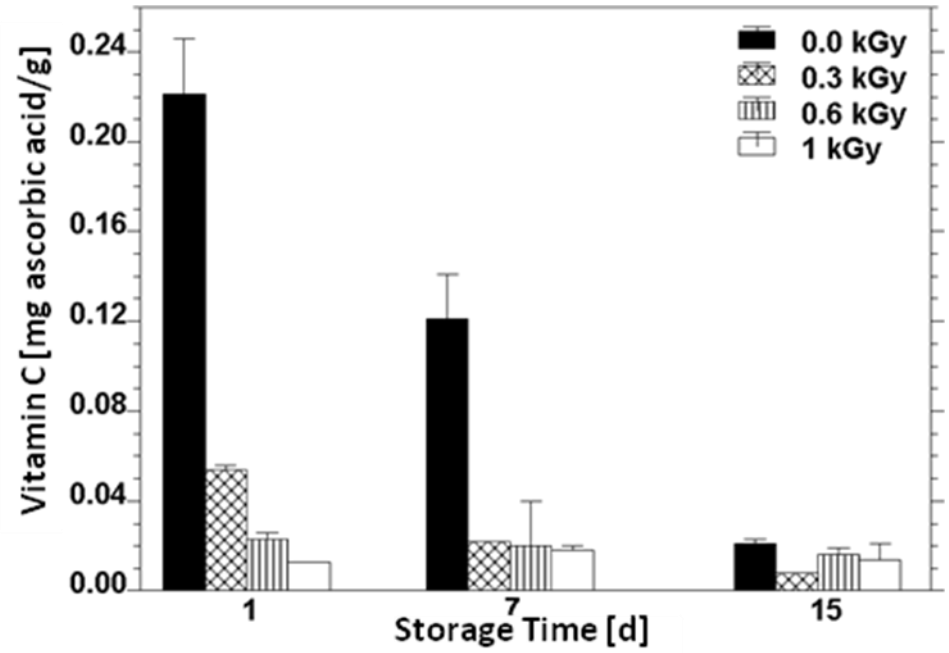

Figure 3.5. Effect of dose and storage (days) on total vitamin C content (mg ascorbic acid/g d.b.) of baby spinach leaves stored for 15 days at 4^{o}C and 90% R.H.

3.4.2 *Dose Distribution and Microbial Survival within a Bag of Baby Spinach Leaves*

A spinach leaf consists of four parts (Fig 3.6a): the blade (lamina), vein, midrib, and leafstalk. The blade and vein are mostly water and their densities very low (~0.96-0.98 g/cm^3). A midrib is a big line dividing the leaf in two, and a leafstalk is a part of the leaf, attached to the stem. The densities were relatively higher (~1.04 to 1.06 g/cm^3). Figure 3.6b shows these density differences due to spinach composition, including the presence of air pockets around the leaves. The density of the polyethylene bag was around 0.80-0.90 g/cm^3. These density differences and the fact that the leaves are loosely packed with air spaces randomly distributed inside the bag, make the dose distribution in spinach leaves non-uniform and difficult to predict.

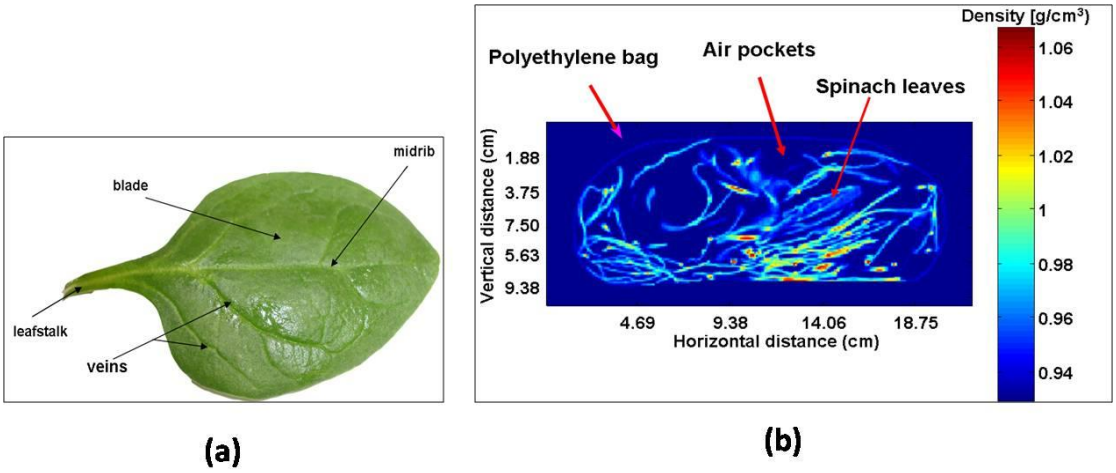

Figure 3.6. (a) A leaf of baby spinach; (b) Density distribution within a bag of spinach leaves using CT data.

Figure 3.7a shows the simulated dose distribution within a bag of spinach leaves using 10- MeV electrons in the single-beam fixture (bags irradiated using the top-beam source only) at an entrance dose of 0.5 kGy. The minimum dose the spinach leaves received was 0.02 kGy, close to the bottom of the bag, which is at a distance of 8 cm from the beam entrance. The upper half of the bag received between 0.3 and 0.6 kGy while the lower half received between 0.02 and 0.3 kGy (blue regions in Fig. 3.7a), which confirmed the non-uniformity of dose within the bag observed at the tightly packed side of the bag (0.02 kGy). Thus, electrons lost less kinetic energy while they passed through air gaps.

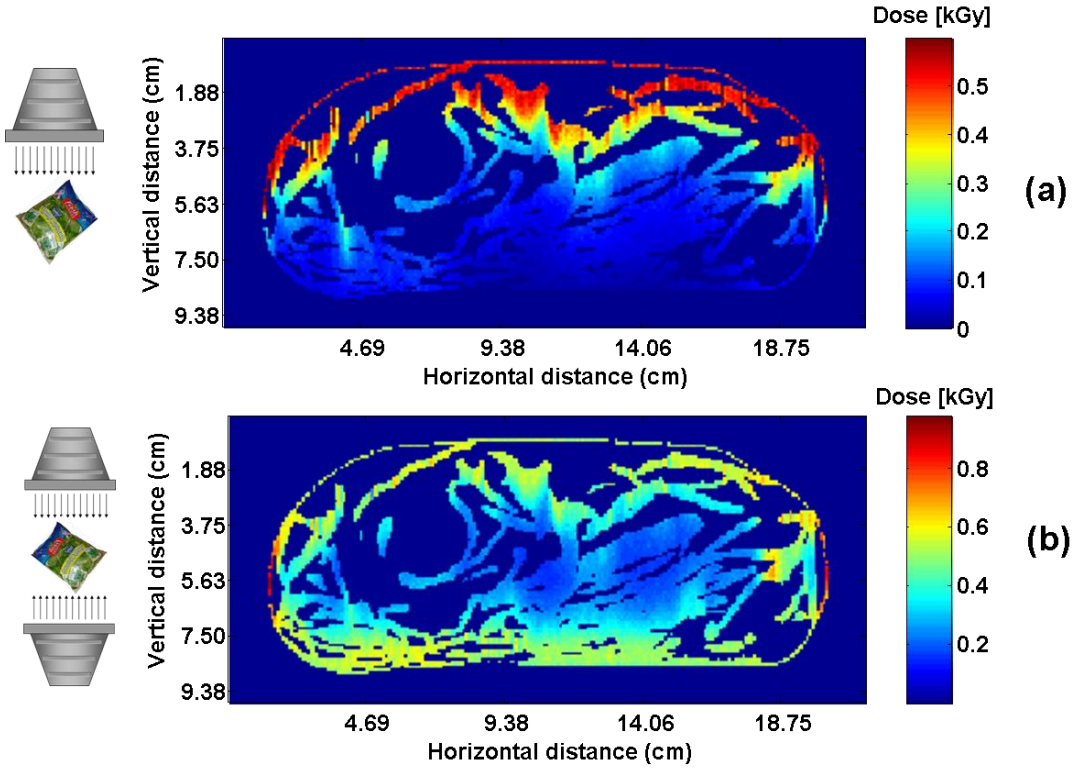

Figure 3.7. Simulated dose distribution within a bag of baby spinach leaves (a) single-top-beam configuration, 10-MeV, entrance dose 0.5 kGy; (b) double-beam configuration, 10- MeV, entrance dose 0.5 kGy/beam.

Two horizontal points were chosen, 6.56 and 14.10 cm (Fig. 3.8a), to compare the depth-dose curve along the vertical direction. Doses along the horizontal point, 14.10 cm, represented the section of the bag where the leaves are tightly packed. Although some air gaps were present inside the bag, the overall electron depth-dose curve followed the typical behavior, with entrance, peak, and exit doses of 0.5, 0.55, and 0.02 kGy, respectively. At the 6.56-cm horizontal point, where the leaves were more loosely packed (with more air gaps) the overall electron depth-dose curve trend was still the same. Absorbed doses, therefore, are determined by the total effects of all scattering electrons. The exit dose in this case was 0.1 kGy, higher than the value observed at the

tightly packed side of the bag (0.02 kGy). Thus, electrons lost less kinetic energy while they passed through air gaps.

The double-beam fixture has been shown to improve dose uniformity in food products (Molins, 2001), including complex-shaped foods (Kim et al., 2007). Our simulation study using both the top and bottom beams with 0.5 kGy entrance dose (Fig. 3.7b) showed that dose values at the center of the spinach bag were considerably lower (0.2-0.4 kGy) than the values at the edges of the bag (0.4-0.6 kGy). These results illustrate, for this entrance dose, the phenomena of double-beam electron scattering at the bag edges, which caused higher energy absorption at the edges compared to the center of the bag.

The dose distribution at the vertical point of 5.63 cm (Fig. 3.8b) illustrates how different parts of the bag receive different doses. At the denser region (tightly-packed), the dose distribution was lower than at the loosely-packed region. The area around each side (at the central line); however, received relatively high doses. These results indicate that specific placement of the spinach leaves inside the bag (or a better package design) would improve the dose distribution. For instance, by placing more spinach leaves around the sides than at the center of the bag, the dose would be more uniformly distributed within the bag.

In this study, all simulations were based on a bag height of 8 cm resulting in wide energy distribution from the top to the center of the bag; however, compared to the single beam exposure (Fig. 3.7a), the uniformity of the dose distribution along the vertical direction with the double beam fixture improved significantly (Fig. 3.8c and d).

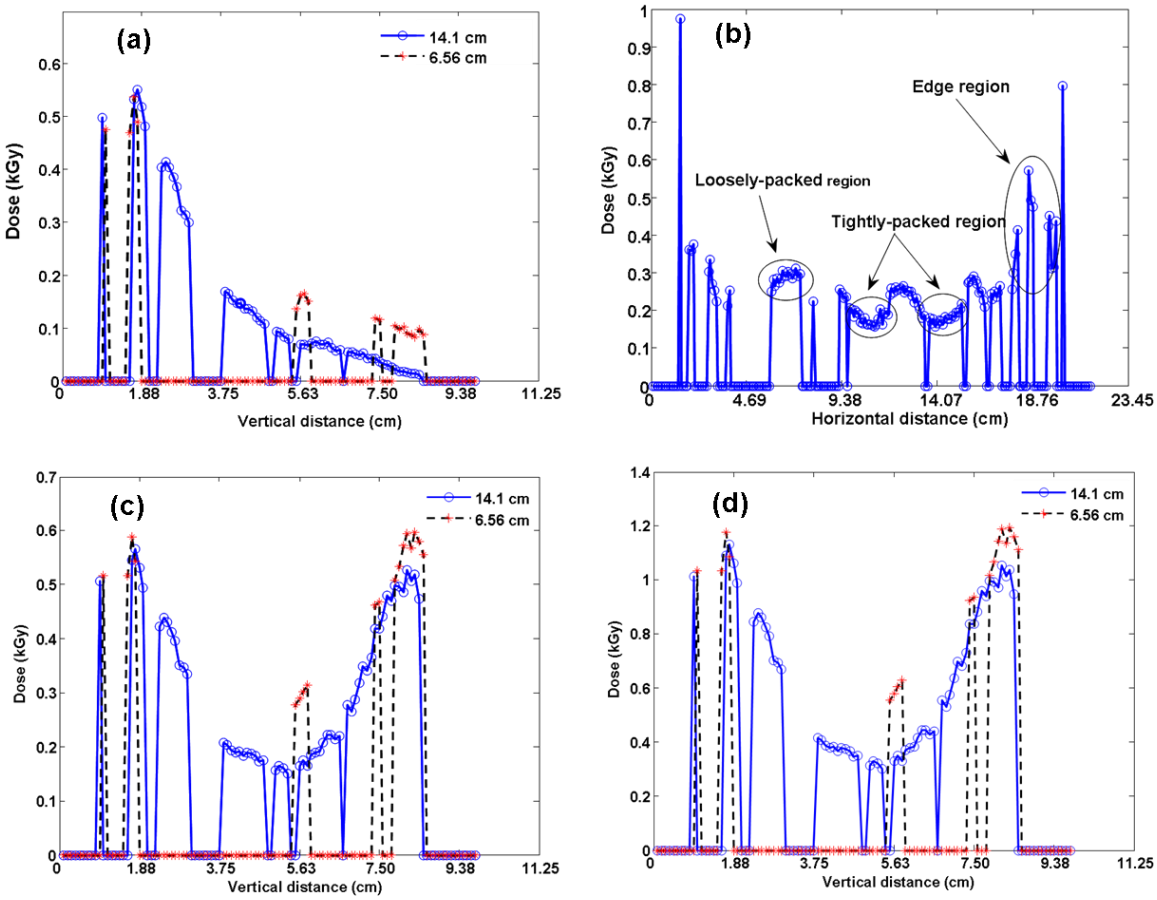

Figure 3.8. Spinach dose data (a) along the vertical direction at the horizontal points (6.56 and 14.1 cm) with single (top) beam direction, entrance dose = 0.5 kGy; (b) along the horizontal direction in the vertical point of 5.63 cm with double (top and bottom) beam direction , entrance dose for each beam = 0.5 kGy ; (c) along the vertical direction at the horizontal points (6.56 and 14.1 cm) with double beam direction, entrance dose for each beam = 0.5 kGy; (d) along the vertical direction at the horizontal points (6.56 and 14.1 cm) with double beam direction, the entrance dose for each beam = 1 kGy.

Doses at the horizontal distances of 14.10 and 6.56 cm varied from 0.2 to 0.6 kGy and 0.3 to 0.6 kGy, respectively, compared to the single beam fixture (0.02 to 0.5 kGy and 0.1 to 0.5 kGy, respectively).

These results indicate that due to the bag configuration, higher entrance dose would be required to destroy the pathogens within the leaves. The simulated dose distribution within a bag of spinach leaves treated with a 10-MeV double-beam for an entrance dose of 1 kGy for both top and bottom beam sources (Figure 3.9a), provided the input for the simulation of *E. coli* survival distribution inside the bag using the D_{10} value of 0.186 kGy and Eq. (3.7). The dose uniformity ratio (D_{max}/D_{min}) values were 3 and 2 at 14.1 and 6.56 cm horizontal distances (Fig.3.8d), respectively, well within the commercial value. The maximum dose obtained at the centerline edges was 2 kGy. The level of pathogen inactivation was dependent on the dose applied, with 99% (2-logs reduction) on most areas and 99.999% (5-logs reduction) on both centerline edges of the bag. This result illustrates that, when conducted properly, e-beam treatment effectively eliminates internalized *E. coli* O157:H7 cells from spinach leaves.

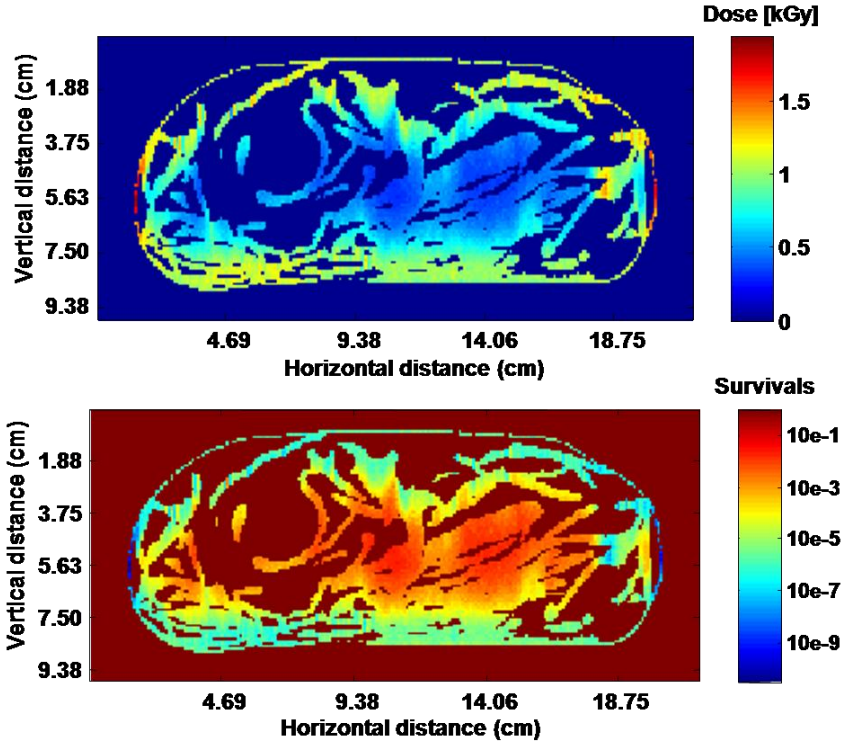

Figure 3.9. (a) Simulated dose distribution within a bag of spinach leaves: double-beam, 10-MeV, entrance dose 1.0 kGy/beam; (b) Simulated microbial (*E. coli* O157:H7) survival distribution within a bag of spinach leaves: double beam, 10-MeV, entrance dose 1.0 kGy/beam.

3.5 Conclusions

A suitable irradiation process can be designed for effective decontamination of bagged, ready-to-eat baby spinach leaves. Treatment with up to 1 kGy did not cause significant changes in produce quality. This study showed that when using a 10-MeV linear accelerator, the uniformity of dose distribution in a bag of spinach leaves depends on the arrangement of the leaves inside the bag (relative to the direction of the electron beam). Thus, treatment of leafy vegetables with a 10-MeV LINAC requires a well controlled operating process as well as package design and positioning to ensure

reduction of a population of a particular pathogen to the desired level using the lowest dose possible without detriment to produce quality.

CHAPTER IV

UNDERSTANDING *E. COLI* INTERNALIZATION IN LETTUCE LEAVES FOR OPTIMIZATION OF IRRADIATION TREATMENT*

4.1 Overview

Irradiation penetrates food tissues and effectively reduces the number of food microorganisms in fresh produce, but the efficacy of the process against internalized bacteria is unknown. The objective of this study was to understand the mechanisms of pathogen colonization of plants relative to lettuce leaf structures so that radiation treatment of fresh leafy vegetables can be optimized. Leaves of iceberg, Boston, green leaf, and red leaf lettuces were cut into pieces, submerged in a cocktail mixture of two isolates of *Escherichia coli* (Rifampicin resistant), and subjected to a vacuum perfusion process to force the bacterial cells into the intercellular spaces in the leaves. Sixty bags containing 20g of lettuce each were tested. The inoculated leaves were gamma irradiated (lanthanum-140, 0.16 kGy/hr) at 0.25-1.0-kGy (surface dose values), with increments of 0.25 kGy at 15^{o}C. Microbial analysis was performed right after irradiation, including non-irradiated leaf pieces (controls). A dose uniformity ratio (max/min dose) of 2.8 was set to confirm the effect of non-uniform dose distribution. Calculated D_{10}-values varied between 48-62% based on the dose distribution from the entrance dose. However, despite the subtle differences in composition and structure among the four lettuce

---

varieties, the D_{10}-values were not significantly different. Irradiation up to 1.0-kGy resulted in 3-4-log reduction of internalized *E. coli* on the lettuce leaves. The SEM images suggest that the contamination sites of pathogens in leafy vegetables are mainly localized on crevices and into the stomata. This study shows that irradiation effectively reduces viable *E. coli* cells internalized in lettuce, and decontamination is not influenced by lettuce variety. Ionizing irradiation effectively reduced the population of internalized pathogen in a dose-dependent manner and could be used as an effective killing step to mitigate the risk of foodborne disease outbreaks.

4.2 Introduction

There has been an increase in the number of foodborne illnesses linked to the consumption of fresh and minimally processed fruits and vegetables (Beuchat, 2002; Sivapalasingam et al., 2004; Tauxe et al., 1997). In 2006, pre-bagged baby spinach contaminated with *Escherichia coli* O157:H7 caused 199 illnesses and three deaths across 26 U.S. states and one Canadian province ((USFDA), 2006). *Escherichia coli* O157:H7 is clearly a public health concern since it is the second most important causal agent of outbreaks from fresh produce (Sivapalasingam et al., 2004).

The pathogen's low infective dose of < 10 CFU ingested and high risk of complications are cause for concern since it can cause hemolytic uremic syndrome and lead to death, particularly in children, the elderly, and the immune-compromised (Armstrong et al., 1996; Rangel et al., 2005; Willshaw et al., 1994). Therefore, actions are required to reduce its prevalence and levels in fresh produce. Furthermore, there are a number of ways in which the pathogen internalizes into produce tissues. Internalization

of bacterial pathogens into the edible portions of plants is of particular concern as these microorganisms are unlikely to be removed by washing or surface sanitization methods ((USFDA), 1999; Jablasone et al., 2005).

The production practices of leafy vegetables commonly include sanitation using tap water containing 100 to 200 ppm of free chlorine (Beuchat, 1998). Surface-sanitizing agents have shown to be ineffective in reducing *E. coli* O157:H7 cells from leafy tissue surfaces (Beuchat, 1999). The problem is that these pathogens may penetrate into the stomata and junction zones of cut leaves, which protect them from surface disinfectants (Seo, 1999). To achieve further reduction of viable cells at these open sites, it is necessary to develop alternative decontamination methods with better penetration ability and stability than chlorination.

Irradiation is a non-thermal treatment that has the ability to effectively eliminate internalized bacteria from different produces. The value of ionizing radiation has been clearly demonstrated with a variety of foodstuffs and pathogenic bacteria including *Salmonella, Listeria monocytogenes, E. coli*, and *Yersinia enterocolitica* (Farkas, 1987). In 2008, the U. S. Food and Drug Administration ((USFDA), 2008b) published a final rule that allows the use of irradiation to make fresh iceberg lettuce and fresh spinach safer and last longer without spoiling, which reinforces the need to understanding of irradiation processing in order to make it more efficient. Radiation treatment causes practically no temperature rise in the product, keeping product freshness and making it ideal for fresh fruits and vegetables processing. The technology can be applied through any type of packaging materials, thus avoiding recontamination (Farkas, 1997).

One challenge is that the mechanisms by which the pathogen is introduced into the leaf are not fully understood. Despite a wealth of information on the interaction of enteric pathogens with their human and animal hosts, acquisition of fundamental knowledge about their behavior on plants has just begun. Attachment and penetration of *E. coli* O157:H7 varies depending on the food type and the cut surface. This variation in attachment to different foods and the different depths of penetration indicate that data obtained for one food cannot be extrapolated to another (Auty et al., 2005). Even small differences among types of produces, such as varietal differences (stomatal distribution and size) could significantly influence the mechanisms of internalization (Huang, 1986; McLean, 1921).

Scanning electron microscopy (SEM) has been used to produce high-resolution images of leafy vegetables, revealing details about 1 to 5 nm in size such as the stomata in leaf surfaces. This imaging technique can also provide detailed three-dimensional non-destructive visualization of pathogens relative to plant structures with magnifications up to 200,000x (Bozzola and Russell, 1999). Therefore, the objectives of this study were: (1) to verify the radiation sensitivity of internalized *E. coli* cells in lettuce leaves; (2) to determine the effect of lettuce variety on the efficacy of the irradiation treatment; and (3) to understand the mechanisms of pathogen colonization of plants relative to lettuce leaf structures using microscopy.

4.3 Materials and Methods

4.3.1 *Determination of Radiation D_{10}-values*

Microorganisms: All isolates utilized in this study were obtained from Dr. Alejandro Castillo's (Department of Animal Science, Texas A&M University) culture collection. For this challenge study, two strains of *E. coli* were used. For differential purposes, Rifampicin-resistant (Rif^{+}) mutants were selected from the parent strains following the procedure described by Kaspar and Tamplin (1993). Preliminary trials were conducted to ensure that the modified organisms had the same resistance to heat, acid, and irradiation, as well as the same growth characteristics, as the parent strains.

The microorganisms were kept frozen in beads with 1% glycerol (cryoprotective agent). Before use, the organisms were resuscitated by 2 consecutive transfers to tryptic soy broth (TSB, Difco, Sparks, MD, U.S.A.), incubating at 37^{o}C for 18h. The cell concentration of these individual cultures was approximately 10^{9} CFU/mL, as determined by serial dilution and plate count on tryptic soy agar (TSA – Difco, Sparks, MD., U.S.A.) with RIF^{+} (100μg/mL) incubated overnight at 37^{o}C.

Produce: Whole heads (7 heads for each variety) of iceberg (*Lactuca sativa* var. *capitata*), Boston (*Lactuca sativa* var. *capitata*), green leaf (*Lactuca sativa* var. *crispa*), and red leaf (*Lactuca sativa* var. *crispa*) lettuce were purchased from local markets and stored at 4^{o}C. Each lettuce variety was evaluated separately. All leaves showing decay, cuts, or bruises were removed and then the basal portion of the head was removed, approximately 5 cm from the end. Leaves from each head were sliced into pieces of ~5 cm^{2} and mixed altogether to get a homogenous material.

Inoculation: The leaves were inoculated using vacuum perfusion (Niemira, 2008), a method which irrigates the intercellular spaces without damaging the cell walls. The description below follows the method of Niemira (2007) with slightly changes. Briefly, sterile Butterfield's phosphate buffer (BPB, 4050 mL) was placed into sterile glass vacuum desiccators (250 mm I.D. x 325 mm H, approximately 10 L capacity) inside a biological safety cabinet. The two *E. coli* cultures (225 mL each) were combined with the BPB to make a 1:10 diluted cocktail inoculum (final volume 4500 mL). Four hundred and fifty grams (450g) of lettuce pieces were added to the desiccator and gently submerged with a fry skimmer; also a sterilized plate was used to keep the leaves submerged during perfusion. Two 0.1 μm filters (VACU-GUARD, Whatman, Florham Park, NJ, U.S.A.) were placed in the vacuum line between the desiccator and the vacuum pump (KNF Neuberger, Trenton, NJ, U.S.A.) and also at the pump outlet to prevent contamination of the vacuum system (operating at 28 in-Hg (50 Torr)).

Vacuum was drawn on the system for 5 min to pull gas from the intercellular spaces of the leaf pieces. After 5 min, the vacuum was broken by quickly opening the vacuum desiccator to the atmosphere, thereby pulling the inoculums into the leaf pieces. The vacuum perfusion process was repeated 3 times (30 min total) to fully perfuse the leaf pieces. Next, the fully perfused leaves were removed from the inoculums bath and spun to visible dryness in a salad spinner (Oxo Intl., New York, NY, U.S.A) inside the biological safety cabinet, typically with 5 to 6 cycles. The spun-dried fully perfused leaves were weighed into 20 g samples and placed inside quart size Zip-loc® bags (17.7 x 195 cm, polyethylene) for irradiation treatment (described below). For each batch of

perfusion run, the weight of the lettuce leaves prior to and after perfusion was recorded to measure the water intake for each lettuce variety.

The relative counts for each strain was 1.9 x 10^8 cfu i.e., a total of approximately 8.8 logs/ml of *E. coli* in the perfusion water. Based on the water intake, it was possible to calculate the amount of inoculums infused to the lettuce leaf. The lettuce leaves pieces took up from 45 to 51% of their normal weight during perfusion process. Based on the water intake, that was obtained by weighting the lettuce leaves before and after the perfusion was completed, and on the amount of inoculums present in the water perfused. Based on that and later on the counts for the control samples, the lettuce leaf had approximately 7 logs of microorganisms per gram of lettuce leaf.

Irradiation: The inoculated leaf pieces were bagged in 20-g samples as described above and treated with 0.25, 0.50, 0.75, and 1.0 kGy, the maximum recommended by the FDA ((USFDA), 2008b) for treatment of lettuce. In all cases, the irradiation was conducted at 15^{o}C. As with the non-irradiated controls, each irradiation treatment was performed with 3 replications. The samples were irradiated using a lanthanum oxide plate (1 m^2). The gamma ray emitter (lanthanum-140) was produced by bombarding the La plate with neutrons. The gamma ray had a half-life of 1.6 days and an average dose rate of 0.16 kGy/h. The dose and dose rate were recorded using two gas ion chambers and radiochromic films (RCF) (GEX Corp., Centennial, CO, U.S.A.) placed at different locations inside the irradiation chamber. Figure 4.1 shows the experimental setup. Samples were piled in stacks of 12 bags for each dose and usually 2 stacks were inside the chamber at one time. The radiochromic films were read after stabilization (1 hour

after irradiation) using a scanner (Far West Technology Inc., Goleta, CA, U.S.A.) and compared with a previously determined standard curve, which was developed with gas ion chamber dosimeters.

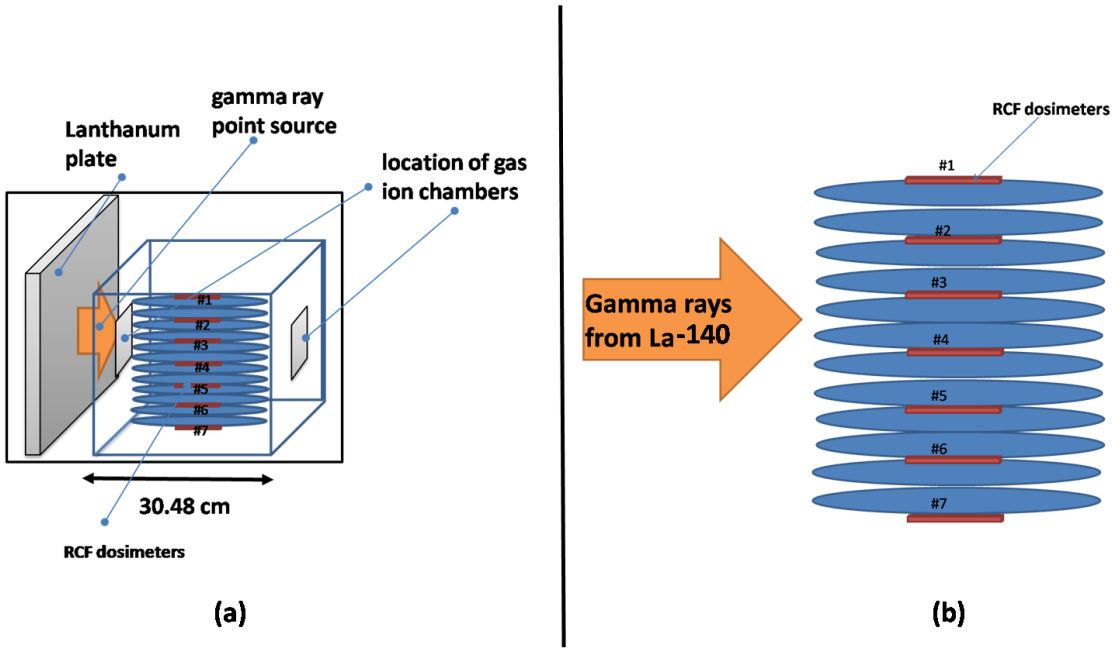

Figure 4.1. (a) Experimental setup showing gas ion-chamber dosimeters locations at the front and back of the box holding the samples; (b) location of RCF (radio-chromic films) dosimeters between the sample bags. Dimensions for the lanthanum plate and the box were 1m x1m and 30.48cm x 30.48cm, respectively.

Sampling: Initially, the bags containing the treated leaf pieces were hammered with the aid of a meat hammer for about 2 min (until samples were reduced to small pieces). Next, 80 mL of BPB was added to each bag, making a 5:1 ratio of total solution: leaf by weight. The bags were stomached at 260 rpm for 8 min to homogenize the material using a stomacher (Seward Stomacher Lab Blenders, Brinkman, USA). Aliquots of the homogenized samples were drawn and decimal dilutions were made BPW (buffered

peptone water, Difco, Sparks, MD, U.S.A.). Appropriate dilutions for each treatment were spread-plated on TSA with RIF^+ plates and incubated overnight at 37°C. For each of the 3 replications, 2 plates per dilution were counted. Each bag containing 20 g of lettuce was considered a replication, and there were 3 bags for each treatment (lettuce variety and dose).

Statistical analysis: Linear regression and significance test among the slopes (i.e., D_{10}-value) for each bacterial survival curve (iceberg, Boston, green leaf, and red leaf) was determined using SPSS software for Windows, v. 16.0 (SPSS, 2007). Linear regression and analysis of covariance with 95% confidence interval ($P \leq 0.05$) were used respectively. The radiation D_{10}-values for the *E. coli* cocktail were calculated based on the negative reciprocal of the slope of the linear regression line.

4.3.2 *Scanning Electron Microscopy*

SEM images of inoculated controls (non-irradiated, 0.0 kGy) and irradiated (1.0 kGy) lettuce leaves were obtained for each variety. The inoculation procedure was the same as described above.

Sample preparation for SEM observation: This part of the study was carried out at the Microscopy and Imaging Center of Texas A&M University. For each lettuce variety, leaf samples were cross-sectioned by using a razor blade and fixed using Trump's fixative (McDowell and Trump, 1976) overnight at 25°C. Fixed samples were submitted to microwave cycles (30 minutes cycle (5 min under vacuum/ 5 min under atmosphere)) at 250 watts (Model Pelco® , Biowave ™, Ted Pella Inc., Redding, CA, U.S.A. – equipped with ColdSpot™) and rinsed three times with Trump's buffer to remove the

glutaraldehyde. Samples were post fixed with 1% osmium tetroxide (Electron Microscopy Sciences, Hatfield, PA, U.S.A.) in Trump's buffer overnight at 4^{o}C as previously reported by Araujo et al. (2003). All samples were dehydrated further in an ethanol/water mixture of 5% increments up to 100%. Dehydration in 100% ethanol was carried out three times. Dehydrated samples were submitted to HMDS (hexamethyldisilazane - Electron Microscopy Sciences, Hatfield, PA, U.S.A.). Following samples were coated with gold/palladium mixture (50/50) under vacuum using a Hummer I Sputter Coater (Anatech Ltd., Union City, CA, U.S.A.)

Observations were made using a scanning electron microscope (SEM, model JEOL JSM 6400, JEOL USA, Peabody, MA) operated at an accelerating voltage of 15 kV and 39 mm working distance.

4.4 Results and Discussion

4.4.1 *Radiation Sensitivity of Internalized Microorganisms*

The vacuum perfusion process effectively introduced the inoculums into the leaf pieces, as confirmed by the SEM images discussed below in the text. Visually, it was observed a change on the leaf appearance from opaque to translucent as the inoculated water perfused into the leaf throughout its major vascular system, creating a water-soaked appearance as previously observed by Niemira (2008). Moreover, the samples were not washed after perfusion, therefore bacteria cells would presumably also be found on leaf surfaces. The concentration of bacterial cells per gram of leaf vegetable was determined directly by sampling the untreated (control) and by calculation from the concentration of the diluted inoculums and the known amount of inoculums taken up

during the perfusion process. The water intake among lettuce varieties ranged from 44.0%, 44.7%, 48.1%, and 50.8% for iceberg, green leaf, red leaf, and Boston varieties, respectively. Even though there was a difference on the amount of inoculums intake among lettuce varieties, it was not significant ($P > 0.05$). Moreover, the inoculums intake did not mathematically influence the calculation of the D_{10}-values.

In this study, we deliberately positioned the radiation source just on one side of the samples to demonstrate the effect of over- or under-estimation of the absorbed dose on the inactivation of the microorganism. Table 4.1 shows the effect of dose distribution within the lettuce samples on the calculation of D_{10}-values for *E. coli*. Note that the different readings (column 3) refer to the dose values given by the different dosimeters, i.e., front (single ion chamber value), center (average values for all seven RCF dosimeters), or back of the samples (single ion chamber value). The ratio of max/min dose (dose uniformity ratio) was 2.8, which is high in this example (desired ratio should be < 1.5), although many food applications can tolerate a higher uniformity ratio of 2 or even 3 ((IAEA), 2002). Figure 4.2a shows the dose distribution along the center line of the process load (depth-dose distribution). The depth–dose uniformity depends on the product density, thickness, and the radiation energy and type and it can be improved by irradiating the process load from two or more sides, using a multipass irradiator system, and reducing the thickness of the process load ((IAEA), 2002).

Table 4.1. Target and measured doses and calculated D_{10}-values for different locations in different bags of lettuces (see Figure 4.1 for location of the dosimeters).

Target Dose [kGy]	**Dosimeter Position**	**Reading [kGy]**	**Lettuce Type**	**D_{10} – values [kGy]**
0.25	**Front**[1]	0.25	Iceberg	0.32
0.50		0.50	Red-leaf	0.33
0.75		0.75	Green-leaf	0.34
1.00		1.00	Boston	0.35
0.25	**Center**[2]	0.13±0.03	Iceberg	0.19
0.50		0.21±0.02	Red-leaf	0.16
0.75		0.32±0.05	Green-leaf	0.16
1.00		0.50±0.09	Boston	0.18
0.25	**Back**[1]	0.09	Iceberg	0.13
0.50		0.18	Red-leaf	0.12
0.75		0.27	Green-leaf	0.12
1.00		0.36	Boston	0.13

[1]measured with ion chamber;[2] measured with radio-chromic film (RCF); max/min = 2.8

The process of energy transfer from photons to the irradiated sample takes place in two distinct stages: (a) at the surface of the sample - interaction of photons (via Compton, pair production, and photoelectric effect) which set secondary (high energy) electrons in motion; and (b) within the sample - transfer of energy from these secondary electrons to the medium through excitation and ionization of the atoms of the medium (Attix, 1986).

If the incident radiation is essentially monoenergetic and the angle of incidence at the irradiated surface is approximately perpendicular and monodirectional, there is initially a marked increase (buildup) of energy deposition near the surface. This region extends up to the depth corresponding to the average range of the first interaction secondary electrons. This is then followed by an exponential decay of dose to greater

depths as shown in Fig. 4.2b. The approximate value of the buildup depth, in units of millimeters of water for lanthanum-140 (E_γ ~ 1.5 MeV) is 7 mm (Turner, 1995).

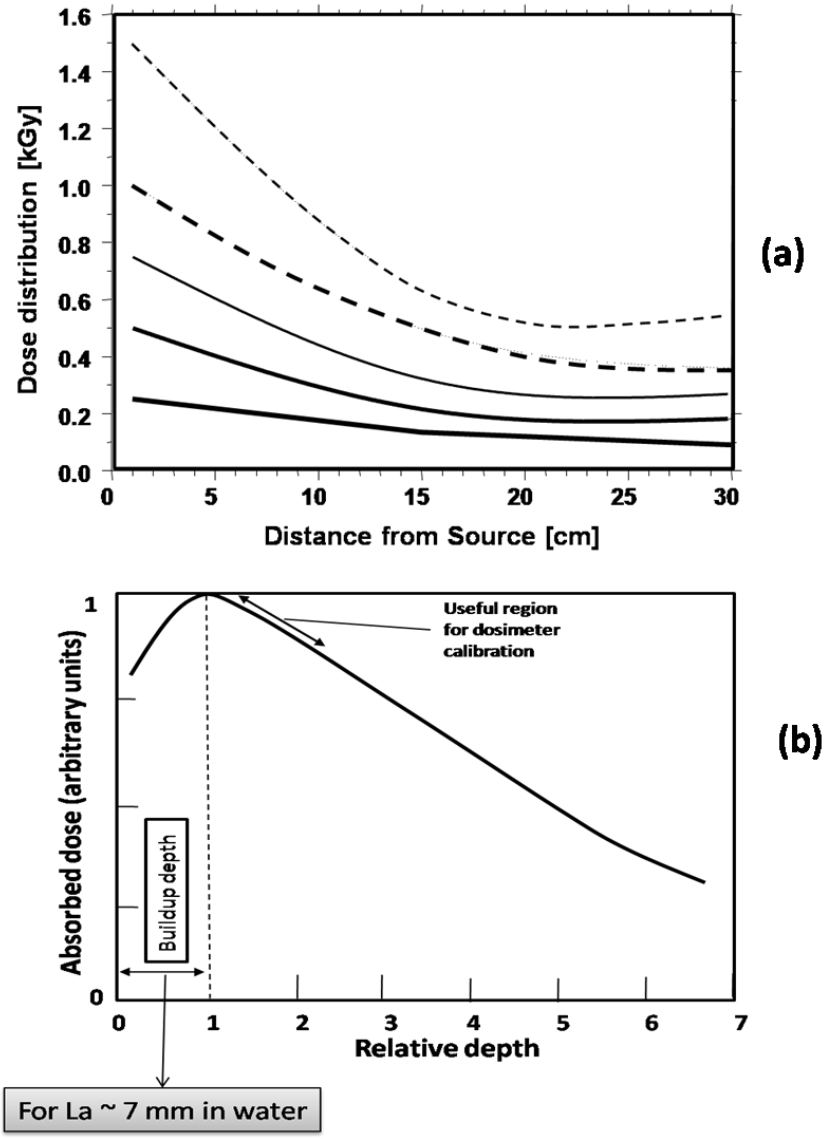

Figure 4.2. (a) Dose distribution within the lettuce bag samples; (b) buildup region for gamma rays in water.

Irradiation treatments effectively reduced ($P < 0.05$) the population of *E. coli* in all the lettuce varieties examined. Figure 4.3 shows the log-reduction as a function of

dose (kGy) for each lettuce variety. The three different lines refer to the dose values given by the different dosimeters, i.e., front, center, or back of the samples. Based on the readings taken from the dosimeter located in front (entrance dose) of the samples, the calculated D_{10}-values were 0.32, 0.33, 0.34, and 0.35 kGy for iceberg, green leaf, red leaf, and Boston lettuce, respectively (Table 4.1). These results agree with those found by Niemira (2008). However, the D_{10}-values were about 48% and 62% lower, based on the dosimeters located at the center and back of the samples, respectively. The D_{10}-values obtained at the center and back of the samples clearly show that the dose required to reduce the pathogens population by 90% could be overestimated. Although this is not a bad thing for safety purposes, quality of the lettuce could be affected if irradiation treatment is based on the higher D_{10}-value. These results also show that, for gamma-ray treatment, if the dose uniformity ratio is ~ 1.0, the D_{10}-values should be similar for surface and internalized pathogens in the different lettuce varieties.

Analysis of covariance showed that the radiation sensitivity of the internalized *E. coli* on the lettuces was not significantly ($P < 0.05$) influenced by lettuce variety. The D_{10}-value for *E. coli* was established as 0.34±0.04 kGy (front); 0.17$\pm$0.02 kGy (center), and 0.13$\pm$0.005 kGy (back). The radiation treatment reduced approximately 3 to 4-logs of internalized *E. coli* on the lettuce leaves at a dose up to1.0 kGy. Niemira (2008) found differences among lettuce varieties and one explanation for that is the fact that his analysis was based on pooled data. Whenever a pooled statistical analysis is conducted, equal variance among the treatments is assumed. However, if that is not the case, then ANOVA and ANCOVA should not be used to determine differences among the samples.

If ANOVA and ANCOVA are used, the chances to find differences among treatments increase, thus resulting in a false conclusion.

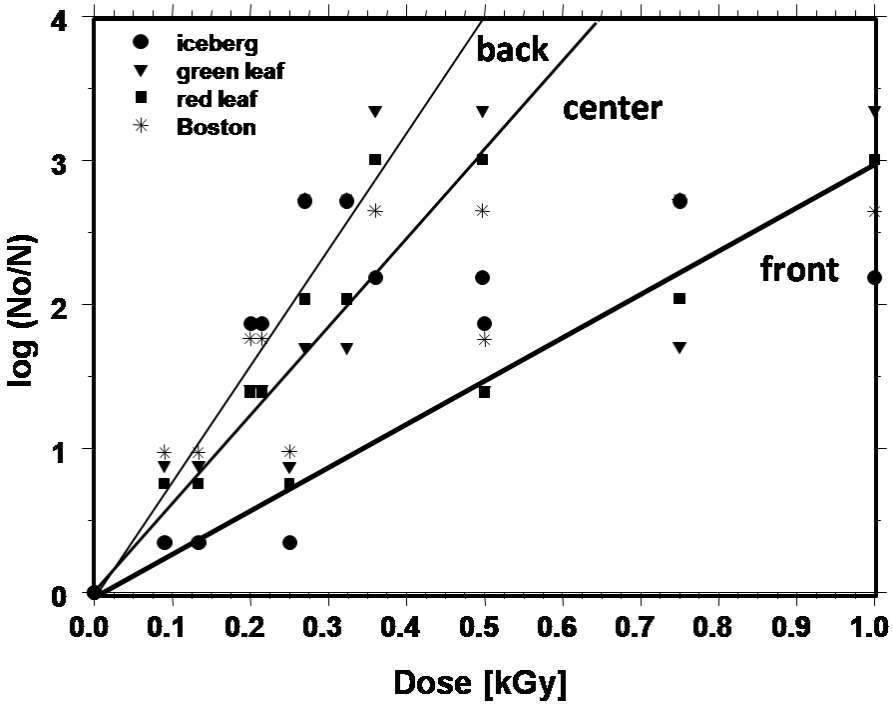

Figure 4.3. Log reduction (log No/N) of internalized *E. coli* in lettuce leaf pieces of four lettuce varieties (iceberg, green leaf, red leaf, and Boston) (dots = experimental data; line = linear regression).

The results from the bacterial counts of the four varieties of lettuce showed that irradiation effectively reduced the internalized bacterial population. These results are well supported by SEM observations, where the bacteria at the stomata of the lettuces (Fig 4.4-top) disappeared after irradiation (Fig 4.4-bottom). The structure of the lettuce leaf was not affected by the irradiation treatment as can be seen when comparing the non-contaminated control images (Figure 4.5) to other treatments, for example the 1 kGy (Fig 4-bottom) treatment which shows no damage to the lettuce structure. Therefore,

irradiation proves to be one, if not the only, treatment to effectively eliminate internalized microorganisms without affecting the product quality (low dose). It has been previously demonstrated that leafy vegetables will tolerate irradiation doses comparable to those used in this study (Castell-Perez et al., 2004; Gomes et al., 2008a; Gomes et al., 2008b; Han et al., 2004; Moreno et al., 2006; Moreno et al., 2007a, 2008; Moreno et al., 2007b).

4.4.2 *Does Variety Affect Radiation Sensitivity?*

This study shows that lettuce variety does not play a role in the inactivation effect of irradiation. This is in disagreement with other studies that concluded that radiation sensitivity of associated bacteria may vary with commodity variety or subtype (Niemira, 2003, 2008; Niemira et al., 2002). The $Z_{effective}$, the effective atomic number (average atomic number for a mixture of components), accounts for all the elements (composition) in the produce. This parameter is important to predict how electrons and photons (gamma-rays) interact with matter and is defined as the number of electrons per atom of an element or per molecule of a compound. The higher the $Z_{effective}$, the denser the target, thus the greater the probability of photon interaction with the material. Based on the (USFDA) composition database (2008c), the calculated $Z_{effective}$ of iceberg, Boston, green leaf and red leaf are 6.63, 6.65, 6.65, and 6.65, respectively (Table 4.2). Thus, our study confirms that materials with similar effective atomic number such as the different lettuce varieties, will have similar dose distribution and consequently the inactivation effect of irradiation on microorganisms will be similar. A better understanding of irradiation (photon and electrons) interaction with matter, its

mechanisms, and the physics of radiation processing are indeed necessary to further clarify this subject.

Table 4.2. Composition of selected lettuces and calculated effective atomic number (Z_{eff}).

	Z	**A**	**Boston**	**Red leaf**	**Iceberg**	**Green leaf**
C	6	12.01	0.018080	0.018102	0.018232	0.019945
H	1	1.008	0.107740	0.107755	0.107773	0.107394
O	8	16	0.868088	0.868207	0.870061	0.866328
N	7	14.01	0.002160	0.002128	0.001440	0.002176
Ca	20	40.08	0.000423	0.000439	0.000229	0.000496
Fe	26	55.85	0.000015	0.000016	0.000006	0.000012
Mg	12	24.3	0.000157	0.000159	0.000089	0.000179
P	15	30.97	0.000399	0.000372	0.000254	0.000400
K	19	39.1	0.002873	0.002486	0.001786	0.002678
Na	11	22.99	0.000061	0.000332	0.000127	0.000387
Zn	30	65.38	0.000002	0.000002	0.000002	0.000002
Mn	25	54.94	0.000002	0.000002	0.000001	0.000003
Cu	29	63.55				
Total			**1.000000**	**1.000000**	**1.000000**	**1.000000**
		Z_{eff}	6.648	6.645	6.634	6.648

Source: USDA (2008).

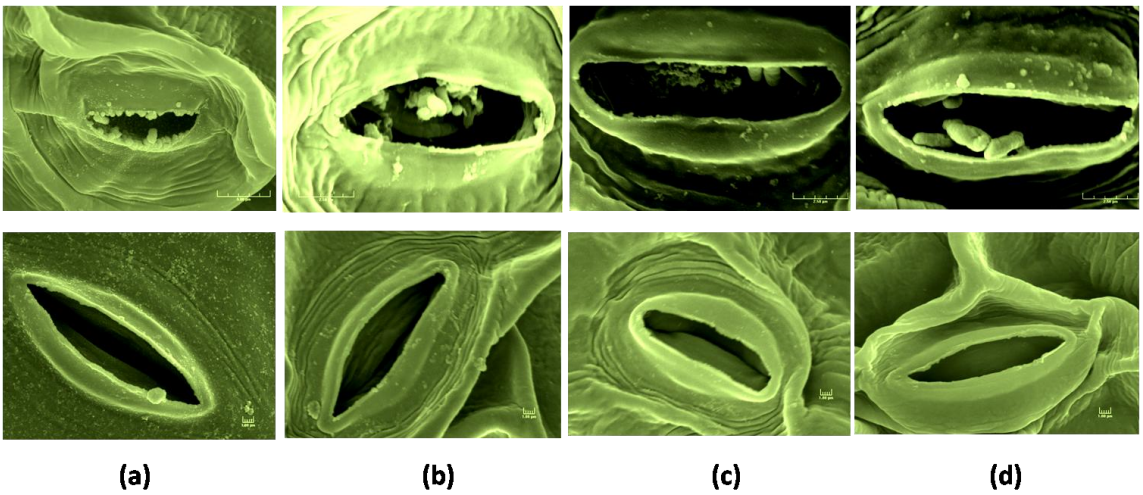

Figure 4.4. Microflora density of the surface of lettuce leaf of (a) iceberg, (b) Boston, (c) green leaf, and (d) red leaf inoculated with *E. coli*. Inoculated (top) and irradiated at 1.0 kGy (bottom).

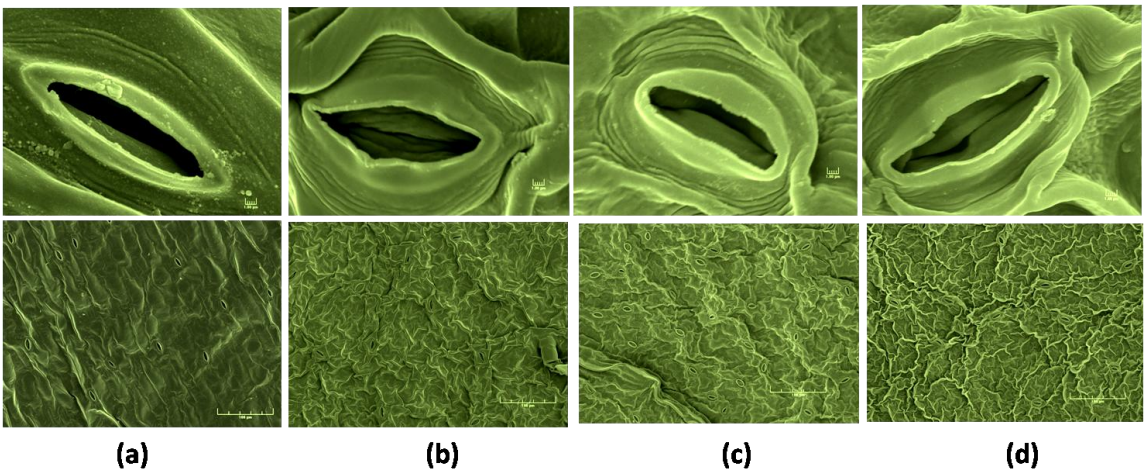

Figure 4.5. Images of (a) iceberg, (b) Boston (b), (c) green leaf, and (d) red leaf (d) surface of non-inoculated control.

4.4.3 *Mechanisms of Internalization*

SEM images (Figure 4.6) from the four different varieties of lettuce confirm that the preferential port of entry of *E. coli* internalization to the vegetable leaf is throughout

the stomatal cavity. Even though the inoculation method utilized in this study was by forcing the infiltration of the bacteria to these openings, our results could help elucidate how this process would occur naturally. Conventional internalizations via wounds into stomatal cavities, hydathodes, or other natural openings are clear means by which pathogens may internalize and avoid contact with antimicrobial chemical treatments. In this particular study, however, the *E. coli* cells were consistently found inside, at the edges and/or surrounding areas of the stomatal cavities for all lettuce varieties. Some bacteria cells were also found on the crevices in the proximity of the stomata, especially on the lettuces with a rougher surface, such as the Boston variety (Figure 4.7). On the other hand, no bacteria were found on the cut edges of lettuce leaf (Figure 4.8). More information is needed to understand how the microenvironment within leaves influences the internalization of human pathogens.

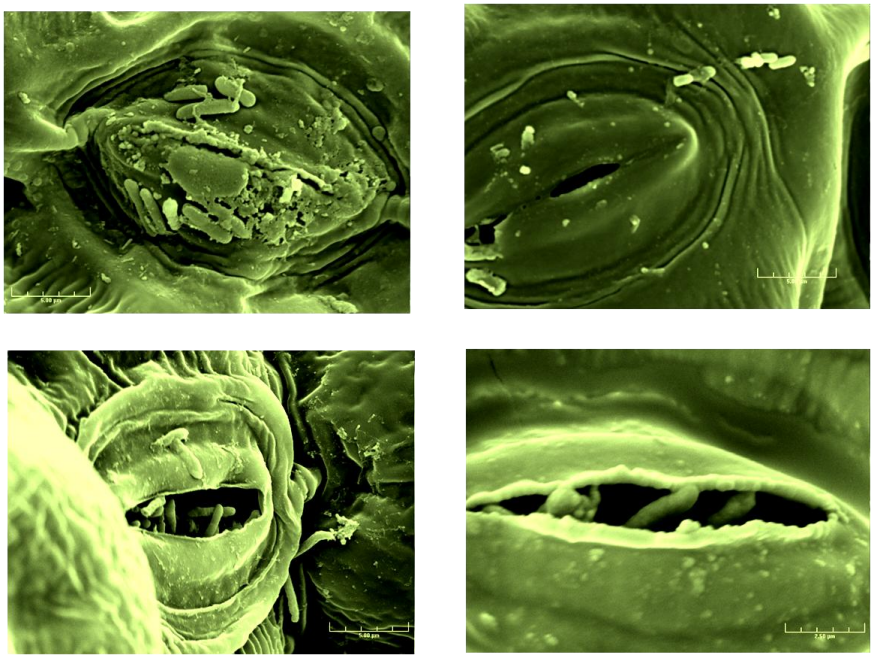

Figure 4.6. Deep internalization of inoculated *E. coli* cells in lettuce leaf stomata (clockwise from top-left - iceberg, Boston, red leaf, green leaf).

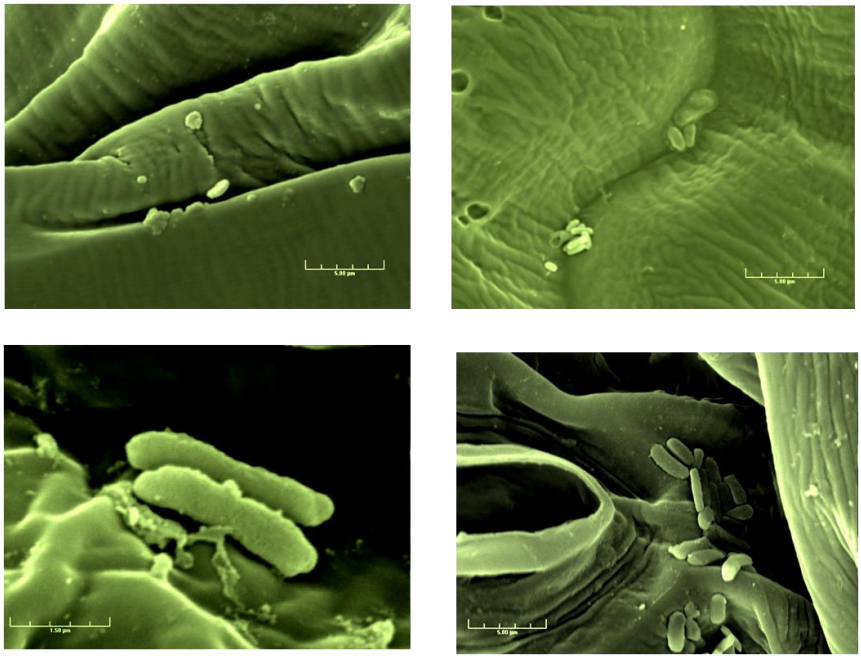

Figure 4.7. Localization of *E. coli* cells on crevices in lettuce leaf. (clockwise from top-left - iceberg, Boston, red leaf, green leaf).

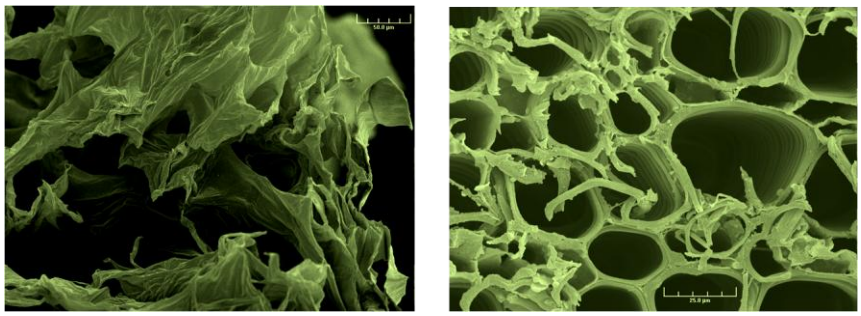

Figure 4.8. Absence of *E. coli* cells on cut edges of lettuce leaf (showing iceberg lettuce).

There was evidence of extracellular material connecting the aggregated bacterial cells, as would be the case with a developing biofilm. Figure 4.9 shows images of stomata and surface with biofilm produced by *E. coli*. A number of plant-pathogenic bacteria enter their respective hosts through the stomata. Immediately after spray or win-drain inoculation, the bacteria are randomly dispersed over the leaf surface, but most of them soon disappear, with the exception of those on or near the stomata. Bacteria in the stomatal cavities multiply rapidly and exude in mass before the infection is visible to the unaided eye. Substomatal cavities, therefore, function as shelters for the bacteria. Bacterial masses emerging from the substomatal cavities are enmeshed in strands of an unidentified substance, possibly polysaccharide slime of bacterial origin. The exuding bacteria serve as inoculums for secondary infection (Huang, 1986). Seemingly, human pathogens could use plants as a secondary host before infection of a new host (Brandl, 2006; Melotto et al., 2006). However, more information is needed to confirm this conclusion.

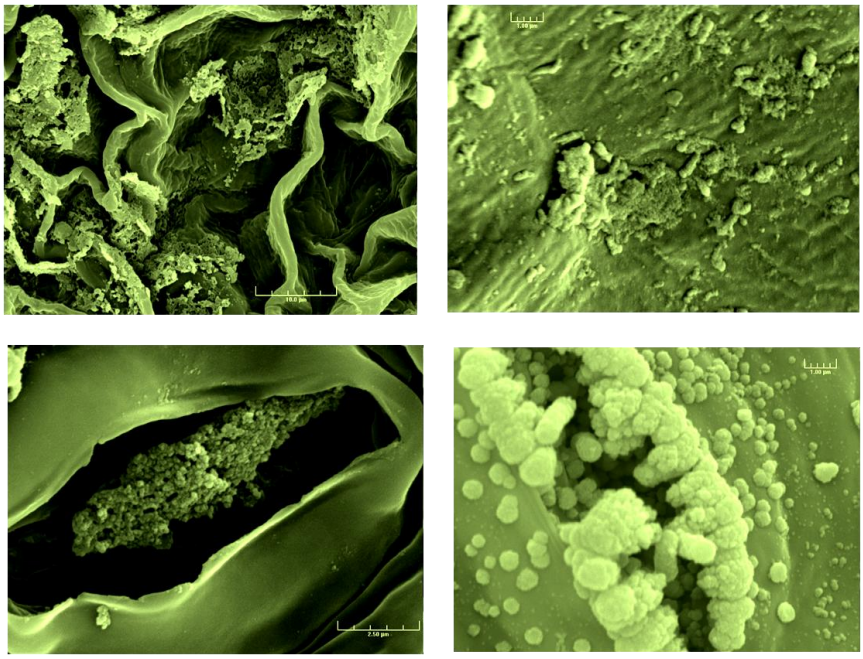

Figure 4.9. Biofilm formation by *E. coli* on lettuce surface and stomata after 24 hours. (Clockwise from top-left – Boston, iceberg, red leaf, green leaf).

A recent study conducted by Plotnikova et al. (2000) analyzed the stages of the *P. aeruginosa* infection process in Arabidopsis. The infection steps include attachment to the leaf surface, congregation of bacteria at and invasion through stomata. This suggests that the *E. coli* cells could have a similar mechanism of internalization on leafy vegetables such as lettuce using stomata as port of entry.

In some instances, morphology and structure of the stoma may play a role in disease/internalization resistance by limiting pathogen penetration. Reductions in stomatal density and aperture could provide pathogens with fewer and smaller points of entry, respectively. To measure stomatal density and size, images were taken using SEM under 250 x magnification. For each treatment, ten field-of-view images were taken. Figure 4.10 shows a field-of-view example for each variety. Stomatal density (the number of stomata per mm^2) was counted and averaged. The length of the stomatal aperture was calculated by measuring the length between the junctions of the guard cells at each end of the stomata (Malone et al., 1993). Stomata and leaf surface topography structure analyzed from the SEM images appeared similar among lettuce varieties. No significant difference ($P < 0.05$) in stomatal density and size was found among the varieties (Figure 4.11). Motility may also help *E. coli* find a protected niche (i.e. stomata on the leaf surface) for extended colonization of the plant.

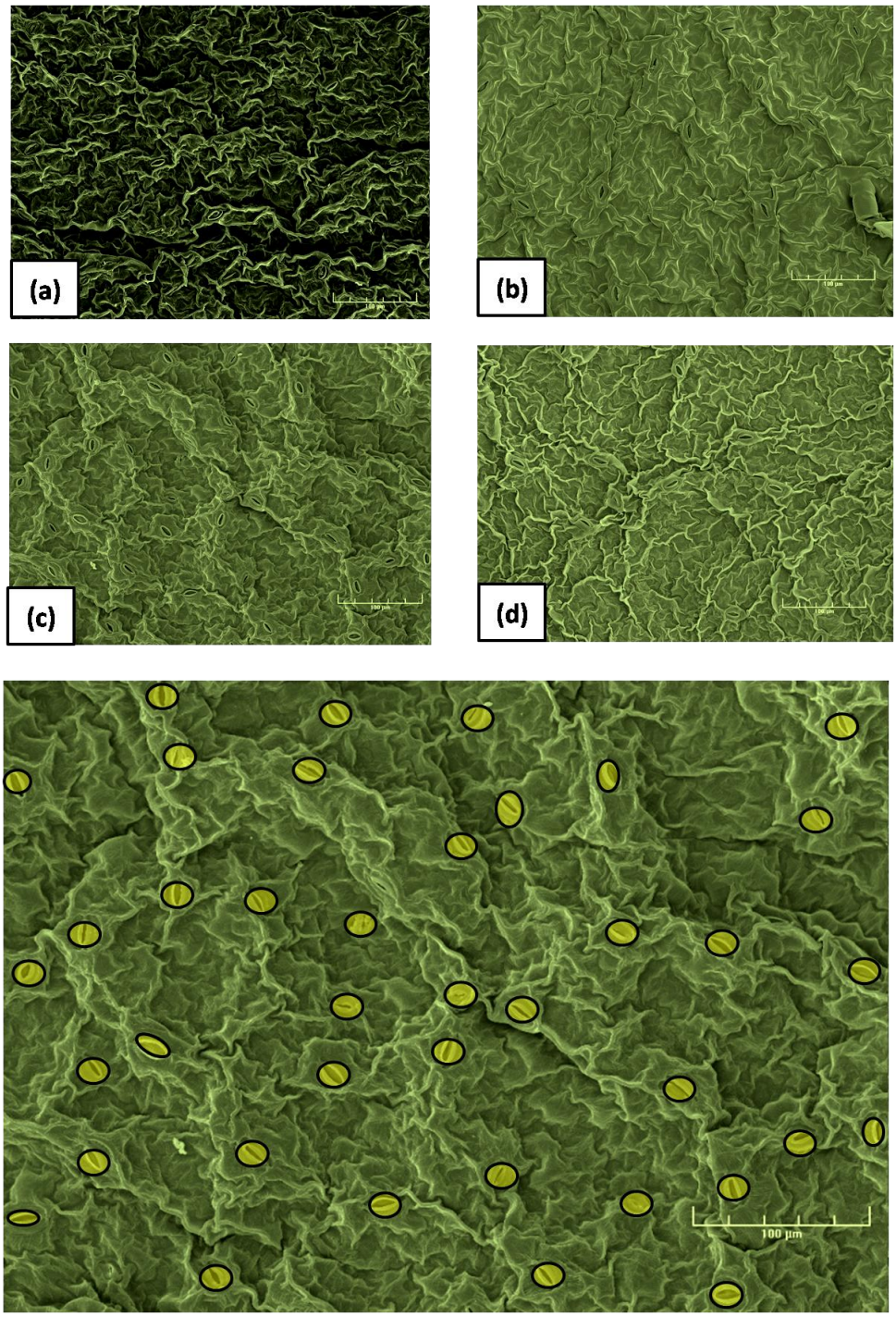

Figure 4.10. Lettuce surface field-of-view (a) iceberg, (b) Boston, (c) green leaf, and (d) red leaf for the determination of stomata density and size. Bottom image shows a zoom of image (c) showing location of stomata.

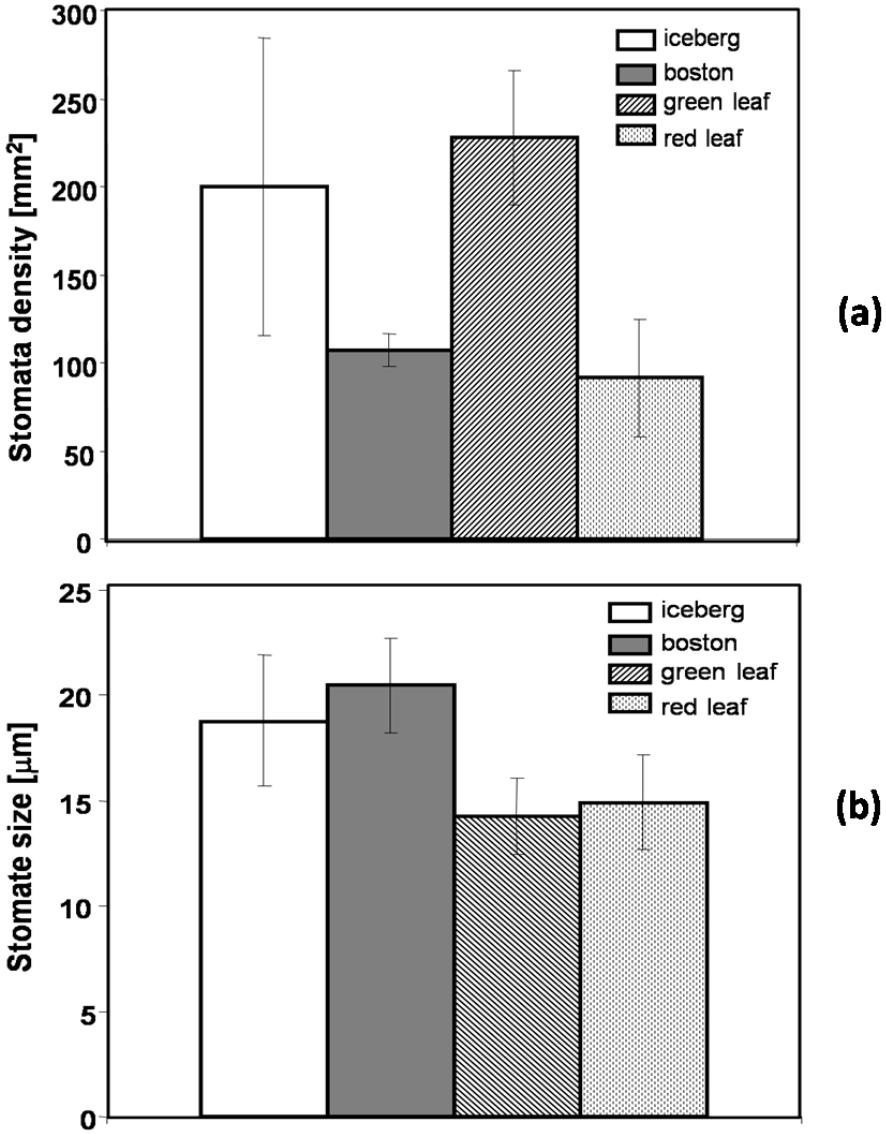

Figure 4.11. Structural characteristics: (a) stomatal density; and (b) length of the stomatal aperture; (error bars indicate standard deviation).

4.5 Conclusions

The current study shows the potential for lettuce leaves to provide a microenvironment for *E. coli*, where they are protected from removal by decontamination processes such as washing and surface sanitizing. All of the SEM

images suggest that the contamination sites of pathogens in fresh leafy vegetables are mainly localized on crevices and into the stomata. The internalization of pathogenic bacteria is particularly important for *E. coli* O157:H7, because a small number of surviving cells can be potentially lethal. Therefore, there is a need for new methods of inactivation. Ionizing irradiation is an effective method to reduce the population of internalized pathogens in a dose-dependent manner and could be used as a killing step to mitigate the risks of foodborne disease outbreaks. However, a clear understanding of irradiation interaction with matter for different irradiation sources (i.e., gamma and electron beam) is needed to obtain uniform dose distribution within the samples. Over-irradiation can be costly and degrade the product quality; however, under-irradiation can have a great impact on produce safety and wholesomeness, so proper design of the process is required for effective treatment of fresh produces.

CHAPTER V

RADIOSENSITIZATION OF *SALMONELLA* SPP. AND *LISTERIA* SPP. IN READY-TO-EAT BABY SPINACH LEAVES

5.1 Overview

The FDA recently approved irradiation treatment of leafy greens such as spinach up to 1.0 kGy. However it is important to reduce the dose required to decontaminate the produce while maintaining its quality. Thus, the objectives of this study were to: (1) assess the radiation sensitivities of S*almonella* spp. and *Listeria* spp. inoculated in ready-to-eat baby spinach leaves under modified atmosphere packaging (MAP) and irradiated using a 1.53-MeV Van de Graff accelerator. The leaves were irradiated both at room temperature and at -5^{o}C; and (2) to understand and optimize the synergistic effect of MAP and irradiation, by studying the radiolysis of ozone formation under different temperatures, the effect of dose rate on its formation, and its decomposition.

Results showed that increase concentrations of oxygen in the packaging significantly increased the radiation sensitivity of the test organisms, ranging from 7% up to 25% reduction in D_{10}-values. In particular, radiation sensitization could be effected ($P<0.05$) by production of ozone, which increases with increasing dose-rate and oxygen concentration, and reducing temperatures. Radiosensitization was demonstrated for both microorganisms with irradiation of either fresh or frozen (-5^{o}C) baby spinach.

These results suggest that low-dose (below 1 kGy) e-beam radiation under modified atmosphere packaging (100% O_2 and N_2:O_2 (1:1)) may be a viable tool for

reducing microbial populations or eliminating *Salmonella* spp. and *Listeria* spp. from baby spinach. A suggested treatment to achieve a 5-log reduction of the test organisms would be irradiation at room temperature under 100% O_2 atmosphere at a dose level of 0.7 kGy.

5.2 Introduction

There has been an increase in the number of foodborne illnesses associated with fresh produce in the past 30 years (Alkerturse and Swerdlow, 1996; Hedberg and Osterhold, 1994; Sivapalasingam et al., 2004). These outbreaks can be attributed to changing dietary habits, new production and processing technologies, sources of produce, as well as the manifestation of pathogens previously not associated with raw produce (Alkerturse and Swerdlow, 1996; Babic et al., 1995; Burnett and Beuchat, 2001; Sivapalasingam et al., 2004).

Early outbreaks of foodborne disease epidemiologically linked to fresh produce were initially suspected to result from cross-contamination of fruits or vegetables during food preparation, particularly with meat products. However, more recent surveys conducted by the U.S. Food and Drug Administration indicated that 1.6% ((USFDA), 2001c) and 4.4 % ((USFDA), 2001b) of the domestic and imported produce, respectively, were contaminated with human pathogens (Brandl, 2006).

Several bacterial pathogens have caused fresh produce-associated epidemics of enteric illness, including *Salmonella enterica*, pathogenic *Escherichia coli*, *Shigella* spp., *Campylobacter* spp., *Listeria monocytogenes*, *Staphylococcus aureus*, *Yersinia* spp., and

Bacillus cereus. *S. enterica*, caused 48% of such outbreaks with a known etiology between 1973 and 1997 in the United States (Brandl, 2006; Sivapalasingam et al., 2004).

Listeria monocytogenes has been associated with a number of serious foodborne outbreaks and product recalls (Anonymous, 1998; Farber and Peterkin, 1991). The bacterium is psychrotrophic and can survive and grow at temperature as low as 4^{o}C; thus, it can be a significant problem in refrigerated foods (Francis et al., 1999; Ukuku and Fett, 2002). Because of the high case fatality rate associated with *L. monocytogenes* infections, the U. S. Food and Drug Administration and the U. S. Department of Agriculture, Food Safety and Inspection Service have established a zero tolerance policy (no detectable level permitted) for *L. monocytogenes* in ready-to-eat foods, including minimally processed fresh and fresh-cut fruits and vegetables (Bari et al., 2005). Therefore, researchers are studying ways to reduce the food safety risks associated with fresh produce. Despite the use of proper hygiene and good agricultural practices, contamination of fresh produce may occur at any point along the farm to table chain ((USFDA), 2008a).

Irradiation is a process with excellent potential to control or eliminate foodborne pathogens in food. Ionizing radiation is able to penetrate into protected areas of produce (surface, subsurface, and interior) to injure or inactivate bacteria. Two of its most promising applications are the assurance of innocuity and the shelf-life extension. However, radiation processing of some foods can be limited by undesirable effects on the sensory quality at the dose required to achieve the desired microbial inactivation (Gomes et al., 2008b; Han et al., 2004; Neal et al., 2008; Sudarmadji and Urbain, 1972).

In 2008, the U. S. Food and Drug administration published a final rule that allows the use of irradiation to make fresh iceberg lettuce and fresh spinach safer and last longer without spoiling, which reinforces the need to understand irradiation processing to make it more efficient ((USFDA), 2008a). Currently, there is an interest in developing methods to reduce the radiation dose necessary to achieve these objectives.

The phenomenon of radiosensitization is well known in both radiation biology and therapy (Faizur Rahman et al., 1972; Schubert and Stegeman, 1981), but its application in food system has not been systematically investigated experimentally. The radiosensitization effect offers significant potential benefits, both technical and economic, to the radiation processing of food (Borsa et al., 2004).

The use of modified atmosphere packaging (MAP) can help to control bacterial populations in food products (Chiasson et al., 2005). MAP and irradiation have been studied to increase the sensitivity of bacteria to radiation; however, the mechanism behind this sensitivity is poorly elucidated. One theory is that the presence of oxygen in modified atmosphere conditions could increase the radiosensitivity of bacteria because of the formation of free radicals (Thakur and Singh, 1994) and the production of ozone gas (Miller, 2005). Ozone is a strong antimicrobial agent with numerous potential applications in the food industry, effective against bacteria in their vegetative as well as spore forms, fungi, protozoa, and viruses (James et al., 2002; Kim et al., 1999). Microbial studies typically show a 2-log reduction of total counts and significant reduction of spoilage and potentially pathogenic species most commonly associated with fruit and vegetable products when using ozone alone (gas and aqueous) (Khadre et al.,

2001). Therefore, the understanding of the composition and concentration of gases in a MAP subjected to ionizing radiation could make the irradiation process more effective in terms of quality and safety assurance.

The objectives of this project were (1) to assess the degree of radiosensitization of *Salmonella* spp. and *Listeria* spp. in baby spinach leaves packaged under different atmospheres at different irradiation temperatures, and (2) to study the radiochemistry of ozone by electron beam irradiation.

5.3 Materials and Methods

5.3.1 *Bacterial Cultures*

Nalidixic acid and Novobiocin resistant mutants were derived from two parent strains of *Salmonella entereditis* and *Salmonella Typhimurium*, according to the method published by Kaspar and Tamplin (1993). In addition, *Listeria monocytogenes* (ATCC 15313, ATCC 33090), Scott A, Strain A and *Listeria innocua* (NRCC B33076) were used to inoculate fresh baby spinach to be treated in this study. All strains were obtained from the Texas A&M Food Microbiology Laboratory (College Station, TX) culture collection. These bacteria were chosen as representatives of Gram–negative and Gram-positive bacteria.

Preliminary trials were conducted to ensure that the modified organisms had the same resistance to heat, acid, and irradiation, as well as the same growth characteristics, as the parent strains. The microorganisms were kept frozen at -80^{o}C in Tryptic Soy Broth (TSB; Difco Laboratory, Sparks, MD, U.S.A.) containing glycerol (10% v/v).

Before use, the stock cultures were resuscitated through 2 consecutive 24 h growth cycles in TSB at 37^{o}C to obtain working cultures containing approximately 10^{9} CFU/ml.

5.3.2. *Inoculation and Preparation of Baby Spinach*

Salmonella spp. and *Listeria* spp. were studied separately. The two *Salmonella* spp. cultures (50 ml each in TSB) were combined to make a cocktail inoculum, final volume 100 ml (containing ca. 9 log CFU/ml). Similar procedure was carried out with *Listeria* spp. cultures, where the 5 strains of *Listeria* spp. (20 ml each) were combined to make 100 ml of cocktail inoculum.

Fresh baby spinach leaves were purchased from a local market and stored at 4^{o}C for no more than 1 day prior to the experiments. All leaves showing decay, cuts, or bruises were removed and then 60-g were weighted and dispensed into a sterile stomacher bag and inoculated with the cocktail containing either *Salmonella* spp. or *Listeria* spp. The bag was then vigorously shaken manually for 10 min to spread the inoculum over the sample. Next, the samples were transferred to a salad spinner-type centrifuge (Oxo Intl, New York, NY, U.S.A.) to remove the excess surface inoculum inside the biological safety cabinet. This design of salad spinner incorporates a container base that captures all of the excess liquid (inoculum) removed from the leaf surface, and prevents the formation of aerosolized droplets. The spun-dried baby spinach leaves were weighed into subsamples of 2-g and bagged into mylar bags (ZipSeal™, 8.64 x 10.16 cm, 48GaPET/PE/0.00035 Foil/LLDPE, Sorbent Systems, Impak Co., Los Angeles, CA, U.S.A.) and sealed using a heat sealer (IPK-305H, Sorbent Systems). The bags were stored at 4^{o}C until irradiation treatment (approximately 15h). Mylar (biaxially-oriented

polyethylene terephthalate polyester) was used because of its excellent gas barrier and moisture properties (water vapor transmission rate of 0.0003g/100 in^2/24hrs and oxygen transmission rate of 0.0006 cm^3/100 in^2/24hrs) Furthermore, mylar is approved by FDA for use during irradiation of prepackaged foods ((CFR), 2009a).

Baby spinach leaves proximal composition was characterized by 91.4% of moisture, 2.86g/100g of total proteins, 0.39g/100g of total lipids, 3.63g/100g of carbohydrates, and 1.2g/100g of ash.

5.3.3 *Irradiation*

Prior to irradiation, the spinach sample bags were sealed under three different atmospheres: under air (78.1% N_2, 20.9% O_2, 0.036% CO_2), under O_2:N_2 (1:1), and under 100% O_2 research grade from Praxair (College Station, TX, U.S.A.) was without further purification. Sample bags were flushed for approximately 10 seconds with the atmosphere chosen using a hose with a thin syringe tip at one end and then quickly sealed. Irradiation of samples was carried out with a Van De Graaff accelerator (2.0 MeV) located at Texas A&M University. The amount used in each bag (2-g – about 3 leaves) of baby spinach was in accordance with the penetration depth of the accelerator (~ 5 mm in water). Irradiation dosage was measured by placing radiochromic film dosimeters (GEX Corp., Centennial, CO, U.S.A.) at the center of the bags (front and back) containing the spinach leaves, for a total of 2 dosimeters. The radiochromic films were read after stabilization (1h after irradiation) using a Radiochromic reader model 92 (Far West Technology Inc., Goleta, CA, U.S.A.) and compared with a previously determined standard curve developed with gas ion chamber dosimeters.

Inoculated spinach samples were exposed to 0.20, 0.5, 0.75, 1.0, and 1.25 kGy. Non-irradiated spinach served as the control. One set of irradiation treatments was conducted at room temperature (21^{o}C) and another set at -5^{o}C to test the effect of radiolytic ozone formation at lower temperatures on bacteria population reduction. At -5^{o}C, temperature control was maintained using a styrofoam box filled up with dry ice. The styrofoam box had a hole at the center of one of its sides (10 cm diameter), and the spinach bags were placed inside this hole (2.54 cm deep). The box was positioned inside the irradiator such as the electron beams would hit the spinach samples. The dry ice pellets were refilled in a regular basis during irradiation treatment by following its weight variation. Samples were analyzed immediately after irradiation. All experiments, accounting for each condition and organism, were replicated three times. The degree of radiation sensitivity was the difference of control D_{10}-value (without antimicrobial) and the D_{10}-value of samples treated with microencapsulated antimicrobial divided by the control D_{10}-value.

5.3.4 *Microbiological Analysis*

Initially, the bags containing the treated spinach were transferred to sterile stomacher bags and hammered with the aid of a meat hammer for about 1 min (until samples were reduced to small pieces). Next, 10 ml of sterile buffer peptone water (BPW, Laboratory, Sparks, MD, U.S.A.) was added to each of the spinach samples, making a ratio of 5:1 of total solution: leaf by weight. The bags were stomached at 260 rpm for 2 min to homogenize the material using a stomacher (Seward Stomacher Lab Blenders, London, U.K.). This time period resulted in a homogenized sample, with the

liquid being as dark green as could be obtained from the pulped leaves. Aliquots of the homogenized samples were drawn and serially diluted using BPW. Appropriate dilutions for each treatment were spread-plated on Tryptic Soy Agar (TSA, Difco) with 20 mg/l Nalidixic acid (Sigma-Aldrich, St. Louis, MO, U.S.A.) and 25 mg/l Novobiocin (Sigma-Aldrich) inverted, and incubated 24h at 37^{o}C for *Salmonella* spp. enumeration. For *Listeria* spp. enumeration, the dilutions were spread-plated on TSA containing 0.6% (w/v) yeast extract (Difco), 0.1% (w/v) esculin (Sigma-Aldrich), and 0.05%(w/v) Ferric Ammonium Citrate (FAC – Mallinckrodt Baker, Inc., Phillipsburg, NJ, U.S.A.), inverted, and incubated 24h at 37^{o}C. For each of the 3 replications, 2 plates per dilution were counted.

5.3.5 *Radiosynthesis Study of Ozone by Electron Beam Irradiation*

Additional experiments were conducted to determine the kinetics of ozone formation inside the bags and degradation by electron beam irradiation. Research grade air (78.1% N_2, 20.9% O_2, 0.036%CO_2), oxygen, and nitrogen and oxygen (1:1) mixture from Praxair (College Station, TX, U.S.A.) was used in most of the experiments without further purification. The gases were flushed into mylar bags (ZipSeal™, 8.64 x 10.16 cm, 48GaPET/PE/0.00035 Foil/LLDPE, Sorbent Systems, Impak Co., Los Angeles, CA, U.S.A.) until completely filled (50.45 ±2.70 ml) and then sealed using a heat sealer (IPK-305H, Sorbent Systems). Irradiation of bags was carried out with the Van De Graaff accelerator (2.0 MeV) located at Texas A&M University.

5.3.6 *Ozone Radiosynthesis under Different Atmospheres*

Bags containing three different atmospheres (air, oxygen, or oxygen-nitrogen mixtures) were irradiated at doses ranging from 0 to 5 kGy with 1 kGy increments at room temperature (21^{o}C) and at -5^{o}C. Immediately after irradiation, ozone concentration was measured with a UV-100 ozone analyzer (Ozone Solutions Inc., Hull, IA, U.S.A.). Experimental settings (temperature control, size of the bag, dose measurements, etc) were similar to the radiosensitization studies described before. Experiments were carried out in triplicates.

5.3.7 *Effect of Dose Rate on Ozone Radiosynthesis*

The effect of dose rate on ozone radiosynthesis was tested to address the effect of using different irradiation sources (i.e. X-ray, e-beam, or isotopes) which are characterized by quite different dose rates. Maybe you should explain why the need for this experiment. Bags containing oxygen (50.45 ±2.70 ml) were irradiated at 1 kGy at different dose rates ranging from 0.003 to 0.001 kGy/s at 21^{o}C. The different dose rates were obtained by varying the cathode temperature of the Van de Graaff accelerator. More drastic changes in dose rate would have been achieved by using different radiation sources (i.e. x-ray, cobalt-60, and 10MeV linear accelerator). Immediately after irradiation, ozone concentration was measured with a UV-100 ozone analyzer (Ozone Solutions Inc., Hull, IA, U.S.A.). Experiments were carried out in triplicates.

5.3.8 *Ozone Decomposition with Time*

Bags containing 100% oxygen were (50.45 ±2.70 ml) irradiated at 1kGy at 21^{o}C. After irradiation at different time intervals of time (0, 5, 10, 30, 45 and 60 minutes)

samples were taken and ozone concentration was measured with a UV-100 ozone analyzer (Ozone Solutions Inc., Hull, IA, U.S.A.). Time intervals in minutes were chosen based on previous studies of ozone decomposition (George et al., 1965; Swanson, 1979). Experiments were carried out in triplicates.

5.3.9 *Statistical Analysis*

Bacterial counts (log CFU/g) were plotted against irradiation dose in kGy. Linear regression and significance test among the slopes for each bacterial survival curve (*Listeria* spp., and *Salmonella* spp. under different atmosphere and temperature) was determined using SPSS software for Windows, v. 16.0 (SPSS, 2007). Linear regression and analysis of covariance with 95 % confidence interval ($P \leq 0.05$) were used, respectively. The radiation D_{10}-values for the *Salmonella* spp. and *Listeria* spp. cocktail were calculated based on the negative reciprocal of the slope for the linear regression line.

The degree of radiation sensitivity was defined as:

$$RS = \left(\frac{D_{10}(\text{control}) - D_{10}(\text{treatment})}{D_{10}(\text{control})} \right) * 100 \qquad [5.1]$$

Where D_{10} (control) is the D_{10}-value (without antimicrobial) and D_{10}(treatment) is the D_{10}-value of samples treated with microencapsulated antimicrobial.

For the ozone radiosynthesis study, linear regression and analysis of covariance with 95 % confidence interval ($P \leq 0.05$) were also used to compare treatments (different atmospheres).

5.4 Results and Discussion

5.4.1 *Bacterial Radiosensitization under Different Atmospheres*

Table 5.1 shows the effect of different atmospheres (MAP) and temperature on the radiation sensitivity (D_{10} values) of *Salmonella* spp. and *Listeria* spp. For both microorganisms and temperatures tested, radiation sensitivity increased ($P < 0.05$) with increasing oxygen concentration (Table 5.1). Figures 5.1 and 5.2 show the effects of different atmospheres (air, N_2:O_2 (1:1), and 100% O_2) on the slope (D_{10} value) of the radiation survival curve of *Salmonella* spp. and *Listeria* spp. at room temperature, respectively. The different atmosphere conditions affected ($P < 0.05$) the degree of radiosensitivity of both bacterial populations, with the 100% oxygen atmosphere being the most effective in increasing pathogen radiosensitivity. Similar results were observed with *Listeria* spp. (Figure 5.2). Compared to air, the percentage increase in radiation sensitivity ranged from 18.6 % to 24.8% between *Salmonella* spp. and *Listeria* spp. and the two MAPs. Statistical analysis showed that the calculated D_{10}-values for 100% O_2 and N_2:O_2 (1:1) atmospheres were not different for either microorganism.

Figures 5.3 and 5.4 show the effect of different packaging atmospheres on the radiation survival curves of *Salmonella* spp. and *Listeria* spp. inoculated on baby spinach leaves and irradiated at -5^{o}C. Similar to the results at room temperature, an increase in the concentration of oxygen in the atmosphere, significantly ($P < 0.05$) increased the radiation sensitivity for either microorganism. The use of N_2:O_2 (1:1) reduced the radiation D_{10}-value to 0.227 ± 0.017 kGy and 0.238 ± 0.009 kGy for *Salmonella* spp. and *Listeria* spp., respectively (Table 5.1). These values are equivalent

to an increase in radiation sensitivity of 15.9% and 16.2%, respectively. The D_{10}-values for 100% O_2 were 0.206 ± 0.014kGy and 0.213 ± 0.005 kGy, for *Salmonella* spp. and *Listeria* spp., respectively; which corresponded to an increase in radiation sensitivity of 23.6% and 25%. Nevertheless, the D_{10}-values for 100% O_2 and N_2:O_2 (1:1) atmospheres were not significantly different for *Salmonella* spp., however 100% O_2 showed the lowest ($P<0.05$) D_{10}-value for *Listeria* spp.

Table 5.1. Radiation sensitivity of *Salmonella* spp. or *Listeria* spp. inoculated in baby spinach leaves irradiated at room temperature (21°C) and at -5°C under MAP.

Treatment	***Salmonella*** spp.			***Listeria*** spp.		
Irradiation at 21°C						
	D_{10}-value [kGy]	**[1]R^2**	**[2]RS**	**D_{10}-value [kGy]**	**R^2**	**RS**
Air (control)	[b] 0.190±0.004 $_w$	0.99		[b, c] 0.213±0.008 $_x$	0.99	
N_2:O_2 (1:1)	[a] 0.155±0.009 $_w$	0.98	18.6%	[a] 0.164±0.005 $_w$	0.99	22.8%
100% Oxygen	[a] 0.143±0.006 $_w$	0.99	24.8%	[a] 0.170±0.005 $_x$	0.99	20.3%
Irradiation at -5°C						
Air (control)	[d] 0.269±0.016 $_w$	0.98		[d] 0.284±0.016 $_w$	0.98	
N_2:O_2 (1:1)	[c] 0.227±0.017 $_w$	0.97	15.9%	[c] 0.238± 0.009 $_w$	0.99	16.2%
100% Oxygen	[b, c] 0.206±0.014 $_w$	0.97	23.6%	[b] 0.213± 0.005 $_w$	0.99	25.0%

[a-c]Means within a column which are not followed by a common superscript letter are significantly different ($P < 0.05$).
$_{w,x}$Means within a row for the same temperature of irradiation, which are not followed by a common superscript letter, are significantly different ($P < 0.05$).
[1] coefficient of determination of the linear regression between Log(No/N) vs. Dose.

[2]RS - Percentage of increase on radiation sensitivity = $\left(\frac{D_{10}(control) - D_{10}(treatment)}{D_{10}(control)}\right) * 100$

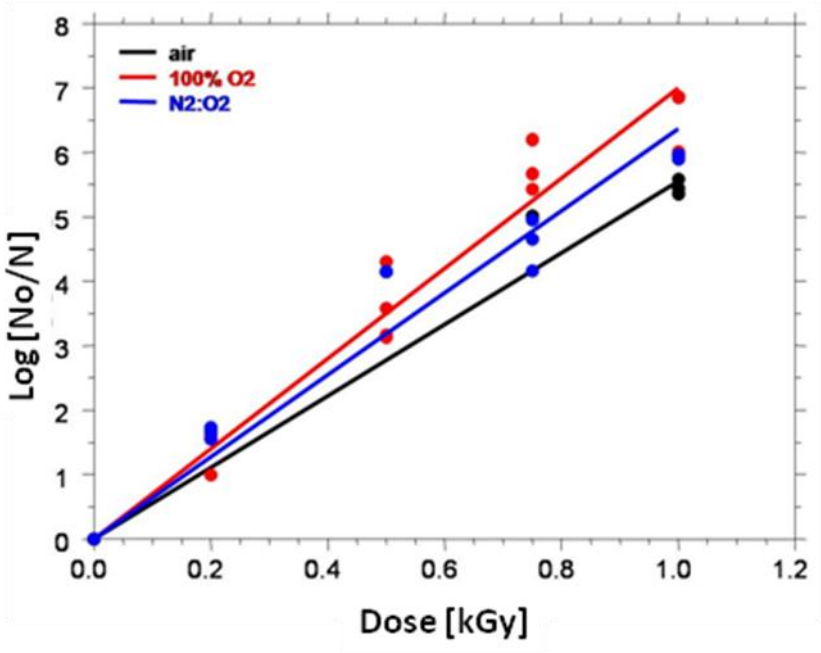

Figure 5.1. Radiosensitization of *Salmonella* spp. in baby spinach under different atmospheres (air, N_2:O_2 (1:1) and 100% O_2) irradiated at room temperature (21^{o}C).

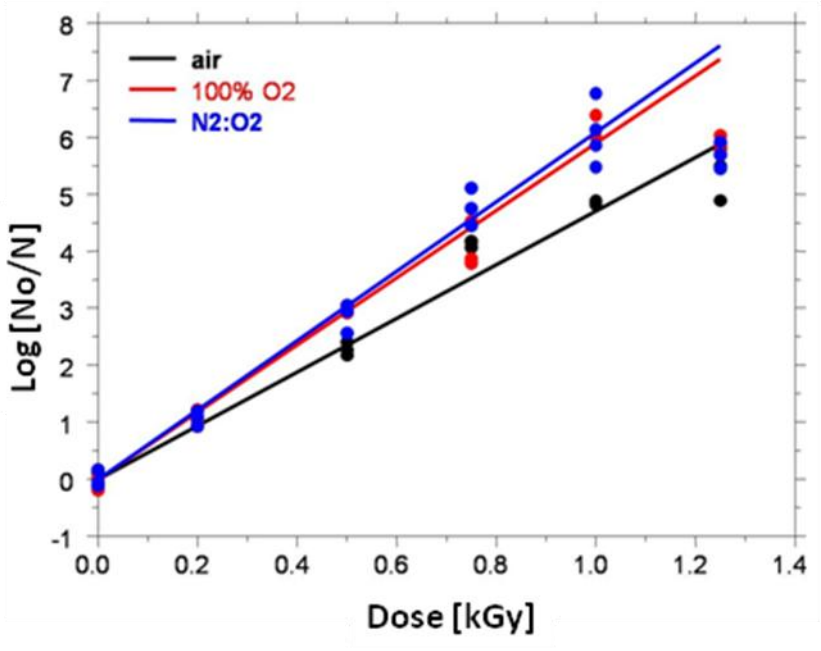

Figure 5.2. Radiosensitization of *Listeria* spp. in baby spinach under different atmospheres (air, N_2:O_2 (1:1) and 100% O_2) irradiated at room temperature (21^{o}C).

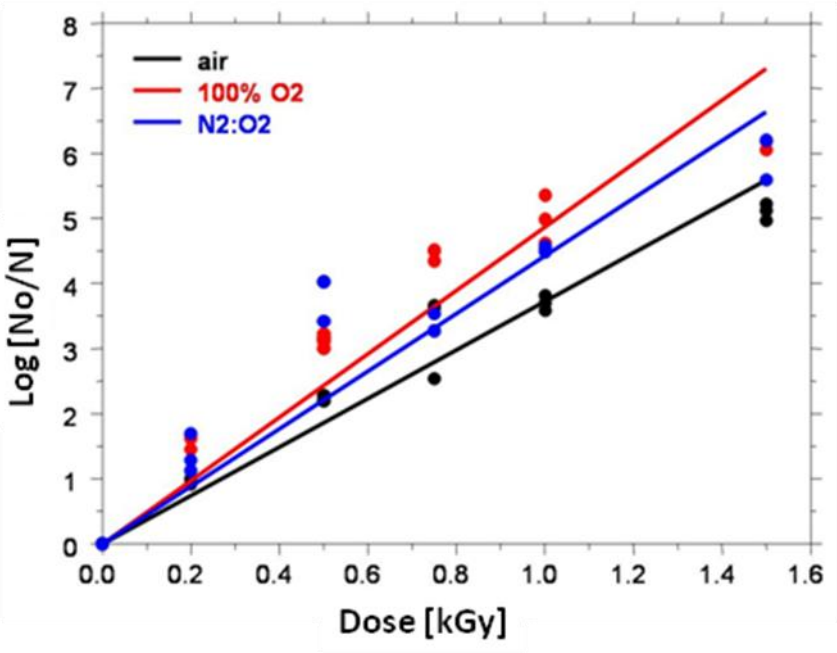

Figure 5.3. Radiosensitization of *Salmonella* spp. in baby spinach under different atmospheres (air, N_2:O_2 (1:1) and 100% O_2) irradiated at -5^{o}C.

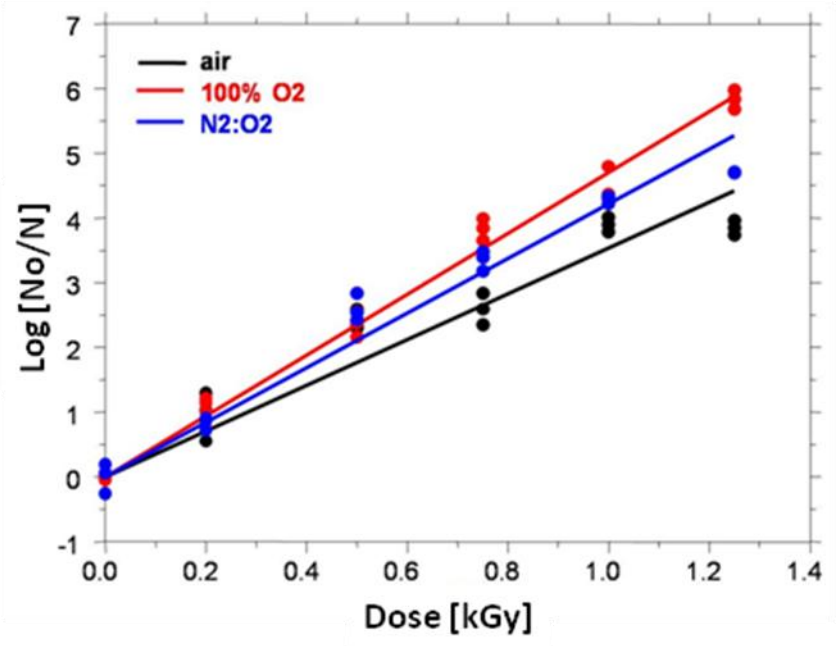

Figure 5.4. Radiosensitization of *Listeria* spp. in baby spinach under different atmospheres (air, N_2:O_2 (1:1) and 100% O_2) irradiated at -5^{o}C.

The experimental data show that MAP (N_2:O_2 (1:1) and 100% O_2) and irradiation have a synergistic effect on microbial decontamination for gram-positive and gram-negative bacteria. Oxygen behaves as a radiation sensitizer, since it increases the response to ionizing radiation and enhances the lethal effect of radiation due to oxygen radicals and ozone formation during the treatment. In general, the most common free radicals created following irradiation treatment stem from oxygen and water (Ewing, 1987). Ozone formation will be discussed in more detail in the next session.

One reason that the D_{10}-values of N_2:O_2 (1:1) and 100% O_2 atmospheres were not significantly different ($P < 0.05$) for the majority of the treatments (exception *Listeria* spp. irradiated at -5^{o}C) is that irradiation of a mixture of nitrogen and oxygen, besides producing free radicals and ozone, also generates nitrogen dioxide and nitrous oxide with the former being an antimicrobial gas and a potent radiation sensitizer (Ewing, 1987; Harteck and Dondes, 1959).

It is common knowledge that Gram-negative bacteria (e.g. *Salmonella* spp.), including common food spoilage microorganisms and enteric species, including pathogens, are more sensitive to irradiation than are Gram-positive bacteria (e.g. *Listeria* spp.). However, the ranges of radiation sensitivities are narrow (Barbosa-Canovas et al., 1998). For this study, although the D_{10}-values for *Listeria* spp. were higher for all treatments, they were not significantly different ($P < 0.05$) from those of *Salmonella* spp. The only exception was for the samples irradiated at room temperature under air and 100% O_2, with *Listeria* spp. showing higher ($P < 0.05$) radiation resistance than *Salmonella* spp.

Another interesting observation was the effect of temperature on the D_{10}-values for both types of bacteria. The D_{10}-values at -5^{o}C (freezing temperatures) were all higher than those obtained at room temperature for all treatments (Table 5.1). This has to do with the mechanism of inactivation of a microorganism by irradiation. The protective effect of freezing can be explained as a result of the suppression of OH radicals from water radiolysis. The OH radicals formed in the hydration layer around the DNA molecule are responsible for 90% of DNA damage. Thus, in living cells, the indirect radiation damage is predominant (Farkas, 1997). Cell water under freezing conditions is essentially immobilized and the metabolism is arrested. The indirect effect of irradiation is the interaction of radiation with other atoms or molecules in the cell, particularly water, to produce free radicals which can diffuse far enough to reach and damage the DNA (Diehl, 1995a).

Overall, the results presented above demonstrate that significant radiosensitization of *Salmonella* spp. (19-25% increase) and *Listeria* spp. (16-25% increase) inoculated into baby spinach can be achieved by utilizing modified atmosphere packaging with increasing concentration of oxygen. For a 5-log reduction (5D performance standard) ((USFDA), 2001a) for either microorganisms irradiated at room temperature, it would be necessary a dose of 0.95 kGy and 1.07 kGy under air for *Salmonella* spp. and *Listeria* spp., respectively. A dose of 0.78 kGy and 0.82 kGy under N_2:O_2 (1:1) atmosphere for *Salmonella* spp. and *Listeria* spp., respectively. And, a dose of 0.72 kGy and 0.85 kGy under 100% oxygen for *Salmonella* spp. and *Listeria* spp., respectively. At -5^{o}C, a 5-log reduction under air would require 1.35 kGy and 1.42 kGy

for *Salmonella* spp. and *Listeria* spp., respectively. A dose of 1.14 kGy and 1.19kGy under N_2:O_2 (1:1) atmosphere for *Salmonella* spp. and *Listeria* spp., respectively. Lastly, under 100% oxygen a dose of 1.03 kGy and 1.07 kGy would be required for *Salmonella* spp. and *Listeria* spp., respectively. In summary, a treatment to achieve a 5-log reduction for both microorganisms would be irradiation at room temperature under 100% O_2 atmosphere at a dose level of 0.7 kGy.

5.4.2 *Radiosynthesis Study of Ozone by Electron Beam Irradiation*

Ozone radiosynthesis under different atmospheres: Figures 5.5 and 5.6 shows ozone production (ppm) by electron beam irradiation under different gas compositions and temperatures as a function of dose. The higher the concentration of oxygen on the gas mixture the higher the ozone production for the same absorbed dose. The relationship between dose and ozone production was linear with a coefficient of determination (R^2) higher than 0.90. Ozone was formed more efficiently (higher concentrations) at low temperatures (-5^{o}C) than at room temperature as previously observed from other studies (Lewis, 1933; Sears and Sutherland, 1968). These results reassure that formation of ozone may be a factor in the germicidal activity of ionizing radiation (Kertesz and Parsons, 1963; Shah and Maxie, 1966).

Even though more ozone ($P < 0.05$) is formed under lower temperatures (-5^{o}C) for the same absorbed dose, the D_{10}-values calculated for *Salmonella* spp. and *Listeria* spp. inoculated in baby spinach leaves were higher compared to those irradiated at room temperature. This difference is because water will freeze at temperatures below-5^{o}C (at P_{atm}). Therefore, the free radicals formed by water inside the cytoplasm of the bacteria

during irradiation will be immobilized and their inactivating will be halted. Most of the damage to "critical molecules" such as DNA, RNA, or protein in the living cell occurs by this "indirect" mechanism (Biaglow, 1987). This indirect effect of radiation is important in vegetative cells, which the cytoplasm contains about 80% water (Diehl, 1995a). The life span of free radicals is extremely short (~ 10^{-9}s) and the indirect effects occurring inside the cytoplasm are more determinant on cell death than the free radicals that are formed on the cell surroundings. Therefore, the effect of temperature was clearly more predominant than ozone concentration on radiation sensitivity for both microorganisms. Probably, an intermediate temperature, such as refrigeration temperature (4^{o}C) would meet both ends and present a higher synergistic effect, since water would not be frozen and radiolytic ozone formation would still be higher than at room temperature.

Visual inspection of the baby spinach samples after irradiation treatment for all MAPs did not show any detrimental aspects on produce quality. A previous study showed that treatment with up to 1 kGy by e-beam irradiation on ready-to-eat baby spinach did not cause significant changes in produce quality (Gomes et al., 2008b). Therefore, the use of MAP can help decrease the dose required (by up to 30%) to reduce, for example, 5-log of initial pathogen population, with preserved quality attributes (color, texture, nutrients). A recent study on the quality of minimally processed baby spinach leaves stored under super atmospheric oxygen (80% and 100% O_2) MAP showed less tissue injury in addition to reducing microbial growth with a beneficial quality retention of fresh-cut baby spinach for 12 days of storage at 5^{o}C (Allende et al.,

2004). Therefore, irradiation of baby spinach under high concentrations of oxygen should retain its quality throughout storage and could be successfully applied to foods to control disease and deterioration caused by microorganisms. Once ozone has completely decomposed ca. 1.5 hr after irradiation, the headspace composition inside the bag throughout the shelf-life of spinach will be mainly oxygen and this modified atmosphere should not affect product quality during storage period.

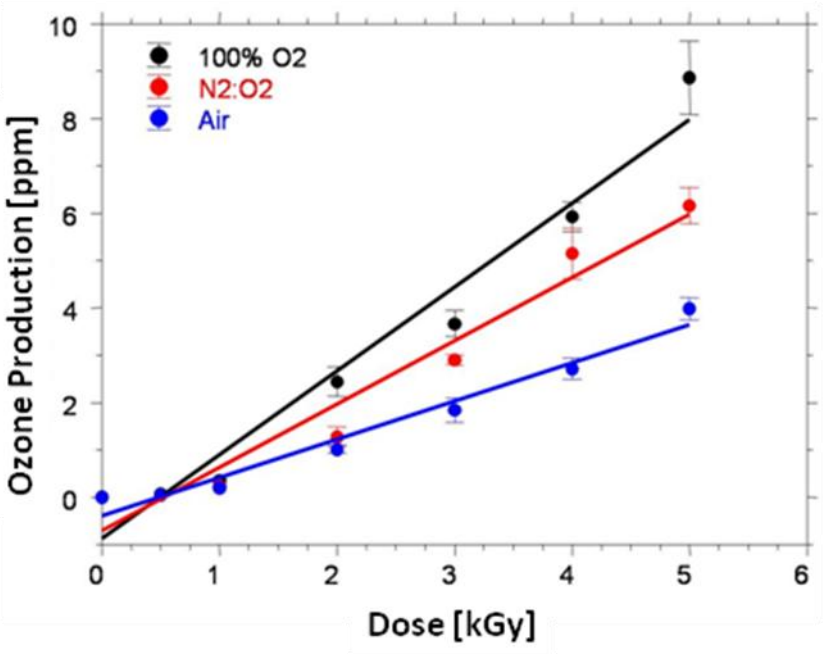

Figure 5.5. Ozone production as a function of dose at room temperature (21^{o}C) under different package atmospheres.

Ozone clearly acts synergistically with irradiation (as shown on the results of microorganism sensitization). It is the potent oxidation capacity (E^{o} = + 2.075 Volts) that makes ozone very effective in inactivating microorganism. The bactericidal effects of ozone have been studied and documented on a wide variety of organisms, including

Gram-positive and Gram-negative bacteria as well as spores and vegetative cells (Guzel-Seydim et al., 2004). When a cell becomes stressed by viral, bacterial, or fungal attack, its energy level is reduced by the outflow of electrons, and becomes electropositive. Ozone possesses the third atom of oxygen, which is electrophilic. Diseased cells, viruses, harmful bacteria, and other pathogens carry such a charge and so attract ozone and its by-products (Mahapatra et al., 2005). Understanding the mechanism of ozone formation under irradiation is paramount to optimize its production and enhance irradiation effectiveness of fresh produce.

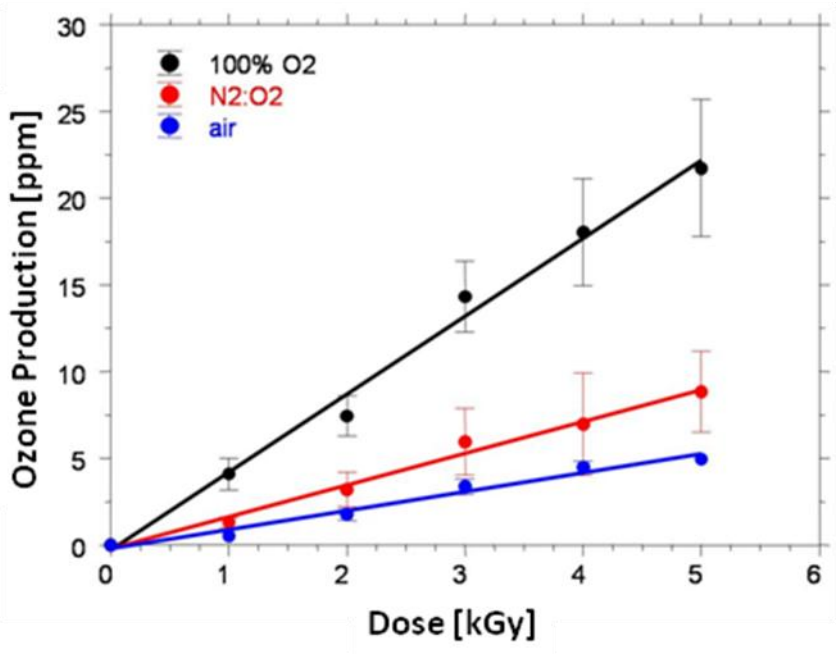

Figure 5.6. Ozone formation as a function of dose at -5^{o}C under different package atmospheres.

Effect of dose rate on ozone radiosynthesis: The dependence of the concentration of ozone produced upon dose rate is illustrated in Figure 5.7 the ozone concentration at a given dose rises with dose rate as observed previously by other authors (Less and Swallow, 1964; Sears and Sutherland, 1968). Even though Figure 5.7 only shows a small range of dose rate, it is still possible to notice its effect on ozone concentration (R^2 = 0.92).

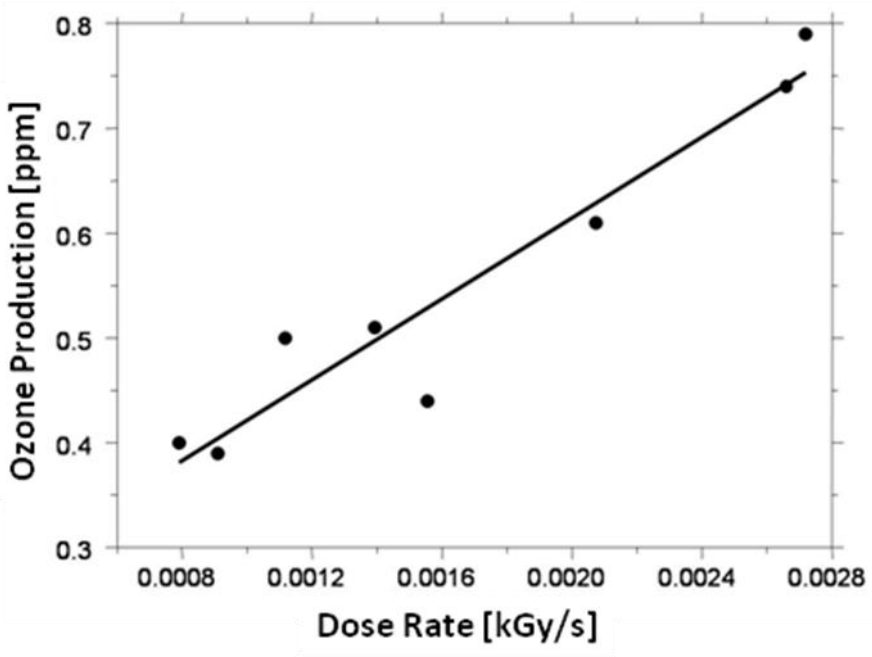

Figure 5.7. Ozone concentration at 1 kGy as a function of dose rate (100% O_2 atmosphere).

Some authors state that ozone is produced very efficiently by the unshielded electron beam in a gas path (George et al., 1965; Swanson, 1979). This is about ten times more efficient than the yield from Bremsstrahlung irradiation (X-ray), the reason being

that a considerable loss of kinetic energy to X-ray energies takes place when converting e-beams to X-rays (George et al., 1965). Therefore, a careful choice of irradiation source (i.e. X-ray, e-beam, Co-60 among others) should be taken into account if one wants to optimize ozone formation inside a package.

Ozone decomposition with time: Non-radiolytic decomposition of ozone at room temperature after electron beam irradiation of 100% O_2 (50.45 ±2.70 ml) at 1 kGy with a dose rate of 0.002512 kGy/s ± 0.0001909 is shown in Figure 5.8. The rate of ozone decomposition was found to be exponential with time (O_3[ppm] = 0.8688*exp(-0.01448**t*[min]; R^2 =0.90) and was characterized by a half-life of 48 min (the time necessary for half of the initial amount of a substance to decay) (Turner, 1995). Similar results were obtained by George et al. (1965) where they found that ozone decomposition was exponential. Ozone decomposes spontaneously, with an effective decomposition time that depends on size of container, material surrounding it, temperature, and impurities. For radiological safety aspects when designing an electron accelerator it is usually assumed a decomposition time for ozone of 50 min (Swanson, 1979).

Based on the decomposition profile of ozone inside the package used for this study, it is possible to determine the concentration and exposure time needed to decontaminate a product with ozone.

Previous studies showed that in aqueous medium, ozone alone showed that for inactivation of *Listeria monocytogenes* at room temperature it was required 0.1 ppm for 10 minutes to obtain 60-70% of the cells injured (Farooq and Akhlaque, 1983; Lee et al.,

1998). Another study showed that 0.1-1.8 ppm for 0.5 minutes at room temperature was enough to get 0.7-7 log reductions. For *Salmonella enteritidis* a concentration of 0.5-6.5 ppm and 0.5 minutes of exposure resulted in 0.6-4 log reductions (Rodriguez Romo, 2004). For *Salmonella typhimurium*, 0.23-0.26 ppm and 1.67 minutes resulted in 4.3 log reductions (Farooq and Akhlaque, 1983). Clearly, from Figures 5.5 and 5.6, the ozone concentrations necessary to achieve inactivation of these microorganisms will be produced under e-beam irradiation of oxygen-containing atmospheres. Obviously, these results will vary depending on the material on which these microorganisms are present (i.e. liquid (water) or solid (food surface)) and if the microorganism is internalized inside the product, where ozone would have limited access. Other factors to consider are that ozone has a longer half-life in the gaseous state than in aqueous solutions and that ozone decomposition is faster at higher water temperatures (Rice, 1986). In addition, gaseous decontamination methods have been more successful than wet methods for inactivation of pathogens on surfaces of fresh produce.

5.5 Conclusions

A suitable irradiation process can be designed for effective decontamination of ready-to-eat baby spinach leaves. D_{10}-values showed that a combination of irradiation at dose levels < 1kGy and modified atmosphere with increasing concentrations of oxygen played a role in bacteria radiosensitization, for either Gram-positive (*Listeria* spp.) or Gram-negative (*Salmonella* spp.) bacteria. By understanding the mechanism of radiolysis of ozone and its decomposition, it is possible to optimize its production to enhance irradiation effectiveness in eliminating pathogenic microorganisms while

maintaining the overall quality of fresh and fresh-cut produce. Hence, a treatment by e-beam irradiation of 0.7 kGy on baby spinach leaves under 100% oxygen at room temperature would assure a 5-log reduction of either *Salmonella* spp. and *Listeria* spp. without detrimental effects on product quality.

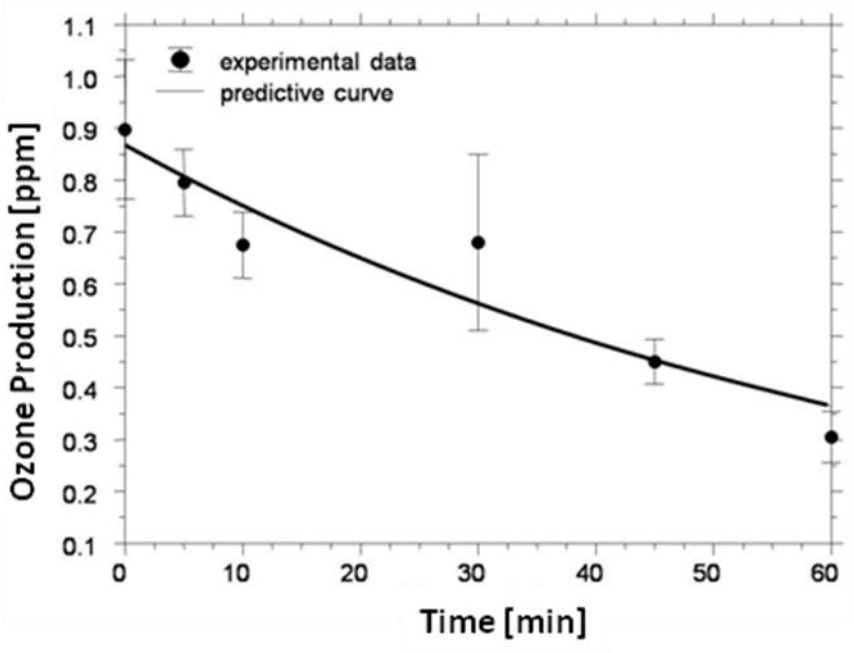

Figure 5.8. Ozone decomposition within time after electron beam irradiation at 1 kGy at room temperature, and with a dose rate of 0.002512 kGy/s ± 0.0001909 .

CHAPTER VI

MICROENCAPSULATED ANTIMICROBIAL COMPOUNDS AS A MEANS TO ENHANCE ELECTRON BEAM IRRADIATION TREATMENT OF FRESH PRODUCE

6.1 Overview

The minimum inhibitory concentration (MIC) of five natural compounds and extracts (*trans*-cinnamaldehyde, eugenol, garlic extract, propolis extract and lysozyme with EDTA (ethylenediaminetetraacetate acid disodium salt dehydrate) was determined against *Salmonella* spp. and *Listeria* spp. All compounds showed ($P<0.05$) bacteriostatic effect at different levels for both bacteria. In order to mask odor and off-flavor inherent of several compounds, and to increase their solubility, complexes of these natural compounds and extracts with β-cyclodextrin (β-CD) were prepared by the freeze-drying method. The formation of the inclusion complexes was confirmed by differential scanning calorimetry (DSC). Oxidative DSC revealed that the microencapsulated compounds in the β-CD cavity were protected against oxidation, remaining intact at temperatures where the free compounds were oxidized. Furthermore, all the inclusion complexes showed antimicrobial activity (determined by their MICs) against *Salmonella* spp. and *Listeria* spp.

The effectiveness of the microencapsulated compounds was tested by spraying them on the surface of baby spinach leaves inoculated with *Salmonella* spp. The dose (D_{10} value) required to reduce the population of bacterial population by 1 log using a

1.35 MeV accelerator was 0.180 kGy. The increase in radiation sensitivity (up to 40%) varied with the antimicrobial compound. These results confirm that the combination of spraying of microencapsulated antimicrobials with electron beam irradiation was effective in increasing the killing effect of irradiation (increased bacterial radiosensitization), demonstrating the potential of this technology to reduce the required radiation dose to control microbial contamination thus minimizing produce quality detriment..

6.2 Introduction

Fresh fruits and vegetables have gained considerable popularity in recent years due to their health benefits and availability year round. Consequently, the increase in consumption has lead to an increase in the number of foodborne illnesses linked to these products (Gombas et al., 2003; Horby et al., 2003; Tauxe et al., 1997). Leafy green vegetables, for example, were associated with 22 outbreaks and recalls from 1995 through 2007 ((USFDA), 2005).

Several bacterial pathogens have caused fresh produce-associated epidemics of enteric illness, including *Salmonella enterica*, pathogenic *Escherichia coli*, *Shigella* spp., *Campylobacter* spp., *Listeria monocytogenes*, *Staphylococcus aureus*, *Yersinia* spp., and *Bacillus cereus* (Brandl, 2006). Although the prevention of the initial contamination by pathogens, spoilage organisms, or both is critical to assure the quality and safety of fresh and minimally processed produce, some produce may be inadvertently contaminated. While decontamination procedures may be applied to fresh produce, current procedures cannot eliminate the contaminating microorganisms (Takeuchi et al., 2000). It is well

known that the difference of total microbial counts between vegetables either water washed or treated with 200 ppm chlorine, is usually not more than 1 log CFU/g (Beuchat, 2002), probably due to the presence of protective hydrophobic pockets and crevices on the leaf surface (Adams et al., 1989).

Irradiation is a nonthermal process, which can effectively inactivate pathogenic bacteria including *Salmonella, L. monocytogenes, E. coli*, and *Yersinia enterocolitica* (Farkas, 1987). Radiation can be applied after packaging, thus avoiding recontamination and reinsfestation (Farkas, 1997). Two of the most promising applications of this technology are the assurance of safety and shelf-life extension. In 2008, the U. S. Food and Drug administration ((USFDA), 2008b) published a final rule that allows the use of irradiation to make fresh Iceberg lettuce and spinach safer and last longer. However, the actual radiation dose used should be a balance between what is needed and what can be tolerated by the product without unwanted changes. Thus, radiosensitization of microorganisms can be obtained by physical and chemical means in combination with other preservation methods such as mild heat treatment, modified atmosphere packaging, addition of antimicrobial agents, and their combinations (Lacroix and Ouattara, 2000).

Recently, there has been a growing interest in natural antimicrobial products due to their availability, fewer side effects or toxicity as well as better biodegradability as compared to the available preservatives (Kalemba and Kunicka, 2003). Cinnamon aldehyde (cinnamaldehyde or 3-phenyl-2-propenal) is the major antimicrobial compound in cinnamon and it has been reported to inhibit the growth *Listeria monocytogenes, E. coli* O157:H7, *Salmonella Hadar,* and *S. entereditis* (Raybaudi-Massilia et al., 2009). In

addition to exhibiting antibacterial activity, cinnamic aldehyde also inhibits mold growth and mycotoxin production (Beuchat, 1994). Eugenol (2-methoxy-4-(2-propenyl)-phenol) is a major constituent in clove oil that possesses antimicrobial activity against a number of bacterial species, molds, and yeasts.

Eugenol and *trans*-cinnamaldehyde are phenolic in nature. The mode of action of phenolic compounds is generally thought to involve interference with functions of the cytoplasmic membrane and membrane proteins including proton motive force and active transport, degradation of the cell wall, and coagulation of cytoplasm (Davidson, 1997; Raybaudi-Massilia et al., 2009).

Bee resin (propolis) is a resinous mixture of substances collected by honey bees (*Apis mellifera*) from various plant sources. It is used by the bees. to seal holes in their honeycombs and protect the hive entrance. Propolis has been used in the traditional medicine since the primordial times of humanity (Moreira et al., 2008) and its biological and therapeutic actions are attributed to the phenolic composition.

Garlic (*Allim sativum*) has been used as a medicine since ancient times and has long been known to have antibacterial, antifungal and antiviral properties (Block, 1985). The main antimicrobial constituent of garlic has been identified as the oxygenated sulphur compound, 2-propenyl-2-propenethiol sulfinate, which is usually referred to as allicin. Allicin is not present in raw garlic. It is formed rapidly by the action of the enzyme, allinase on S-ally-L-cysteine-sulphoxide (alliin) when the garlic is crushed. Garlic sap inhibits the growth of several food spoilage and pathogenic bacteria (Davidson, 1997).

Lysozyme (1,4-β-N-acetylmuramidase, EC 3.2.1.17) is a lytic enzyme present in avian eggs, milk, tears and others secretions, insects, and fish. It has bactericidal power because the enzyme catalyzes hydrolysis of the β-1,4 glycosidic bonds between N-acetylmuramic acid and N-acetylglucosamine of the peptidoglycan of bacterial cell walls, causing cell wall degradation and lysis. Lysozyme is most active against Gram-positive bacteria, most likely because the peptidoglycan of the cell wall is more exposed. Gram-negative susceptibility can be increased by pretreatment with chelators (e.g. EDTA) that bind Ca^{+2} or Mg^{+2}, which are essential for maintaining integrity of the lipopolysaccharide layer (Cannarsi et al., 2008; Davidson, 1997). Hughey and Johnson (1987) reported that lysozyme is inhibitory to several food spoilage organisms as well as some pathogenic organisms, including *Listeria monocytogenes, Campylobacter jejuni, Salmonella typhimurium, Bacillus cereus, and Clostridium botulinum.* Lysozyme is one of the few naturally occurring antimicrobials approved by regulatory agencies for use in foods ((IFT), 2006).

The antimicrobial action of essential oils in model food systems or in real foods is well documented in the literature (Kalemba and Kunicka, 2003; Raybaudi-Massilia et al., 2009). Although the majority of the essential oils are classified as Generally Recognized As Safe (GRAS) food flavoring by FDA based on 21 CFR part 172.515 ((CFR), 2009a), their use in foods as preservatives is often limited due to flavor considerations, since effective antimicrobial doses may exceed organoleptically acceptable levels. Therefore, there is demand for accurate knowledge of the minimum

inhibitory (effective) concentrations (MIC) of essential oils to enable a balance between the sensory acceptability and antimicrobial efficacy.

In the antimicrobial action of essential oil components, the lipophilic character of their hydrocarbon skeleton and the hydrophilic character of their functional groups are of main importance. The activity rank of essential oil components is as follows: phenols> aldehydes> ketones> alcohols> ether> hydrocarbons (Kalemba and Kunicka, 2003). According to Davidson (1997) cloves, cinnamon, oregano, and thyme and to a lesser extent sage and rosemary have the strongest antimicrobial activity among spices.

The restrictive factors for fragrance ingredients are their high volatility and irritant effect that make difficult to formulate preparations containing them (Carlotti et al., 2007; Cheung et al., 2003). The ability of cyclodextrins to form an inclusion complex with a guest molecule could overcome these problems (Gouin, 2004). In fact, inclusion complexation exerts a strong effect on the guest's physicochemical properties; among which solubility enhancement of highly insoluble guests, stabilization of labile guests against the degradative effects of oxidation (e.g. visible or UV light and heat), control of volatility and sublimation, physical isolation of incompatible compounds, chromatographic separations, taste modification by masking off flavors, unpleasant odors and controlled release of drugs and flavors (Del Valle, 2004).

Considering the requirements of effectiveness and convenience of the application of natural antimicrobial products, the objectives of this study were to: (1) determine the levels of antimicrobial activity of essential oils, extracts, and enzymes against gram-positive and negative bacteria; (2) microencapsulate the essential oil and extracts within

β-cyclodextrin and verify the antimicrobial activity of the complexes formed; (3) evaluate the degree of radiosensitization of *Salmonella* spp. in baby spinach leaves sprayed with several microencapsulated antimicrobial compounds.

6.3 Materials and Methods

6.3.1 *Materials*

trans-Cinnamaldehyde, 99% (C80687), eugenol, 99% (E51791), Lysozyme from chicken egg white (~50,000 units/mg protein – L7001), ethylenediaminetetraacetate acid disodium salt dehydrate (EDTA- E4884), and β-cyclodextrin (C4767) were purchased from Sigma-Aldrich (St. Louis, MO, U.S.A.).

Garlic extract and characterization: Fresh garlic cloves (*Allium sativum*) (395.17g) were blended (Waring blender, Waring Laboratory, Torrington, CT, U.S.A.) in 200 ml of distilled water, centrifuged at 20125g for 20 min (Allegra 25R centrifuge, Beckman Coulter, Fullerton, CA, U.S.A.), and the supernatant was ultrafiltered using a Millipore-Labscale^{TM} TFF system equipped with a 5kDa cutoff Pellicon XL-Millipore (Millipore Co, Kankakee, IL, U.S.A.). Aliquots were stored at -20^{o}C until required. The concentration of allicin in each preparation was determined spectrophotometrically (UV-Vis Shimadzu 1600 spectrophotometer, Shimadzu Scientific Instruments, Columbia, MD, U.S.A.) by reaction with the thiol, 4-mercaptopyridine (4-MP, Sigma-Aldrich – 148202) (Miron et al., 2002). Briefly, varying quantities of garlic extract were incubated at room temperature for 30 min in 1 ml of 4-mercaptopyridine (10^{-4} M) in 50 mM Na-phosphate buffer, 2 mM EDTA (pH 7.2) which results in the formation of a mixed disulphide, 4-allylmercaptothipyridine, and the consequent shift in absorbance at 324 nm

(ΔA_{324}) (was monitored. A molar extinction coefficient (ε_M) of 39,600 $M^{-1}cm^{-1}$ at 324 nm was used for the calculation of allicin concentration. The molar concentration (mols/liter) of allicin was calculated as (Miron et al., 2002):

$$[allicin] = \frac{\Delta A_{324} \times dilution}{39{,}600}$$

$$\Delta A_{324} = \left[A_{324}(4 - MP\ without\ allicin) - A_{324}(4 - MP\ with\ allicin)\right] \qquad [6.1]$$

where 4-MP is 4-mercaptopyridine (λ_{max}= 324nm).

Bee resin extract and characterization: Bee resin (propolis) powder samples (Y. S. organic bee farms, IL, U.S.A.) were purchased from a local natural food grocery store. According to the producer, propolis was collected from different areas, mainly North Dakota, South Dakota, Minnesota, and Canada. Samples were vacuum dried at 37^oC for 24hr. The dried propolis powder was stored in airtight glass bottle in a desiccator; 80 mg was suspended in 10 ml ethanol under stirring for 24 hrs at room temperature. Next, the ethanol extracts were filtered through a 0.2 μm filter (Acrodisc, Pall life Sciences Port Washington, NY, U.S.A.) and stored at 4^oC for no longer than a week.

A Dionex Summit HPLC system (Dionex, Germering, Germany) equipped with P680 pump with high-speed gradient, ASI-100 autosampler, SOR-100 degasser running Chromeleon version 6.6 software was used with photodiode array detection (PDA-100). All wavelengths between 250 and 601 nm were collected while 280 nm wavelengths were monitored during runs. Determinations were made in triplicates.

The chromatographic analysis of propolis extract was performed using a High Performance Liquid Chromatograph (HPLC). A Dionex Summit HPLC system (Dionex,

Germering, Germany) equipped with P680 pump with high speed gradient, ASI-100 autosampler, SOR-100 degasser, running Chromeleon version 6.6 software was used with photodiode array detection (PDA-100). All wavelengths between 250 and 601 nm were collected while 280 nm and 320 nm wavelengths were monitored during runs. Phenolics were separated on a Supelco 2.1 mm x 250 mm, 5μm discovery Bio Wide Pore C18 column with Supelguard (C18) column cartridge at 0.25 ml/min using a method similar to that described by Woodard et al. (2009). The solvents consisted of (A) 0.25% phosphoric acid in water and (B) acetonitrile. The gradient used was from 0 to 50 min, 0-60% B; 50 to 70 min, 60-100% B. Each 10μl sample was run at room temperature (22^{o}C). The phenolic compounds were identified by comparison with the authentic chromatographic standards available at the compounds library of the Bioseparations Laboratory at Texas A&M University.

6.3.2 β-*cyclodextrins Inclusion Complexes with Antimicrobial Compounds*

Preparation of the inclusion complex: The inclusion complexes of *trans*-cinnamaldehyde, eugenol, garlic, and bee resin extract in β-cyclodextrin (CD) were prepared by freeze-drying (Del Valle, 2004). There was no need to prepare a complex for the lysozyme because it does not have off-flavor problems. *trans*-cinnamaldehyde or eugenol were dispersed in 500 ml of β-cyclodextrin aqueous solution (16 mM – 9.08g) in molecular ratio 1:1 and mixed in a laboratory stirrer for 24 h at room temperature (Karathanos et al., 2007). For the garlic and bee resin extract inclusion complexes, 5g of the extract were dispersed in 500ml of β-cyclodextrin aqueous solution (16 mM) and then mixed in a laboratory stirrer for 24 h at room temperature. All suspensions were

filtered through a 0.45 μm nylon filter (VWR® vacuum filtration systems, VWR International, West Chester, PA, U.S.A.). The filtrate was frozen at –20°C and freeze-dried at -50°C under 5 mtorr (9.67 x 10^{-5} psi) vacuum for 48 h in a Labconco Freeze Dry-5 unit (Labconco, Kansas City, MO, U.S.A.). Finally, the lyophilized samples were stored in a desiccator placed inside a freezer (-20°C) until further use.

Preparation of the physical mixture: A physical mixture consisting of *trans*-cinnamaldehyde, eugenol, garlic extract, or bee resin extract and β-cyclodextrin in the same weight ratio as the freeze-dried complex was prepared. The compounds and β-cyclodextrin were mixed together in a mortar and pestle for 5 min to obtain a homogeneous blend.

Study of complex formation by Differential Scanning Calorimetry (DSC): A Perkin-Elmer DSC instrument (Pyris 1 – DSC, Boston, MA, U.S.A.) was used for this study. The enthalpy calibration was carried out with Indium metal. Four different types of samples were used: β-cyclodextrin alone, compounds alone, physical mixtures and inclusion complexes, to identify differences in the DSC curves. The scan rate was 10°C/min between 70 and 230°C under nitrogen environment. The sample was accurately weighed at an accuracy of ± 0.01 mg and was placed in 40μl closed aluminum pans. The purge gas was nitrogen. Duplicate determinations were carried out for each sample (Mourtizinos et al., 2007).

Study of oxidation of compounds and its complex by DSC: DSC studies were performed to study `the stability against thermal oxidation of the samples. Samples of each compound and extract and their inclusion complexes were accurately weighed and

placed in aluminum pans with one hole in their lid. The specimens were heated from room temperature to 120^{o}C in an oxygen atmosphere at a heating rate of 90^{o}C/min. The oxygen atmosphere was provided by connecting the DSC unit to an oxygen container that provides the gas. Samples remained at 120^{o}C for 1 min to ensure a homogeneous temperature distribution within the sample and then heated up to 400^{o}C at a heating rate of 10^{o}C/min (Mourtizinos et al., 2007).

6.3.3 *Minimum Inhibitory Concentration (MIC)*

Bacterial cultures: Nalidixic acid and Novobiocin resistant mutants were derived from two parent strains of *Salmonella entereditis* and *Salmonella Typhimurium*, according to Kaspar and Tamplin (1993). In addition, *Listeria monocytogenes* (ATCC 15313, ATCC 33090), Scott A, Strain A and *Listeria innocua* (NRCC B33076) were used to inoculate fresh baby spinach leaves. All strains were obtained from the Texas A&M Food Microbiology Laboratory (College Station, TX) culture collection. These bacteria were chosen as representatives of Gram–negative and Gram-positive bacteria.

Preliminary trials were conducted to ensure that the modified organisms had the same resistance to heat, acid, and irradiation, as well as the same growth characteristics, as the parent strains. The microorganisms were kept frozen at -80^{o}C in Tryptic Soy Broth (TSB; Difco Laboratory, Sparks, MD, U.S.A.) containing glycerol (10% v/v). Before use, the stock cultures were resuscitated through 2 consecutive 24 h growth cycles in TSB at 37^{o}C to obtain working cultures containing approximately 10^{9} CFU/ml.

Antimicrobial activity: Overnight cultures of *Salmonella* spp. *(Salmonella entereditis and Salmonella typhimurium)* and *Listeria* spp. (*Listeria monocytogenes* ATCC 15313,

Listeria monocytogenes Scott A 46, *Listeria monocytogenes* strain A, *Listeria innocua* NRCC B33076, *Listeria monocytogenes* ATCC 33090), were grown in tryptic soy broth (TSB). Based on turbidity measurements, correlated with plate counts, the cultures were diluted to approximately 10^5 CFU/ml. An appropriate volume of 10^5 CFU/ml dilution was added to sterile TSB to give approximately 10^3 CFU/ml level of organism. Each of the wells of a 96-well microtiter plate (sterilized 300 μl volume – MicroWell, 96-Well Plates, NUNC, flat-bottom, Thermo Scientific, West Palm Beach, FL, U.S.A.) was charged with 125 μl of seeded TSB using a multichannel pipettor. To the first well of a row, 125 μL of the natural compound (containing either *trans*-cinnamaldehyde, eugenol, garlic extract, bee resin extract, or lysozyme + EDTA (ethylenediaminetetraacetate acid disodium salt dehydrate) was added and mixed well. After mixing, 125 μL of the well contents was transferred to the next well. This transfer procedure continued for 10 of the 12 rows of wells. The last row of well acted as a growth control. Along with each antimicrobial being screened, sterilized water blank was used in an identical fashion to ensure that the sterilized water (where the compounds were suspended) effect, if present, was not misinterpreted. The test compound concentration in the wells ranged from 4000 to 7.8 μg/ml (Kalemba and Kunicka, 2003). Similarly, the inclusion complexes with β-cyclodextrin (*t*-cinnamaldehyde-CD, eugenol-CD, propolis-CD, and garlic-CD) were tested with concentration ranging from 35000 μg/ml to 68 μg/ml. Given the volatile nature of some of the compounds, to avoid possible vapor-phase transfer between wells in a microtiter plate and losses due to evaporation, the microplates were covered with a Mylar plate sealer (Thermo Scientific).

The microtiter plates were placed into a microplate reader (Tecan SpectraFluor plus, Tecan US Inc., Durham, NC, U.S.A.) equipped with Magellan^{TM} software. The microtiter plates were incubated at 35^{o}C with agitation (100 rpm) and at every 3 hours for 36 hours absorbance of each well was measured at 550 nm. The MIC was defined as the concentration of the last row of wells where no growth occurred (no change in optical density within time). All experiments were conducted in duplicate.

6.3.4 *Radiosensitization Analysis*

Inoculation and preparation of baby spinach leaves: The two *Salmonella* spp. cultures (50 ml each in TSB) were combined to make a cocktail inoculum, final volume of 100 ml (containing ca. 9 log CFU/ml). *Salmonella* spp. was chosen it is the most frequent etiologic agent of outbreaks from fresh produce, caused 48% of such outbreaks with a known etiology between 1973 and 1997 in the United States (Sivapalasingam et al., 2004). Fresh baby spinach leaves were purchased from a local market and stored at 4^{o}C for no more than 1 day prior to the experiments. All leaves showing decay, cuts, or bruises were removed and then 50-g were weighed and dispensed into a sterile stomacher bag and inoculated with the cocktail containing *Salmonella* spp. The bag was then vigorously shaken manually for 15 min to spread the inoculum over the sample. Next, the samples were transferred to a salad spinner-type centrifuge (Oxo Intl, New York, NY, U.S.A.) to remove the excess surface inoculum inside the biological safety cabinet. This design of salad spinner incorporates a container base that captures all of the excess liquid (inoculum) removed from the leaf surface, and prevents the formation of aerosolized droplets. The spun-dried baby spinach leaves were distributed in a tray and

treated by spraying the corresponding microencapsulated antimicrobial solution (eugenol-CD complex, *t*-cinnamaldehyde-CD complex, garlic-CD complex, propolis-CD complex, and lysozyme in 30mM EDTA) at ca. 1ml/spinach leaf under a biological safety containment hood. Concentration of the antimicrobial compounds was 0.5% w/v. A drying period of 15 min for each side of the spinach leaf was allowed. After drying, samples were weighed into subsamples of 2-g, bagged into Mylar bags (ZipSeal™, 8.64 x 10.16 cm, 48GaPET/PE/0.00035 Foil/LLDPE, Sorbent Systems, Impak Co., Los Angeles, CA, U.S.A.) and sealed using a heat sealer (IPK-305H, Sorbent Systems). The bags were stored at 4^{o}C until irradiation treatment (approximately 15 h). Mylar (biaxially-oriented polyethylene terephthalate polyester) was used because of its excellent gas barrier and moisture properties (water vapor transmission rate of 0.0003g/100 in^{2}/24hrs and oxygen transmission rate of 0.0006 cm^{3}/100 in^{2}/24hrs) Furthermore, Mylar is approved by the FDA for use during irradiation of prepackaged foods ((CFR), 2009b).

6.3.5 *Irradiation*

Irradiation of samples was carried out with a 1.35 Me Van De Graaff accelerator located at Texas A&M University. The amount used in each bag (2-g – about 3 leaves of baby spinach) was in accordance with the penetration depth of the accelerator (~ 5 mm in water). Irradiation dosage was measured by placing radiochromic film dosimeters (GEX Corp., Centennial, CO, U.S.A.) at the center of the bags (front and back) containing the spinach leaves, for 2 dosimeters. The radiochromic films were read after stabilization (1h after irradiation) using a Radiochromic reader model 92 (Far West

Technology Inc., Goleta, CA, U.S.A.) and compared with a previously determined standard curve developed with gas ion chamber dosimeters.

Inoculated spinach samples were exposed to 0.2, 0.4, 0.6, 0.8, and 1.0 kGy. Non-irradiated spinach served as the control. Samples were analyzed immediately after irradiation. All experiments were done in triplicate for each antimicrobial. The degree of radiation sensitivity was defined as:

$$RS = \left(\frac{D_{10}(\text{control}) - D_{10}(\text{treatment})}{D_{10}(\text{control})} \right) * 100 \qquad [6.2]$$

Where D_{10} (control) is the D_{10}-value (without antimicrobial) and D_{10} (treatment) is the D_{10}-value of samples treated with microencapsulated antimicrobial.

6.3.6 ***Microbiological Analysis***

Initially, the bags containing the treated spinach leaves were transferred to sterile stomacher bags and hammered with the aid of a meat hammer for about 1 min (until samples were reduced to small pieces). Next, 10 ml of sterile buffer peptone water (BPW, Laboratory, Sparks, MD, U.S.A.) was added to each of the spinach samples, making a ratio of 5:1 of total solution: leaf by weight. The bags were stomached at 260 rpm for 2 min to homogenize the material using a stomacher (Seward Stomacher Lab Blenders, London, U.K.). This time period resulted in a homogenized sample, with the liquid being as dark green as could be obtained from the pulped leaves. Aliquots of the homogenized samples were drawn and serially diluted using BPW. Appropriate dilutions for each treatment were spread-plated on Tryptic Soy Agar (TSA, Difco) with 20 mg/l Nalidixic acid (Sigma-Aldrich, St. Louis, MO, U.S.A.) and 25 mg/l Novobiocin (Sigma-

Aldrich) inverted, and incubated 24h at 37^{o}C for *Salmonella* spp. enumeration. For each of the 3 replications, 2 plates per dilution were counted.

6.3.7 *Statistical Analysis*

Bacterial counts (log CFU/g) were plotted against irradiation dose in kGy. Linear regression and significance test among the slopes for each bacterial survival curve (*Salmonella* spp. under different microencapsulated antimicrobial) was determined using SPSS software for Windows, v. 16.0 (SPSS, 2007). Linear regression and analysis of covariance with 95 % confidence interval ($P \leq 0.05$) were used. The radiation D_{10}-values for the *Salmonella* spp. cocktail were calculated based on the negative reciprocal of the slope for the linear regression line.

6.4 Results and Discussion

6.4.1 *Garlic Extract and Characterization*

The garlic extract employed was 1.98g/ml (total weight of garlic per milliliter) and contained an estimated 988.2 μg/ml of allicin, as determined spectrophometrically. Allicin represents about 70% of the overall thiosulfinates present or formed upon crushing the garlic cloves (Miron et al., 2002).

6.4.2 *Bee Resin Extract and Characterization*

The results of HPLC analysis (Figure 6.1) allowed the identification of the following major phenolic compounds: *p*-coumaric (retention time of 23.13 min), ferulic acid (RT = 22.36 min), cinnamic acid (RT = 33.70 min), benzoic acid (RT = 31.91 min) as well as the flavonoids quercetin (RT =30.56 min) and kampferol (RT = 38.36 min). Absorption spectra obtained with a photodiode detector were used to compare and

distinguish peaks. The flavonoids and phenolic compounds act on the microbial membrane or cell wall site, causing functional and structural damages (Scazzocchio et al., 2006), conferring the antimicrobial capability of propolis extracts.

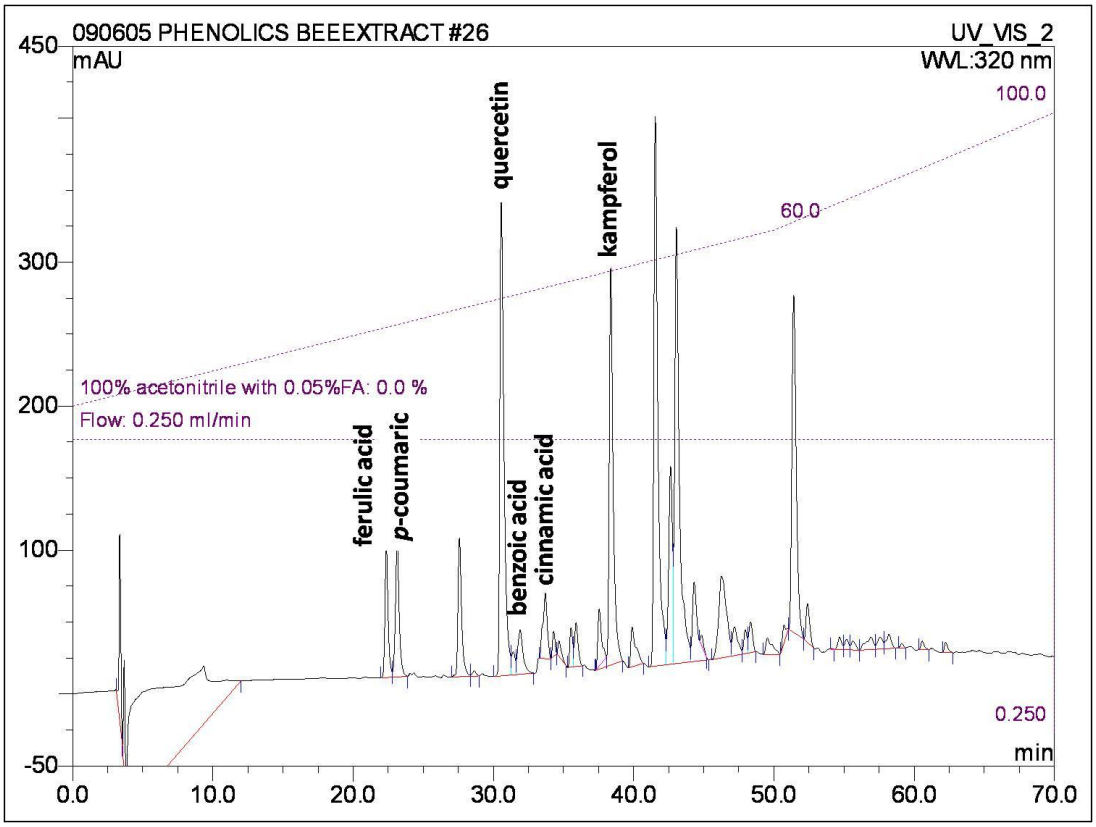

Figure 6.1. HPLC chromatogram of ethanolic extract of propolis.

6.4.3 β-*cyclodextrins Inclusion Complexes with Antimicrobial Compounds*

The formation of the inclusion complexes was confirmed by DSC in an inert atmosphere. Figures 6.2 and 6.3 show the DSC results for the different types of samples. Propolis extract DSC scan exhibited an endothermic peak at 82.3^{o}C, possibly due to

melting point of phenolic compounds and ethanol present on the extract (Figure 6.2a). The DSC thermogram of β-CD showed an endothermic peak at 165.5^{o}C (Figure 6.2b), possibly due to elimination of the contained water. The DSC scan of the physical mixture showed an endothermic peak at 128.8^{o}C, (Figure 6.2c) which could possibly indicate a partial complex formation by paste complexation (only a small amount of water is added to form a paste, which is mixed with the cyclodextrin using a mortar and pestle) (Del Valle, 2004). On the other hand, the disappearance of the endothermic peaks assigned to the constituents of the propolis extract at 82.3^{o}C (Figure 6.2d) indicate an inclusion complex was produced between propolis extract constituents and β-CD and not simply a physical mixture.

Similarly, for garlic extract (Figure 6.3a), an endothermic peak is observed at 120^{o}C. The DSC thermogram of the physical mixture shows a few more peaks (93^{o}C, 110^{o}C, and 135^{o}C) which could indicate a partial complex formation between garlic extract components and β-CD by paste complexation (Figure 6.3b). The elimination of the endothermic peak at 120^{o}C, assigned to pure garlic extract, and the other peaks on the physical mixture (Figure 6.3a and 6.3b) imply that an inclusion complex rather than a simple physical mixture has been formed between garlic extract constituents and β-CD.

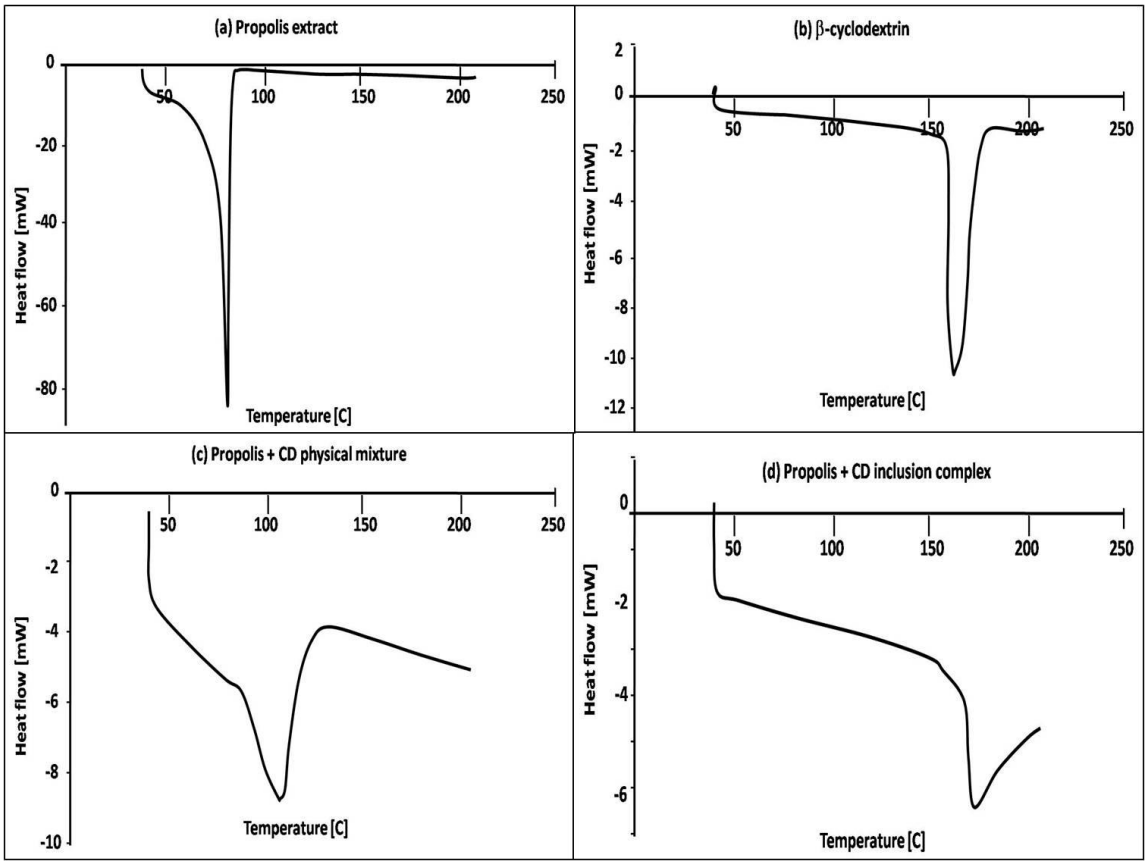

Figure 6.2. DSC thermograms of a) propolis extract, b) β-cyclodextrin, c) physical mixture of propolis and β-cyclodextrin, d) inclusion complex of propolis and β-cyclodextrin.

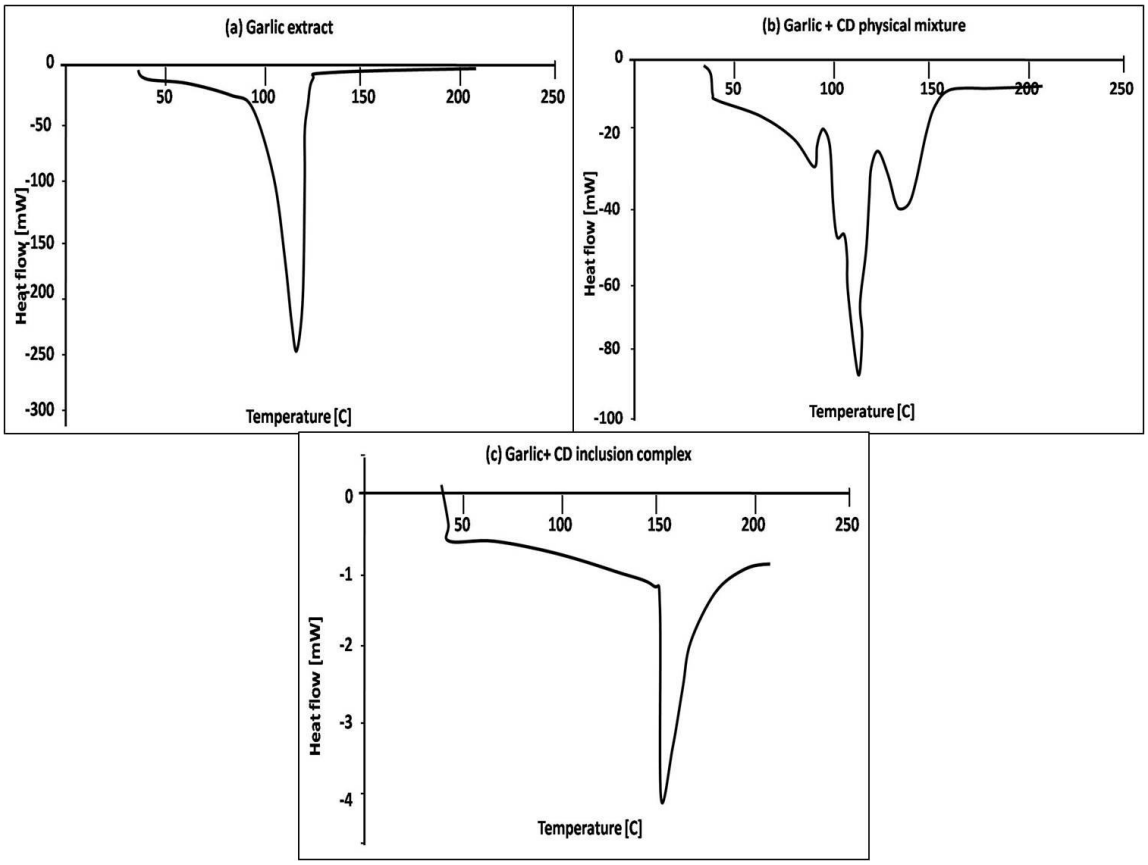

Figure 6.3. DSC thermograms of a) garlic extract, b) β-cyclodextrin, c) garlic extract β-cyclodextrin inclusion complex.

Since *trans*-cinnamaldehyde and eugenol are liquid at room temperature, no DSC thermographs can be obtained for these substances in order to prove the formation of its inclusion complexes. The inclusion of *trans*-cinnamaldehyde and eugenol can be confirmed using DSC indirectly by comparing the thermal stability of the free compound with the encapsulated form (inclusion complex with β-CD). The expected higher thermal stability of the encapsulated compound may be considered as an indirect proof of inclusion (Karathanos et al., 2007). Exothermic peaks observed at 265^{o}C and 260^{o}C for pure *trans*-cinnamaldehyde and eugenol, respectively, are related to their oxidation

(Figure 6.4 and 6.5). These peaks are not present in the DSC thermogram of their inclusion complexes, indicating that both *trans*-cinnamaldehyde and eugenol are protected from oxidation, being inside the β-CD cavity, and providing an indirect proof of *trans*-cinnamaldehyde and eugenol inclusions. The exothermic curves emerging after 350^{o}C for either *trans*-cinnamaldehyde and eugenol β-CD complexes in their respective thermographs are probably due to the decomposition of β-CD.

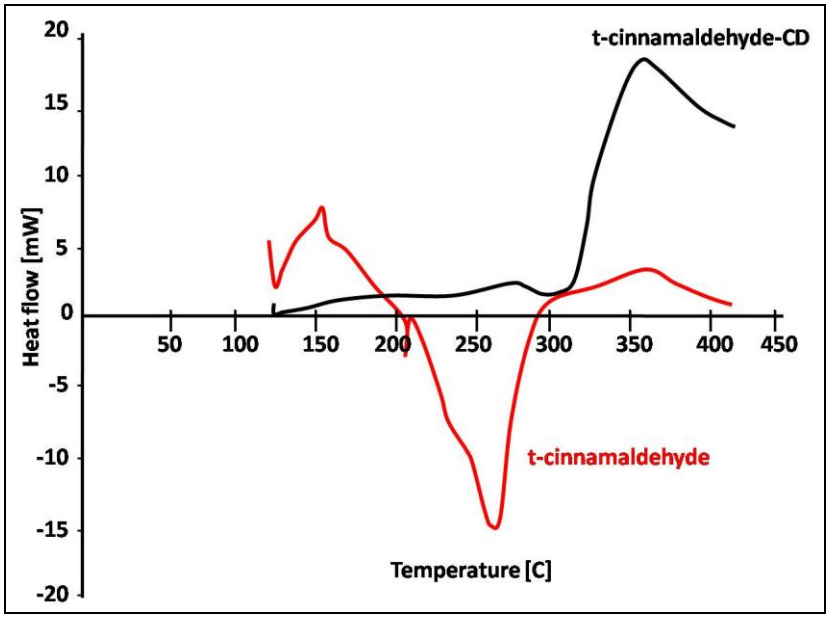

Figure 6.4. DSC thermograms of pure *trans*-cinnamaldehyde and inclusion complex of *trans*-cinnamaldehyde and β-cyclodextrin under oxidative conditions.

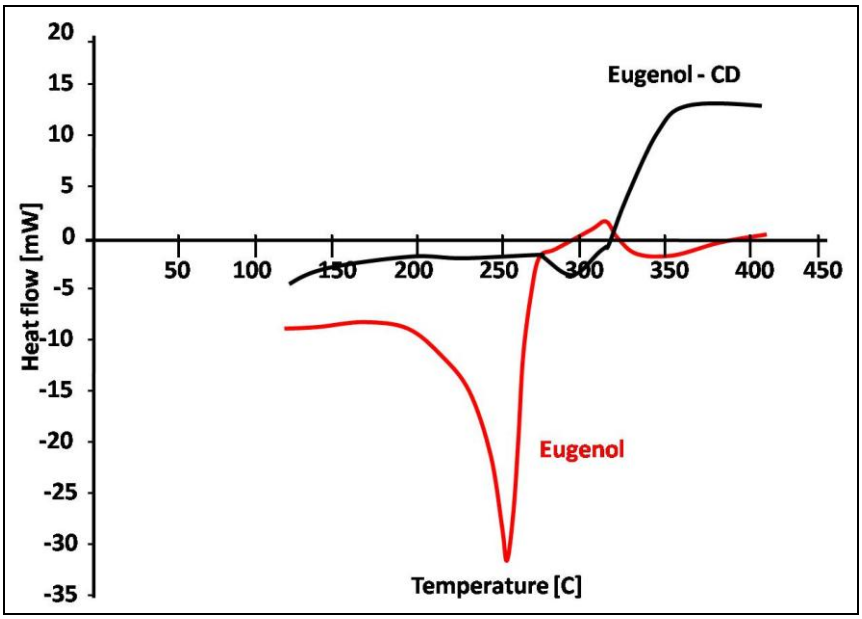

Figure 6.5. DSC thermograms of eugenol and inclusion complex of eugenol and β-cyclodextrin under oxidative conditions.

6.4.4 *Minimum Inhibitory Concentration (MIC)*

All the natural compounds including their inclusion complexes with β-cyclodextrin tested showed, at different levels, activity in inhibiting the growth of both microorganisms (*Salmonella* spp. and *Listeria* spp.) by the broth dilution method (Figures 6.6 to 6.9). The growth of *Salmonella* spp. and *Listeria* spp. was inhibited by *trans*-cinnamaldehyde and propolis extract at 500 μl/ml (Table 6.1) which demonstrates the broad range of action and effectiveness of these two antimicrobial compounds.

Eugenol inhibited bacterial growth at 500 and 2000 μg/ml (Table 6.1) for *Salmonella* spp. and *Listeria* spp., respectively. It is commonly know that Gram-positive bacteria are more susceptible to essential oils and Gram-negative ones are less sensitive.

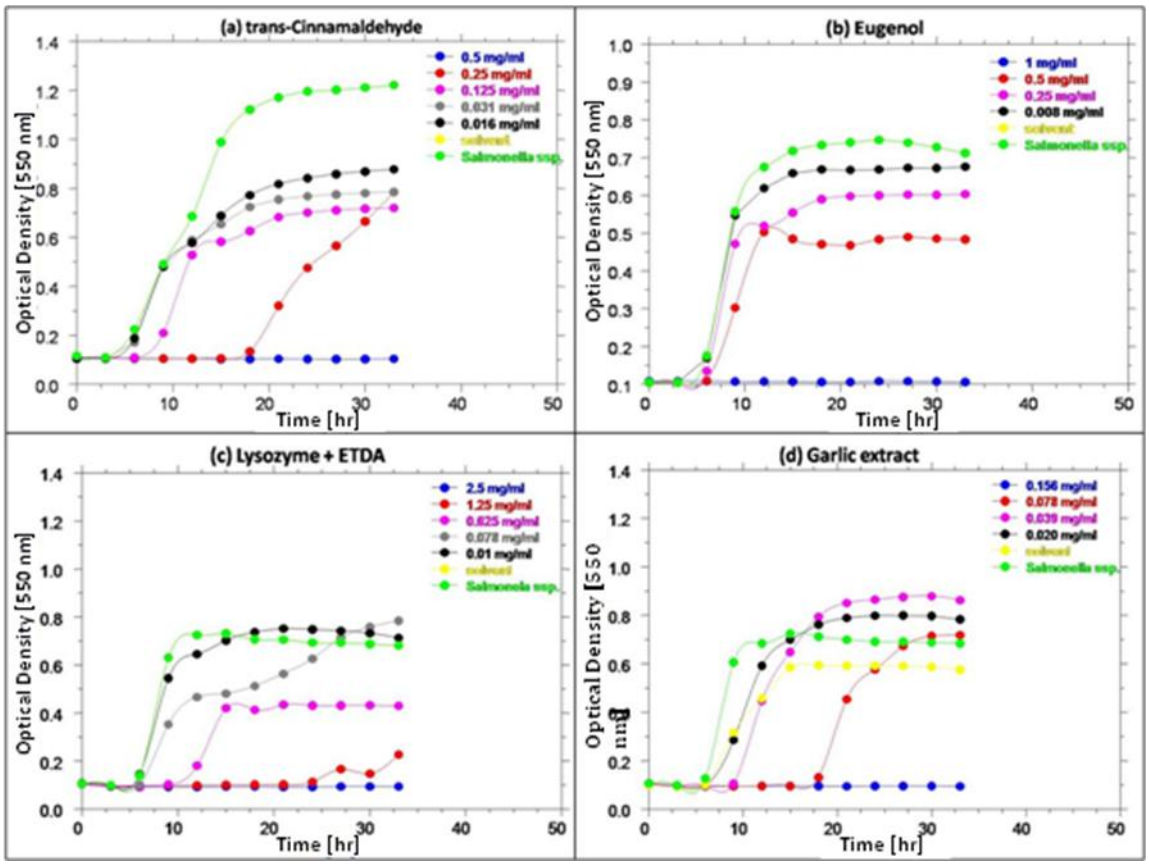

Figure 6.6. Growth of *Salmonella* spp. in tryptic soy broth as a function of active compound.

The growth of *Salmonella* spp. and *Listeria* spp. were inhibited by Lysozyme with EDTA at 2000 and 78.12 μg/ml with 15mM and 0.5mM EDTA (Table 6.1), respectively. These results are in agreement with other studies (Wilkins and Board, 1989). Furthermore, EDTA enhances penetration of the lysozyme to the peptidoglycan; without the addition of EDTA the growth of *Salmonella* spp. was not inhibited by lysozyme at the concentrations used (data not shown).

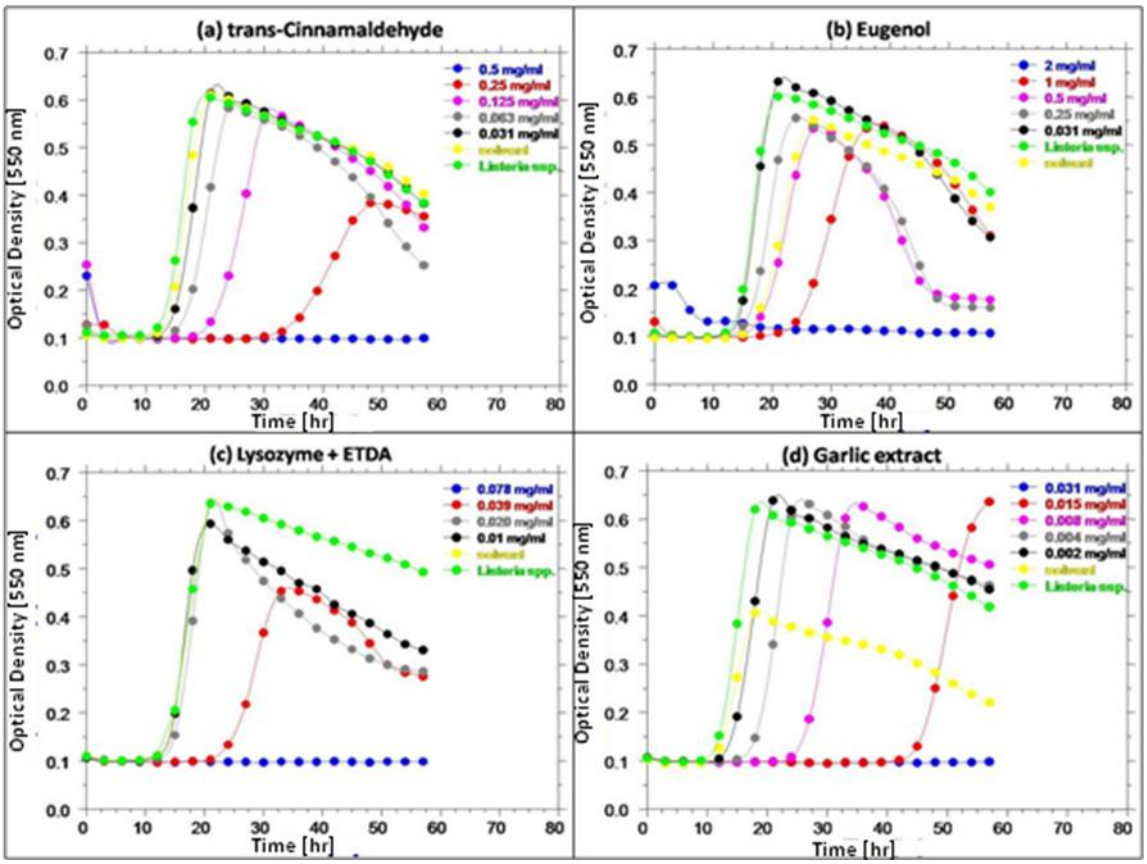

Figure 6.7. Growth of *Listeria* spp. in tryptic soy broth as a function of active compound.

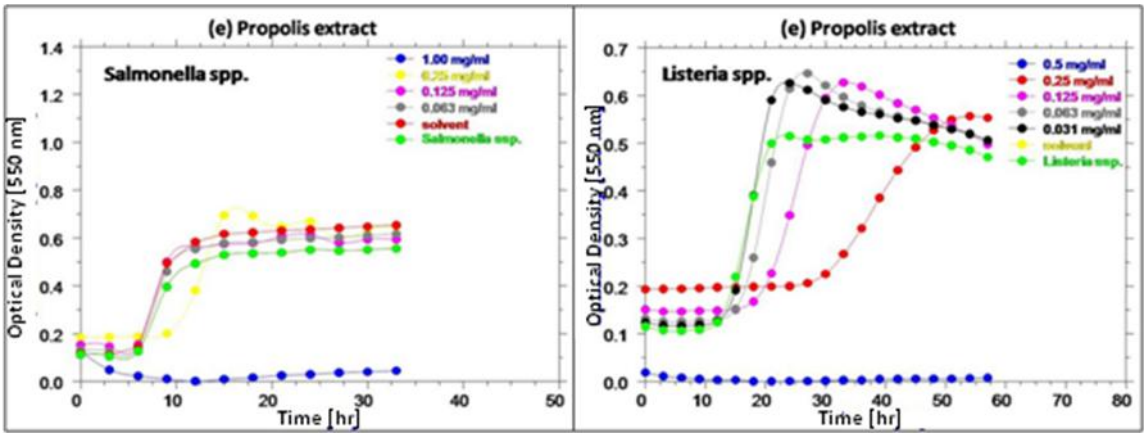

Figure 6.8. Growth of *Salmonella* spp. and *Listeria* spp.in tryptic soy broth as a function of active compound.

Growth of *Salmonella* spp. and *Listeria* spp. were fully inhibited by garlic extract at the concentrations of 15.4 μg/ml and 30.8 μg/ml in terms of allicin content, respectively. These values would be equivalent to a concentration of 62 mg/ml and 31 mg/ml of garlic extract, respectively. The structural differences of the bacterial strains may play a role in the bacterial susceptibility to garlic constituents. While the main active agent in garlic, allicin, is known to be able to penetrate cell membranes (Tynecka and Gos, 1975) it is tempting to speculate that features of the bacterial cell envelope my influence its access to periplasmic and cytoplasmic enzymes (Bakri and Douglas, 2005; Miron et al., 2000). The lipid content of the membranes will have an effect on the permeability of allicin and other garlic constituents (Sivam, 2001). Furthermore, perhaps the thick peptidoglycan layer in the Gram-positive cell envelope might impair access of the allicin to some extent to the Gram-positive cell membrane, and consequently making them more resistant to garlic extract as observed in this study.

Table 6.1. Minimal Inhibitory Concentration (MIC) of natural compounds and their respective inclusion complexes with β-cyclodextrin against Gram-positive and negative bacteria.

Antimicrobial compound	***Salmonella* spp. [μg/ml]**	***Listeria* spp. [μg/ml]**
trans-Cinnamaldehyde	500	500
Eugenol	500	2,000
Lysozyme + EDTA	2,000	78
Garlic Extract*	15	31
Propolis Extract	500	500
trans-cinnamaldehyde-CD	5,000	2,500
Eugenol-CD	5,000	10,000
Garlic extract-CD	10,000	20,000
Propolis extract-CD	10,000	10,000

*allicin

A similar pattern was observed for the microencapsulated complexes of the natural compounds. The MIC concentrations of the inclusion complexes were higher ($P<0.05$) than the respective pure constituents (Figures 6.7-6.8 and 6.9-6.10 and Table 6.1). Therefore, the inclusion complexes could be used as antimicrobial agents with the added advantage of masking their characteristic strong odor/off-flavor and stability during storage (i.e. protected from oxidation), and consequently broadening their range of application in food products.

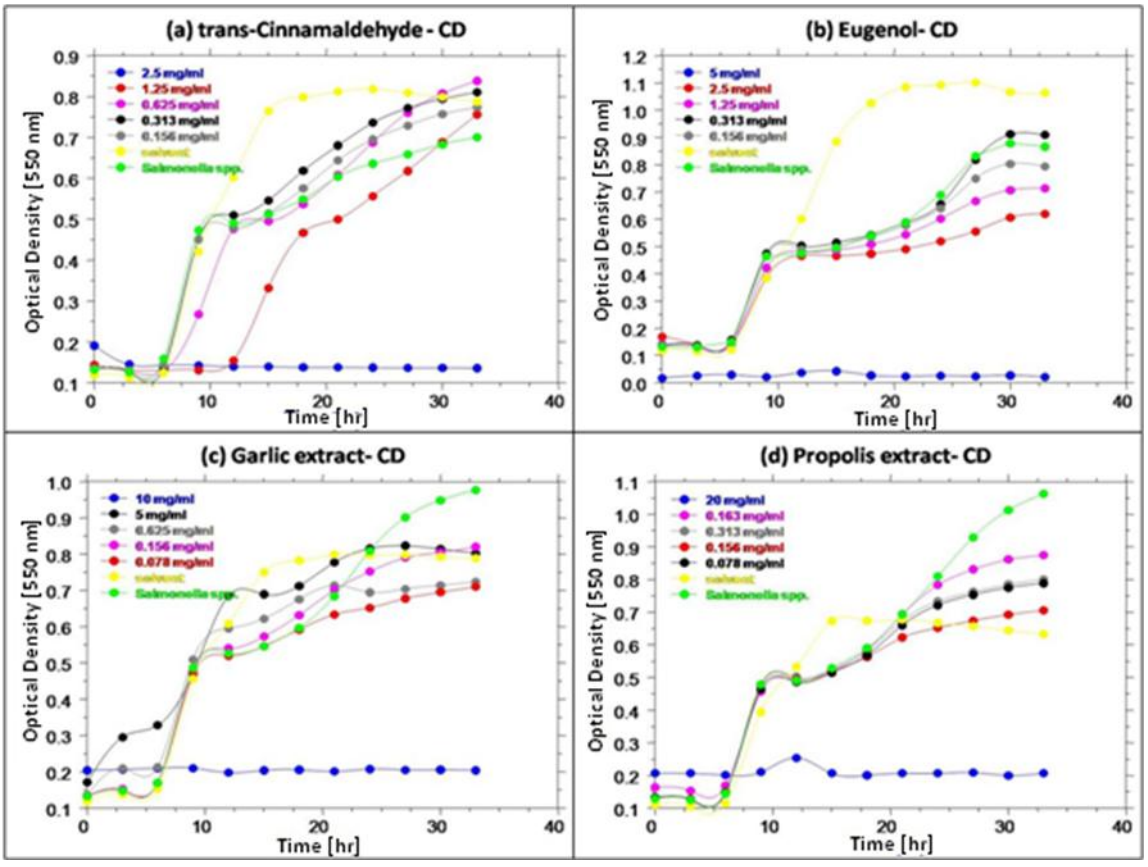

Figure 6.9. Growth of *Salmonella* spp. in tryptic soy broth as a function of active compounds and their respective inclusion complexes with β-cyclodextrin.

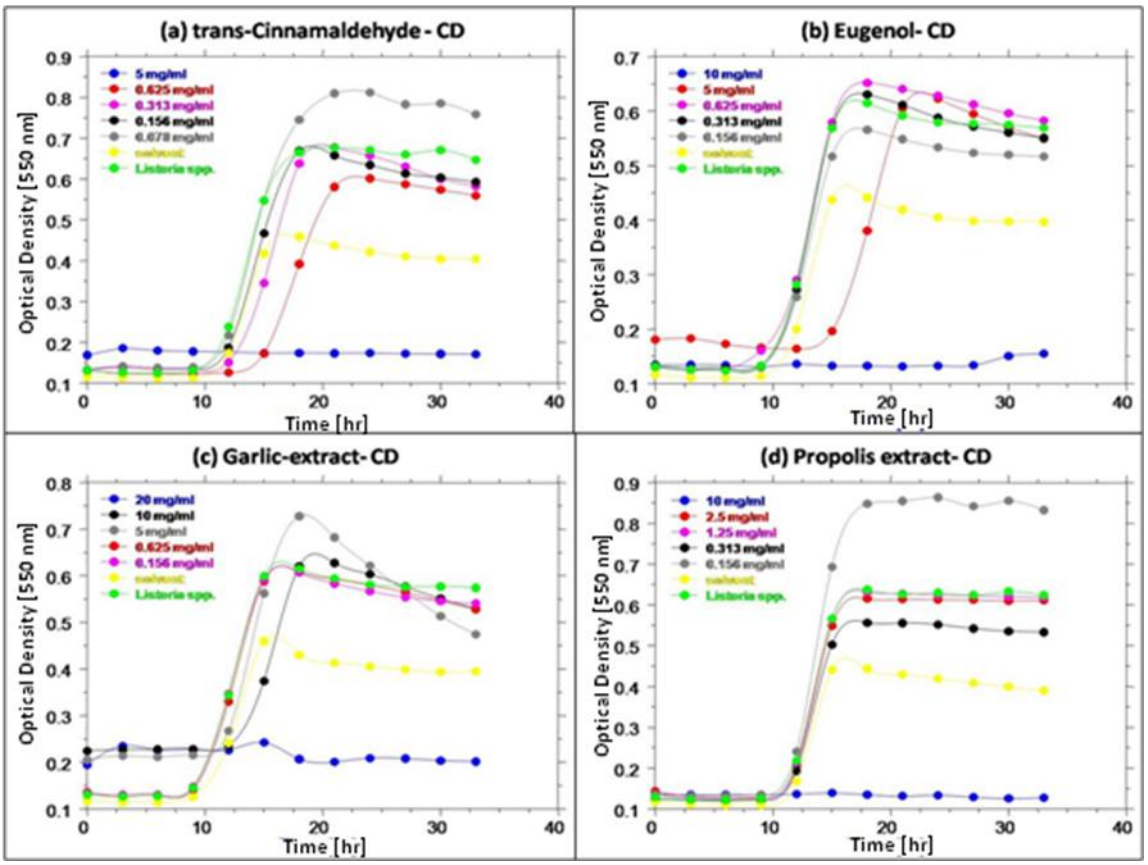

Figure 6.10. Growth of *Salmonella* spp. and *Listeria* spp.in tryptic soy broth as a function of active compounds and their respective inclusion complexes with β-cyclodextrin.

The solvents were the natural compounds were suspended (sterilized water, ethanol, and EDTA alone (at the concentration levels tested) were not bactericidal to any of the strains. MICs for all the compounds and their respective microencapsulated complexes with the two bacteria species are summarized in Table 6.1.

Concentration of the natural compounds and their respective inclusion complex below the MIC slowed the growth rate of both microorganisms. sub-MIC levels of natural compounds have a marked effect on cell growth, decreasing the final absorbance

achieved at the stationary phase (12 hr and 21 hr for *Salmonella* spp. and *Listeria* spp., respectively) and prolonging the lag phase.

These results confirm the potential application of essential oils and other natural components as effective antimicrobial agents to control foodborne pathogens.

6.4.5 *Radiosensitization Analysis*

The influence of the microencapsulated compounds and lysozyme with EDTA on the radiosensitization of *Salmonella* spp. in baby spinach leaves is shown in Table 6.2. Figure 6.11 shows the effects of different antimicrobial compounds (*trans*-cinnamaldehyde-CD, eugenol-CD, propolis extract -CD, garlic extract, and lysozyme + 30mM EDTA) on the slope (D_{10}-value) of the radiation survival curve of *Salmonella* spp. at room temperature.

Table 6.2. Radiation sensitivity of *Salmonella* spp. in baby spinach leaves when sprayed with antimicrobial compounds and irradiated at room temperature (20°C).

Treatment	***Salmonella* spp.**		
Antimicrobial compounds	**D_{10}-value [kGy]**	**[1]R²**	**[2]RS**
Air (control)	[c] 0.19±0.00	0.99	-
trans-cinnamaldehyde-CD	[b] 0.14±0.01	0.99	28%
Eugenol-CD	[b] 0.14±0.01	0.99	24%
Propolis extract-CD	[a, b] 0.13±0.00	0.99	33%
Garlic extract-CD	[a, b] 0.13±0.00	0.99	34%
Lysozyme with EDTA	[a] 0.11±0.01	0.98	43%

[a,b]Means within a column which are not followed by a common superscript letter are significantly different (P < 0.05).
[1] coefficient of determination of the linear regression between Log(No/N) vs. Dose.

[2]RS - Percentage of increase on radiation sensitivity = $\left(\frac{D_{10}(control) - D_{10}(treatment)}{D_{10}(control)}\right) * 100$

The presence of antimicrobial compounds affected (P<0.05) the radiosensitivity of *Salmonella* spp. for all the compounds tested. The radiation sensitivity (RS) of *Salmonella* spp. in baby spinach leaves without antimicrobial compounds was 0.190

kGy. The most effective active compound was Lysozyme with 30mM EDTA, with a D_{10}-value of 0.108 kGy, which represents a 43% increase in radiation sensitivity. Spraying microencapsulated garlic and propolis extract had a significant improvement ($P<0.05$) of 33-34% in the radiation sensitivity, with a D_{10}-value of 0.127 kGy. In the presence of microencapsulated *trans*-cinnamaldehyde and eugenol, the D_{10}-values obtained were 0.137 and 0.144 kGy, with an improvement in the radiation sensitivity of 28 and 24%, respectively. Among the microencapsulated antimicrobial compounds, even though their D_{10}-values were numerically different not statistically they are not different, showing a maximum improvement in *Salmonella* spp. sensitivity of 34%. Clearly, the spraying of antimicrobial compounds had a strong effect on the radiation dose required to eliminate *Salmonella* spp. in baby spinach leaves.

As shown in Table 6.3, less than 2 logs reduction in *Salmonella* spp. was observed when the antimicrobial compounds were used alone, without irradiation. The microbial population decreased and then increased again during the 15-day period and varied with the antimicrobial agent. However, it was observed that the microbial population growth weakened, indicated by the smaller cluster sizes. It seems that the microencapsulated compounds would diffuse faster with the help of ionizing radiation.

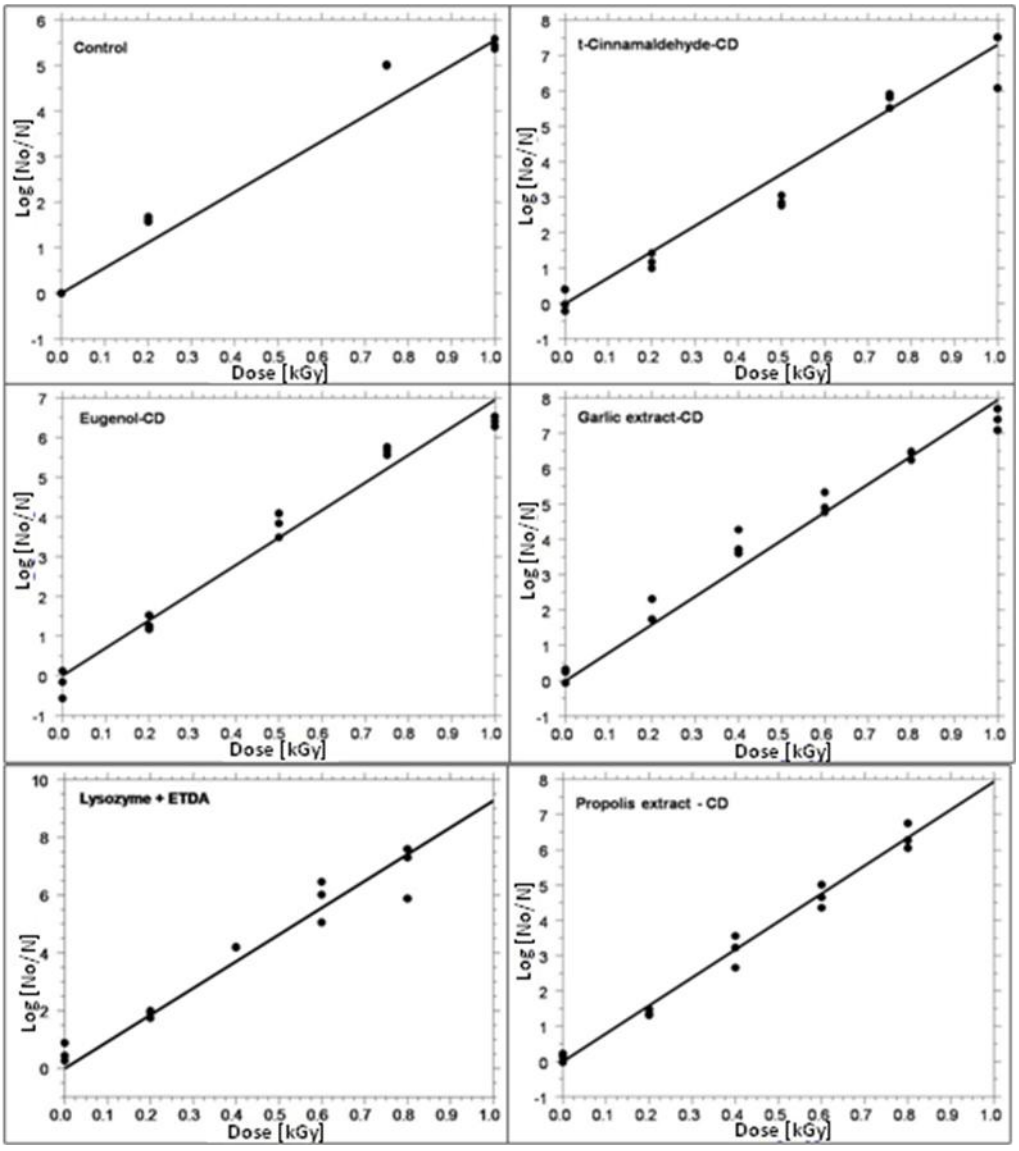

Figure 6.11. Effect of microencapsulated antimicrobial compounds (0.5% w/v) sprayed on baby spinach on radiation inactivation of *Salmonella* spp. at room temperature.

One factor that could explain why Lysozyme with EDTA was the most effective antimicrobial compound would be because that it was not microencapsulated. By being free in the medium Lysozyme probably had more opportunity to interact with the bacteria while the microencapsulated compounds had first to be released from the β-

cyclodextrin ring, which is controlled by an equilibrium constant. The rate of release will depend upon the relative affinities of the guest and its concentration (Hedges et al., 1998). These also would explain the difference in radiation sensitivity among the microencapsulated compounds, since each of them would have their characteristic release profile.

Therefore, the application of antimicrobial compounds with electron beam irradiation had a synergistic effect on the radiation sensitivity of *Salmonella* spp. in baby spinach leaves. A combination of antimicrobial compounds with irradiation effected the inactivation of *Salmonella* spp. than could be achieved by either treatment applied alone. An effective treatment of 0.5 kGy at room temperature would assure a 5-log reduction of *Salmonella* spp. in baby spinach leaves if sprayed with a solution of 0.5% w/v lysozyme and EDTA.

Table 6.3. Log reduction of *Salmonella* spp. in baby spinach leaves when sprayed with antimicrobial compounds during storage at 4^{o}C for 15 days.

	Log reduction (No/N) of *Salmonella* spp.			
Storage time	**CD-cinnamaldehyde**	**CD-eugenol**	**CD-garlic**	**CD-propolis**
Day 0	1.25	0.97	0.85	0.78
Day 1	1.28	1.23	0.97	1.16
Day 3	1.16	1.44	0.94	1.25
Day 6	NA	1.12	1.27	1.32
Day 9	1.58	0.47	1.00	1.21
Day 15	0.31	0.47	0.20	1.74

6.5 Conclusions

This study shows that the natural compounds and extracts investigated were effective in inhibiting growth of both Gram-positive and Gram-negative microorganisms, at different levels. All of the substances studied show potential for use

as antimicrobial agents in food systems. Inclusion complexes containing natural compounds and extracts with β-cyclodextrin were successfully obtained and their inclusion complexes were protected from oxidation. Moreover, encapsulation of the natural compounds and extracts preserved their antimicrobial activity, which contributes to the successful application of such natural preservatives in foods, by masking their strong flavor and odor.

The spraying of microencapsulated natural antimicrobial compounds increased the irradiation sensitivity of *Salmonella* spp. in baby spinach by 34%, and Lysozyme with EDTA being the best treatment increasing sensitivity up to 43%. The best treatment to achieve a 5-log reduction would be irradiation at 0.5 kGy at room temperature with baby spinach leaves sprayed with 0.5 % (w/v) Lysozyme and EDTA. Further work will be conducted to investigate in more detail the effect of the suggested treatment on product quality throughout shelf-life.

CHAPTER VII

POLY (DL-LACTIDE-CO-GLYCOLIDE) (PLGA) NANOPARTICLES WITH ENTRAPPED *TRANS*-CINNAMALDEHYDE AND EUGENOL FOR ANTIMICROBIAL DELIVERY APPLICATIONS

7.1 Overview

Eugenol and *trans*-cinnamaldehyde are natural compounds known to be highly effective antimicrobials. However, both are hydrophobic molecules, a limitation to their use within the food industry. The goal of this study was to synthesize spherical poly (DL-lactide-co-glycolide) (PLGA) nanoparticles with entrapped eugenol and *trans*-cinnamaldehyde for future antimicrobial delivery applications. The emulsion evaporation method was used to form the nanoparticles in the presence of poly (vinyl alcohol) (PVA) as a surfactant. The inclusion of antimicrobial compounds into the PLGA nanoparticles was accomplished in the organic phase. Synthesis was followed by ultrafiltration (performed to eliminate the excess of PVA and antimicrobial compound) and freeze-drying. The nanoparticles were characterized by their shape, size, entrapment efficiency and, antimicrobial efficiency. The entrapment efficiency for eugenol and *trans*-cinnamaldehyde was approximately 98% and 92%, respectively. Controlled release experiments conducted *in vitro* at 37^{o}C and 100 rpm for 72 hrs showed an initial burst followed by a slower rate of release of the antimicrobial entrapped inside the PLGA matrix. All loaded nanoparticles formulations proved to be efficient in inhibiting growth of *Salmonella* spp. (Gram-negative) and *Listeria* spp. (Gram-positive) with

concentrations ranging from 20 to 10 mg/ml. Results suggest that the application of these antimicrobial nanoparticles in food systems may be effective at inhibiting specific pathogens.

7.2 Introduction

Natural compounds that do not have any significant medical or environmental impact could potentially serve as effective alternatives to conventional antibacterial or antifungal agents. In this context, the activity of several essential oils against both important human pathogenic and food spoilage microorganisms should be studied (Burt, 2004; Hammer et al., 1999).

Although the majority of the essential oils are classified as Generally Recognized As Safe (GRAS), their use in foods as preservatives is often limited due to flavor considerations, since effective antimicrobial doses may exceed organoleptically acceptable levels.

In antimicrobial action of essential oil components, the lipophilic character of their hydrocarbon skeleton and the hydrophilic character of their functional groups are of great importance. The activity rank of essential oil components is as follows: phenols > aldehydes > ketones > alcohols > hydrocarbons. The Phenols include thyme, savory and oregano oils containing thymol and carvacrol as well as clove oil containing eugenol. Cinnamon oil with cinnamaldehyde as the main component is also a member of this group (Kalemba and Kunicka, 2003; Knobloch et al., 1989).

Cinnamaldehyde (cinnamic aldehyde or 3-phenyl-2-propenal)) is the main component in cassia oil as well as cinnamon bark oil, and is a GRAS for food use based

on 21 CFR (Code of Federal Regulation) part 172.515 ((CFR), 2009a). It has been shown to be the major antimicrobial compound in cinnamon. In addition to exhibiting antibacterial activity, cinnamic aldehyde also inhibits mold growth and mycotoxin production (Beuchat, 1994).

Eugenol (2-methodxy-4-(2-propenyl) phenol) is a major constituent in clove oil and present in considerable amounts in the essential oil of allspice. It is also a GRAS for food use based on 21 CFR part 172.515 ((CFR), 2009a). Karapinar and Aktug (1987) reported that eugenol was more effective against *Salmonella typhimurium, Staphylococcus aureus,* and *Vibrio parahaemolyticus* than were thymol, anethol, and menthol (Beuchat, 1994).

In the last decades, micro and nanosized colloidal carriers have received a growing scientific and industrial interest (Thies, 1996). These vectors may be capsules (with liquid core surrounded by a solid shell), particles (polymeric matrices), vesicles or liposomes, multiple or single emulsions and have found a wide range of applications. They may be loaded by living cells, enzymes, flavor oils, pharmaceuticals, vitamins, adhesives, agrochemicals, catalysts, and offer considerable advantages at use. Liquids can be handled as solids, odor or taste can be effectively masked in a food product, sensitive substances can be protected from deleterious effects of the surrounding environment, toxic materials can be safely handled, and drug delivery can be controlled and targeted (Robinson, 1997).

Synthetic polymers and natural macromolecules have been extensively researched as colloidal materials for nanoparticles production designed for drug delivery.

Synthetic polymers have the advantage of high purity and reproducibility over natural polymers; with the polyester family (i.e., poly (lactic acid) (PLA), poly(e-caprolactone) (PCL), and poly (glycolic acid) (PGA) being of great interest in the biomedical area because of their biocompatibility and biodegradability properties. In particular, poly (lactide-co-glycolide) (PLGA) has been FDA approved for human therapy (Anderson and Shive, 1997).

Along with other physical characteristics, the size and size distribution of the PLGA nanoparticles, are affected by the technique used for nanoparticle production and the pertinent synthesis parameters, i.e., PLGA molecular mass, the addition of active components, surfactants, and other additives (Barrat et al., 2000; Brigger et al., 2002; Chorny et al., 2002; Hans and Lowman, 2002; Nakache et al., 2000; Westesen, 2001).

Emulsion evaporation, emulsion diffusion, salting out, nanoprecipitation, and solvent displacement are some of the common methods used to form nanoparticles from preformed polymers (Astete and Sabliov, 2006).

Spices and herbs have been used for millennia to provide distinctive flavor for foods and beverages around the world. In addition to contributing flavor to foods, many spices also exhibit antimicrobial activity. Essential oils are the odorous, volatile products of plant secondary metabolism, normally formed in special cells or groups of cells or as glandular hairs, found on many leaves and stems (Bernfeld, 1967). The antimicrobial action of essential oils in model food systems or in real food is well documented in the literature (Koutsoumanis, 1998; Lambert et al., 2001).

Despite the development of antibiotics, bacterial and fungal infections are still a major issue in medicine, and the presence of numerous drug-resistant strains poses a new challenge. Herbal drugs have been extensively used in this field for many centuries. Recently, there has been a growing interest in natural products due to their availability, fewer side effects or toxicity as well as better biodegradability as compared to the available antibiotics and preservatives (Kalemba and Kunicka, 2003).

Delivery of eugenol and *trans*-cinnamaldehyde entrapped in polymeric nanoparticles has definite advantages over the delivery of non-entrapped antimicrobials. The release rate of these compounds can be controlled and the dose frequency reduced. Furthermore, the bioactivity and stability of the active substance entrapped in the nanoparticles is protected by encapsulation (Lamprecht et al., 2001; Uhrich et al., 1999; Zigoneanu et al., 2008). Also, it will prevent the loss of volatiles and improve their solubility in a hydrophilic medium, which broadens its application. In the food industry, it has become apparent that inclusion of lipophilic bioactives in food matrices is one of the major problems that manufacturers have when developing health-and-wellness-promoting foods.

There has been very little published on the release mechanism and kinetics of antimicrobial agents from nanoparticles. Most studies have measured the release of drugs from micro or nanoparticles (Anderson and Shive, 1997; Astete, 2006). In order to understand the release of antimicrobial agents, the parameters of *trans*-cinnamaldehyde and eugenol diffusion kinetics must be determined.

Thus, the objectives of this study were: (1) to synthesize poly (D,L-lactide-co-glycolide) (PLGA) nanoparticles with entrapped *trans*-cinnamaldehyde and eugenol with poly (vinyl alcohol) (PVA) as surfactant; (2) to characterize the size, size distribution, morphology, entrapment efficiency and controlled release profile of the synthesized nanoparticles; (3) to determine the minimum inhibitory concentration (MIC) in order to establish their antimicrobial efficiency; and (4) to determine the diffusion kinetics of *trans*-cinnamaldehyde and eugenol from the nanoparticles.

7.3 Materials and Methods

7.3.1 *Materials*

Poly (D,L-lactide-co-glycolide acid) (PLGA), with a copolymer ratio of DL-lactide to glycolide of 65:35 (M_w 40,000-75,000 g/mol, P2066 , Sigma-Aldrich -St. Louis, MO, U.S.A.) was used in this study. The surfactant used in the emulsification process was poly (vinyl alcohol) (PVA) (98-99% hydrolysis degree and average M_w 30,000-50,000 g/mol, 363138, Sigma-Aldrich, St. Louis, MO, U.S.A.). *trans*-Cinnamaldehyde, 99% (C80687),and eugenol, 99% (E51791), were also purchased from Sigma-Aldrich (St. Louis, MO, U.S.A.). Sodium chloride, 99.5%, sodium dodecyl sulfate (SDS), 99%, acetonitrile (HPLC grade), D(+) trehalose, 98% were obtained from VWR International (West Chester, PA, U.S.A.). Nanopure water was obtained using Nanopure Diamond (Barnsted International, Dubuque, IA, U.S.A.).

7.3.2 *Synthesis of Nanoparticles with Entrapped* trans-*Cinnamaldehyde and Eugenol*

The nanoparticles were prepared by an emulsion evaporation method (Figure 7.1) similar to Zigoneanu et al. (2008). Unloaded PLGA nanoparticles were also synthesized

and used as control systems. Normally, the organic phase was formed by dissolving 50 mg of PLGA in 2 ml of dichloromethane, with or without *trans*-cinnamaldehyde or eugenol (16% w/w – relative to PLGA). An aqueous phase (20 ml) was formed with 0.3% (w/v) PVA in nanopure water. The organic phase was added in droplets to the aqueous phase, and the emulsion was formed under homogenization (Ultra-Turrax T25 basic Ika®-Works, Inc., Wilmington, NC, U.S.A.) for 2 min at 95000 rpm. Next, the emulsion was sonicated in an ice bath at 2^{o}C at 70 W of energy output (Cole Parmer 8890 ultrasonic cleaner, Vernon Hills, IL, U.S.A.) during 10 min. Dichloromethane was evaporated under vacuum (operating at 28 inHg (50 torr)) for 20 min in a rotoevaporator (Buchi R-210 Rotavapor, Buchi Co., New Castle, DE, U.S.A.) (Zigoneanu et al., 2008). Unloaded (control) nanoparticles were prepared using the same procedure described above, without addition of *trans*-cinnamaldehyde or eugenol to the organic solvent.

Following synthesis, the nanoparticles were purified by ultrafiltration to remove the excess of surfactant (PVA) and *trans*-cinnamaldehyde or eugenol. A Millipore-Labscale^{TM} TFF system equipped with a 10kDa cutoff Pellicon XL-Millipore (Millipore Co, Kankakee, IL, U.S.A.) was used. The nanoparticles were ultrafiltered with 300 ml of water and 50 ml was collected (retentate). Inlet pressure was 40 psi and outlet pressure in the system was 40 psi and 10 psi, respectively. After ultrafiltration, nanoparticles were kept for 2 h at -80^{o}C and freeze-dried at -50^{o}C under 5 mtorr (9.67 x 10^{-5} psi) vacuum for 48 h in a Labconco Freeze Dry-5 unit (Labconco, Kansas City, MO, U.S.A.). D(+) trehalose was added to the nanoparticles suspension before precoooling at a ratio of 1:1

(w/w) relative to the amount of nanoparticles. Finally, the lyophilized samples were stored in desiccator placed in the freezer (-20^{o}C) for further use (Astete, 2006).

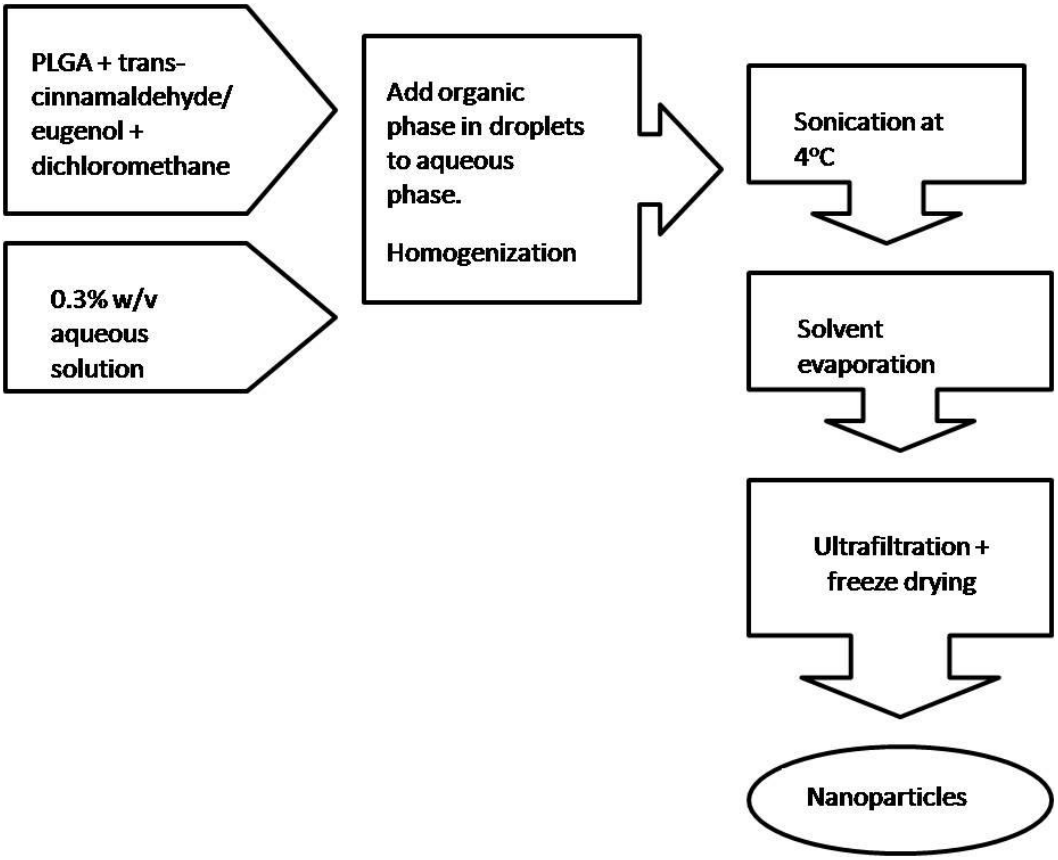

Figure 7.1. Schematic diagram of nanoparticle synthesis with entrapped *trans*-cinnamaldehyde and eugenol using PVA as surfactant

7.3.3 *Size and Size Distribution*

The size distribution of the nanoparticles was determined in nano-pure water at 25^{o}C temperature using a particle size analyzer (90 Plus particle size analyzer, Brookhaven Instruments Co., Holtsville, NY, U.S.A.). For the measurements, 200μL of the nanoparticles suspension was dispersed in 2 ml. The water was previously filtered

using a 0.02 μm filter (Anotop 10, Whatman, Piscataway, NJ, U.S.A.). The analysis was performed at a scattering angle of 90^{o}, refractive index of 1.590 and at a temperature of 25^{o}C. A standard of 100 nm (nanosphere size standards, Duke Scientific Co., Palo Alto, CA, U.S.A.) of a polymer microsphere in water (polymer density of 1.05 g/cm^{3}, refractive index of 1.590 at 589 nm) was used to verify equipment calibration. Measurements of size and polydispersity index (particle size distribution - PDI) were made for freshly synthesized nanoparticles (prior ultrafiltration), ultrafiltered nanoparticles, and re-suspended nanoparticles (after freeze-drying). For each sample, the mean diameter and the standard deviation of nine determinations were calculated.

7.3.4 *Nanoparticle Morphology Characterization*

The morphology of nanoparticles was examined by transmission electron microscopy (TEM) using a JEOL 1200 EX TEM (JEOL USA Inc., Peabody, MA, U.S.A.) system at the Microscopy Imaging Center of the Biology Department at Texas A&M University. A droplet of the aqueous phase containing nanoparticles was placed on a copper grid of 400 mesh with carbon film. The sample excess was removed with a filter paper. Uranium acetate 2% was used as a stain; the excess uranium acetate was removed after 1 min with a filter paper. The sample was dried before analysis by TEM. Observations were performed at 60 kV (Astete, 2006; Panyam et al., 2003).

7.3.5 *Determination of* **trans**-*Cinnamaldehyde and Eugenol Entrapment Efficiency*

The entrapment efficiency of *trans*-cinnamaldehyde and eugenol in the PLGA nanoparticles was measured by reverse-phase (RP)-HPLC. A sample of 2 mg lyophilized nanoparticles was dissolved in 2 ml acetonitrile: water (95:5). Each sample was passed

through a syringe filter (pore size 0.2μm, Acrodisc, Pall life Sciences Port Washington, NY, U.S.A.) before HPLC measurements. The entrapment efficiency of both active substances was determined by injecting 25 μl of previously prepared samples into the HPLC column. A Dionex Summit HPLC system (Dionex, Germering, Germany) equipped with P680 pump with high-speed gradient, ASI-100 autosampler, SOR-100 degasser running Chromeleon version 6.6. software was used with photodiode array detection (PDA-100). All wavelengths between 250 and 601 nm were collected while 280 nm wavelengths were monitored during runs. The column was a Supelco 2.1mm x 250 mm, 5 μm Discovery Bio Wide Pore C_{18} column with Supelguard (C_{18}) column cartridge (Supelco, Bellefonte, PA, U.S.A.). The mobile phase consisted of acetonitrile: water: acetic acid in a ratio of 50:50:0.01, isocratic with a flow rate of 0.25 ml/min and a total run time of 15 min per sample.

A standard curve (concentrations ranged from 2 to 200 μg/ml, 25μl injection volume) was prepared under the same conditions. *trans*-cinnamaldehyde and eugenol entrapment efficiency was expressed as the percentage of active substance entrapped in the nanoparticles reported to the initial amount of each used for nanoparticles preparation. Determinations were made in triplicates.

7.3.6 *Controlled Release Study*

Lyophilized resuspended nanoparticles were dissolved in the release medium, containing phosphate saline buffer (PBS, 0.15 M, pH 7.4), at a concentration of 1mg/ml (sufficient to establish sink conditions – *trans*-cinnamaldehyde and eugenol concentration in the medium was kept five times lower than their saturation solubility in

buffer) similar to Zigoneanu et al. (2008). The sample was divided into 10 vials (1.5 ml Eppendorf tube) of 1 ml. The *in vitro* controlled release study was performed at 37^{o}C and 100 rpm (Orbit shaker, Lab line instruments, Melrose Park, IL, U.S.A.). At predetermined time intervals, samples were withdrawn and filtered with a 0.2μm pore size filter (Acrodisc, Pall life Sciences Port Washington, NY, U.S.A.) and the *trans*-cinnamaldehyde and eugenol concentrations were assessed by RP-HPLC. The mobile phase was acetonitrile: water: acetic acid in the ratio 50:50:0.01, the injected volume was 25μl and the flow rate 0.25 ml/min. The column was a Supelco 2.1mm x 250 mm, 5 μm Discovery Bio Wide Pore C_{18} column with Supelguard (C_{18}) column cartridge (Supelco, Bellefonte, PA, U.S.A.) in a Dionex Summit HPLC system (Dionex, Germering, Germany) equipped with P680 pump with high-speed gradient, ASI-100 autosampler, SOR-100 degasser running Chromeleon version 6.6 software was used with photodiode array detection (PDA-100). All wavelengths between 250 and 601 nm were collected while 280 nm wavelengths were monitored during runs. Determinations were made in triplicates.

Most of the models used for describing the controlled release of substances have been based on solutions of the Fickian diffusion equation (Siepmann and Peppas, 2001). For one-dimensional radial antimicrobial content in a sphere of radius *r*, under perfect sink initial and boundary conditions, with constant diffusion coefficient *D*, the series expansion of Fick's law for unsteady state diffusion is (Crank, 1975):

$$\frac{M(t)}{M_o} = \frac{6}{\pi^2}\sum_{n=1}^{\alpha}\frac{1}{n^2}\exp\left[-\frac{Dn^2\pi^2 t}{r^2}\right] \qquad [7.1]$$

where M (t) is the nanoparticles antimicrobial content at time t, and M_o the initial antimicrobial content. A simplification of the solution of Eqn. (7.1) was used to predict the antimicrobial release from PLGA nano-systems. Instead of an infinite number of terms, only the first term of Eqn.(7.1) was employed to calculate the release rate:

$$\frac{M(t)}{M_o} = \frac{6}{\pi^2}\exp\left(-\frac{D\pi^2 t}{r^2}\right) = \frac{6}{\pi^2}\exp(-Kt) \qquad [7.2]$$

Equations (7.1) and (7.2) give significantly different results only for small values of t. The difference between the series solution of Eqn. (7.1) and the one-term solution of Eqn. (7.2) is less than 5% if the dimensionless ratio $K = D\pi^2 t / r^2 > 0.52$ (i.e. for larger times > 6500 s assuming average D of $6.12\text{x}10^{-20}$ m^2/s and average r of $8.6875\text{x}10^{-8}$ m). Shorter times can be assumed if more terms are added to Eqn. (7.2), (i.e., 1000 s for the same D and r values for the two-term solution).

However, Eqn. (7.2) often predicts the shape of drug releasing curves from polymers poorly (Ritger and Peppas, 1987); the initial release rate is too low and the approach to the final drug content in the polymeric delivery system is too rapid.

A simple semi-empirical equation also used to describe the amount of drug released from a wide variety of matrix delivery systems is the so-called power law (Gamsiz et al. 2008., (Costa and Lobo, 2001; Siepmann and Peppas, 2001; Xiong et al., 2005; Zuleger and Lippold, 2001). The power law model is similar in form to the short-time approximation of the exact solution of Fick's second law of diffusion (Ritger and Peppas, 1986). So, it does not provide a good fitting for antimicrobial release data.

In this work we are proposing a modified empirical equation to describe the release of *trans*-cinnamaldehyde and eugenol compounds from PLGA-nanoparticles:

$$\frac{M(t)}{M_o} = b_1 * \exp(-k_1 t) + b_2 * \exp(-k_2 t) \qquad [7.3]$$

where b_1, b_2, k_1, and k_2 are constants. This model can be seen as a generalized form of the solution of the Fickian model when employing only the 1st two terms of Eqn. (7.2). The values k_1, and k_2 are defined as the antimicrobial release rate constants.

The experimental data were fitted to the Eqn. (7.3) using SPSS software for Windows, v. 16.0 (SPPS, 2007).

7.3.7 *Minimum Inhibitory Concentration (MIC)*

Overnight cultures of *Salmonella* spp. *(Salmonella entereditis and Salmonella typhimurium)* and *Listeria* spp. (*Listeria monocytogenes* ATCC 15313, *Listeria monocytogenes* Scott A 46, *Listeria monocytogenes* strain A, *Listeria innocua* NRCC B33076, *Listeria monocytogenes* ATCC 33090), used as representative of the Gram-negative and Gram-positive bacteria, respectively; were grown in tryptic soy broth (TSB). Based on turbidity measurements, correlated with plate counts, the cultures were diluted to approximately 10^5 CFU/ml. An appropriate volume of 10^5 CFU/ml dilution was added to sterile TSB to give approximately 10^3 CFU/ml level of organism. Each of the wells of a 96-well microtiter plate (sterilized 300 μl volume – MicroWell, 96-Well Plates, NUNC, flat-bottom, Thermo Scientific, West Palm Beach, FL, U.S.A.) was charged with 125 μl of seeded TSB using a multichannel pipettor. To the first well of a row, 125 μL of the antimicrobial nanoparticles (containing either *trans*-cinnamaldehyde

or eugenol) was added and mixed well. After mixing, 125 μL of the well contents was transferred to the next well. This transfer procedure continued for 10 of the 12 rows of wells. The last row of well acted as a growth control. Along with each antimicrobial being screened, sterilized water blank was used in an identical fashion to ensure that the sterilized water (where the nanoparticles were suspended) effect, if present, was not misinterpreted. The test compound concentration in the wells ranged from 20000 to 20 μg/ml of nanoparticle (Kalemba and Kunicka, 2003).

The microtiter plates were placed into a microplate reader (Tecan SpectraFluor plus, Tecan US Inc., Durham, NC, U.S.A.) equipped with Magellan^{TM} software. The microtiter plates were incubated at 35^{o}C with agitation (100 rpm) and at every 3 hours for 36 hours absorbance of each well was measured at 550 nm. The MIC was defined as the concentration of the last row of well where no growth occurred (no change in optical density within time).

7.3.8 ***Statistical Analysis***

Data analysis was performed using the SPSS software for Windows, v. 16.0 (SPPS, 2007) for size, PDI of nanoparticles, and entrapment efficiency. Differences between variables were tested for significance by one-way ANOVA. Significantly different means ($P<0.05$) were separated by the Tukey test. The kinetic data (controlled release study) were analyzed by the nonlinear procedure to determine k_1 and k_2 and correlation coefficient, R^2.

7.4 Results and Discussion

7.4.1 *Size and Polydispersity of Nanoparticles*

Size and polydispersity of nanoparticles was measured after evaporation, ultrafiltration, and freeze-drying steps, as shown in Tables 7.1 and 7.2. The processing steps (i.e. evaporation, ultrafiltration, and freeze-drying) affected the size of unloaded PLGA nanoparticles, which decreased ($P < 0.05$) from 317 to 174 nm. The same effect was observed with the entrapment of the antimicrobial compounds, though it was not significant. Initially, the unloaded PLGA nanoparticles were significantly ($P < 0.05$) of larger size than the other antimicrobial loaded nanoparticles, but they decreased ($P < 0.05$) in size during the subsequent evaporation step. With the exception of the evaporation step, there was no significant difference in size among the antimicrobial loaded and unloaded nanoparticles throughout the processing steps. The nanoparticles had a mean diameter of 180 ± 4 nm (Table 7.1).

The presence of antimicrobial did not affect ($P < 0.05$) the mean diameter of the nanoparticles with the eugenol loaded particles being slightly larger (Table 7.1). The presence of antimicrobial agent yielded a more viscous dispersed phase, making it difficult for the mutual dispersion of the phases and therefore resulting in larger particles. Similar results were observed in previous studies using PVA as emulsifier (Mainardes and Evangelista, 2005; Zigoneanu et al., 2008).

Table 7.1. Effect of treatment (unloaded PLGA, PLGA loaded with *trans*-cinnamaldehyde (PLGA-C), PLGA loaded with eugenol (PLGA-E), and processing parameter (evaporation, ultrafiltration, and freeze-drying) during synthesis on size of nanoparticles.

	Size (nm)		
	Processing parameters		
Treatments	After evaporation	After ultrafiltration	After freeze-drying
Unloaded PLGA	$_{x}$ 317.1 ^{b} (14.2)	$_{w, x}$ 234.7 ^{a} (52.8)	$_{w}$ 174.0 ^{a} (83.3)
PLGA-C	$_{w}$ 225.3 $^{a, b}$ (5.08)	$_{w}$ 222.6 ^{a} (12.87)	$_{w}$ 173.8 ^{a} (40.4)
PLGA–E	$_{w}$ 185.2 ^{b} (96.8)	$_{w}$ 167.2 ^{a} (47.0)	$_{w}$ 179.3 ^{a} (36.5)

[1]Standard deviation
[a,b]Means within a column which are not followed by a common superscript letter are significantly different ($P < 0.05$).
[w,x]Means within a row, which are not followed by a common superscript letter, are significantly different ($P < 0.05$).

The processing steps (i.e. evaporation, ultrafiltration, and freeze-drying) did not ($P < 0.05$) affect the polydispersity for all treatments, including whether or not the nanoparticles were unloaded or loaded with the antimicrobial agents. The only exception occurred with the unloaded PLGA nanoparticles during the freezing-drying steps, where a significant size decrease ($P < 0.05$) occurred (Table 7.2).

All the treatments evaluated showed different families of particles with different sizes. The advantage of a monodisperse system (PDI < 0.100) is related to its ability to deliver a consistent amount of compound, as compared to a mixture of polydisperse particles, of different loading capacities (Astete, 2006). In this study, the polydispersity was higher (above 0.100) probably because important amounts of PVA were removed

during the ultrafiltration process and this could cause some agglomeration of nanoparticles, though it did not affect its antimicrobial capacity.

Table 7.2. Polydispersity of nanoparticles as a function of treatments (unloaded PLGA, PLGA loaded with *trans*-cinnamaldehyde (PLGA-C), PLGA loaded with eugenol (PLGA-E)), and processing parameter during synthesis.

	Polydispersity (-)		
	Processing parameters		
Treatments	After evaporation	After ultrafiltration	After freeze-drying
Unloaded PLGA	$_{x}$ 0.32 ^{a} [1](0.03)	$_{x}$ 0.33 ^{a} (0.04)	$_{w}$ 0.25 ^{a} (0.05)
PLGA-C	$_{w}$ 0.31 ^{a} (0.01)	$_{w}$ 0.30 ^{a} (0.02)	$_{w}$ 0.29 ^{a} (0.03)
PLGA–E	$_{w}$ 0.33 ^{a} (0.03)	$_{w}$ 0.30 ^{a} (0.06)	$_{w}$ 0.33 ^{a} (0.04)

[1]Standard deviation
[a,b]Means within a column which are not followed by a common superscript letter are significantly different ($P < 0.05$).
[w,x]Means within a row, which are not followed by a common superscript letter, are significantly different ($P < 0.05$).

In the emulsion-solvent evaporation method, the emulsification and stabilization of the globules are crucial factors. The higher energy released during homogenization and sonication in the process leads to a rapid dispersion of polymeric organic phase as nanodroplets of small size and monomodal distribution profile. The emulsification can be considered one of the most important steps of the process, because an insufficient dispersion of phases results in large particles with wide size distribution. A reduction of the emulsion globule size allows the formation of smaller nanoparticles (Mainardes and Evangelista, 2005). Also, the amount of surfactant plays an important role in the emulsification process and in the protection of the droplets, because it can avoid the

coalescence of globules (Murakami and Yoshino, 1999; Quintanar-Guerrero et al., 1996). Therefore, to reduce the polydispersity of this study (Table 7.2), one could increase the energy release during homogenization (by increasing rpm) and/or sonication (increasing power (wattage)). Another alternative would be selecting a different emulsifier with surface charge (it increases repulsion and consequently avoids coalescence of globules).

7.4.2 *Nanoparticle Morphology Characterization*

Figures 7.2- 7.4 show the morphology of the unloaded PLGA, *trans*-cinnamaldehyde-PLGA and eugenol-PLGA loaded particles. All particles showed a spherical shape and smooth surface with a broad size distribution and a strong tendency to form clusters. No distinct difference in size and shape was noticed, however, among treatments. The aggregation present on all particles was likely due to natural clustering due to insufficient steric stabilization by the PVA which is a non-ionic surfactant. The size of the nanoparticles measured by the particle analyzer is consistent with the particle sizes estimated from TEM (in the range of 200 nm) images.

The PVA chain is formed from alternating hydrophilic and hydrophobic segments. The hydrophobic moieties of PVA interconnect with the PLGA chains to create a matrix, whereas the hydrophilic PVA moieties face the water phase. This arrangement is conducive to the formation of the PVA “corona”, observed by TEM (Zigoneanu et al., 2008). The affinity of PVA with water pulled the PVA to the surface of micelles by the bulk water molecules in the emulsion process. At the same time, the hydrophobic polylactide segments were directed into the inner core of the micelles.

Corona type microspheres were formed after solvent evaporation as observed by the TEM images.

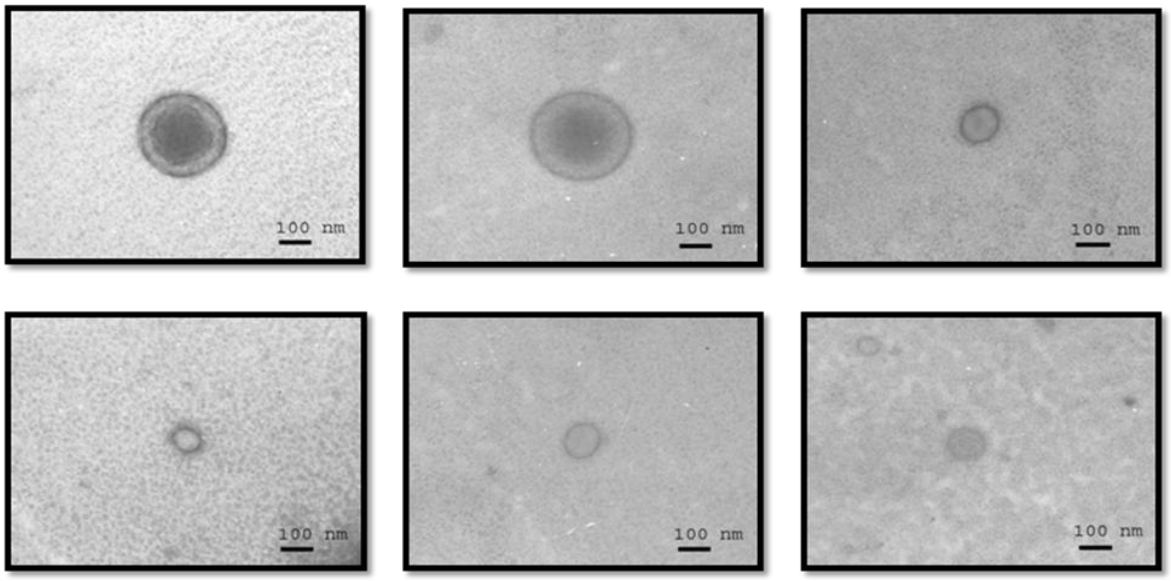

Figure 7.2. TEM images of unloaded PLGA nanoparticles (x 50,000 magnification).

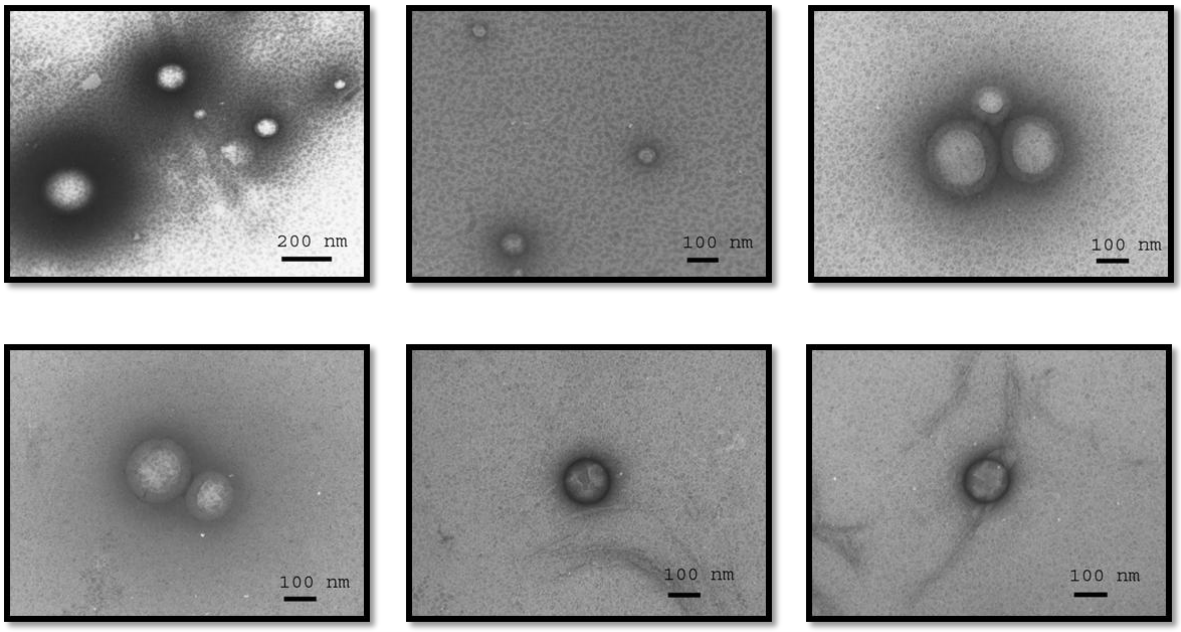

Figure 7.3. TEM images of PLGA-*trans*-cinnamaldehyde loaded nanoparticles (x 50,000 magnification).

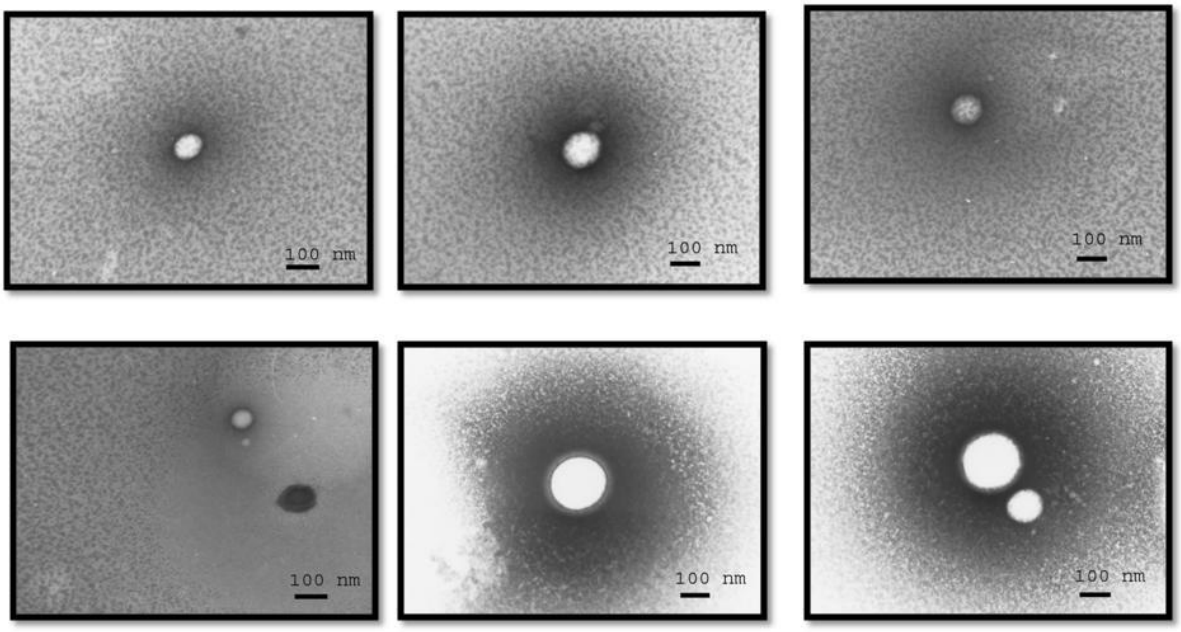

Figure 7.4. TEM images of PLGA-eugenol loaded nanoparticles (x 50,000 magnification).

7.4.3 *Determination of* trans-*Cinnamaldehyde and Eugenol Entrapment Efficiency*

Entrapment efficiency is used to indicate the amount of compound entrapped into the polymeric matrix. The entrapment efficiency for eugenol was 98.27% and for *trans*-cinnamaldehyde was 92.56%. This is in agreement with the data found in the literature about hydrophobic components whose entrapment is usually greater than 90% (Brigelius-Flohe and Traber, 1999; Zigoneanu et al., 2008).

7.4.4 *Controlled Release Study*

The *trans*-cinnamaldehyde and eugenol release profiles were evaluated *in vitro* as a function of time. The results over 72 hrs releasing time are shown in Figures 7.5 and 7.6. The release profiles for both agents were biphasic, showing an initial burst effect in the first couple of hours followed by uniform release within time.

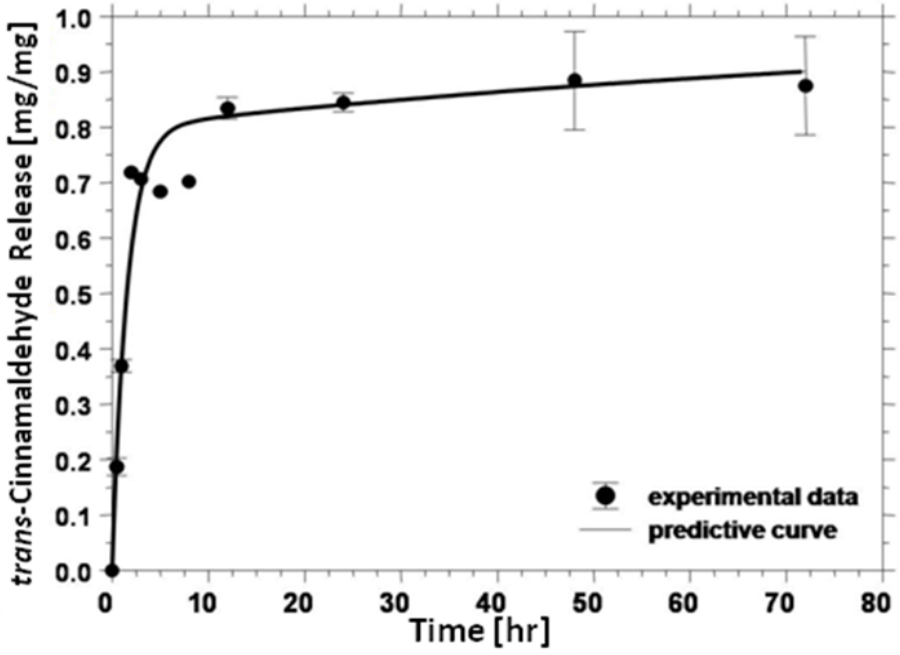

Figure 7.5. *trans*-cinnamaldehyde release kinetic by PLGA nanospheres as a function of time (hours). See text for equations used in the fitting procedure.

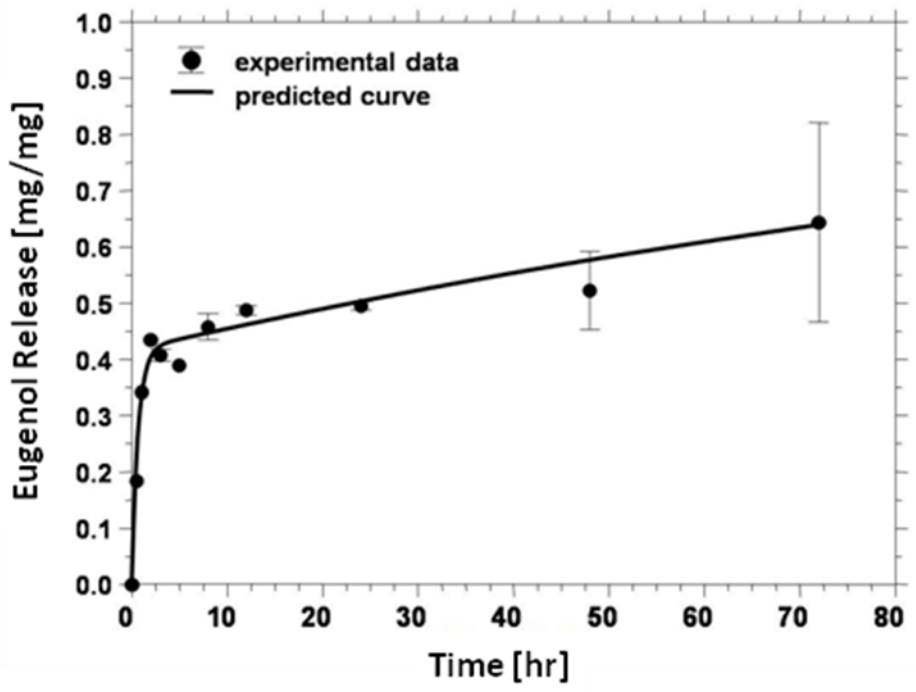

Figure 7.6. Eugenol release kinetic by PLGA nanospheres as a function of time (hours). See text for equations used in the fitting procedure.

The 2-term exponential model (Eqn.7.3) fitted well the experimental data for both antimicrobial releasing profiles. The values for the release constant rates and the coefficient of determination, R^2, are shown in Table 7.3. The sum of the exponential series yields a rate that initially is steeper and then slows down at long times compared to the one-term exponential equation; this result emphasizes the difficulty in obtaining a sustained release effect from a monodisperse sphere formulation of this type, and indeed the rapid initial release may be indistinguishable from the burst effect observed in many systems. For *trans*-cinnamaldehyde, the release rate constants were obtained by fitting the experimental data to Eqn. (7.3) were $k_1 = 1.76 \times 10^{-4}$ 1/s and $k_2 = 2.75 \times 10^{-6}$ 1/s compared to the values of $k_1 = 4.10 \times 10^{-4}$ 1/s and $k_2 = 1.65 \times 10^{-6}$ 1/s obtained for eugenol.

These values show the differences between the two nanoparticles release characteristics, with almost 80% of the *trans*-cinnamaldehyde being released in the first 5 hours compared to only 45% of eugenol being released during the same time period. Even after 72 hours of incubation, eugenol did not completely release into the medium.

Table 7.3. Release constant values for *trans*-cinnamaldehyde and eugenol antimicrobial agents determined by fitting Eqn. (7.3) to the experimental data

Product	k_1 **[1/s]**	k_2 **[1/s]**	R^2
trans-cinnamaldehyde	1.76×10^{-4}	2.75×10^{-6}	0.96
Eugenol	4.10×10^{-4}	1.65×10^{-6}	0.97

As illustrated by the chemical structures of *trans*-cinnamaldehyde and eugenol (Figure 7.7), the steric conformation of eugenol and the fact that eugenol is more lipophilic than *trans*-cinnamaldehyde, it may be more difficult for the eugenol to diffuse from the innermost parts of the PLGA nanoparticles to the outside medium. Future work is needed in this area.

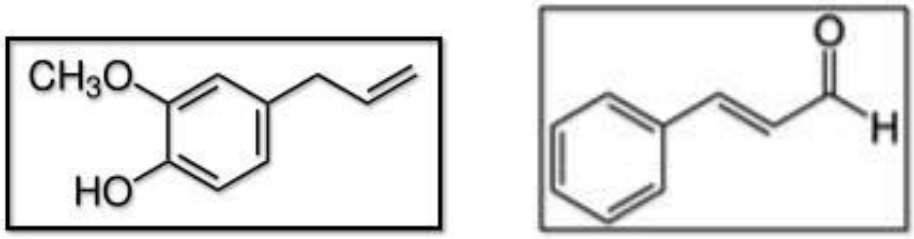

Figure 7.7. Eugenol (left) and *trans*-cinnamaldehyde (right) chemical structures.

The release rate constant, k_1, for eugenol was higher than for *trans*-cinnamaldehyde, which could be caused by more eugenol than *trans*-cinnamaldehyde being adsorbed to the outside of the particle, consequently yielding a steeper burst effect on the dilution.

The fraction of antimicrobial released in the initial burst is thus dependent on the composition of the nanoparticles. Generally, the mechanisms by which active agents can be released from a delivery system are the combination of diffusion of the active agent passing through the polymer, polymeric erosion, swelling, and degradation. Usually, the degradation of PLGA is slow, therefore the release mechanism of the antimicrobial substances from the nanoparticles may depend on the substance diffusion and the PLGA surface and bulk erosions or swelling (Mu and Feng, 2003). In our antimicrobial release system, the diffusion occurred when the substance passed through the polymeric matrix into the external environment, by passing between polymer chains. In this type of system, the release rate normally decreases with long time, because the substance has a progressively longer distance to travel and thus requires a longer time to escape. In the 72 hours period of incubation, the average released amount of antimicrobial was ca. 64% and 87% of the total antimicrobial load for eugenol and *trans*-cinnamaldehyde, respectively.

The rapid release (under 0.5 hr ca. 20% of antimicrobial load) can be attributed to the diffusion of the encapsulated or adsorbed antimicrobial in the external surface of the nanoparticles. The second release period (after 5 hrs) shows a dependency with time

and is related to the antimicrobial diffusivity inside the matrix system, the surface area and, obviously, the antimicrobial agent.

7.4.5 *Minimum Inhibitory Concentration (MIC)*

The two antimicrobial nanoparticles (loaded with *trans*-cinnamaldehydeand eugenol) showed different degrees of growth inhibition against *Salmonella* spp. and *Listeria* spp. using the broth micro dilution method (Figures 7.8 and 7.9).

The growth of *Salmonella* spp. was inhibited by both compounds, PLGA-*trans*-cinnamaldehyde (Top Figure 7.8) and PLGA-eugenol (Bottom Figure 7.8), at 10,000 μg/ml, being this concentration the minimum inhibitory concentration, or the lowest antimicrobial compound concentration in the broth resulting in lack of visible microorganism growth changes.

Furthermore, *Listeria* spp. growth was inhibited by both compounds, PLGA-*trans*-cinnamaldehyde (Top Figure 7.9) and PLGA-eugenol (Bottom Figure 7.9), at 20,000 μg/ml. At 10,000 μg/ml, a delay in the lag phase, a slower growth rate, and thus a lower final cell concentration of microorganism were observed for both nanoparticles. It is commonly known that Gram-positive bacteria are more susceptible to essential oils than Gram-negative microorganisms (Kalemba and Kunicka, 2003). However, there are some exceptions, with *Vibrio vulnificus* (Gram-negative) proven to be most susceptible to the essential oil constituents, with *Listeria monocytogenes* (Gram-positive) the least sensitive among a number of tested bacteria (Kim et al., 1995), as confirmed in this study.

The concentrations of nanoparticles would correspond to a MIC of approximately 800 and 1600 μg/ml of antimicrobial compound (eugenol and *trans*-cinnamaldehyde) for *Salmonella* spp. and *Listeria* spp., respectively; considering the loaded amount of antimicrobial into the nanoparticles and its entrapment efficiency.

These results show the spectrum of eugenol and *trans*-cinnamaldehyde antimicrobial nanoparticles, which are able to effectively inhibit the growth of both Gram-positive and Gram-negative bacteria.

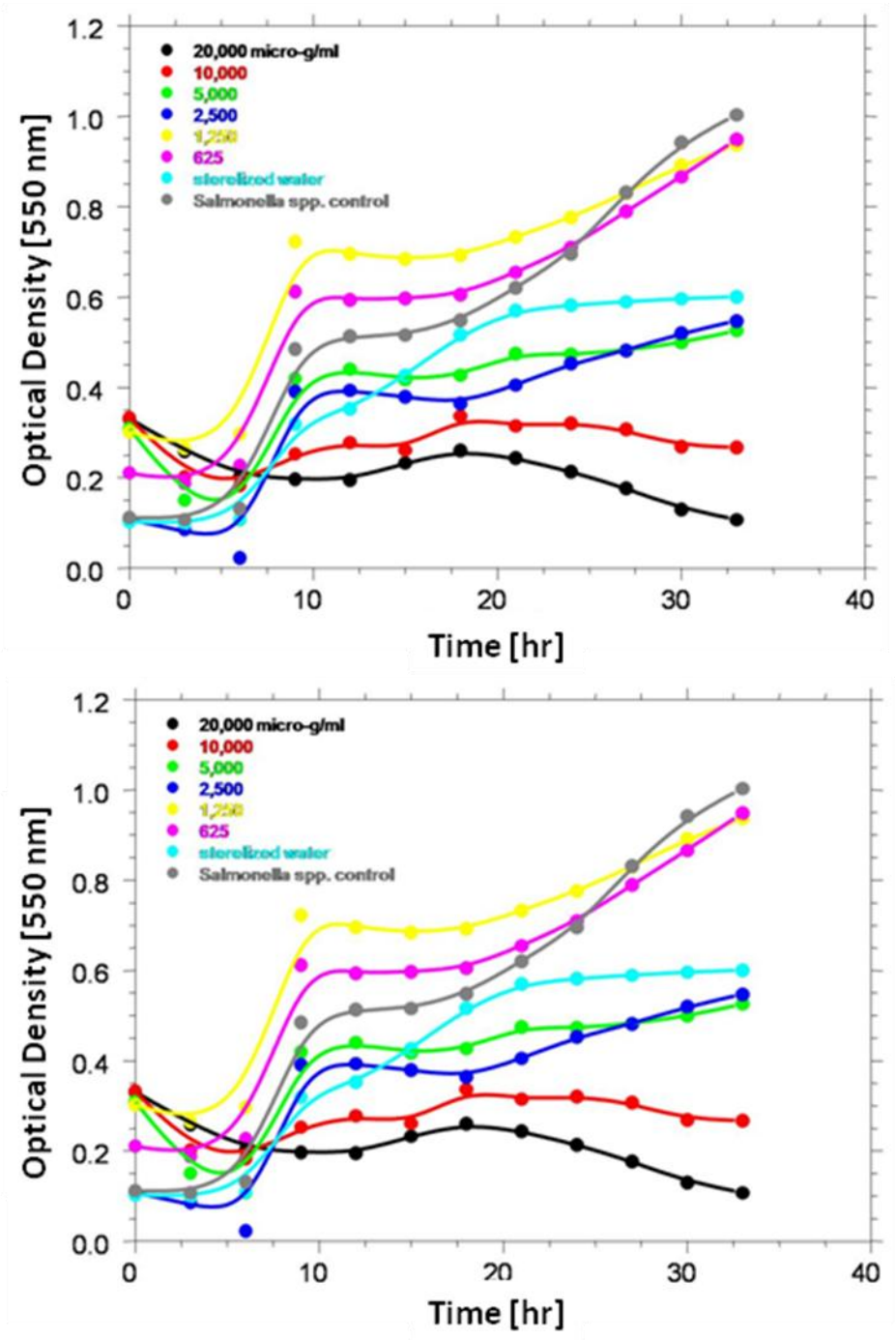

Figure 7.8. Growth of *Salmonella* spp. in tryptic soy broth as a function of active compound concentration (Top: PLGA-*trans*-cinnamaldehyde; Bottom: PLGA-eugenol). Concentration units are μg/ml.

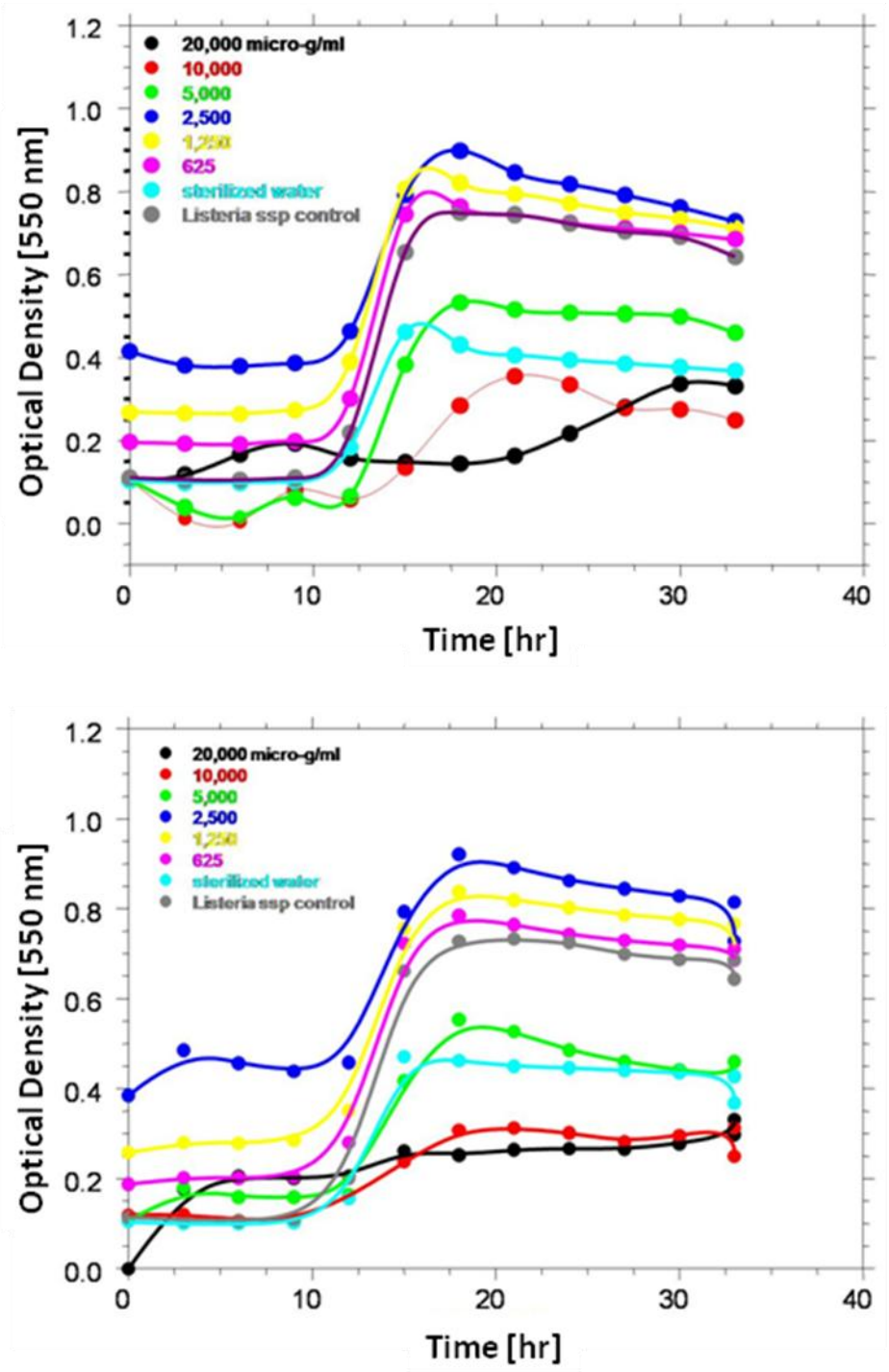

Figure 7.9. Growth of *Listeria* spp. in tryptic soy broth as a function of active compound concentration (Top: PLGA-*trans*-cinnamaldehyde; Bottom: PLGA-eugenol). Concentration units are μg/ml.

Therefore, the use of nanoparticles to encapsulate antimicrobial hydrophobic compounds could improve their efficacy due to three main factors: improved hydrophilicity, sustained release, and small size, as observed in the present study, *trans*-cinnamaldehyde and eugenol increased their solubility in water due to microencapsulation with PLGA (an aqueous suspension of 1mg/ml was translucid). Furthermore, the nanoparticles showed a sustained release with continuous migration of the antimicrobial with time. In addition, their small size (ca. 200 nm) would not present a barrier to access the cytomembranes of bacteria.

7.5 Conclusions

The emulsion evaporation method allowed the preparation of an antimicrobial loaded system of biodegradable PLGA carrier containing natural compounds derived from essential oils (i.e. *trans*-cinnamaldehyde and eugenol) incorporated in the polymeric matrix. These nanoparticles are suitable for hydrophobic antimicrobial release carriers, with an entrapment efficiency ranging from 92 to 98% for both compounds and final mean size under 200 nm, for a 16% w/w antimicrobial theoretical loading.

The *in vitro* release kinetics of antimicrobial compounds was governed by an initial burst followed by a slow and continuous release profile. The two-term exponential kinetic model predicted well the *trans*-cinnamaldehyde and eugenol release. In 72 hrs, 64% and 87% of the initial load was released in the medium for eugenol and *trans*-cinnamaldehyde, respectively. The release rate constants were k_1 =1.76x10^{-4} 1/s and k_2 =2.75x10^{-6} 1/s for *trans*-cinnamaldehyde compared to k_1 = 4.10x10^{-4} 1/s and k_2 =1.65x10^{-6} 1/s for eugenol. Furthermore, the controlled release profile showed that these

biodegradable PLGA/antimicrobial delivery systems have great potential and should be given particular consideration in the design of new active packaging or even for direct food application.

The antimicrobial efficacy of these nanoparticles was evaluated against *Salmonella* spp. (Gram-negative) and *Listeria* spp. (Gram-positive) with MICs ranging from 10 mg/ml to 20 mg/ml, respectively for both nanoparticles, demonstrating a broad spectrum of application in food systems where both types of microorganism could present a risk. These results indicate that such nanoparticles could be useful antimicrobial delivery systems capable of inhibiting growth of either Gram-positive or negative pathogenic bacteria with continuous releasing during 72 hrs.

CHAPTER VIII

CONCLUSIONS

This research focused on validating the application of ionizing irradiation to decontaminate fresh leafy vegetables.

The first part of this research confirmed the effectiveness of ionizing irradiation treatment for fresh produce (i.e. baby spinach and lettuce) in terms of quality and safety. The following conclusions were reached:

1. Packaged baby spinach leaves can be irradiated using electron beam irradiation up to 1.0 kGy dose without detrimental effects to produce quality.
2. Color, texture, vitamin C, total carotenoids, and chlorophyll content were not significantly different ($P > 0.05$) from non irradiated controls throughout storage time (15 days at $4^{o}C$).
3. Sensory analysis (consumer acceptance tests using a 9-point hedonic scale) demonstrated that irradiation had little or no effect on the overall quality of baby spinach. Only at the end of refrigerated storage (day 15), irradiated samples received slightly lower odor scores than the non-irradiated controls.
4. Ionizing irradiation effectively inactivated internalized bacteria (*Escherichia coli* spp.) in lettuce leaves in a dose-dependent manner (3-4 log reduction at 1.0 kGy) and can be used as an effective killing step to mitigate the risk of foodborne illness in fresh leafy vegetables..

5. Despite of the subtle differences in composition and structure among the four lettuce varieties evaluated, the D_{10}-values were not different ($P>0.05$). Therefore, decontamination of internalized bacteria by irradiation is not dependent ($P>0.05$) on lettuce varieties (i.e., boston, iceberg, green leaf, and red leaf).
6. Understanding of irradiation interaction with matter from different irradiation sources (i.e., gamma and electron beam) is needed to obtain uniform dose distribution within the samples and consequently uniform inactivation of microorganism (internalized or on surface) present on the produce.
7. Scanning Electron Microscopy (SEM) images indicate that the contamination sites of pathogens in leafy vegetables are mainly localized on crevices in the proximity and into the stomata.

The second part of this research consisted on combining different treatments with irradiation to increase foodborne pathogens sensitivity to ionizing radiation and consequently reduce the dose required to achieve safety standards without affecting produce quality. The following conclusions were drawn from this study:

8. Modified Atmosphere Packaging (MAP) in combination with irradiation (up to 1 kGy) had a positive effect ($P<0.05$) in increasing the radiosensitization of bacteria (*Salmonella* spp. and *Listeria* spp.).
9. Increasing concentrations of oxygen in the packaging ($P<0.05$) increased the radiation sensitivity of both microorganisms tested (up to 25% reduction in the D_{10}-values).

10. Irradiation temperature significantly affected microorganism sensitivity. Compared to irradiating at room temperature (21^{o}C), irradiation at -5^{o}C increased ($P<0.05$) D_{10}-values of both microorganisms up to ca. 60%.
11. Radiation sensitization could be effected ($P<0.05$) by production of ozone, which increases with increasing dose-rate and oxygen concentration, and reducing temperatures.
12. The rate of ozone decomposition was found to be exponential with time (100% of oxygen irradiated at room temperature at 1kGy) with a half-life of 48 min, which would provide enough exposure time for reducing microorganism population.
13. The antimicrobial activity of natural compounds was clearly demonstrated against *Listeria* spp. and *Salmonella* spp. Their inclusion complexes with β-cyclodextrin were confirmed by differential scanning calorimetry (DSC).
14. The inclusion complexes of the natural compounds together with Lysozyme with EDTA increased ($P<0.05$) the radiation sensitivity (up to 40%) of *Salmonella* spp. when sprayed at the surface of baby spinach leaves.
15. Eugenol and *trans*-cinnamaldehyde were used to synthesize spherical poly (DL-lactide-co-glycolide) (PLGA) nanoparticles for future antimicrobial delivery applications. The emulsion evaporation method was used to form the nanoparticles in the presence of poly (vinyl alcohol) (PVA) as a surfactant.
16. The entrapment efficiency for eugenol and *trans*-cinnamaldehyde was approximately 98% and 92%, respectively. Controlled release experiments

conducted *in vitro* at 37^{o}C and 100 rpm for 72 hrs showed an initial burst followed by a slower rate of release of the antimicrobial entrapped inside the PLGA matrix. All loaded nanoparticles formulations proved to be efficient in inhibiting growth of *Salmonella* spp. (Gram-negative) and *Listeria* spp. (Gram-positive). Results suggest that the application of these antimicrobial nanoparticles in food systems may be effective at inhibiting specific pathogens.

CHAPTER IX

RECOMMENDATIONS FOR FURTHER STUDY

Recommendations for future research on radiosensitization strategies to enhance irradiation treatment of fresh produce are to:

1. Incorporate these novel antimicrobial delivery systems (β-cyclodextrin inclusion complexes and nanoparticles) into different packaging materials such as biodegradable/edible polymers. Verify their applicability and controlled release with irradiation on treatment of fresh produce.
2. Verify the effect of different MAP (modified atmosphere packaging - air, N_2:O_2 and 100% O_2) combined with irradiation treatment on the quality parameters (physico-chemical and organoleptic) of fresh produce throughout shelf-life.
3. Similarly, verify the effect of irradiation combined with spraying of the novel antimicrobial compounds on the surface of fresh produce on their quality (physico-chemical and organoleptic) parameters throughout storage.
4. Study the release profile of the antimicrobial inclusion complexes with β−cyclodextrin. Determine their stability constant and solubility in water.
5. Study the effect of combining irradiation, MAP and antimicrobials on the radiosensitization of foodborne pathogens. Ultimately, determine the optimum treatment to achieve a 5-log reduction while preserving produce quality.

6. Similarly, study the effect of combining irradiation, MAP and antimicrobial packaging on the radiosensitization of foodborne pathogens. Ultimately, determine the optimum treatment to achieve a 5-log reduction while ensuring produce quality.
7. Verify the antimicrobial effect of these treatments (MAP and/or novel antimicrobial compounds with irradiation) on foodborne pathogens during shelf-life of fresh produce.
8. Optimize nanoparticle preparation with alternative and cost effective encapsulating materials.
9. Verify the application of the antimicrobial nanoparticle materials on food products.
10. Verify the antimicrobial activity of the nanoparticle under the effect of ionizing irradiation.

REFERENCES

Adams, M.R., Harley, A.D., Cox, L.J., (1989). Factors affecting the efficacy of washing procedures used in the production of prepared salads. Food Microbiology 6 (2), 69-77.

Adams, M.R., Moss, M.O., (2000). *Food Microbiology* (2nd ed). The Royal Society of Chemistry, Cambrigde, UK, p. 479.

Alkerturse, S., Swerdlow, D., (1996). The changing epidemiology of foodborne diseases. The American Journal of the Medical Sciences 311, 23-29.

Allende, A., Jacxsens, L., Devlieghere, F., Debevere, J., Artes, F., (2002). Effect of super atmospheric oxygen packaging on sensorial quality, spoilage, and *Listeria monocytogenes* and *Aeromonas caviae* growth in fresh processed mixed salads. Journal of Food Protection 65, 1565-1573.

Allende, A., Luo, Y., McEvoy, J., Artes, F., Wang, C., (2004). Microbial and quality changes in minimally processed baby spinach leaves stored under super atmospheric oxygen and modified atmosphere conditions. Postharvest Biology and Technology 33, 51-59.

Alpen, E.L., (1998). *Radiation Biophysics* (2nd ed). Academic Press, New York, p. 484.

Amanatidou, A., Smid, E.J., Gorris, L.G.M., (1999). Effect of elevated oxygen and carbon dioxide on the surface growth of the vegetable-associated microorganisms. Journal of Applied Microbiology 86, 429-438.

Anderson, J.M., Shive, M.S., (1997). Biodegradation and biocompatibility of PLA and PLGA microspheres. Advanced Drug Delivery Reviews 28 (1), 5-24.

Anonymous, (1998). Multistate outbreak of listeriosis - United States. Morbidity and Mortality Weekly Report 47, 1085-1086.

AOAC, Association of Official Analytical Chemists, (1990). Official method 930.04. Moisture in plants. Official Methods of Analysis. AOAC A. International.

AOAC, Association of Official Analytical Chemists, (1998). Official method 985.33. Vitamin C (Reduced Ascorbic Acid) in ready-to-feed milk-based infant formula - 2,6-dichloroindophenol titrimetric method. Official Methods of Analysis. AOAC A. International.

Araujo, J.C., Teran, F.C., Oliveira, R.A., Nour, E.A., Montenegro, M.A., Campos, J.R., Vazoler, R.F., (2003). Comparison of hexamethyldisilazane and critical point drying treatments for SEM analysis of anaerobic biolfims and granular sludge. Journal of Electron Microscopy 52 (4), 429-433.

Armstrong, G.L., Hollingsworth, J., Morris, J.G., (1996). Emerging foodborne pathogens: *Escherichia coli* O157:H7 as a model of entry of a new pathogen into the food supply of the developed world. Epidemiologic Reviews 18, 29-51.

Astete, C.E., Sabliov, C.M., (2006). Synthesis of poly(DL-lactide-co-glycolide) nanoparticles with entrapped magnetite by emulsion evaporation method. Particulate Science and Technology 24, 321-328.

Astete, C.E., Sabliov, C. M., (2006). Synthesis and characterization of PLGA nanoparticles. Journal of Biomaterial Science, Polymer Edition 17 (3), 247-289.

Attix, F.H., (1986). Gamma- and X-ray interactions in matter. In: Attix, F.H. (Ed.), *Introduction to Radiological Physics and Radiation Dosimetry*. John Wiley & Sons, Hoboken, NJ, pp. 124-159.

Auty, M., Duffy, G., O'Beirne, D., McGovern, A., Gleeson, E., Jordan, K., (2005). In situ localization of *Escherichia coli* O157:H7 in food by confocal scanning laser microscopy. Journal of Food Protection 68 (3), 482-486.

Babic, I., Roy, S., Watada, A., Wergin, W., (1995). Changes in microbial populations on fresh cut spinach. International Journal of Food Microbiology 31, 107-119.

Bakri, I.M., Douglas, C.W.I., (2005). Inhibitory effect of garlic extract on oral bacteria Archives of oral biology 50, 645-651.

Barbosa-Canovas, G.V., Pothakamury, U.R., Palou, E., (1998). *Nonthermal Preservation of Foods*. Marcel Dekker, Inc., New York, p. 276.

Bari, M.L., Nakauma, M., Todoriki, S., Juneja, V.K., Isshiki, K., Kawamoto, S., (2005). Effectiveness of irradiation treatments in inactivating *Listeria monocytogenes* on fresh vegetables at refrigeration temperature. Journal of Food Protection 68 (2), 318-323.

Barrat, G., Courraze, G., Couvreur, C., Fattal, E., Gref, R., Labarre, D., Legrand, P., Ponchel, G., Vauthier, C., (2000). Polymeric micro- and nanoparticles as drug carries. In: Dumitriu, S. (Ed.), *Polymeric Biomaterials*, 2nd ed. Marcel Dekker, New York, p. 753.

Bergquist, S.A.M., Gertsson, U.E., Olsson, M.E., (2006). Influence of growth stage and postharvest storage on ascorbic acid and carotenoid content and visual quality of

baby spinach (*Spinacia oleracea* L.). Journal of the Science of Food and Agriculture 86 (3), 346-355.

Bernfeld, P., (1967). *Biogenesis of Natural Compounds* (2nd ed). Pergamon Press, Oxford, NY, p. 1209.

Beuchat, L.R., (1994). Antimicrobial properties of spices and their essential oils. In: Dillon, V.M., Board, R.G. (Eds.), *Natural Antimicrobial Systems and Food Preservation*. CAB International, Wallingford, UK, pp. 167-180.

Beuchat, L.R., (1996). *Listeria monocytogenes*: incidence on vegetables. Food Control 7, 223-228.

Beuchat, L.R., (1998). Surface decontamination of fruits and vegetables eaten raw: a review. WHO/FSF/FOS/98.2, p. 42.

Beuchat, L.R., (1999). Survival of enterohemorrhagic *Escherichia coli* O157:H7 in bovine feces applied to lettuce and the effectiveness of chlorinated water as a disinfectant. Journal of Food Protection 62, 845-849.

Beuchat, L.R., (2002). Ecological factors influencing survival and growth of human pathogens on raw fruit and vegetables. Microbes and Infection 4 (4), 413-423.

Beuchat, L.R., Brackett, R.E., (1990). Survival and growth of *Listeria monocytogenes* on lettuce as influenced by shredding, chlorine treatment, modified atmosphere packaging and temperature. Journal of Food Science 55 (3), 755-758.

Beuchat, L.R., Golden, D.A., (1989). Antimicrobials occurring naturally in foods. Food Technology 43 (1), 134-142.

Biaglow, J.E., (1987). The effects of ionizing radiation on mammalian cells. In: Farhataziz, Rodgers, M. (Eds.), *Radiation Chemistry: Principles and Application*. VCH, New York, pp. 527-563.

Block, E., (1985). The chemistry of garlic and onions. Scientific American 252, 114-119.

Borsa, J., Lacroix, M., Ouattara, B., Chiasson, F., (2004). Radiosensitization: enhancing the radiation inactivation of foodborne bacteria. Radiation Physics and Chemistry 71, 135-139.

Bozzola, J.J., Russell, L.D., (1999). The scanning electron microscope. In: Bozzola, J.J., Russell, L.D. (Eds.), *Electron Microscopy: Principles and Techniques for Biologists*, 2nd ed. Jones and Bartlett, Sudbury, MA, pp. 203-240.

Brandl, M.T., (2006). Fitness of human enteric pathogens on plants and implications for food safety. Annual Review of Phytopathology 44, 367-392.

Brigelius-Flohe, R., Traber, M.G., (1999). Vitamin E: function and metabolism. Journal of the Federation of American Society of Experimental Biology 13, 1145-1455.

Brigger, I., Dubernet, C., Couvreur, P., (2002). Nanoparticles in cancer therapy and diagnosis. Advanced Drug Delivery Reviews 54 (5), 631-651.

Burnett, S., Beuchat, L., (2001). Human pathogens associated with raw produce and unpasteurized juices, and difficulties in decontamination. Journal of Industrial Microbiology & Biotechnology 27, 104-110.

Burt, S., (2004). Essential oils: their antibacterial properties and potential applications in foods - a review. International Journal of Food Microbiology 94, 223-253.

Burton, W.G., (1982). *Post-harvest Physiology of Food Crops*. Longman., London, UK, p. 339.

Cannarsi, M., Baiano, A., Sinigaglia, M., Ferrara, L., Baculo, R., Nobile, M.A.D., (2008). Use of nisin, lysozyme and EDTA for inhibiting microbial growth in chilled buffalo meat. International Journal of Food Science and Technology 43, 573-578.

Carlotti, M.E., Sapino, S., Cavalli, R., Trotta, M., Trotta, F., Martina, K., (2007). Inclusion of cinnamaldehyde in modified γ-cyclodextrins. Journal of Inclusion Phenomena and Macrocyclic Chemistry 57 (1-4), 445-450 (6).

Castell-Perez, E., Moreno, M., Rodriguez, O., Moreira, R.G., (2004). Electron beam irradiation treatment of cantaloupes: effect on product quality. Food Science and Technology International 10 (6), 383-390.

Castillo, A., (2006). Personal communication. Department of Animal Science, Texas A&M University, College Station, TX.

Castillo, A., Lucia, L.M., Goodson, K.J., Savell, J.W., Acuff., G.R., (1998). Use of hot water for beef carcass decontamination. Journal of Food Protection 61, 19-25.

(CFR), (2009a). Code of Federal Regulations. Title 21, Part 172.515. Food additives permitted for direct addition to food for human consumption: synthetic flavoring substances and adjuvants. 3, 59-65.

(CFR), (2009a). Code of Federal Regulations. Title 21, Part 179.45. Irradiation in the production, processing and handling of food: packaging materials for use during the irradiation of prepackaged foods. 3, 458-460.

(CFR), (2009c). Code of Federal Regulations. Title 21, Part 184.1563. Direct generally recognized as safe: ozone. 3, 553.

Cheung, C., Hotchkiss, S.A.M., Smith Pease, C.K., (2003). Cinnamic compound metabolism in human skin and the role metabolism may play in determining relative sensitisation potency. Journal of Dermatological Science 31, 9-19.

Chiasson, F., Borsa, J., Lacroix, M., (2005). Combined effect of carvacrol and packaging conditions on radiosensitivity of *Escherichia coli* and *Salmonella* Typhi in ground beef. Journal of Food Protection 68 (12), 2567-2570.

Chorny, M., Fishbein, I., Danenberg, H.D., Golomb, G., (2002). Lipophilic drug loaded nanospheres prepared by nanoprecipitation: effect of formulation variables on size, drug recovery and release kinetics. Journal of Controlled Release 83 (3), 389-400.

D'Aoust, J.-Y., (1997). *Salmonella* species. In: Doyle, M.P., Beuchat, L.R., Montivelle, T.J. (Eds.), *Food Microbiology: Fundamentals and Frontiers*. ASM Press, Washington, DC, pp. 129-158.

Davidson, P.M., (1997). Chemical preservatives and natural antimicrobial compounds. In: Doyle, P.M., Beuchat, L.R., Montville, T.J. (Eds.), *Food Microbiology: Fundamentals and Frontiers*. American Society for Microbiology, Washington, DC, pp. 520-556.

Day, B., (1996). High oxygen modified atmosphere packaging for fresh prepared produce. Postharvest News and Information. 7, 31-34.

Day, B., (2000). Novel MAP for freshly prepared fruit and vegetable products. Postharvest News and Information. 11, 27-31.

Del Valle, E.M.M., (2004). Cyclodextrins and their uses: a review. Process Biochemistry 39 (9), 1033-1046.

Diehl, J.F., (1995a). Biological effects of ionizing radiation. In: Diehl, J.F. (Ed.), *Safety of Irradiated Foods*, 2nd ed. Marcel Dekker, New York, pp. 89-142.

Diehl, J.F., (1995b). *Safety of Irradiated Foods* (2nd ed). Marcel Dekker, Inc., New York, p.454.

Doyle, M.P., Zhao, T., Meng, J., Zhao, S., (1997). *Escherichia coli* O157:H7. In: Doyle, M.P., Beuchat, L.R., Montivelle, T.J. (Eds.), *Food Microbiology: Fundamentals and Frontiers*. ASM Press, Washington, DC, pp. 171-191.

Ewing, D., (1987). Application of radiation chemistry to studies in the radiation biology of microorganisms. In: Farhataziz, Rodgers, M.A.J. (Eds.), *Radiation Chemistry: Principles and Applications*. VCH Publisher, Inc., New York, pp. 501-526.

Faizur Rahman, A.T.M., Siddiqui, A.K., Amin, R., (1972). Microbiological problems in food irradiation: radiosensitivity, induced radioresistance and radiosensitization. Nuclear Science Applications Series A 6, 66-76.

Farber, J.M., (1991). Microbiological aspects of modified-atmosphere packaging technology - a review. Journal of Food Protection 54, 58-70.

Farber, J.M., Peterkin, P.I., (1991). *Listeria monocytogenes*, a foodborne pathogen. Microbiological Reviews 55, 476-511.

Farkas, J., (1987). Decontamination, including parasite control, of dried, chilled and frozen food by irradiation. Acta Alimentaria 16, 351-384.

Farkas, J., (1997). Physical methods of food preservation. In: Doyle, M.P., Beuchat, L.R., Montville, T.J. (Eds.), *Food Microbiology - Fundamentals and Frontiers*. ASM Press, Washington, DC, pp. 495-577.

Farooq, S., Akhlaque, S., (1983). Comparative response of mixed cultures of bacteria and viruses to ozonation. Water Research 17, 809-812.

Favell, D.J., (1998). A comparison of the vitamin C content of fresh and frozen vegetables. Food Chemistry 62, 59-64.

Francis, G.A., Thomas, C., O'Beirne, D., (1999). The microbial safety of minimally processed vegetables. International Journal of Food Science and Technology 34, 1-22.

George, A.C., Breslin, A.J., Haskins, J.W., Ryan, R.M. (1965). Evaluation of the hazard from radioactive gas and ozone at linear electron accelerators. In: *Proceedings of the U.S. Atomic Energy Commission 1st Symposium on Accelerator Radiation Dosimetry and Experience*. Brookhaven National Laboratory, 3-5 November, 1965, USAEC Report No. CONF-651109, Washington, DC, p.539.

Ghisalberti, E.L., (1979). Propolis: a review. Bee World 60, 59-84.

Gombas, D.M., Chen, Y., Clavero, R.S., Scott, V.N., (2003). Survey of *Listeria monocytogenes* in ready-to-eat foods. Journal of Food Protection 66, 559-569.

Gomes, C., Da Silva, P., Chimbombi, E., Kim, J., Castell-Perez, E., Moreira, R.G., (2008a). Electron-beam irradiation of fresh broccoli heads (Brassica *oleracea* L. italica). Lwt-Food Science and Technology 41 (10), 1828-1833.

Gomes, C., Moreira, R.G., Castell-Perez, M.E., Kim, J., Da Silva, P., Castillo, A., (2008b). E-beam irradiation of bagged, ready-to-eat spinach leaves (*Spinacea oleracea*): an engineering approach. Journal of Food Science 73 (2), E95-E102.

Gouin, S., (2004). Microencapsulation: industrial appraisal of existing technologies and trends. Trends in Food Science & Technology 15, 330-347.

Grecz, N., Rowley, D.B., Matsuyama, A., (1983). The action of radiation on bacteria and viruses. In: Josephson, E.S., Peterson, M.S. (Eds.), *Preservation of Food by Ionizing Radiation*. CRC Press, Inc, Boca Raton, FL. pp. 167-218.

Greenaway, W., Scaysbrook, T., Whatley, F.R., (1990). The composition and plant origins of propolis. Bee World 71, 107-118.

Guzel-Seydim, Z., Greene, A., Seydim, A., (2004). Use of ozone in the food industry. Lebensmittel-Wissenschaft Und-Technologie-Food Science and Technology 37, 453-460.

Hammer, K.A., Carson, C.F., Riley, T.V., (1999). Antimicrobial activity of essential oils and other plant extracts. Journal of Applied Microbiology 29, 130-135.

Han, J., Gomes-Feitosa, C.L., Castell-Perez, M.E., Moreira, R.G., Silva, P.F., (2004). Quality of packaged romaine lettuce hearts exposed to low-dose electron beam irradiation. Lebensmittel Wissenschaft und Technologie-Food Science and Technology 37 (7), 705-715.

Hans, M.L., Lowman, A.M., (2002). Biodegradable nanoparticles for drug delivery and targeting. Current Opinion in Solid State and Materials Science 6 (4), 319-327.

Harteck, P., Dondes, S., (1959). The kinetic radiation equilibrium of air. Journal of Physical Chemistry 63 (6), 956-961.

Hedberg, C., Osterhold, M., (1994). Changing epidemiology of food-borne diseases: a Minnesota perspective. Clinical Infectious Diseases 18, 671-682.

Hedges, A.R., Shieh, W.J., Sikorski, C.T., (1998). Use of cyclodextrins for encapsulation in the use and treatment of food products. In: Risch, S.J., Reineccius, G.A. (Eds.), *Encapsulation and Controlled Release of Food Ingredients*. Oxford University Press, New York, pp. 60-71.

Hintlian, C.B., Hotchkiss, J.H., (1986). The safety of modified atmosphere packaging: a review. Food Technology 40, 70-76.

Hodges, D.M., Forney, C.F., (2003). Postharvest ascorbate metabolism in two cultivars of spinach differing in their senescence rates. Journal of American Society of Horticultural Science 128, 930-935.

Hora, R., Warriner, K., Shelp, B.J., Griffiths, M.W., (2005). Internalization of *Escherichia coli* O157:H7 following biological and mechanical disruption of growing spinach plants. Journal of Food Protection 68, 2506-2509.

Horby, P.W., O'Brien, S.J., Adak, G.K., Graham, C., Hawker, J.I., Hunter, P., Lane, C., Lawson, A.J., Mitchell, R.T., Reacher, M.H., Threlfall, E.J., Ward, L.R., (2003). A national outbreak of multiresistant *Salmonella enterica* serovar Typhimurium definitive phage type (DT) 104 associated with consumption of lettuce. Epidemiology and Infection 130, 169-178.

Huang, J., (1986). Ultrastructure of bacterial penetration in plants. Annual Review of Phytopathology 24, 141-157.

Hughey, V.L., Johnson, E.A., (1987). Antimicrobial activity of lysozyme against bacteria involved in food spoilage and foodborne disease. Applied and Environmental Microbiology 53 (9), 2165-2170.

(IAEA), (2002). International Atomic Energy Agency. Dosimetry for food irradiation. Technical Report Series 409, Vienna, Austria, p. 161.

Ibarra-Sanchez, L.S., Alvarado-Casillas, S., Rodriguez-Garcia, M.O., Martinez-Gonzales, N.E., Castillo, A., (2004). Internalization of bacterial pathogens in tomatoes and their control by selected chemicals. Journal of Food Protection 67, 1353-1358.

(IFT), (2006). An Expert Report, Funded by the IFT Foundation. Antimicrobial resistance: Implications for the food system. Comprehensive Reviews in Food Science and Food Safety 5 (3), 71-137.

Izumi, H.N.T., Muraoka, T., (1997). Physiology and quality of fresh-cut spinach stored in low O_2 controlled atmospheres at various temperatures. In: Gorny, J.R. (Ed.), *CA'97 Proceedings Vol 5: Fresh-cut fruits and vegetables and MAP*. Davis, CA: University of California, pp. 130-133.

Jablasone, J., Warriner, K., Griffiths, M., (2005). Interactions of *Escherichia coli* O157:H7 in a gnotobiotic system. International Journal of Food Microbiology 99, 7-18.

Jacobsson, A., Nielsen, T., Sjoholm, I., (2004). Effects of type of packaging material on shelf-life of fresh broccoli by means of changes in weight, colour and texture. European Food Research and Technology 218, 158-163.

Jacxsens, L., Devlieghere, F., Van der Steen, C., Debevere, J., (2001). Effect of high oxygen modified atmosphere packaging on microbial growth and sensorial qualities of fresh-cut produce. International Journal of Food Microbiology 71 (2-3), 197-210.

James, L., Puniya, A.K., Mishra, V., Singh, K., (2002). Ozone: a potent disinfectant for application in food industry - an overview. Journal of Scientific & Industrial Research 61, 504-509.

Kalemba, D., Kunicka, A., (2003). Antibacterial and antifungal properties of essential oils. Current Medicinal Chemistry 10, 813-829.

Karapinar, M., Aktug, S.E., (1987). Inhibition of foodborne pathogens by thymol, eugenol, menthol and anethole. International Journal of Food Microbiology 4, 161-166.

Karathanos, V., Mourtzinos, I., Yannakopoulou, K., Andrikopoulos, N., (2007). Study of the solubility, antioxidant activity and structure of inclusion complex of vanillin with β-cyclodextrin. Food Chemistry 101, 652-658.

Kaspar, C.W., Tamplin, M.L., (1993). Effects of temperature and salinity on the survival of *Vibrio vulnificus* in seawater and shellfish. Applied Environmental Microbiology 59, 2425-2429.

Kertesz, Z.I., Parsons, G.F., (1963). Ozone formation in air exposed to cobalt-60 gamma radiation. Science 142 (3597), 1289-1290.

Keteleer, A., Tobback, P.P., (1994). Modified atmosphere storage of respiring product. In: Leistner, L., Gorris, L.G.M. (Eds.), *Food Preservation by Combined Processes*. Final Report, FLAIR Concerted Action no. 7, Subgroup B. EUR 15776 EN. European Commission, Brussels, pp. 59-64.

Khadre, M.A., Yousef, A.E., Kim, J.G., (2001). Microbiological aspects of ozone applications in food: A review. Journal of Food Science 66 (9), 1242-1252.

Kim, J., Moreira, R.G., Huang, Y., Castell-Perez, M.E., (2007). 3-D dose distributions for optimum radiation treatment planning of complex foods. Journal of Food Engineering 79, 312-321.

Kim, J., Yousef, A.E., Dave, S., (1999). Application of ozone for enhancing the microbiological safety and quality of foods: a review. Journal of Food Protection 62 (9), 1071-1087.

Kim, J.M., Marshall, M.R., Wei, C., (1995). Antibacterial activity of some essential oil components against 5 foodborne pathogens. Journal of Agricultural and Food Chemistry 43 (11), 2839-2845.

Knobloch, K., Pauli, A., Iberl, B., Weigand, H., Weis, N., (1989). Antibacterial and antifungal properties of essential oil components. Journal Essential Oil Research 1, 119-128.

Koutsoumanis, K., Tassou, C.C., Taoukis, P.S., Nychas, G.-J.E., , (1998). Modelling the effectiveness of a natural antimicrobial on *Salmonella enteriditis* as a function of

concentration, temperature and pH, using conductance measurements. Journal of Applied Microbiology 84, 981-987.

Lacroix, M., Ouattara, B., (2000). Combined industrial processes with irradiation to assure innocuity and preservation of food products: a review. Food Research International 33, 719-724.

Lambert, R.J.W., Skandamis, P.N., Coote, P.J., Nychas, G.-J.E., (2001). A study of the minimum inhibitory concentration and mode of action of oregano essential oil, thymol and carvacrol. Journal of Applied Microbiology 91, 453-462.

Lamprecht, A., Ubrich, N., Yamamoto, H., Schafer, U., Takeuchi, H., Maincent, P., Kawashima, Y., Lehr, C.M., (2001). Biodegradable nanoparticles for targeted drug delivery in treatment of inflammatory bowel disease. Journal of Pharmacology and Experimental Therapeutics 299, 755-781.

Lea, D.E., (1955). *Actions of Radiation on Living Cells* (2nd ed). Cambridge University Press, New York, p. 416.

Lee, D., Martin, S.E., Yoon, H., Park, Y., Kim, C., (1998). Metabolic sites of ozone injury in *Listeria monocytogenes*. Food Science and Biotechnology 7 (3), 201-204.

Less, L.N., Swallow, A.J., (1964). Estimating the hazard due to radiolytic products from air. Nucleonics 22 (9), 58-61.

Lewis, B., (1933). Communications to the editor - the decomposition of ozone by alpha particles and by thermal means. Journal of Physical Chemistry 37 (4), 533-534.

Lichtenthaler, H.K., (1987). Chlorophylls and caroteinoids: pigments of photosynthetic biomembranes. Methods in Enzymology 148, 350-382.

Lipton, W.J., (1990). Postharvest biology of fresh asparagus. Horticultural Reviews 12 (2), 65-155.

Mahapatra, A.K., Muthukumarappan, K., and Julson, J. L., (2005). Applications of ozone, bacteriocins and irradiation in food processing: a review. Critical Reviews in Food Science and Nutrition 45, 447-461.

Mainardes, R.M., Evangelista, R.C., (2005). PLGA nanoparticles containing praziquantel: effect of formulation variables on size distribution. International Journal of Pharmaceutics 290, 135-144.

Malone, S.R., Mayeux, H.S., Johnson, H.B., Polley, H.W., (1993). Stomatal density and aperture length in four plant species grown across a subambient CO_2 gradient. American Journal of Botany 49, 443-452.

McLean, F.T., (1921). A study of the structure of the stomata of two species of citrus in relation to citrus canker. Bulletin of the Torrey Botanical Club 48, 101-106.

Meilgaard, M., Civille, G.V., Carr, B.T., (1999). *Sensory Evaluation Techniques* (3rd ed). CRC Press, Boca Raton, FL, p. 387.

Melotto, M., Underwood, W., Koczan, J., Nomura, K., He, S.Y., (2006). Plant stomata function in innate immunity against bacterial invasion. Cell 126, 969-980.

Miller, R.B., (2005). *Electronic Irradiation of Foods: An Introduction to the Technology*. Springer, New York, p. 295.

Miron, T., Rabinkov, A., Mirelman, D., Wichek, M., Weiner, L., (2000). The mode of action of allicin: its ready permeability through phospholid membranes may contribute to its biological activity. Biochimica et Biophysica Acta 1463, 20-30.

Miron, T., Shin, I., Feigenblat, G., Weiner, L., Mirelman, D., Wilchek, M., Rabinkov, A., (2002). A spectrophotomectric assay for allicin, alliin, and alliinase (alliin lyase) with a chromogenic thiol: reaction of 4-mercaptopyridine with thiosulfinates. Analytical Biochemistry 307, 76-83.

Molins, R.A., (2001). *Food Irradiation: Principles and Applications.* Wiley-Interscience, New York, p. 469.

Moreira, L., Dias, L.G., Pereira, J.A., Estevinho, L., (2008). Antioxidant properties, total phenols and pollen analysis of propolis samples from Portugal. Food and Chemical Toxicology 46, 3482-3485.

Moreno, M., Castell-Perez, M.E., Gomes, C., Da Silva, P.F., Moreira, R.G., (2006). Effects of electron beam irradiation on physical, textural, and microstructural properties of "Tommy Atkins" mangoes (*Mangifera indica* L.). Journal of Food Science 71 (2), E80-E86.

Moreno, M.A., Castell-Perez, M.E., Gomes, C., Da Silva, P.F., Kim, J., Moreira, R.G., (2007a). Optimizing electron beam irradiation of "Tommy Atkins" mangoes (*Mangifera Indica* L.). Journal of Food Process Engineering 30 (4), 436-457.

Moreno, M.A., Castell-Perez, M.E., Gomes, C., Da Silva, P.F., Kim, J., Moreira, R.G., (2008). Treatment of cultivated highbush blueberries (*Vaccinium corymbosum* L.) with electron beam irradiation: Dosimetry and product quality. Journal of Food Process Engineering 31 (2), 155-172.

Moreno, M.A., Castell-Perez, M.E., Gomes, C., Da Silva, P.F., Moreira, R.G., (2007b). Quality of electron beam irradiation of blueberries (*Vaccinium corymbosum* L.) at

medium dose levels (1.0-3.2 kGy). Lwt-Food Science and Technology 40 (7), 1123-1132.

Moseley, B.E.B., (1989). Ionizing radiation: action and repair. In: Gould, G.W. (Ed.), *Mechanisms of Action of Food Preservation Procedures*. Elsevier Applied Science, London, UK, pp. 43-70.

Mourtizinos, I., Salta, F., Yannakopoulou, K., Chiou, A., Karathanos, V., (2007). Encapsulation of olive leaf extract in β-cyclodextrin. Journal of Agricultural and Food Chemistry 55, 8088-8094.

Mu, L., Feng, S., (2003). PLGA/TPGS nanoparticles for controlled release of paclitaxel: effects of the emulsifier and drug loading ratio. Pharmaceutical Research 20 (11), 1864-1872.

Murakami, Y., Yoshino, H., (1999). Preparation of poly(DL-lactide-co-glycolide) nanoparticles by modified spontaneous emulsification solvent diffusion method. International Journal of Pharmaceutics 187, 143-152.

Nakache, E., Poulain, N., Candau, F., Orecchioni, A., Irache, J., (2000). Biopolymer and polymer nanoparticles and their biomedical applications. In: Nalwa, H.S. (Ed.), *Handbook of Nanostructured Materials and Nanotechnology*. Academic Press, San Diego, CA, p. 577.

Neal, J.A., Cabrera-Diaz, E., Marquez-Gonzalez, M., Maxim, J.E., Castillo, A., (2008). Reduction of *Escherichia coli O157:H7* and *Salmonella* on baby spinach, using electron beam radiation. Journal of Food Protection 71 (12), 2415-2420.

Niemira, B., (2003). Radiation sensitivity and recoverability of *Listeria monocytogenes* and *Salmonella* on 4 lettuce types. Journal of Food Science 68 (9), 2784-2787.

Niemira, B., (2007). Relative efficacy of sodium hypochlorite wash vs. irradiation to inactivate *Escherichia coli* O157:H7 internalized in leaves of romaine lettuce and baby spinach. Journal of Food Protection 70 (11), 2526-2532.

Niemira, B., (2008). Irradiation compared with chlorination for elimination of *Escherichia coli* O157:H7 internalized in lettuce leaves: influence of lettuce variety. Journal of Food Science 73 (5), 208-212.

Niemira, B., Sommers, C., Fan, X., (2002). Suspending lettuce type influences recoverability and radiation sensitivity of *Escherichia coli* O157:H7. Journal of Food Protection 65 (9), 1388-1393.

Panyam, J., Sahoo, S.K., Prabha, S., Bargar, T., Labhasetwar, V., (2003). Fluorescence and electron microscopy probes for cellular and tissue uptake of poly(D,L-lactide-co-glycolide) nanoparticles. International Journal of Pharmaceutics 262 (1-2), 1-11.

Pirovani, M.E., Piagentini, A.M., Guemes, D.R., Di Pentima, J.H., (1998). Quality of minimally processed lettuce as influenced by packaging and chemical treatments. Journal of Food Quality 22, 475-484.

Plotnikova, J.M., Rahme, L.G., Ausubel, F.M., (2000). Pathogenesis of the human opportunistic pathogen *Pseudomonas aeruginosa* PA14 in *Arabidopsis*. Plant Physiology 124 (4), 1766-1774.

Quintanar-Guerrero, D., Allemann, E., Fessi, H., Doelker, E., (1998). Preparation techniques and mechanisms of formation of biodegradable nanoparticles from preformed polymers. Drug Development and Industrial Pharmacy 24 (12), 1113-1128.

Quintanar-Guerrero, D., Fessi, H., Allemann, E., Doelker, E., (1996). Influence of stabilizing agents and preparatives variables on the formation of poly(D,L-lactic acid) nanoparticles by an emulsification-diffusion technique. International Journal of Pharmaceutics 143, 133-141.

Rangel, J.M., Sparlling P.H., Crowe C., Griffin P.M., Swerdlow, D.L., (2005). Epidemiology of *Escherichia coli* O157:H7 outbreaks, United States, 1982-2002. Emerging Infectious Disease 11, 603-609.

Raybaudi-Massilia, R.M., Mosqueda-Melgar, J., Soliva-Fortuny, R., Martin-Belloso, O., (2009). Control of pathogenic and spoilage microorganisms in fresh-cut fruits and fruit juices by traditional and alternative natural antimicrobials. Comprehensive Reviews in Food Science and Food Safety 8, 157-180.

Rice, R.G., (1986). Application of ozone in water and wastewater treatment. In: Rice, R.G., Brollyky,L. J., Lacy, W. J. (Eds.), *Analytical Aspects of Ozone Treatment of Water and Wastewater*. Lewis Publisher, Chelsea, MI, pp. 7-26.

Rittinger, P.A., Biggs, A.R., Peirson, D.R., (1987). Histochemistry of lignin and suberin deposition in boundary-layers formed after wounding in various plant-species and organs. Canadian Journal of Botany-Revue Canadienne De Botanique 65 (9), 1886-1892.

Robinson, J.R., (1997). Controlled drug delivery. past, present, and future. In: Park, K. (Ed.), *Controlled Drug Delivery: Challenges and Strategies*. American Chemical Society, Washington, DC, pp. 1-7.

Rodriguez Romo, L.A., (2004). Control of *Salmonella enterica* serovar *enteritidis* in shell eggs by ozone, ultraviolet radiation, and heat. The Ohio State University, United States, Ohio, p. 185.

Scazzocchio, F., D'auria, F.D., Alessandrini, D., Pantanella, F., (2006). Multifactorial aspects of antimicrobial activity of propolis. Microbiological Research 161, 327-333.

Schubert, J., Stegeman, H., (1981). Sensitization of microorganisms and enzymes by radiation-induced selective inorganic radical anions, *Proceedings of a Symposium, Colombo (Sri Lanka), 24-28 November1980*. Jointly organized by IAEA and FAO, Vienna, Austria: International Atomic Energy Agency, pp. 35-65.

Sears, J.T., Sutherland, J.W., (1968). Radiolytic formation and decomposition of ozone. The Journal of Physical Chemistry 72 (4), 1166-1171.

Seo, K.H.F., J. F., (1999). Attachment of *Escherichia coli* O157:H7 to lettuce leaf surface and bacterial viability in response to chlorine treatment as demonstrated by using confocal scanning laser microscopy. Journal of Food Protection 62 (1), 3-9.

Shah, J., Maxie, E.C., (1966). Gamma-ray radiosynthesis of ozone from air. International Journal of Applied Radiation and Isotopes 17, 155-159.

Sivam, G.P., (2001). Protection against *Helicobacter pylori* and other bacterial infections by garlic. Journal of Nutrition Supplement 131, 1106S-1108S.

Sivapalasingam, S., Friedman, C., Cohen, L., Tauxe, R., (2004). Fresh produce: a growing cause of outbreaks of foodborne illness in the United States, 1973 through 1997. Journal of Food Protection 67, 2342-2353.

Spears, J.T., Sutherland, J.W., (1968). Radiolytic formation and decomposition of ozone. Journal of Physical Chemistry. 72 (4), 1166-1171.

SPSS, (2002). SPSS for Windows. Chicago: SPSS Inc.

SPSS, (2007). SPSS for Windows, Chicago, IL. SPSS Inc.

Sudarmadji, S., Urbain, W.M., (1972). Flavor sensitivity of selected animal protein to gamma irradiation. Journal of Food Science 37, 671-672.

Swanson, W.P., (1979). Radiological safety aspects of the operation of electron linear accelerators. In: International Atomic Energy Agency (Ed.), *Technical Reports Series no. 188,* Vienna, p. 327.

Takeuchi, K., Matute, C.M., Ashraf, N.H., Frank, J.F., (2000). Comparison of the attachment of *Escherichia coli* O157:H7, *Listeria monocytogenes*, *Salmonella Typhimurium*, and *Pseudomonas fluorescens* to lettuce leaves. Journal of Food Protection 63 (10), 1433-1437.

Tauxe, R., Kruse, H., Hedberg, C., Potter, M., Madden, J., Wachsmuth, K., (1997). Microbial hazards and emerging issues associated with produce: a preliminary report to the national advisory committee on Microbiologic Criteria for Foods. Journal of Food Protection 65, 1093-1099.

Thakur, B.R., Singh, R.K., (1994). Food irradiation - chemistry and applications. Food Reviews International 10, 437-473.

Thayer, D.W., Josephson, E.S., Brynjolfsson, A., Gidding, G.G., (1996). Radiation pasteurization of food. Council for Agricultural Science and Technology. Issue Paper 7, 1-12.

Thies, C., (1996). A survey of microencapsulation processes. In: Benita, S. (Ed.), *Microencapsulation: Methods and Industrial Applications*. Marcel Dekker, New York, pp. 1-19.

Thomson, N., Evert, R.F., Kelman, A., (1995). Wound healing in whole potato tubers: A cytochemical, fluorescence, and ultrastructural analysis of cut and bruise wounds Canadian Journal of Botany-Revue Canadienne De Botanique 73 (12), 2028-2029.

Turner, J.E., (1995). Interaction of photons with matter. In: Turner, J.E. (Ed.), *Atoms, Radiation, and Radiation Protection*, 2nd ed. John Wiley & Sons, New York, pp. 170-207.

Tynecka, Z., Gos, Z., (1975). The fungistatic activity of garlic *(Allium sativum) in vitro*. Annales Universitatis Mariae Curie-Skłodowska. Sectio D, Medicina 30, 5-13.

Uhrich, K., Cannizaro, S.M., Langer, R., Shakesheff, K.M., (1999). Polymeric systems for controlled drug release. Chemical Reviews 99, 3181-3198.

Ukuku, D., Fett, W.F., (2002). Behavior of *Listeria monocytogenes* inoculated on cantaloupe surfaces and efficacy of washing treatments to reduce transfer from rind to fresh-cut pieces. Journal of Food Protection 65, 709-725.

(USFDA), (1999). U. S. Food and Drug Administration. Potential for infiltration, survival and growth of human pathogens within fruits and vegetables. http://www.cfsan.fda.gov/~comm/juicback.html.

(USFDA), (2001a). U. S. Food and Drug Administration. Chapter 6. Microbiology challenge testing. In: *Evaluation and definition of potentially hazardous foods. A report of the Institute of Food Technology for the Food and Drug Administration of the U.S. Department of Health and Human Services*. http://www.fda.gov/Food/ScienceResearch/ResearchAreas/SafePracticesforFoodProcesses/ucm094141.htm.

(USFDA), (2001b). U. S. Food and Drug Administration. FDA survey of imported fresh produce. The Center for Food Safety and Applied Nutrition. http://www.cfsan.fda.gov/~dms/prodsur6.html.

(USFDA), (2001c). U. S. Food and Drug Administration. Survey of domestic fresh produce. The Center for Food Safety and Applied Nutrition. http://www.csfan.fda.gov/~dms/prodsur9.html.

(USFDA), (2005). U. S. Food and Drug Administration. Letter to California firms that grow, pack, process, or ship fresh and fresh-cut lettuce. http://www.fda.gov/Food/FoodSafety/Product-SpecificInformation/FruitsVegetablesJuices/GuidanceComplianceRegulatoryInformation/ucm118911.htm.

(USFDA), (2006). U. S. Food and Drug Administration. FDA finalizes report on 2006 spinach outbreak. http://www.fda.gov/NewsEvents/Newsroom/PressAnnouncements/2007/ucm108873.htm.

(USFDA), (2008a). U. S. Food and Drug Administration. Guidance for industry. Guide to minimize microbial food safety hazards of fresh-cut fruits and vegetables. http://www.fda.gov/food/guidancecomplianceregulatoryinformation/guidancedocuments/produceandplanproducts/ucm064458.htm.

(USFDA), (2008b). U. S. Food and Drug Administration. Irradiation: a safe measure for safer iceberg lettuce and spinach. http://www.fda.gov/ForConsumers/ConsumerUpdates/ucm093651.htm

(USFDA), (2008c). U. S. Food and Drug Administration. National nutrient database for standard reference. Release 21. http://www.nal.usda.gov/fnic/foodcomp/search/.

Velikov, K.P., Pelan, E., (2008). Colloidal delivery systems for micronutrients and nutraceuticals. Soft Matter 4, 1964-1980.

Watada, A.E., Kim, S.D., Kim, K.S., Harris, T.C., (1987). Quality of green beans, bell peppers and spinach stored in polyethylene bags. Journal of Food Science 52, 1637-1644.

Weiss, J., Takhistov, P., McClements, J., (2006). Functional materials in food nanotechnology. Journal of Food Science 71 (9), R107-R116.

Westesen, K., Bunjes, H., Hammer, G., Siekmann, B., (2001). Novel colloidal drug delivery systems. PDA Journal of Pharmaceutical Science and Technology 55, 240-247.

Wilkins, K.M., Board, R.G., (1989). Natural antimicrobial systems. In: Gould, G.W. (Ed.), *Mechanism of Action of Food Preservation Procedures*. Elsevier Applied Science, London, UK, pp. 285-362.

Willshaw, G.A., Thirlwell, J., Jones, A.P., Parry, S., Salmon, R.L., Hickey, M., (1994). Vero cytotoxin-producing *Escherichia coli* O157:H7 in beef burgers linked to an outbreak of diarrhea, haemorrhagic colitis and haemolytic uraemic syndrome in Britain. Letters Applied Microbiology 19, 304-307.

Woodard, S., Wilken, L., Barros, G., White, S., Nikolov, Z., (2009). Evaluation of monoclonal antibody and phenolic extraction from transgenic *Lemna* for purification process development. Biotechnology and Bioengineering 104 (3), 562-571.

Zigoneanu, I.G., Astete, C.E., Sabliov, C.M., (2008). Nanoparticles with entrapped alpha-tocopherol: synthesis, characterization, and controlled release. Nanotechnology 19 (10), 1-8.

APPENDIX

Table A1. Growth data for *Salmonella enteriditis (SE)* and *Salmonella typhimurium (ST)*

1st replication			2nd replication		
time [hours]	**Absorbance @ 540nm**	**log CFU-SE**	**Time [hours]**	**Absorbance @540 nm**	**log CFU-SE**
0	0.017	3.3979	0	0.015	3.1139
4	0.018	5.0899	4	0.001	4.9005
6	0.035	7.0000	6	0.005	6.2636
8	0.253	8.0722	8	0.133	7.4329
10	0.746	8.7404	10	0.552	8.3786
12	0.790	9.0846	12	0.615	8.3539
15	0.800	9.1599	15	0.645	8.5502
23	0.866	9.2405	23	0.666	8.5250
26	0.948	9.1688	26	0.850	8.8663
1st replication			**2nd replication**		
time [hours]	**Absorbance @ 540nm**	**log CFU-ST**	**Time [hours]**	**Absorbance @540 nm**	**log CFU-ST**
0	0.019	3.6752	0	0.015	3.4548
4	0.018	5.2041	4	0.001	5.0149
6	0.028	6.6990	6	0.008	6.2542
8	0.171	7.9191	8	0.088	7.4624
10	0.653	8.7889	10	0.575	8.7559
12	0.822	9.0374	12	0.797	8.9934
15	0.836	9.0212	15	0.805	8.9890
23	0.783	9.2279	23	0.856	9.2014
26	1.025	9.3284	26	0.995	9.2393

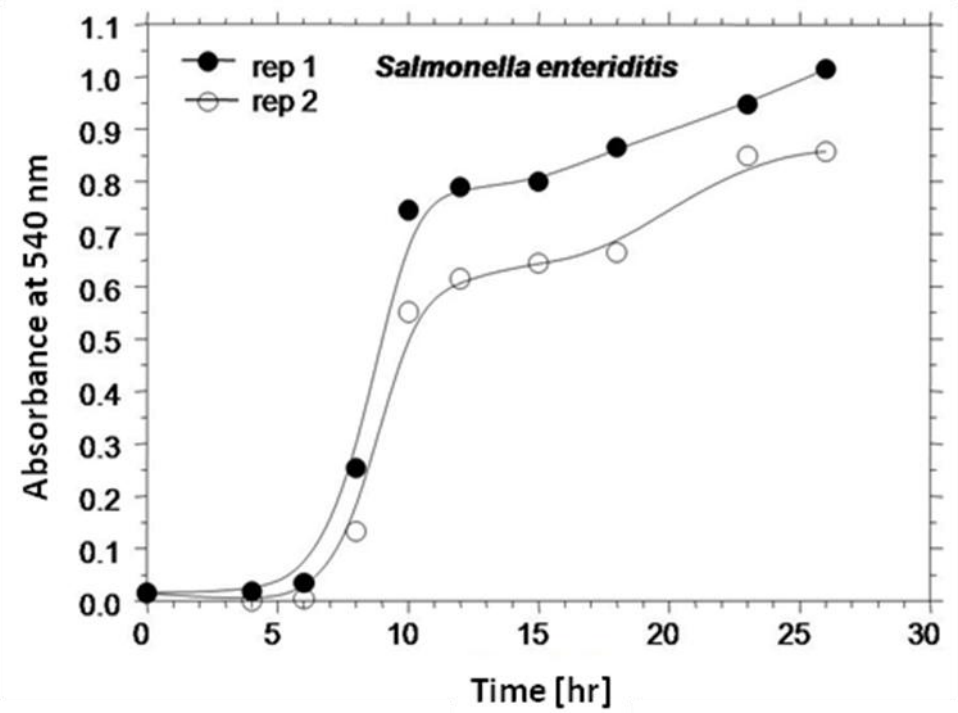

Figure 1A. Absorbance growth curves for *Salmonella enteriditis*.

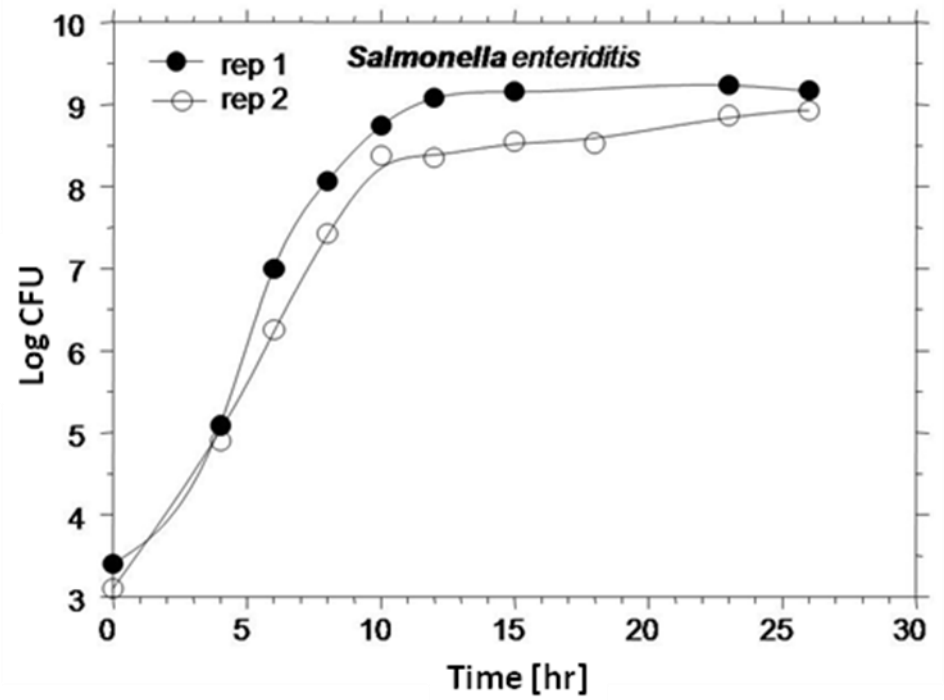

Figure 2A. Log CFU growth curves for *Salmonella enteriditis*.

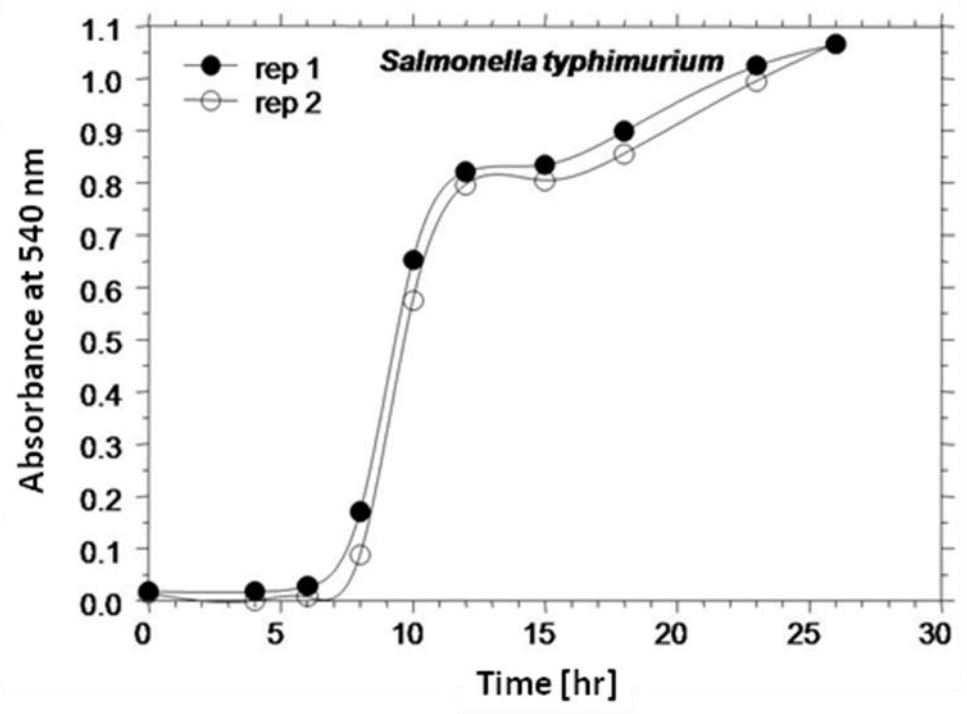

Figure 3A. Absorbance growth curves for *Salmonella typhimurium.*

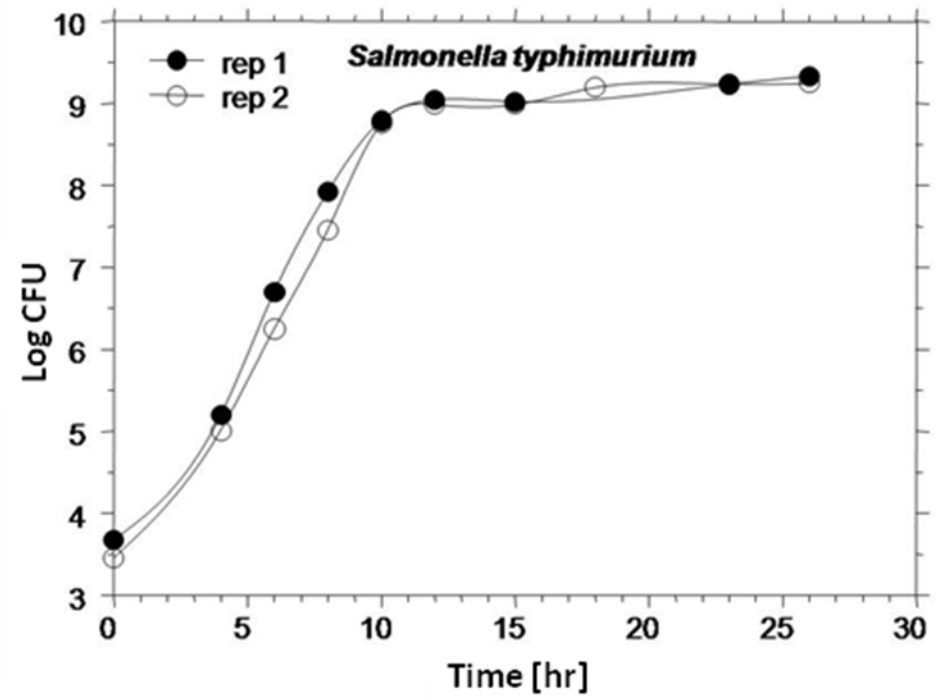

Figure 4A. Log CFU growth curves for *Salmonella typhimurium.*

Table A2. Growth data for *Listeria strain A (LA)* and *Listeria Scott A (LS)*

1st replication			2nd replication		
time [hours]	**Absorbance @ 540nm**	**log CFU-LA**	**time [hours]**	**Absorbance @540nm**	**log CFU-LA**
0	0.004	4.6675	0	0.013	4.4191
2	0.001	4.8293	2	0.016	4.7243
4	0.005	5.4372	4	0.017	5.2788
6	0.008	6.3424	6	0.021	6.1475
8	0.009	8.0512	8	0.028	6.9112
10	0.009	7.4771	10	0.057	7.6946
14	0.255	8.8388	14	0.426	8.7959
17	0.672	9.3306	17	0.862	9.3406
20	0.944	9.4692	20	1.021	9.4042
24	0.960	9.5203	24	1.000	9.2860
1st replication			**2nd replication**		
time [hours]	**Absorbance @ 540nm**	**log CFU-LS**	**time [hours]**	**Absorbance @540nm**	**log CFU-LS**
0	0.000	4.9058	0	0.011	4.4350
2	0.003	4.7482	2	0.019	4.7597
4	0.006	5.4292	4	0.021	5.2971
6	0.008	6.3160	6	0.027	6.2068
8	0.012	7.9638	8	0.027	7.0917
10	0.020	7.7482	10	0.042	7.8692
14	0.292	8.9004	14	0.446	8.9345
17	0.799	9.2175	17	0.918	9.4559
20	0.950	9.4379	20	0.970	9.4555
24	0.932	9.4188	24	0.949	9.4142

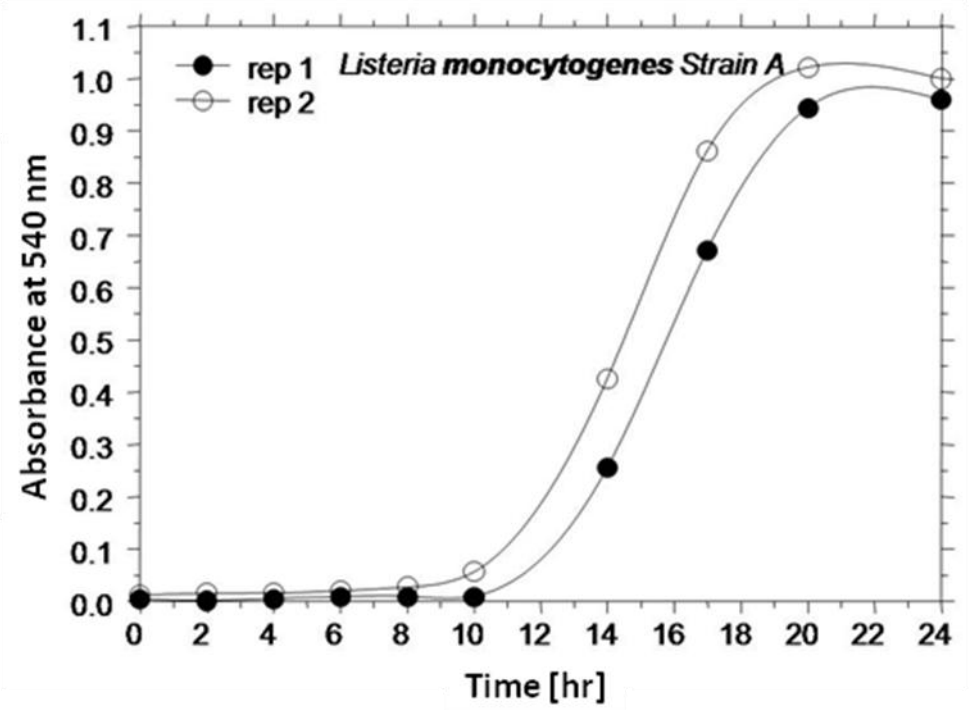

Figure 5A. Absorbance growth curves for *Listeria monocytogenes Strain A.*

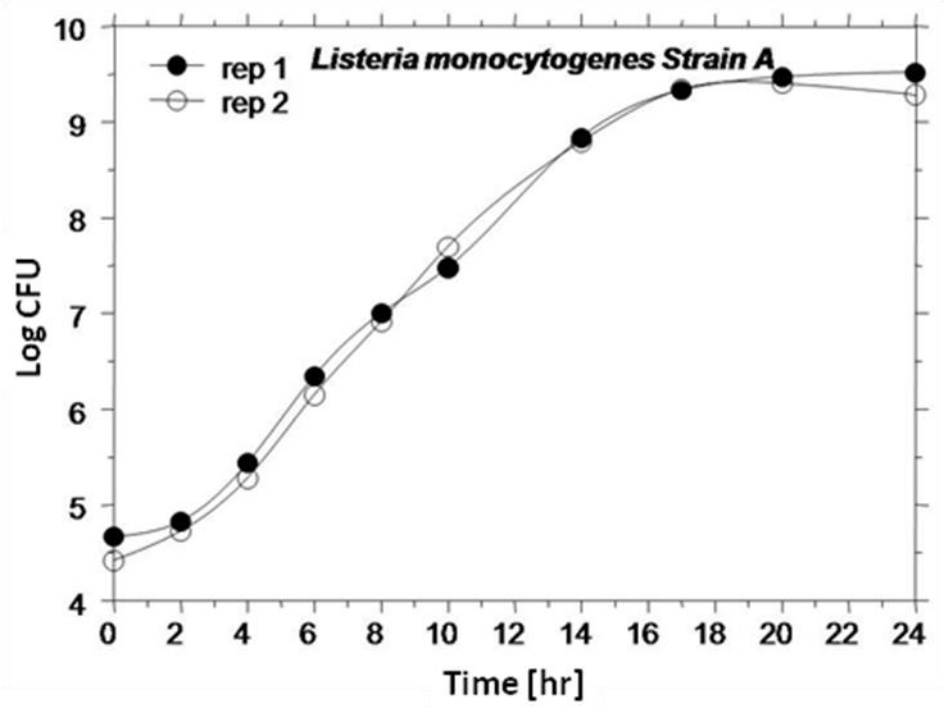

Figure 6A. Log CFU growth curves for *Listeria monocytogenes Strain A*

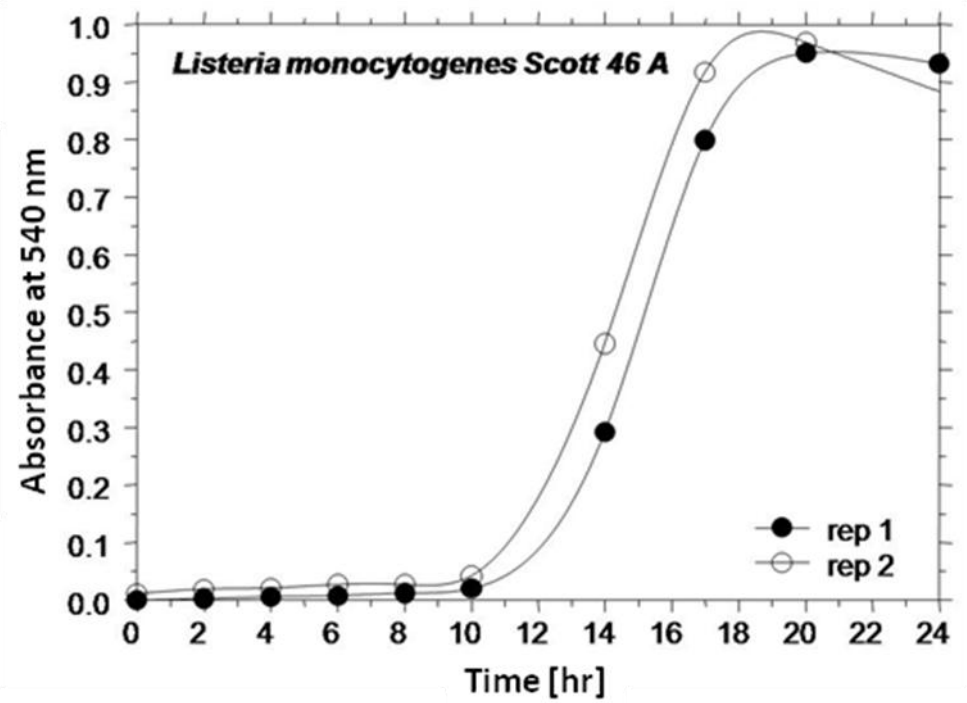

Figure 7A. Absorbance growth curves for *Listeria monocytogenes Scott A.*

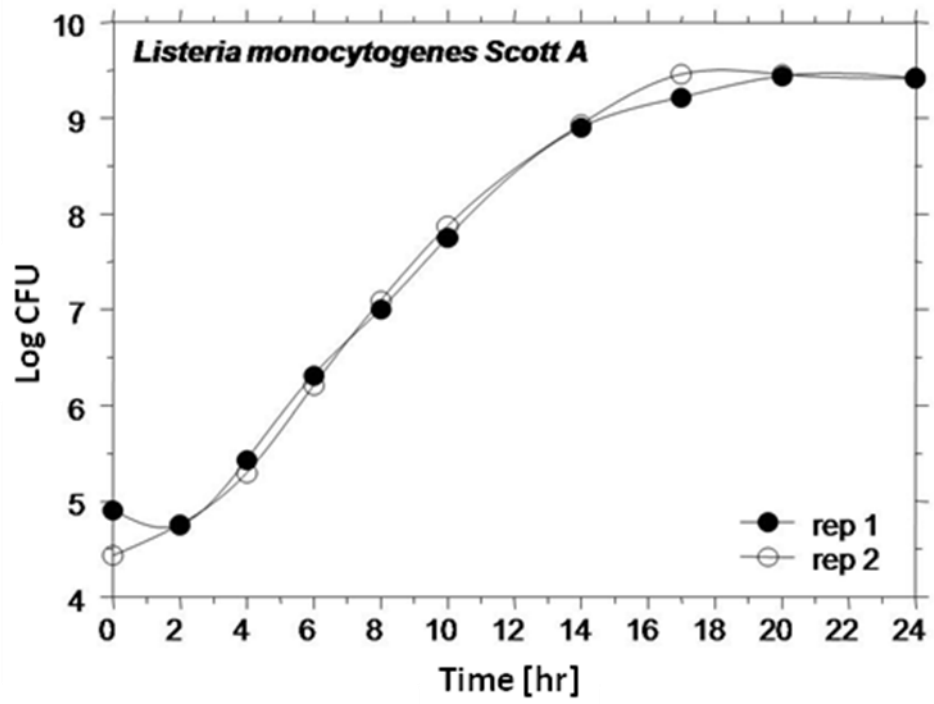

Figure 8A. Log CFU growth curves for *Listeria monocytogenes Scott A.*

Table A3. Growth of *Salmonella* spp. in tryptic soy broth as a function of active compound.

		(a) Trans-cinnamaldehyde vs. *Salmonella*										
Time	**4 mg/ml**	**2 mg/ml**	**1 mg/ml**	**0.5 g/ml**	**0.25 mg/ml**	**0.125 mg/ml**	**0.063 mg/ml**	**0.031 mg/ml**	**0.016 mg/ml**	**0.008 mg/ml**	**Solvent**	***Salmonella* spp. only**
0	0.22829	0.10974	0.10622	0.10711	0.11078	0.10657	0.10581	0.10643	0.10529	0.10869	0.11704	0.1170375
3	0.22829	0.10974	0.10622	0.10711	0.11078	0.10657	0.10581	0.10643	0.10529	0.10869	0.1088	0.1088
6	0.13682	0.10624	0.1053	0.10487	0.10641	0.10994	0.13717	0.17135	0.18771	0.21054	0.22456	0.22456
9	0.11733	0.10629	0.10567	0.10487	0.10579	0.2096	0.43845	0.48443	0.4797	0.48185	0.49146	0.49146
12	0.11389	0.10475	0.10501	0.10498	0.1053	0.52866	0.57794	0.58815	0.57783	0.57888	0.68624	0.68624
15	0.1103	0.1053	0.10339	0.10364	0.106	0.58283	0.63435	0.65399	0.68866	0.69009	0.98899	0.98899
18	0.11178	0.10525	0.10421	0.10392	0.13516	0.62663	0.7274	0.72459	0.77223	0.76891	1.1221	1.1221
21	0.10742	0.10566	0.10401	0.10445	0.3204	0.68271	0.76117	0.75472	0.81773	0.79813	1.1717	1.1717
24	0.10634	0.10559	0.10452	0.10354	0.47558	0.70111	0.78119	0.76772	0.84114	0.82192	1.1958	1.1958
27	0.10664	0.10543	0.10503	0.10284	0.56558	0.7107	0.79321	0.77548	0.85829	0.83442	1.2021	1.2021
30	0.10745	0.10572	0.10522	0.10341	0.66539	0.7162	0.79927	0.78024	0.8688	0.84342	1.2116	1.2116
33	0.10935	0.10638	0.10504	0.10479	0.78419	0.72013	0.80467	0.78578	0.87757	0.84948	1.2218	1.2218

		(b) Eugenol										
Time	**4 mg/ml**	**2 mg/ml**	**1 mg/ml**	**0.5 mg/ml**	**0.25 mg/ml**	**0.125 mg/ml**	**0.063 mg/ml**	**0.031 mg/ml**	**0.016 mg/ml**	**0.008 mg/ml**	**Solvent**	***Salmonella* spp. only**
0	0.12302	0.13838	0.10817	0.10442	0.10380	0.10270	0.10360	0.10365	0.10415	0.10502	0.10497	0.10497
3	0.12302	0.13838	0.10817	0.10442	0.10380	0.10270	0.10360	0.10365	0.10415	0.10502	0.10497	0.10497
6	0.09605	0.10767	0.10873	0.10970	0.13503	0.15413	0.16260	0.16410	0.17038	0.16937	0.17565	0.17565
9	0.09462	0.10323	0.10723	0.30247	0.47152	0.52257	0.54197	0.52888	0.56262	0.54710	0.55725	0.55725
12	0.09468	0.10225	0.10750	0.50377	0.51867	0.58943	0.59530	0.58650	0.63330	0.61910	0.67525	0.67525
15	0.09473	0.10252	0.10730	0.48480	0.55383	0.65097	0.64952	0.64382	0.70008	0.65877	0.71780	0.71780
18	0.09368	0.10073	0.10600	0.47073	0.58960	0.67908	0.66487	0.65933	0.72273	0.66855	0.73338	0.73338
21	0.09450	0.10103	0.10600	0.46842	0.59788	0.67977	0.66987	0.66055	0.73285	0.66688	0.74050	0.74050
24	0.09482	0.10222	0.10830	0.48395	0.60007	0.67512	0.66873	0.65922	0.74297	0.66863	0.74657	0.74657
27	0.09417	0.10385	0.10788	0.49025	0.60183	0.67037	0.66620	0.65345	0.74925	0.67287	0.73987	0.73987
30	0.09525	0.10318	0.10713	0.48553	0.60178	0.66763	0.66375	0.65108	0.75373	0.67247	0.72747	0.72747
33	0.09528	0.10288	0.10625	0.48330	0.60308	0.66610	0.66305	0.64895	0.75695	0.67540	0.71203	0.71203

		(c) Lysozyme + 60 mM EDTA										
Time	**5 mg/ml**	**2.5 mg/ml**	**1.25 mg/ml**	**0.625 mg/ml**	**0.313 mg/ml**	**0.156 mg/ml**	**0.078 mg/ml**	**0.039 mg/ml**	**0.020 mg/ml**	**0.010 mg/ml**	**Solvent**	***Salmonella* spp. only**
0	0.09965	0.10274	0.10601	0.10463	0.10324	0.10295	0.10356	0.10424	0.10558	0.10716	0.10568	0.10568
3	0.09293	0.09334	0.09748	0.09565	0.09496	0.09605	0.09480	0.09490	0.09800	0.09799	0.09883	0.09883
6	0.09224	0.09229	0.09770	0.09553	0.09489	0.09530	0.10100	0.12118	0.14361	0.14483	0.14025	0.14025
9	0.09146	0.09224	0.09854	0.10348	0.12211	0.12776	0.35215	0.44509	0.53858	0.54530	0.63040	0.63040
12	0.09240	0.09249	0.09916	0.18136	0.35269	0.50173	0.46650	0.51795	0.64714	0.64598	0.72579	0.72579
15	0.09174	0.09349	0.10103	0.41991	0.48183	0.50144	0.48181	0.58981	0.72636	0.70209	0.73088	0.73088
18	0.09228	0.09404	0.10224	0.41273	0.48331	0.51470	0.51228	0.66576	0.75593	0.73673	0.70691	0.70691
21	0.09131	0.09300	0.10214	0.43371	0.48220	0.53979	0.56386	0.70821	0.76131	0.75074	0.70588	0.70588
24	0.09025	0.09268	0.11410	0.43158	0.48568	0.57758	0.62560	0.72199	0.76528	0.74788	0.69289	0.69289
27	0.09141	0.09446	0.16630	0.43125	0.48978	0.63134	0.71338	0.72766	0.77071	0.74265	0.69284	0.69284
30	0.09123	0.09461	0.14800	0.43185	0.49901	0.67403	0.75801	0.72823	0.75468	0.73263	0.68729	0.68729
33	0.09170	0.09366	0.22818	0.42943	0.50578	0.73679	0.78436	0.71988	0.73618	0.71305	0.68231	0.68231

		(d) Garlic extract										
Time	**0.494 mg/ml**	**0.247 mg/ml**	**0.124 mg/ml**	**0.062 mg/ml**	**0.031 mg/ml**	**0.015 mg/ml**	**0.008 mg/ml**	**0.004 mg/ml**	**0.002 mg/ml**	**0.001 mg/ml**	**Solvent**	***Salmonella* spp. only**
0	0.10061	0.10543	0.10740	0.10470	0.10444	0.10398	0.10393	0.10490	0.10613	0.10631	0.10113	0.10700
3	0.09728	0.09470	0.10003	0.09540	0.09551	0.09555	0.09488	0.09634	0.09748	0.09784	0.09208	0.09824
6	0.10026	0.09500	0.10004	0.09571	0.09686	0.09591	0.09594	0.09754	0.09956	0.10529	0.10106	0.12888
9	0.09671	0.09418	0.09938	0.09515	0.09528	0.09536	0.09520	0.10609	0.28591	0.47641	0.31670	0.60558
12	0.09676	0.09491	0.09976	0.09540	0.09601	0.09580	0.09690	0.44659	0.59293	0.59371	0.45753	0.68423
15	0.09684	0.09444	0.09913	0.09561	0.09534	0.09603	0.09690	0.64858	0.70033	0.69494	0.58549	0.72426
18	0.09769	0.09479	0.09944	0.09570	0.09580	0.09580	0.13243	0.79389	0.76223	0.74223	0.59390	0.71271
21	0.09795	0.09526	0.09916	0.09600	0.09683	0.09528	0.45440	0.85079	0.79028	0.76876	0.59201	0.70044
24	0.09670	0.09399	0.09924	0.09525	0.09668	0.09620	0.57678	0.86458	0.79909	0.77086	0.59299	0.69130
27	0.09676	0.09496	0.09955	0.09549	0.09629	0.09603	0.67361	0.87623	0.79934	0.76823	0.59125	0.69134
30	0.09886	0.09550	0.09951	0.09613	0.09631	0.09621	0.71451	0.87969	0.79734	0.76268	0.58731	0.68764
33	0.09891	0.09494	0.09900	0.09576	0.09561	0.09551	0.71808	0.86309	0.78426	0.75464	0.57523	0.68470

		(e) Propolis extract										
Time	**4 mg/ml**	**2 mg/ml**	**1 mg/ml**	**0.5 mg/ml**	**0.25 mg/ml**	**0.125 mg/ml**	**0.063 mg/ml**	**0.031 mg/ml**	**0.016 mg/ml**	**0.008 mg/ml**	**Solvent**	***Salmonella* spp. only**
0	0.10179	0.24387	0.12472	0.02144	0.18549	0.15316	0.13184	0.15234	0.11750	0.11830	0.11316	0.11316
3	0.11205	0.01470	0.04925	0.01033	0.18610	0.14681	0.12390	0.11496	0.11116	0.10974	0.10573	0.10573
6	0.09535	0.01416	0.02345	0.00686	0.18884	0.15489	0.14578	0.14619	0.14464	0.14221	0.12738	0.12738
9	0.05999	0.00214	0.01068	0.00437	0.20158	0.50028	0.45936	0.48093	0.49544	0.48428	0.39633	0.39633
12	0.00259	0.01365	0.00117	0.00106	0.38059	0.56310	0.55484	0.56664	0.58471	0.56856	0.49310	0.49310
15	0.01900	0.01268	0.01006	0.00138	0.69509	0.57516	0.57870	0.59535	0.61681	0.59718	0.52946	0.52946
18	0.03427	0.03519	0.01723	0.00340	0.69315	0.57906	0.58389	0.60241	0.62308	0.60480	0.53660	0.53660
21	0.04406	0.04460	0.02552	0.00621	0.64669	0.60694	0.59290	0.60329	0.63104	0.61284	0.53866	0.53866
24	0.05686	0.03719	0.03092	0.00575	0.66889	0.61441	0.59833	0.60321	0.63625	0.61831	0.55100	0.55100
27	0.06489	0.07679	0.03676	0.00795	0.59890	0.58084	0.60389	0.60763	0.64213	0.62371	0.54800	0.54800
30	0.07259	0.03287	0.04086	0.00915	0.63373	0.59569	0.61133	0.61711	0.64805	0.62893	0.55105	0.55105
33	0.07494	0.01358	0.04558	0.01023	0.64919	0.59448	0.61798	0.62160	0.65466	0.63526	0.55578	0.55578

Table A4. Growth of *Listeria* spp. in tryptic soy broth as a function of active compounds.

		(a) Trans-cinnamaldehyde vs. *Listeria*										
Time	**4 mg/ml**	**2 mg/ml**	**1 mg/ml**	**0.5 mg/ml**	**0.25 mg/ml**	**0.125 mg/ml**	**0.063 mg/ml**	**0.031 mg/ml**	**0.016 mg/ml**	**0.008 mg/ml**	**Solvent**	***Listeria* spp. only**
0	0.26546	0.16471	0.13139	0.23121	0.12843	0.25458	0.12546	0.10764	0.10551	0.10670	0.26910	0.11220
3	0.26546	0.11063	0.10594	0.10241	0.12843	0.10160	0.09931	0.09959	0.09914	0.09904	0.09938	0.10615
6	0.15211	0.10675	0.10348	0.10078	0.10065	0.09996	0.09968	0.09874	0.09854	0.09908	0.09709	0.10579
9	0.12291	0.10568	0.10390	0.10010	0.09980	0.09973	0.09853	0.10028	0.10030	0.10069	0.09805	0.10555
12	0.11126	0.10425	0.10164	0.09831	0.09729	0.09808	0.09989	0.10504	0.10929	0.11335	0.09779	0.12208
15	0.10849	0.10536	0.10283	0.09966	0.09841	0.09965	0.11515	0.16146	0.20714	0.23228	0.11371	0.26266
18	0.10523	0.10374	0.10226	0.09881	0.09755	0.10384	0.20268	0.37328	0.48403	0.51201	0.19109	0.55339
21	0.10419	0.10403	0.10244	0.09931	0.09871	0.13385	0.41685	0.61364	0.61098	0.59131	0.33701	0.60520
24	0.10314	0.10360	0.10201	0.09808	0.09783	0.23084	0.58368	0.60774	0.60211	0.58011	0.51305	0.59373
27	0.10433	0.10474	0.10224	0.09861	0.09861	0.40304	0.57354	0.59261	0.58378	0.56119	0.56213	0.57928
30	0.10360	0.10408	0.10214	0.09849	0.10298	0.56539	0.55904	0.57609	0.56695	0.54601	0.54400	0.56610
33	0.10338	0.10401	0.10210	0.09845	0.11310	0.56661	0.54438	0.55793	0.55104	0.53049	0.52553	0.55275
36	0.10491	0.10596	0.10290	0.09868	0.14301	0.54631	0.52503	0.54055	0.53715	0.51838	0.51101	0.53813
39	0.10351	0.10378	0.10158	0.09766	0.19950	0.52636	0.50020	0.52381	0.52523	0.50714	0.49618	0.52524
42	0.10271	0.10353	0.10131	0.09886	0.27260	0.50325	0.47109	0.50839	0.51258	0.49559	0.48550	0.51198
45	0.10448	0.10480	0.10138	0.09886	0.34778	0.47676	0.43734	0.49205	0.49768	0.48248	0.47305	0.49200
48	0.10444	0.10446	0.10146	0.09784	0.38390	0.45055	0.39571	0.47265	0.48221	0.46716	0.45851	0.47061
51	0.10405	0.10440	0.10214	0.09748	0.38075	0.41861	0.34179	0.44698	0.45998	0.44555	0.44211	0.44290
54	0.10381	0.10460	0.10115	0.09730	0.36946	0.38016	0.29183	0.41516	0.43061	0.42055	0.42106	0.41170
57	0.10584	0.10556	0.10333	0.09930	0.35535	0.33306	0.25243	0.38196	0.40344	0.39734	0.39831	0.38440

		(b) Eugenol										
Time	**4 mg/ml**	**2 mg/ml**	**1 mg/ml**	**0.5 mg/ml**	**0.25 mg/ml**	**0.125 mg/ml**	**0.063 mg/ml**	**0.031 mg/ml**	**0.016 mg/ml**	**0.008 mg/ml**	**Solvent**	***Listeria* spp. only**
0	0.23518	0.20639	0.13066	0.10739	0.10620	0.10500	0.24560	0.09841	0.10965	0.10476	0.09684	0.10738
3	0.23518	0.20639	0.10196	0.09846	0.09808	0.09916	0.10100	0.09841	0.10121	0.09818	0.09684	0.10046
6	0.14899	0.15465	0.09974	0.09786	0.09790	0.09733	0.09629	0.09758	0.10058	0.09724	0.09549	0.09928
9	0.13378	0.13074	0.09813	0.09683	0.09643	0.09766	0.09598	0.09716	0.10034	0.09695	0.09388	0.09900
12	0.12231	0.13150	0.09996	0.09939	0.10083	0.10313	0.10295	0.10559	0.10755	0.10723	0.09575	0.10778
15	0.10904	0.12801	0.09851	0.10441	0.12193	0.14553	0.15940	0.17446	0.18774	0.19285	0.10338	0.19801
18	0.10578	0.11941	0.10094	0.14108	0.23614	0.33695	0.40056	0.45529	0.48029	0.48839	0.15931	0.48695
21	0.10428	0.11654	0.10729	0.25355	0.46830	0.58469	0.61785	0.63233	0.61295	0.58366	0.28965	0.60106
24	0.10140	0.11373	0.12981	0.43638	0.55603	0.58556	0.60241	0.62026	0.60366	0.57253	0.47574	0.59585
27	0.10088	0.11493	0.21074	0.53435	0.53911	0.56710	0.58729	0.60830	0.59273	0.56020	0.55164	0.58434
30	0.10085	0.11563	0.34471	0.52391	0.51425	0.54769	0.57065	0.59173	0.57558	0.54664	0.53634	0.57098
33	0.10219	0.11556	0.47534	0.48819	0.48881	0.52801	0.55240	0.57220	0.55979	0.53371	0.51760	0.55623
36	0.10131	0.11351	0.53410	0.44951	0.45534	0.50380	0.53066	0.55313	0.54028	0.51560	0.50068	0.53933
39	0.10081	0.11145	0.53919	0.39150	0.40798	0.47413	0.50535	0.53421	0.52460	0.49926	0.48671	0.52396
42	0.10193	0.11184	0.51954	0.29993	0.34043	0.43151	0.46833	0.51379	0.51019	0.48613	0.47416	0.51069
45	0.09901	0.10663	0.49728	0.21593	0.24806	0.36934	0.41445	0.48353	0.49276	0.47313	0.45958	0.49758
48	0.09546	0.10811	0.46243	0.18835	0.17928	0.29243	0.34439	0.43900	0.46401	0.45580	0.44245	0.48251
51	0.09529	0.10755	0.41758	0.18159	0.16275	0.22233	0.28405	0.38739	0.42546	0.43283	0.42566	0.46238
54	0.09704	0.10850	0.36369	0.17965	0.16093	0.19493	0.25224	0.34090	0.38136	0.39858	0.39911	0.43496
57	0.09675	0.10668	0.31046	0.17688	0.15998	0.19103	0.24025	0.30663	0.34093	0.36013	0.36955	0.40093

		(c) Lysozyme + 60mM EDTA										
Time	**5 mg/ml**	**2.5 mg/ml**	**1.25 mg/ml**	**0.625 mg/ml**	**0.313 mg/ml**	**0.156 mg/ml**	**0.078 mg/ml**	**0.039 mg/ml**	**0.020 mg/ml**	**0.010 mg/ml**	**Solvent**	***Listeria* spp. only**
0	0.1034	0.1061	0.1102	0.1067	0.1064	0.1058	0.1061	0.1075	0.1082	0.1074	0.1097	0.1097
3	0.0971	0.0981	0.1020	0.0992	0.0998	0.0986	0.0985	0.0991	0.1015	0.1016	0.1011	0.1011
6	0.0968	0.0978	0.1028	0.0993	0.0984	0.0993	0.0988	0.0989	0.1005	0.0999	0.1008	0.1008
9	0.0959	0.0972	0.1018	0.0989	0.0989	0.0986	0.0982	0.0986	0.1003	0.1010	0.1017	0.1017
12	0.0965	0.0971	0.1020	0.0980	0.0990	0.0977	0.0975	0.0977	0.1048	0.1096	0.1107	0.1107
15	0.0959	0.0973	0.1016	0.0976	0.0982	0.0986	0.0976	0.0980	0.1536	0.1981	0.2061	0.2061
18	0.0960	0.0988	0.1025	0.0995	0.0999	0.0982	0.0993	0.0995	0.3916	0.4962	0.4574	0.4574
21	0.0950	0.0966	0.1011	0.0978	0.0975	0.0972	0.0984	0.1026	0.6364	0.5935	0.6359	0.6359
24	0.0946	0.0956	0.1013	0.0977	0.0979	0.0980	0.0977	0.1339	0.5740	0.5599	0.6290	0.6290
27	0.0946	0.0968	0.1008	0.0977	0.0970	0.0976	0.0978	0.2182	0.5181	0.5370	0.6183	0.6183
30	0.0950	0.0963	0.1015	0.0979	0.0980	0.0986	0.0968	0.3672	0.4746	0.5142	0.6054	0.6054
33	0.0969	0.0983	0.1022	0.0992	0.0983	0.0990	0.0986	0.4530	0.4382	0.4954	0.5924	0.5924
36	0.0962	0.0967	0.1009	0.0982	0.0980	0.0976	0.0980	0.4528	0.4063	0.4701	0.5797	0.5797
39	0.0953	0.0973	0.1017	0.0994	0.0987	0.0982	0.0984	0.4365	0.3764	0.4571	0.5665	0.5665
42	0.0968	0.0973	0.1020	0.0996	0.0991	0.0987	0.0993	0.4129	0.3528	0.4256	0.5568	0.5568
45	0.0960	0.0964	0.1018	0.0986	0.0983	0.0979	0.0981	0.3882	0.3323	0.4060	0.5453	0.5453
48	0.0959	0.0954	0.1003	0.0981	0.0972	0.0969	0.0975	0.3450	0.3132	0.3865	0.5322	0.5322
51	0.0961	0.0970	0.1007	0.0985	0.0983	0.0989	0.0985	0.3005	0.3005	0.3638	0.5219	0.5219
54	0.0954	0.0976	0.1010	0.0994	0.0992	0.0979	0.0989	0.2844	0.2909	0.3429	0.5086	0.5086
57	0.0946	0.0973	0.1020	0.0985	0.0987	0.0987	0.0989	0.2755	0.2858	0.3305	0.4930	0.4930

		(d) Garlic extract										
Time	**0.494 mg/ml**	**0.247 mg/ml**	**0.124 mg/ml**	**0.062 mg/ml**	**0.031 mg/ml**	**0.015 mg/ml**	**0.008 mg/ml**	**0.004 mg/ml**	**0.002 mg/ml**	**0.001 mg/ml**	**Solvent**	***Listeria* spp. only**
0	0.10183	0.10604	0.10776	0.10808	0.10599	0.10573	0.10673	0.10744	0.10719	0.10770	0.10293	0.10618
3	0.09789	0.10025	0.10071	0.10078	0.09929	0.09950	0.09910	0.10026	0.10040	0.10033	0.09523	0.09956
6	0.09669	0.09808	0.09989	0.09906	0.09778	0.09785	0.09878	0.09964	0.09935	0.09969	0.09539	0.09881
9	0.09695	0.09821	0.09948	0.09939	0.09773	0.09713	0.09745	0.09865	0.09961	0.10048	0.09670	0.10144
12	0.09621	0.09688	0.09879	0.09878	0.09764	0.09754	0.09689	0.09858	0.10521	0.12539	0.12689	0.15264
15	0.09710	0.09783	0.09900	0.09889	0.09829	0.09798	0.09795	0.10325	0.19216	0.29375	0.27308	0.38433
18	0.09716	0.09720	0.09900	0.09923	0.09825	0.09795	0.09821	0.14775	0.42993	0.59581	0.40531	0.61955
21	0.09795	0.09820	0.09888	0.09888	0.09835	0.09800	0.09944	0.34130	0.63878	0.61900	0.38865	0.60753
24	0.09649	0.09724	0.09856	0.09878	0.09793	0.09761	0.10785	0.60398	0.61821	0.59484	0.37744	0.59336
27	0.09670	0.09616	0.09803	0.09761	0.09606	0.09593	0.18630	0.63144	0.60206	0.57656	0.36523	0.58039
30	0.09509	0.09464	0.09739	0.09673	0.09555	0.09549	0.38683	0.60863	0.58273	0.55456	0.35596	0.56538
33	0.09694	0.09759	0.09821	0.09790	0.09685	0.09696	0.60181	0.58416	0.56434	0.53735	0.34861	0.55264
36	0.09638	0.09601	0.09856	0.09700	0.09688	0.09596	0.62615	0.55801	0.54951	0.52263	0.34111	0.54033
39	0.09714	0.09661	0.09829	0.09811	0.09709	0.09776	0.60514	0.53949	0.53800	0.50929	0.33078	0.52696
42	0.09734	0.09730	0.09948	0.09876	0.09778	0.10194	0.58379	0.52449	0.52794	0.49693	0.31966	0.51446
45	0.09666	0.09574	0.09773	0.09763	0.09618	0.13093	0.56010	0.51043	0.51444	0.47933	0.30186	0.49813
48	0.09858	0.09720	0.09904	0.09915	0.09719	0.25035	0.54490	0.49951	0.50326	0.46586	0.28369	0.48168
51	0.09703	0.09685	0.09841	0.09770	0.09718	0.44134	0.52973	0.48798	0.48830	0.44504	0.26020	0.46209
54	0.09749	0.09609	0.09863	0.09790	0.09740	0.58191	0.51704	0.47603	0.47255	0.42724	0.23784	0.44149
57	0.09879	0.09786	0.09905	0.09961	0.09874	0.63623	0.50680	0.46384	0.45506	0.40754	0.22140	0.41876

		(e) Propolis extract										
Time	4 mg/ml	2 mg/ml	1 mg/ml	0.5 mg/ml	0.25 mg/ml	0.125 mg/ml	0.063mg/ml	0.031 mg/ml	0.016 mg/ml	0.008 mg/ml	**Solvent**	***Listeria* spp. only**
0	0.16106	0.13547	0.11258	0.01857	0.19323	0.15083	0.13155	0.12368	0.12130	0.11701	0.11503	0.11503
3	0.15329	0.07554	0.05467	0.01108	0.19396	0.14616	0.12636	0.11736	0.11671	0.10934	0.10715	0.10715
6	0.09741	0.03116	0.03683	0.00814	0.19461	0.14688	0.12600	0.11700	0.11795	0.11024	0.10625	0.10625
9	0.02608	0.00458	0.02495	0.00504	0.19579	0.14816	0.12703	0.11843	0.11409	0.11136	0.10863	0.10863
12	0.01561	0.04889	0.01585	0.00350	0.19730	0.14841	0.12983	0.12569	0.13273	0.12575	0.12415	0.12415
15	0.00285	0.04721	0.01075	0.00341	0.19793	0.15083	0.15231	0.19145	0.22908	0.23099	0.21984	0.21984
18	0.00534	0.01449	0.00335	0.00056	0.19876	0.16750	0.25946	0.39084	0.45796	0.44245	0.38853	0.38853
21	0.01807	0.05244	0.00057	0.00027	0.19911	0.22690	0.45911	0.59050	0.62058	0.58009	0.49943	0.49943
24	0.02935	0.03091	0.00377	0.00072	0.19973	0.34846	0.61504	0.62633	0.61888	0.58121	0.51465	0.51465
27	0.03430	0.00983	0.00796	0.00097	0.20650	0.49608	0.64664	0.61193	0.59874	0.56416	0.50686	0.50686
30	0.03947	0.01767	0.01080	0.00170	0.22568	0.59453	0.62123	0.59048	0.58058	0.54829	0.50738	0.50738
33	0.03991	0.03473	0.01498	0.00266	0.26709	0.62733	0.59655	0.57593	0.57201	0.53885	0.51188	0.51188
36	0.04322	0.01147	0.01776	0.00237	0.32128	0.61904	0.57859	0.56563	0.56051	0.53211	0.51403	0.51403
39	0.03954	0.00184	0.02165	0.00494	0.38503	0.60124	0.56643	0.56025	0.55598	0.52786	0.51581	0.51581
42	0.04310	0.01214	0.02317	0.00484	0.44296	0.58375	0.55620	0.55235	0.54934	0.52190	0.51170	0.51170
45	0.03705	0.01514	0.02788	0.00544	0.49121	0.56965	0.54948	0.54694	0.54519	0.51786	0.50980	0.50980
48	0.03659	0.00941	0.02840	0.00537	0.52718	0.55291	0.53920	0.53805	0.53824	0.51014	0.50213	0.50213
51	0.03289	0.05304	0.03112	0.00589	0.54905	0.53704	0.53013	0.52911	0.53865	0.50294	0.49544	0.49544
54	0.03121	0.07163	0.03470	0.00671	0.55669	0.51856	0.52098	0.51896	0.52941	0.49395	0.48573	0.48573
57	0.02626	0.04263	0.03623	0.00731	0.55324	0.49744	0.50733	0.50551	0.50801	0.48213	0.47074	0.47074

Table A5. Growth of *Salmonella* spp. in tryptic soy broth as a function of active compounds and their respective inclusion complexes with β-cyclodextrin.

		(a) Trans-cinnamaldehyde - CD										
Time	**40 mg/ml**	**20 mg/ml**	**10 mg/ml**	**5 mg/ml**	**2.5 mg/ml**	**1.25 mg/ml**	**0.625 mg/ml**	**0.313mg/ml**	**0.156 mg/ml**	**0.078 mg/ml**	**Solvent**	***Salmonella* spp. only**
0	0.00397	0.05784	0.10059	0.18193	0.19095	0.14353	0.13538	0.13368	0.13458	0.13238	0.11866	0.13225
3	0.08311	0.07108	0.10495	0.18045	0.14504	0.13064	0.12749	0.12728	0.12988	0.12808	0.11236	0.12650
6	0.10090	0.10346	0.09543	0.19134	0.14335	0.12995	0.12859	0.13640	0.14574	0.15290	0.12415	0.15856
9	0.11154	0.10246	0.11148	0.18885	0.14270	0.13059	0.26715	0.45078	0.45113	0.45989	0.42051	0.47260
12	0.10305	0.08286	0.07324	0.18484	0.13981	0.15436	0.47669	0.50981	0.47936	0.47316	0.60305	0.49090
15	0.09734	0.06956	0.04821	0.18243	0.13913	0.33115	0.49553	0.54604	0.51381	0.50075	0.76494	0.51111
18	0.08916	0.05325	0.03340	0.18111	0.13756	0.46684	0.53719	0.61850	0.57491	0.55166	0.79834	0.54908
21	0.08107	0.03951	0.02256	0.18064	0.13750	0.49986	0.60764	0.68045	0.64436	0.62714	0.81239	0.60375
24	0.07959	0.03319	0.01566	0.18099	0.13688	0.55664	0.68754	0.73603	0.69520	0.70450	0.81834	0.63614
27	0.06861	0.02379	0.00836	0.17974	0.13615	0.61828	0.76056	0.77214	0.72949	0.77191	0.80924	0.65889
30	0.06710	0.00818	0.00199	0.17806	0.13644	0.68835	0.80733	0.79478	0.75705	0.82525	0.79831	0.68330
33	0.06471	-0.00192	-0.00434	0.17788	0.13578	0.75634	0.83834	0.81120	0.77363	0.85501	0.78794	0.70049

		(b) Eugenol -CD										
Time	**40 mg/ml**	**20 mg/ml**	**10 mg/ml**	**5 mg/ml**	**2.5 mg/ml**	**1.25 mg/ml**	**0.625 mg/ml**	**0.313mg/ml**	**0.156 mg/ml**	**0.078 mg/ml**	**Solvent**	***Salmonella* spp. only**
0	-0.00431	0.09530	0.01736	0.01726	0.16878	0.14036	0.13634	0.13466	0.13420	0.13321	0.11778	0.13230
3	0.05258	0.01661	0.01740	0.02598	0.13746	0.13254	0.13198	0.13698	0.13224	0.13104	0.11528	0.13159
6	0.06007	0.01632	0.02298	0.02898	0.14340	0.14234	0.14660	0.15653	0.15043	0.14964	0.12305	0.14945
9	0.05803	0.02318	0.01515	0.02176	0.38523	0.42194	0.44851	0.47305	0.46581	0.46441	0.38586	0.46243
12	0.05223	0.02390	0.01649	0.03646	0.46605	0.48018	0.49125	0.50315	0.48915	0.47604	0.60159	0.47419
15	0.04065	0.01665	0.02236	0.04224	0.46529	0.48709	0.50046	0.51380	0.49768	0.48713	0.88446	0.49440
18	0.03539	0.02250	0.02156	0.02704	0.47333	0.50808	0.52506	0.54265	0.53410	0.54264	1.02639	0.53954
21	0.02904	0.08825	0.03099	0.02295	0.49070	0.54424	0.57283	0.58781	0.57683	0.59269	1.08548	0.58785
24	0.02608	0.06121	0.02321	0.02551	0.51849	0.60210	0.62213	0.65521	0.63945	0.68764	1.09315	0.68803
27	0.01860	0.03989	0.01476	0.02400	0.55608	0.66651	0.69469	0.81779	0.74876	0.80131	1.10141	0.83121
30	0.01534	0.01919	0.01020	0.02685	0.60593	0.70753	0.75503	0.91131	0.80316	0.84594	1.06710	0.87851
33	0.01207	0.00371	0.00396	0.02071	0.61963	0.71394	0.76513	0.90881	0.79370	0.83251	1.06314	0.86616

		(c) Garlic extract -CD										
Time	**40 mg/ml**	**20 mg/ml**	**10 mg/ml**	**5 mg/ml**	**2.5 mg/ml**	**1.25 mg/ml**	**0.625 mg/ml**	**0.313mg/ml**	**0.156 mg/ml**	**0.078 mg/ml**	**Solvent**	***Salmonella* spp. only**
0	0.02479	0.02538	0.20419	0.17075	0.14968	0.13950	0.13650	0.13243	0.13354	0.13194	0.11863	0.13201
3	0.02699	0.02314	0.20614	0.29545	0.26341	0.23975	0.20944	0.16696	0.15220	0.14613	0.13869	0.14833
6	0.02819	0.02098	0.20965	0.32818	0.27884	0.24221	0.21324	0.18863	0.17020	0.16883	0.15348	0.17028
9	0.02556	0.02551	0.20998	0.47199	0.53954	0.53835	0.50994	0.49273	0.47969	0.46708	0.45578	0.48724
12	0.02716	0.02009	0.19729	0.68515	0.66015	0.62980	0.59530	0.56298	0.54050	0.51989	0.60769	0.52701
15	0.01526	0.02599	0.20361	0.68955	0.66381	0.64278	0.62176	0.58916	0.57319	0.54665	0.75115	0.54580
18	0.02242	0.02321	0.20541	0.71261	0.70253	0.69343	0.67530	0.63849	0.63249	0.59220	0.78194	0.59663
21	0.02864	0.02150	0.20084	0.77778	0.75800	0.74583	0.71351	0.68169	0.70195	0.63381	0.79885	0.68466
24	0.02445	0.02863	0.20721	0.81624	0.79396	0.74195	0.69451	0.66535	0.75281	0.65261	0.79795	0.80920
27	0.02721	0.02169	0.20516	0.82338	0.85908	0.73753	0.70410	0.68401	0.79083	0.67778	0.79823	0.90086
30	0.02488	0.02068	0.20538	0.81486	0.90324	0.73654	0.71368	0.70033	0.80623	0.69525	0.79330	0.94858
33	0.02885	0.02069	0.20423	0.80249	0.89869	0.73536	0.72331	0.71435	0.82039	0.71078	0.78868	0.97705

		(d) Propolis extract -CD										
Time	40 mg/ml	20 mg/ml	10 mg/ml	5 mg/ml	2.5 mg/ml	1.25 mg/ml	0.625 mg/ml	0.313mg/ml	0.156 mg/ml	0.078 mg/ml	Solvent	*Salmonella* spp. only
0	0.33564	0.20691	0.20040	0.16315	0.14536	0.13616	0.13400	0.13060	0.13228	0.13234	0.11136	0.12903
3	0.09069	0.20647	0.19843	0.15314	0.13298	0.12564	0.12739	0.12646	0.12708	0.12735	0.10540	0.12439
6	0.00778	0.20107	0.21619	0.16926	0.15199	0.14590	0.14746	0.14875	0.14914	0.14708	0.11325	0.14471
9	-0.00140	0.21009	0.20160	0.45740	0.46185	0.46249	0.46965	0.47813	0.47580	0.46430	0.39394	0.47869
12	0.00326	0.25411	0.20355	0.49165	0.48951	0.48871	0.49415	0.50195	0.49458	0.48560	0.53229	0.49066
15	0.04186	0.20664	0.30459	0.52091	0.51270	0.51441	0.51981	0.52501	0.51783	0.51428	0.67309	0.52863
18	0.06889	0.20063	0.20636	0.58531	0.56656	0.56793	0.57655	0.58128	0.56324	0.56808	0.67481	0.58998
21	0.07330	0.20656	0.26184	0.69328	0.65381	0.65195	0.67328	0.67455	0.62259	0.65951	0.67720	0.69350
24	0.07446	0.20661	0.28270	0.78384	0.71164	0.70858	0.72516	0.73351	0.65241	0.72115	0.66783	0.80984
27	0.06910	0.20911	0.20191	0.83141	0.74669	0.74376	0.75625	0.76293	0.67474	0.75303	0.65728	0.92944
30	0.04103	0.20024	0.21748	0.86224	0.76951	0.76740	0.77803	0.78545	0.69279	0.77478	0.64520	1.01305
33	0.01540	0.20729	0.22693	0.87551	0.78394	0.78294	0.79193	0.80083	0.70576	0.78834	0.63319	1.06399

Table A6. Growth of *Listeria* spp. in tryptic soy broth as a function of active compounds and their respective inclusion complexes with β-cyclodextrin.

		(a) Trans-cinnamaldehyde - CD										
Time	**40 mg/ml**	**20 mg/ml**	**10 mg/ml**	**5 mg/ml**	**2.5 mg/ml**	**1.25 mg/ml**	**0.625 mg/ml**	**0.313 mg/ml**	**0.156 mg/ml**	**0.078 mg/ml**	**solvent**	***Listeria* spp.**
0	0.003312	0.118	0.175938	0.16835	0.169138	0.137725	0.129975	0.131863	0.130663	0.13275	0.11475	0.130138
3	0.066613	0.092413	0.175363	0.185688	0.141275	0.12925	0.124088	0.13665	0.140538	0.14145	0.1135	0.125863
6	0.0872	0.128138	0.176888	0.1792	0.139738	0.12765	0.123138	0.13265	0.136238	0.136988	0.111813	0.12475
9	0.0924	0.123575	0.1726	0.177475	0.138038	0.128088	0.122688	0.1305	0.135038	0.138525	0.11295	0.130575
12	0.097388	0.11035	0.177663	0.175988	0.14005	0.12785	0.126038	0.150725	0.186463	0.21735	0.173538	0.237463
15	0.085125	0.088163	0.171	0.1731	0.139088	0.12855	0.172825	0.34495	0.4669	0.547675	0.416888	0.546988
18	0.07255	0.0651	0.178838	0.173713	0.139388	0.1394	0.391575	0.638138	0.668838	0.745125	0.458838	0.665675
21	0.066325	0.049387	0.1778	0.173188	0.1383	0.205275	0.580875	0.67775	0.658175	0.810088	0.437463	0.67715
24	0.059337	0.03415	0.171325	0.173563	0.13825	0.4015	0.601575	0.65765	0.63435	0.812463	0.421475	0.670463
27	0.051275	0.024412	0.165263	0.17185	0.1379	0.566	0.587825	0.630725	0.613675	0.783275	0.410375	0.660388
30	0.046725	0.009713	0.158413	0.171463	0.138863	0.583325	0.573775	0.600463	0.604013	0.7854	0.404925	0.670163
33	0.04025	-0.00366	0.174538	0.170863	0.1406	0.59575	0.55985	0.582588	0.592575	0.758513	0.404038	0.646863

		(b) Eugenol -CD										
Time	**40 mg/ml**	**20 mg/ml**	**10 mg/ml**	**5 mg/ml**	**2.5 mg/ml**	**1.25 mg/ml**	**0.625 mg/ml**	**0.313 mg/ml**	**0.156 mg/ml**	**0.078 mg/ml**	**Solvent**	***Listeria* spp.**
0	0.1689	0.1318	0.134625	0.181438	0.164225	0.137488	0.132538	0.132538	0.1295	0.1284	0.116725	0.131313
3	0.20345	0.136775	0.134838	0.183288	0.138513	0.127613	0.12725	0.127	0.124575	0.123438	0.111263	0.126363
6	0.20565	0.138138	0.134325	0.173	0.1357	0.126938	0.127075	0.127538	0.124163	0.122525	0.110363	0.124375
9	0.198313	0.137138	0.131638	0.165825	0.136	0.130588	0.160788	0.13325	0.129163	0.128813	0.114	0.13305
12	0.193563	0.136763	0.1359	0.164163	0.1645	0.225888	0.28995	0.272188	0.25925	0.261063	0.199975	0.2828
15	0.185875	0.1389	0.133013	0.196425	0.392275	0.524313	0.57965	0.56945	0.5169	0.518538	0.437788	0.569113
18	0.180013	0.139325	0.132538	0.380988	0.674025	0.650238	0.652475	0.630925	0.566575	0.56745	0.441525	0.614888
21	0.164088	0.131625	0.132088	0.605725	0.696313	0.646588	0.640775	0.611938	0.548825	0.551388	0.419338	0.592525
24	0.1567	0.133363	0.13325	0.6233	0.690163	0.631488	0.628563	0.588675	0.53385	0.540788	0.40545	0.579513
27	0.149875	0.192863	0.133838	0.595125	0.6852	0.6209	0.612488	0.572425	0.524163	0.533963	0.398963	0.5774
30	0.139763	0.172875	0.1512	0.570213	0.680275	0.603713	0.595788	0.561	0.52005	0.533063	0.397975	0.575275

		(c) Garlic extract -CD										
Time	**40 mg/ml**	**20 mg/ml**	**10 mg/ml**	**5 mg/ml**	**2.5 mg/ml**	**1.25 mg/ml**	**0.625 mg/ml**	**0.313 mg/ml**	**0.156 mg/ml**	**0.078 mg/ml**	**Solvent**	***Listeria* spp.**
0	0.220275	0.195025	0.224513	0.205425	0.156538	0.141788	0.135763	0.132375	0.133425	0.133975	0.116913	0.130938
3	0.20755	0.234825	0.22665	0.214125	0.141763	0.12765	0.126075	0.127363	0.129925	0.129138	0.114013	0.126788
6	0.2125	0.226188	0.22785	0.211213	0.140088	0.128613	0.12845	0.1278	0.131113	0.13185	0.114238	0.12785
9	0.2008	0.226975	0.228863	0.214888	0.144038	0.137325	0.141338	0.142963	0.147188	0.148238	0.125575	0.144925
12	0.201213	0.226025	0.235375	0.266913	0.270375	0.306125	0.330713	0.337375	0.346963	0.353038	0.241775	0.344525
15	0.20345	0.242075	0.373925	0.562413	0.5426	0.570425	0.588275	0.5854	0.592063	0.6036	0.4595	0.599675
18	0.204738	0.206825	0.620075	0.727625	0.594388	0.597763	0.609463	0.60535	0.60715	0.65745	0.430813	0.614575
21	0.2019	0.200563	0.627725	0.682113	0.5811	0.58215	0.593238	0.589	0.58345	0.635375	0.413788	0.594125
24	0.202288	0.2089	0.6032	0.621975	0.563075	0.566713	0.58005	0.568	0.566613	0.607963	0.40595	0.581588
27	0.19995	0.208038	0.576875	0.566688	0.540138	0.549988	0.564438	0.548238	0.554163	0.612088	0.398925	0.576038
30	0.19575	0.20365	0.551138	0.513725	0.511888	0.531038	0.5459	0.53325	0.545925	0.601213	0.3935	0.577

		(d) Propolis extract -CD										
Time	**40 mg/ml**	**20 mg/ml**	**10 mg/ml**	**5 mg/ml**	**2.5 mg/ml**	**1.25 mg/ml**	**0.625 mg/ml**	**0.313 mg/ml**	**0.156 mg/ml**	**0.078 mg/ml**	**Solvent**	***Listeria* spp.**
0	0.137813	0.135988	0.13675	0.16455	0.143175	0.136288	0.130488	0.123363	0.135725	0.128138	0.116863	0.129088
3	0.131325	0.134263	0.134513	0.15405	0.13105	0.125825	0.124013	0.121213	0.132188	0.125213	0.111325	0.123688
6	0.1357	0.137788	0.135725	0.1523	0.127338	0.124113	0.122538	0.118913	0.131925	0.123625	0.110425	0.122475
9	0.137413	0.139	0.135388	0.153125	0.128013	0.126188	0.125138	0.121013	0.134975	0.125275	0.110538	0.125463
12	0.131388	0.142288	0.13685	0.222275	0.204788	0.209188	0.203925	0.19285	0.240925	0.212688	0.167413	0.217975
15	0.137813	0.138513	0.139088	0.559688	0.54935	0.565213	0.558663	0.502288	0.693938	0.564125	0.441275	0.566063
18	0.134188	0.13445	0.135213	0.63415	0.61555	0.632263	0.616438	0.5566	0.847688	0.615213	0.44375	0.637663
21	0.135425	0.125288	0.131488	0.62875	0.614225	0.627938	0.613963	0.5555	0.854625	0.604475	0.430213	0.626038
24	0.136163	0.11845	0.134013	0.625	0.61365	0.624738	0.613075	0.551588	0.863438	0.597075	0.41965	0.6303
27	0.133675	0.113175	0.12895	0.623563	0.6124	0.623338	0.608763	0.54205	0.842313	0.59345	0.409363	0.6243
30	0.133638	0.113975	0.125563	0.622488	0.6109	0.620925	0.606175	0.535575	0.854875	0.600313	0.399875	0.63305

Table A7. Growth of *Salmonella* spp. in tryptic soy broth as a function of active compounds loaded nanoparticles.

		(a) Trans-cinnamaldehyde - PLGA										
Time	**20000 mg/ml**	**10000 mg/ml**	**5000 mg/ml**	**2500 mg/ml**	**1250 mg/ml**	**625 mg/ml**	**313 mg/ml**	**156 mg/ml**	**78 mg/ml**	**39 mg/ml**	**Solvent**	***Salmonella* spp. only**
0	0.33051	0.33276	0.30956	0.10718	0.30244	0.21074	0.15926	0.13551	0.12501	0.11679	0.10291	0.11234
3	0.25875	0.20229	0.15090	0.08659	0.26435	0.18874	0.15260	0.12995	0.12021	0.11431	0.09850	0.10718
6	0.20399	0.18350	0.10718	0.02289	0.29708	0.22676	0.19239	0.15886	0.15213	0.14175	0.10916	0.13099
9	0.19705	0.25298	0.41988	0.39158	0.72289	0.61281	0.55205	0.49099	0.47375	0.47461	0.31883	0.48499
12	0.19551	0.27843	0.44040	0.39378	0.69600	0.59339	0.55440	0.51270	0.50250	0.50024	0.35240	0.51323
15	0.23254	0.26113	0.41750	0.37933	0.68451	0.59765	0.56283	0.52374	0.50903	0.51095	0.42654	0.51586
18	0.26031	0.33673	0.42741	0.36459	0.69285	0.60558	0.57418	0.54960	0.52894	0.53953	0.51713	0.54896
21	0.24316	0.31469	0.47531	0.40573	0.73328	0.65509	0.63246	0.60958	0.58459	0.61185	0.57000	0.62090
24	0.21327	0.32119	0.47293	0.45273	0.77619	0.70980	0.69229	0.67969	0.63108	0.68114	0.58185	0.69585
27	0.17695	0.30762	0.48238	0.48136	0.83008	0.79005	0.75566	0.76564	0.66856	0.75600	0.58993	0.83143
30	0.13065	0.26919	0.49899	0.52038	0.89193	0.86640	0.82636	0.85208	0.69354	0.84531	0.59635	0.94203
33	0.10717	0.26759	0.52608	0.54745	0.93695	0.94894	0.88896	0.90126	0.71881	0.89649	0.60070	1.00305

		(b) Eugenol - PLGA										
Time	**20000 mg/ml**	**10000 mg/ml**	**5000 mg/ml**	**2500 mg/ml**	**1250 mg/ml**	**625 mg/ml**	**313 mg/ml**	**156 mg/ml**	**78 mg/ml**	**39 mg/ml**	**Solvent**	***Salmonella* spp. only**
0	0.33051	0.33276	0.30956	0.10718	0.30244	0.21074	0.15926	0.13551	0.12501	0.11679	0.10291	0.11234
3	0.25875	0.20229	0.15090	0.08659	0.26435	0.18874	0.15260	0.12995	0.12021	0.11431	0.09850	0.10718
6	0.20399	0.18350	0.10718	0.02289	0.29708	0.22676	0.19239	0.15886	0.15213	0.14175	0.10916	0.13099
9	0.19705	0.25298	0.41988	0.39158	0.72289	0.61281	0.55205	0.49099	0.47375	0.47461	0.31883	0.48499
12	0.19551	0.27843	0.44040	0.39378	0.69600	0.59339	0.55440	0.51270	0.50250	0.50024	0.35240	0.51323
15	0.23254	0.26113	0.41750	0.37933	0.68451	0.59765	0.56283	0.52374	0.50903	0.51095	0.42654	0.51586
18	0.26031	0.33673	0.42741	0.36459	0.69285	0.60558	0.57418	0.54960	0.52894	0.53953	0.51713	0.54896
21	0.24316	0.31469	0.47531	0.40573	0.73328	0.65509	0.63246	0.60958	0.58459	0.61185	0.57000	0.62090
24	0.21327	0.32119	0.47293	0.45273	0.77619	0.70980	0.69229	0.67969	0.63108	0.68114	0.58185	0.69585
27	0.17695	0.30762	0.48238	0.48136	0.83008	0.79005	0.75566	0.76564	0.66856	0.75600	0.58993	0.83143
30	0.13065	0.26919	0.49899	0.52038	0.89193	0.86640	0.82636	0.85208	0.69354	0.84531	0.59635	0.94203
33	0.10717	0.26759	0.52608	0.54745	0.93695	0.94894	0.88896	0.90126	0.71881	0.89649	0.60070	1.00305

Table A8. Growth of *Listeria* spp. in tryptic soy broth as a function of active compounds loaded nanoparticles.

		(a) Trans-cinnamaldehyde - PLGA										
Time	**20000 mg/ml**	**10000 mg/ml**	**5000 mg/ml**	**2500 mg/ml**	**1250 mg/ml**	**625 mg/ml**	**313 mg/ml**	**156 mg/ml**	**78 mg/ml**	**39 mg/ml**	**Solvent**	***Listeria* spp. only**
0	0.10520	0.10520	0.10520	0.41486	0.26759	0.19613	0.15713	0.13296	0.12201	0.11726	0.10339	0.11093
3	0.11767	0.01206	0.03880	0.38226	0.26539	0.19295	0.15415	0.13335	0.12139	0.11356	0.09861	0.10584
6	0.16745	0.00511	0.01630	0.37941	0.26450	0.19145	0.15391	0.13203	0.12041	0.11319	0.09873	0.10520
9	0.19230	0.08133	0.06241	0.38649	0.27283	0.19854	0.16236	0.13969	0.14738	0.11861	0.10123	0.10999
12	0.15865	0.05923	0.06640	0.46385	0.38979	0.30151	0.27908	0.26396	0.30845	0.23489	0.18379	0.21889
15	0.14882	0.13553	0.38341	0.79234	0.80768	0.74635	0.73473	0.72931	0.71586	0.68279	0.46173	0.65515
18	0.14481	0.28455	0.53320	0.89965	0.82131	0.76464	0.75039	0.74533	0.72479	0.75040	0.43149	0.74928
21	0.16387	0.35501	0.51566	0.84610	0.79509	0.74489	0.73065	0.72894	0.70373	0.74869	0.40598	0.74489
24	0.21729	0.33496	0.50846	0.81796	0.77280	0.72534	0.71355	0.71126	0.68691	0.73663	0.39451	0.72363
27	0.28111	0.27859	0.50560	0.79223	0.74993	0.71184	0.69864	0.70089	0.67403	0.71679	0.38594	0.70413
30	0.33671	0.27573	0.49934	0.76284	0.73450	0.70035	0.68863	0.71194	0.67809	0.71318	0.37698	0.69136
33	0.33179	0.24954	0.46012	0.72860	0.71111	0.68554	0.67571	0.68763	0.65514	0.66788	0.36774	0.64395

		(b) Eugenol - PLGA										
Time	**20000 mg/ml**	**10000 mg/ml**	**5000 mg/ml**	**2500 mg/ml**	**1250 mg/ml**	**625 mg/ml**	**313 mg/ml**	**156 mg/ml**	**78 mg/ml**	**39 mg/ml**	**Solvent**	***Listeria* spp. only**
0	0.00000	0.11913	0.10616	0.38519	0.25760	0.18718	0.15585	0.13328	0.12404	0.11843	0.10439	0.11305
3	0.17656	0.11980	0.17950	0.48515	0.28036	0.20178	0.16038	0.13196	0.11923	0.11430	0.09916	0.10656
6	0.20456	0.10616	0.15840	0.45615	0.27879	0.20098	0.16016	0.13178	0.11841	0.11410	0.09953	0.10616
9	0.20026	0.10864	0.15850	0.43864	0.28511	0.20371	0.16234	0.13598	0.12099	0.11745	0.10186	0.11009
12	0.20496	0.15653	0.16435	0.45841	0.35076	0.28044	0.24966	0.22441	0.20650	0.20804	0.15574	0.20075
15	0.26180	0.23686	0.41741	0.79343	0.75599	0.72314	0.73478	0.70879	0.65751	0.67065	0.47059	0.66188
18	0.25219	0.30704	0.55324	0.92113	0.83800	0.78460	0.85661	0.76665	0.68279	0.74135	0.46236	0.72780
21	0.26415	0.31196	0.52650	0.89165	0.81906	0.76473	0.87681	0.77096	0.68833	0.74863	0.44965	0.73300
24	0.26669	0.30170	0.48516	0.86268	0.80216	0.74348	0.86448	0.75811	0.67783	0.73055	0.44621	0.72545
27	0.26552	0.28100	0.45996	0.84453	0.78608	0.72925	0.85133	0.74443	0.65886	0.68946	0.44036	0.69861
30	0.27770	0.29554	0.44148	0.82828	0.77675	0.71979	0.84200	0.73595	0.64871	0.67369	0.43595	0.68728
33	0.29775	0.31306	0.42735	0.81471	0.76688	0.71061	0.82908	0.73459	0.64576	0.66290	0.42755	0.68716

Table A9. Controlled release data for the nanoparticles loaded with active compounds.

Eugenol				t-cinnamaldehyde			
			mt/mo -				mt/mo -
time [hr]	area [mAu*min]	mt/mo	corrected	Time [hr]	area [mAu*min]	mt/mo	corrected
0	0	0	0	0	0	0	0
0	0	0	0	0	0	0	0
0	0	0	0	0	0	0	0
0.5	3.31260	0.18412	0.29355	0.5	5.78430	0.16933	0.22290
0.5	3.24130	0.18015	0.28724	0.5	6.72030	0.19673	0.25897
0.5	3.22620	0.17931	0.28590	0.5	6.69780	0.19607	0.25811
1	6.07890	0.33787	0.53870	1	12.87550	0.37692	0.49617
1	6.02730	0.33500	0.53412	1	12.19880	0.35711	0.47009
1	5.97910	0.33232	0.52985	1	12.78520	0.37428	0.49269
2	7.80820	0.43399	0.69194	2	24.65640	0.72180	0.95016
2	7.59710	0.42225	0.67324	2	24.63260	0.72110	0.94924
2	7.60010	0.42242	0.67350	2	24.36680	0.71332	0.93900
3	7.39810	0.41119	0.65560	3	24.10550	0.70567	0.92893
3	7.10300	0.39479	0.62945	3	24.22220	0.70909	0.93343
3	7.07040	0.39298	0.62656	3	24.04580	0.70393	0.92663
5	6.86160	0.38137	0.60806	5	23.48540	0.68752	0.90503
5	6.90240	0.38364	0.61167	5	23.39270	0.68481	0.90146
5	6.81820	0.37896	0.60421	5	23.18270	0.67866	0.89337
8	8.49780	0.47231	0.75305	8	24.16560	0.70743	0.93124
8	8.09170	0.44974	0.71707	8	24.03190	0.70352	0.92609
8	7.65780	0.42563	0.67862	8	23.79910	0.69670	0.91712
12	8.56830	0.47623	0.75930	12	28.22050	0.82614	1.08750
12	8.75220	0.48645	0.77560	12	29.27970	0.85714	1.12832
12	8.48240	0.47146	0.75169	12	28.04900	0.82112	1.08089
24	8.69690	0.48338	0.77070	24	28.57400	0.83649	1.10113
24	8.88440	0.49380	0.78731	24	28.46940	0.83342	1.09709
24	8.63150	0.47975	0.76490	24	29.49360	0.86341	1.13656
48	10.59700	0.58899	0.93908	48	28.34800	0.82987	1.09242
48	8.23230	0.45756	0.72953	48	35.21550	0.83313	1.09671
48	8.83950	0.49131	0.78333	48	28.57090	0.83640	1.10101
72	11.15730	0.62013	0.98873	72	27.82990	0.81470	1.07245

72	8.33510	0.46327	0.73864	72	28.46330	0.83325	1.09686
72	14.57910	0.81032	0.86368	72	33.35810	0.97654	1.28549

VITA

Carmen Luiza Feitosa de Lima Gomes received her Bachelor of Science degree in food engineering from Federal University of Vicosa, Brazil in 2002. In 2003, she joined the graduate program at Texas A&M University in the Biological & Agricultural Engineering Department to pursue her Doctor of Philosophy degree. During her graduate study, she has published eleven articles in major scientific journals and received two awards for excellence in research.

Her permanent address is:

Carmen Luiza Feitosa de Lima Gomes

Texas A&M University

Biological & Agricultural Engineering Department

2117 TAMU

College Station, TX – 77843-2117

email: carmen@tamu.edu